arXiv:gr-qc/0610071v1 13 Oct 2006

Alternative Theories of Gravity

Timothy Clifton

King's College

Dissertation submitted for the degree of Doctor of Philosophy

Department of Applied Mathematics and Theoretical Physics
University of Cambridge

August 2006

ACKNOWLEDGEMENTS

This work would not have been possible without the help of a lot of people. I would like to thank my family and friends for their encouragement, my collaborators David Mota and Robert Scherrer for their hard work and my office mate Simon West for innumerable delightful lunches. Most of all I would like to thank my supervisor, John Barrow, for his constant support, his guidance and for his untiring correction of my speling and, grammar.

DECLARATION

The research presented in this thesis was performed in the Department of Applied Mathematics and Theoretical Physics at the University of Cambridge between October 2003 and July 2006. This dissertation is the result of my own work, except as stated below or where explicit reference is made to the results of others.

The content of this thesis is based on the research papers

- *'Spherically Symmetric Solutions to Fourth-Order Theories of Gravity'*

  Timothy Clifton

  gr-qc/0607096

- *'Decaying Gravity'*

  Timothy Clifton and John Barrow

  Physical Review D **73**, 104022 (2006)

- *'Further Exact Cosmological Solutions to Higher-Order Gravity Theories'*

  Timothy Clifton and John Barrow

  Classical and Quantum Gravity **23**, 2951 (2006)

- *'The Existence of Gödel, Einstein and de Sitter Universes'*

  Timothy Clifton and John Barrow

  Physical Review D **72**, 123003 (2005)

- *'Exact Cosmological Solutions of Scale-Invariant Gravity Theories'*

  John Barrow and Timothy Clifton

  Classical and Quantum Gravity **23**, L1-L6 (2006)

- *'The Power of General Relativity'*

  Timothy Clifton and John Barrow

  Physical Review D **72**, 103005 (2005)

- *'Constraints on the Variation of G from Primordial Nucleosynthesis'*

  Timothy Clifton, John Barrow and Robert Scherrer

  Physical Review D **71**, 123526 (2005)

- *'Inhomogeneous Gravity'*

  Timothy Clifton, David Mota and John Barrow

  Monthly Notices of the Royal Astronomical Society **358**, 601 (2005)

A brief discussion of the number of arbitrary functions in section 5.2.1 is due to John Barrow. Section 5.2.3 was written collaboratively with John Barrow where the analysis of R^n theories in this section is due primarily to him. Discussion in the introduction to section 7.1 is also due to John Barrow. Section 7.1.3 was written collaboratively with David Mota where his main contribution was the numerical calculations involved and the production and discussion of figures 7.6 to 7.15. In section 9.1.1 the numerical work and the production of figure 9.1 was performed by Robert Scherrer. John Barrow also provided ideas and guidance which were of use throughout this work. Use was made of the computer programs Mathematica and Maple.

This dissertation is not substantially the same as any that I have submitted, or am submitting, for a degree, diploma or other qualification at any other university.

Signed: ..... Dated: .....

Alternative Theories of Gravity

Timothy Clifton

SUMMARY

This work investigates alternative theories of gravity, the solutions to their field equations and the constraints that can be imposed upon them from observation and experiment. Specifically, we consider the cosmologies and spherically symmetric solutions that can be expected to result from scalar-tensor and fourth-order theories of gravity. We find exact cosmological solutions of various different kinds; isotropic and anisotropic, homogeneous and inhomogeneous. These solutions are used to investigate the behaviour of the Universes at both late and early times, to investigate the effects of corrections to general relativity on approach to an initial singularity and to look for effects which may be observable in the present day Universe. We use physical processes, such as the primordial nucleosynthesis of the light elements, to impose constraints upon any deviations from the standard model. Furthermore, we investigate the vacuum spherically symmetric solutions of these theories. This environment is of particular interest for considerations of the local effects of gravity, where the most accurate experiments and observations of gravitational phenomena can be performed. Exact solutions are obtained for this situation and their stability analysed. It is found that a variety of new behaviour is obtainable in these theories that was not previously possible in the standard model. This new behaviour allows us an extended framework in which to consider gravitational physics, and its cosmological consequences.

Contents

1 Introduction **1**

2 Extended Theories of Gravity **11**

2.1 Actions and Field Equations 11

2.1.1 Scalar-Tensor Theories 12

2.1.2 Fourth-Order Theories 13

2.2 Conformal Transformations 17

2.2.1 Scalar-Tensor Theories 19

2.2.2 Fourth-Order Theories 21

3 Homogeneous and Isotropic Scalar-Tensor Cosmologies **23**

3.1 Friedmann-Robertson-Walker Cosmologies 23

3.2 Brans-Dicke Theory 24

3.2.1 Radiation Domination 25

3.2.2 Matter Domination 29

3.2.3 Vacuum Energy Domination 29

3.2.4 Vacuum Solutions 30

3.3 More General Theories 31

3.3.1 Radiation Domination 32

3.3.2 Matter Domination 33

3.3.3 Vacuum Domination 33

4 Homogeneous and Isotropic Fourth-Order Cosmologies 34
4.1 Freidmann-Robertson-Walker Cosmologies 34
4.2 The Dynamical Systems Approach 36
4.2.1 Locating the Critical Points 37
4.2.2 Stability of the Critical Points 41
4.2.3 Illustration of the Phase Plane 44

5 Other Homogeneous Fourth-Order Cosmologies 50
5.1 Gödel, Einstein and de-Sitter Universes 51
5.1.1 Gödel Universes 52
5.1.2 Einstein Static Universes 58
5.1.3 de Sitter Universes 60
5.2 Anisotropic Cosmologies 60
5.2.1 Field Equations 61
5.2.2 Exact Solutions 62
5.2.3 Investigation of the Effects of Matter 70
5.2.4 Discussion 75

6 Static Solutions 77
6.1 Scalar-Tensor Theories 77
6.2 Fourth-Order Theories 79
6.2.1 Dynamical System 80
6.2.2 Linearised Solution 86

7 Inhomogeneous Cosmological Solutions 90
7.1 Scalar-Tensor Theories 90
7.1.1 Exact Solutions 92
7.1.2 Spherical Collapse Model 98
7.1.3 A More Refined Spherical Collapse Model 101
7.1.4 Discussion 118
7.2 Fourth-Order Theories 123
7.2.1 Exact Solution 123

7.2.2 Linear perturbation analysis . . . 124

8 Scalar-Tensor Cosmologies with Energy Exchange 127

8.1 Field Equations . . . 128
8.2 Transfer of Energy and Entropy . . . 130
8.3 General Solutions . . . 132
8.4 Particular Solutions . . . 134
8.5 Behaviour of Solutions . . . 137
8.6 Physical Consequences . . . 142
8.7 Discussion . . . 145

9 Cosmological Constraints 148

9.1 Scalar-Tensor Theories and Primordial Nucleosynthesis . . . 148
9.1.1 Modelling the Form of $G(t)$ . . . 149
9.1.2 The Effect of a Non-Constant G . . . 152
9.1.3 Constraining the Theory . . . 153
9.1.4 Discussion . . . 162
9.2 Fourth-Order Theories . . . 163
9.2.1 Primordial Nucleosythesis . . . 164
9.2.2 Microwave Background Formation . . . 167

10 Weak-Field Constraints 170

10.1 Parameterised Post-Newtonian Approach . . . 171
10.2 Scalar-Tensor Theories . . . 173
10.3 Fourth-Order Theories . . . 175
10.3.1 Static Space-Time . . . 175
10.3.2 Non-Static Space-Time . . . 182

11 Conclusions 185

Bibliography 189

CHAPTER 1

Introduction

The standard model of gravitation and cosmology is based on the theory of general relativity (GR). GR is one of the cornerstones of modern theoretical physics and has been shown to be enormously successful not just in its conceptual ingenuity and mathematical elegance, but also in its ability to explain real physical phenomena. This is particularly astonishing considering that the vast majority of relativistic gravitational effects were completely unknown at the time of its conception.

Whilst in most branches of physics it has been the case that experiments have been performed and theory developed to fit these observations, this has not been the case for the development of relativity theory. Instead, due to the extreme weakness of gravity, it has been the situation that the theory of relativity was developed with only a minimal input from experiment. The theory then had only to satisfy the few experiments that were available at the time. Today this is no longer the case; an ever increasing body of experimental and observational evidence is being accumulated. This wealth of data has brought gravitational physics up to the status of a real experimental science, and so it must be confirmed that the theory which has been developed does in fact adequately model the observations.

In making any comparison between theory and observation it is useful to have a framework in which to consider the theory. Such frameworks have been con-

structed for gravitational physics by a number of authors for a variety of different circumstances. For example, the parameterised post-Newtonian approach has been developed to provide a framework in which weak field tests of gravity can be interpreted. Once the parameters in this very general approach have been constrained by the appropriate observations, these constraints can then be compared to the predictions of the relativistic theory. However, if we have only a single theory it is difficult to interpret exactly what these observations mean; we can only say if they are consistent with that one theory or not. In order to make a proper evaluation of just how influential these constraints are it is necessary to have a variety of theories, each differing from the others in their own particular modifications. It is the development of just such alternative theories that is the subject of this work.

As well as providing a foil against which to test GR, alternative theories of gravity are also interesting to study in their own right. The very existence of logically consistent alternatives to GR demands investigation to establish their potential compatibility with experiment, how they manifest the usual relativistic phenomena and if any new phenomena can be identified that are not present in the standard model. This avenue of research becomes particularly pressing if one wishes to attempt to explain aspects of gravitational physics which appear unsatisfactorily accounted for in the standard model. A number of these apparent shortcomings present themselves both from observations of physical phenomena as well from more philosophical concerns regarding the theory itself. Examples which are often cited in the literature are the apparent need for more than 95% of our Universe to be made from dark matter and dark energy (neither of which is satisfactorily understood), the anomalous acceleration of Pioneer, the incompatibility of GR with quantum field theory and the lack of application of Mach's principle. Any one of these provides sufficient motivation to investigate potential alternatives to GR.

In considering alternative theories of gravity it is necessary to impose some *a priori* conditions, to limit the number of candidate theories. We proceed as Dicke [81], and choose that

1. Space-time is a differentiable four-manifold with a metric and a connection.

2. The theory must be relativistic.

3. General coordinate covariance should be manifest.

4. There should exist no a priori geometric structure.

5. The field equations should be derivable from an action principle.

6. The theory should be simple.

The first condition is the statement that we are restricting ourselves to what are often called 'metric theories of gravity'. Associating a metric with the curvature of space-time is a powerful idea, leading directly to the equivalence of inertial and gravitational mass as neutral test-particles (those with negligible self-gravity) follow geodesics of the space-time. This equivalence of gravitational and inertial masses has been shown to very high accuracy by Eötvös type experiments. Furthermore, this condition limits our considerations to four dimensional theories with Riemannian geometry.

The second condition can be well justified from both experimental and philosophical considerations and is closely related to the first. It is known that at any point on a smooth manifold we can make a local coordinate transformation to normal coordinates. In such a coordinate system the effects of gravity should be transformed away (up to tidal forces) and we should recover special relativity. This is a manifestation of the weak equivalence principle which states: '*a freely falling frame in a gravitational field is equivalent to an inertial frame in the absence of gravity*'.

The condition of general coordinate covariance implies that we should be free to choose any coordinates to mark the positions of physical events on our space-time manifold. It is the position of the events themselves and the geometry of space-time that is important, not the arbitrary set of coordinates we put on the manifold. This condition requires that the theory should be formulated in terms of tensors.

Condition four is the idea that there should be no absolute space. It is the requirement that the geometry of space-time should be entirely determined by its matter content. This condition is in keeping with Mach's principle which states that the inertial forces acting on a body can only be defined with respect to other bodies, and not with respect to abstract concepts such as absolute space-time.

The condition that the field equations of the theory should be derivable from an action principle gives us covariantly conserved quantities, such as energy-momentum,

via Nöther's theorem and allows us to use Lagrangian mechanics. Further justification for this condition may be found in quantum mechanics; if a satisfactory quantum theory of gravity is to be found this strongly suggests that the theory should be derivable from an action principle.

The last of the above conditions is perhaps the most tenuous and is the one which could be most readily relaxed. We choose to interpret this condition as meaning that the gravitational Lagrangian should be a function of simple contractions of the Riemann tensor and one extra scalar field only. This still leaves us with a great number of alternative theories, including the most general formulation of the scalar-tensor theories as well as the fourth-order theories of gravity. Both of these classes of theory contain GR as a special (or limiting) case and it is these theories which this work will be concerned with.

It is clear that GR satisfies all of the above conditions. However, there are a number of additional conditions that GR also obeys which will not necessarily be obeyed by the theories we will be considering. These conditions are:

1. The strong equivalence principle.

2. The space and time independence of Newton's constant.

3. The linearity of the action in second derivatives of the metric.

The first of these conditions, the strong equivalence principle, is the statement that: '*massive self-gravitating objects should follow geodesics of the space-time*'. Whilst the metric formalism above assures us of this property for neutral test-particles, we are no longer assured that it should be true in general for extended massive bodies. These objects distort the background space-time in which they exist and whilst it is true that in GR they still follow geodesics, this is no longer true in general for the alternative theories we will be considering. This type of violation of the strong equivalence principle is often referred to as the Nordvedt effect.

The second condition that is met by GR is that at any point in space-time one can take the weak-field and slow motion limit to recover Newtonian gravity, with the same value of Newton's constant as is measured on Earth. This condition is explicitly violated by some of the theories we will consider. In fact, the Brans-Dicke theory

was devised specifically in order to create a theory of gravitation in which space-time variations of Newton's constant could occur. Constraining the parameters of these theories is then equivalent to constraining the potential variations of Newton's constant which they model.

The violation of the last of these three conditions is perhaps the most worrying. It is the linearity in second derivatives of the Einstein-Hilbert action that ensures that the field equations of GR are of no higher than second order in derivatives of the metric. Whilst this is also true of scalar-tensor theories, it is no longer true of theories which are constructed from contractions of the Riemann tensor only (except for the Einstein-Hilbert action with a cosmological constant). Generating Lagrangians which are non-linear in second derivatives yield field equations which are fourth-order in derivatives of the metric (with the exception of additional terms in the Lagrangian which are total diverges, such as the Gauss-Bonnet term). Also, variation of the action with respect to the metric is then no longer equivalent to Palatini approach of varying with respect to the metric and an independent connection. In fourth-order theories these two approaches yield two different sets of field equations. In this work we will only be concerned with the metric variation approach.

The investigation of alternative theories of gravity is hampered by the additional complexities that modifications to GR introduce. It seems that GR is unique not only in satisfying all of the conditions listed above, but also in being the simplest relativistic metric theory of gravitation that can be conceived of. Any modification to GR invariably results in a set of field equations that is considerably more complicated than Einstein's equations. In dealing with this complexity there appear in the literature two different ways of proceeding. The first is to look for approximate solutions to a specific theory of interest. This approach is particularly useful in the weak-field and low-velocity regime where frameworks such as the parameterised post-Newtonian approach can often be employed. It is the approach that is most frequently taken up when investigating theories that are motivated by a desire to overcome the perceived shortcomings of the standard theory (examples of which were given above). The second approach is to look for exact solutions of the simplest possible modifications to GR. The idea behind this approach is to understand as well as possible the effect of modifying the standard theory. Once this behaviour is well understood it can then be used as an approximation to more complicated

theories of specific interest, as well for considerations of that particular modification. It is the second approach that will be most closely adhered to in this work.

The program for this study will be to investigate the form of the solutions to the simplest alternative theories that meet the demands listed above; these will be the scalar-tensor theories and the fourth-order theories, which are often collectively referred to as the extended theories of gravity. Particular attention will be focussed on highly symmetric situations. High symmetry space-times are the most readily solved for and are often the ones of most physical interest. These solutions will then be used to model physical processes that occur in the Universe. Comparing these models with observation will allow constraints to be imposed upon the theory, which will limit the allowed deviations of this kind from GR. In performing this analysis we will be able to note new behaviour that was not previously obtainable in the general relativistic case.

We begin in chapter 2 by formally introducing the theories that will be considered. The generating Lagrangians will be explicitly given and the field equations derived from them. The form of these field equations will immediately be seen to be more complicated than the general relativistic case. We will then give a brief discussion of how these theories can be conformally transformed to look like general relativity minimally coupled to a scalar field. This conformal equivalence will be useful in finding solutions to the field equations.

In chapter 3 the homogeneous and isotropic solutions to the scalar-tensor field equations will be given. For the simplest case of a spatially flat Brans-Dicke universe containing a single perfect fluid the general solutions to the problem can be found. These general solutions have a late time power law attractor for the evolution of the scale factor and at early times are generally dominated for a period by the free component of the gravitational scalar itself. For this reason the general solution for the radiation dominated universe is presented explicitly, as it is this component of a realistic universe which is expected to dominate at early times, and the late time attractors are given for dust and vacuum energy densities. Vacuum solutions with non-zero spatial curvature are also given, and will be used in chapter 7 for a discussion of inhomogeneous cosmologies. The spatially-flat perfect fluid solutions will be used in chapter 9 to model the expansion of the Universe during primordial nucleosynthesis. The homogeneous and isotropic cosmological solutions for more

general scalar-tensor theories are also given in this chapter.

In chapter 4 the homogeneous and isotropic spatially flat cosmologies of a simple class of fourth-order gravity theories are investigated. A phase plane analysis is performed of the solutions and it is found that the late time attractor solutions for both vacuum cosmologies and universes filled with perfect fluids are simple power-law functions of time. These solutions are used in chapter 9 to model the expansion of the Universe during both primordial nucleosynthesis and microwave background formation.

In chapter 5 a variety of other homogeneous fourth-order cosmologies are presented. These include solutions of the Gödel type, as well as Einstein static, de-Sitter and Bianchi type I Kasner-like solutions. For the case of the Gödel solutions the existence of closed time-like curves, and hence the theoretical possibility of time travel, is investigated. The Kasner-like solutions are used to perform an analysis of the approach towards an anisotropic cosmological singularity in these theories. It is found that, unlike in the general relativistic case, these cosmologies do not undergo an infinite sequence of chaotic oscillations as the initial singularity is approached. It is also confirmed that matter sources do not generally dominate the evolution of these universes on approach to the singularity.

In chapter 6 static and spherically symmetric vacuum solutions are presented for both the scalar-tensor and fourth-order cases. For the case of the simple class of fourth-order theories that is studied it is found, using a dynamical systems approach, that the general solution to the problem is not asymptotically flat. An explicit r dependent expression is found for the asymptotic attractor and an exact solution is presented which has the same asymptotic behaviour. A perturbative analysis is performed which confirms that the exact solution corresponds to the mode with the appropriate Newtonian limit and also indicates the existence of extra modes which are damped oscillatory waves. This solution is used in chapter 10 to model solar system gravitational experiments in such a space-time.

Chapter 7 investigates the inhomogeneous cosmologies of these alternative theories. In the scalar-tensor case exact solutions are presented for inhomogeneous universes which asymptotically approach the homogeneous and isotropic solutions of chapter 3. A detailed investigation of the spherical collapse model in these theories is also performed: firstly for exact flat and closed vacuum solutions which

are matched at a boundary and secondly for flat and closed universes containing a perfect fluid. For the case of spherical collapse with a perfect fluid numerical simulations are performed, as no exact solutions are know for closed perfect fluid universes. The evolution of the scalar field, and hence Newton's constant, are followed both inside and outside the collapsing region and variations are tracked. For the case of fourth-order theories an exact spherically symmetric vacuum solution is presented which asymptotically approaches the homogeneous and isotropic vacuum solution of chapter 4. This solution is used in chapter 10, as an alternative to the static solution found in chapter 6, to model gravitational experiments that are carried out in the solar system. A linear perturbative analysis is carried out on the background of this solution and it is found that the exact solution does indeed reduce to the appropriate Newtonian limit and that the extra modes present in the general solution are manifest as modes growing as r^2 in the linearisation.

In chapter 8 an analysis is made of scalar-tensor cosmologies where energy is allowed to be exchanged between the gravitational scalar field and a perfect fluid. In such a theory all of the conditions required of the theory above are still met. However, some of the meaning of condition 1 is lost as test-particles no longer follow exact geodesics of the space-time geometry. This is due to the interaction with the gravitational scalar, which acts as an external force on the test-particle. The exchange of energy and entropy between the scalar field and the perfect fluid is discussed and the evolution of homogeneous and isotropic universes is then considered. For a general form of the parameter controlling the energy exchange the field equations for the scale factor and scalar field can be decoupled and integrated to two first order ordinary differential equations. From this point some simple specific functions of the energy exchange parameter are proposed and these equations are then integrated again to give explicit expressions for the evolutions of the scale factor and scalar field.

In chapter 9 cosmological processes are modelled in the solutions that were presented in previous chapters. Specifically, primordial nucleosynthesis is modelled in the general solutions for radiation dominated spatially flat scalar-tensor universes. Previous analyses have been performed on primordial nucleosynthesis in these theories, but have always taken the late time power law solutions to describe the evolution of the Universe. In this study we consider the general form of the solution

and hence allow for Newton's constant to be varying whilst nucleosynthesis occurs. This allows, for the first time, observational constraints to be imposed upon the free scalar-dominated period of such a universe's expansion. In addition, we study primordial nucleosynthesis and microwave background formation in the power law solutions of the fourth-order theories found in chapter 4. These observable processes allow the theory to be constrained from observation.

Chapter 10 provides an analysis of the weak field constraints available on the theory. A brief explanation of the parameterised post-Newtonian approach, and how it can be used to place constraints on the scalar-tensor theories of gravity, is given. The spherically symmetric vacuum solutions to the fourth order theories found in chapters 6 and 7 are then analysed. It is shown that these theories do not fit so readily into the usual formalism, and that in these theories one should expect extra gravitational forces in the weak field limit which are not present in GR. For the static solution this extra force takes the form of a force which drops off as r^{-1} and for the inhomogeneous cosmological solution this force looks like a friction force, for a slowly moving test-particle. The r^{-1} force in the static solution has a dramatic impact on the perihelion precession of closed orbits in such a space-time and, applying observational constraints from the orbit of Mercury, it is possible to constrain the theory dramatically if this solution is used to model the solar system. The inhomogeneous cosmological solution fits better into the parameterised post-Newtonian formalism and, if it is used to model the solar system, can be used to place tight constraints on this theory from the observations of the Shapiro time delay of radio signals from the Cassini space craft as it passes behind the Sun. The extra gravitational forces present in these solutions, and their lack of asymptotic flatness, show explicitly new behaviour in these theories which is not present in GR.

In chapter 11 we summarise our results and provide concluding remarks.

Conventions

The Riemann curvature tensor is

$$R^{a}{}_{bcd} = \Gamma^{a}{}_{bd,c} - \Gamma^{a}{}_{bc,d} + \Gamma^{a}{}_{ce}\Gamma^{e}{}_{bd} - \Gamma^{a}{}_{de}\Gamma^{e}{}_{cb}$$

where Latin indices refer to space-time components and we use Greek indices to refer to space components. The signature of the metric is taken to be $(-,+,+,+)$ and we choose units in which $c = 1$.

CHAPTER 2

Extended Theories of Gravity

'Extended theories of gravity' is the collective term usually applied to the scalar-tensor and fourth-order theories of gravity. In this chapter we will introduce these theories, deriving their field equations and showing their conformal equivalence to GR.

2.1 Actions and Field Equations

We present in this section the generating Lagrangians for the theories that will be considered in the remainder of this work. The actions obtained from integrating these Lagrangians over all space will be extremised to obtain the relevant field equations.

Considering gravitational theories derived from Lagrangians has the advantage of ensuring coordinate independence of the derived field equations, as well as the covariant conservation of quantities via Nöther's constraint.

2.1.1 Scalar-Tensor Theories

A general form of the scalar-tensor theory [46, 143, 187] can be derived from the Langrangian density

$$\mathcal{L} = \frac{1}{16\pi}\sqrt{-g}\left(f(\phi)R - g(\phi)\partial_a\phi\partial^a\phi - 2\Lambda(\phi)\right) + \mathcal{L}_m(\Psi, h(\phi)g_{ab}) \tag{2.1.1}$$

where f, g, h and Λ are arbitrary functions of the scalar field ϕ and $\mathcal{L}_m$ is the Lagrangian density of the matter fields Ψ. The function $h(\phi)$ can be absorbed into the metric by a conformal transformation of the form [80]

$$h(\phi)g_{ab} \rightarrow g_{ab}.$$

The conformal frame picked out by this choice is the one in which there is no direct interaction between the scalar field and matter fields and is usually referred to as the Jordan frame (see section 2.2 for a discussion of conformal transformations in these theories). Test-particles in this conformal frame follow geodesics of the metric and the weak equivalence principle is obeyed. The effect of this transformation on the rest of the Lagrangian can then be absorbed into redefinitions of f, g and Λ.

By a redefinition of the scalar field ϕ we can now set $f(\phi) \rightarrow \phi$, without loss of generality. The Lagrangian density (2.1.1) can then be written as

$$\mathcal{L} = \frac{1}{16\pi}\sqrt{-g}\left(\phi R - \frac{\omega(\phi)}{\phi}\partial_a\phi\partial^a\phi - 2\Lambda(\phi)\right) + \mathcal{L}_m(\Psi, g_{ab}) \tag{2.1.2}$$

where $\omega(\phi)$ is an arbitrary function which has been chosen in analogy with the Brans-Dicke theory and Λ is a ϕ-dependent generalisation of the cosmological constant. This theory reduces to the Brans-Dicke theory in the limit $\omega \rightarrow$constant and $\Lambda \rightarrow 0$, and approaches general relativity in the limit $\omega \rightarrow \infty$, $\omega'/\omega^2 \rightarrow 0$ and $\Lambda \rightarrow 0$.

The variation of the action derived from integrating (2.1.2) over all space is

$$\delta I = \frac{1}{16\pi}\int d\Omega\sqrt{-g}\left[\frac{1}{2}g^{ab}\delta g_{ab}\mathcal{L} + \phi\delta R + \frac{\omega(\phi)}{\phi}\partial^a\phi\partial^b\phi\delta g_{ab} + 8\pi T^{ab}\delta g_{ab}\right] \tag{2.1.3}$$

where use has been made of

$$\delta g^{ab} = -g^{ac}g^{bd}\delta g_{cd}, \qquad \delta\sqrt{-g} = \frac{1}{2}g^{ab}\delta g_{ab} \tag{2.1.4}$$

and

$$T^{ab} = \frac{2}{\sqrt{-g}} \frac{\delta \mathcal{L}_m}{\delta g_{ab}}.$$

Now using the relation [79]

$$\delta R_{ab} = \frac{1}{2} g^{cd} (\delta g_{ac;bd} + \delta g_{bd;ac} - \delta g_{ab;cd} - \delta g_{cd;ab}) \tag{2.1.5}$$

we can write

$$\delta I \simeq \frac{1}{16\pi} \int d\Omega \sqrt{-g} (-S^{ab} + 8\pi T^{ab}) \delta g_{ab} \tag{2.1.6}$$

where

$$S^{ab} = \phi (R^{ab} - \frac{1}{2} g^{ab} R) - (g^{ac} g^{bd} - g^{ab} g^{cd}) \phi_{;cd} - \frac{\omega}{\phi} (g^{ac} g^{bd} - \frac{1}{2} g^{ab} g^{cd}) \phi_{,c} \phi_{,d} + g^{ab} \Lambda$$

and $\simeq$ means equal up to total divergences. Such terms are irrelevant here as they can be transformed via Gauss's theorem to terms on the boundary which are assumed to vanish.

The first variation of the action corresponding to (2.1.2), with respect to the scalar field ϕ, is now

$$\delta I \simeq \frac{1}{16\pi} \int d\Omega \sqrt{-g} \left(R + 2\omega \frac{\Box \phi}{\phi} - \frac{\omega}{\phi^2} \phi_{,c} \phi^{,c} + \frac{\omega'}{\phi} \phi_{,c} \phi^{,c} - 2\Lambda' \right) \delta \phi \tag{2.1.7}$$

where primes denote differentiation with respect to ϕ. Eliminating R with the trace of (2.1.6) and looking for stationary points of the action, by setting the first variation to zero, then gives the field equations

$$\phi (R_{ab} - \frac{1}{2} g_{ab} R) = 8\pi T_{ab} + (\delta^c_a \delta^d_b - g_{ab} g^{cd}) \phi_{;cd} + \frac{\omega}{\phi} (\delta^c_a \delta^d_b - \frac{1}{2} g_{ab} g^{cd}) \phi_{,c} \phi_{,d} - g_{ab} \Lambda \tag{2.1.8}$$

and

$$(2\omega + 3) \Box \phi = 8\pi T - \omega' \phi_{,a} \phi^{,a} - 4\Lambda + 2\phi \Lambda'. \tag{2.1.9}$$

2.1.2 Fourth-Order Theories

The fourth-order theories we shall consider are derived from functions of the three possible linear and quadratic contractions of the Riemann curvature tensor: R,

$R_{ab}R^{ab}$ and $R_{abcd}R^{abcd}$ [1] . The relevant weight-zero scalar density for this general class of theories is then given by

$$\mathcal{L} = \chi^{-1}\sqrt{-g}f(X,Y,Z) \tag{2.1.10}$$

where $f(X,Y,Z)$ is an arbitrary function of X, Y and Z which are defined by $X \equiv R$, $Y \equiv R_{ab}R^{ab}$ and $Z \equiv R_{abcd}R^{abcd}$, and χ is an arbitrary constant which can be determined from the appropriate Newtonian limit. The action is obtained, as usual, by integrating this density, together with that of the matter fields, over all space. The addition of supplementary terms to the density (2.1.10) in order to cancel total divergences which can be transformed to integrals on the boundary can be problematic (see e.g. [121]) and so, for simplicity, they will all be assumed to vanish.

The variation of the action derived from integrating the density (2.1.10) over all space is

$$\begin{aligned}\delta I &= \chi^{-1}\int d\Omega\sqrt{-g}\Big[\frac{1}{2}fg^{ab}\delta g_{ab} + f_X\delta X + f_Y\delta Y + f_Z\delta Z\Big] \\ &= \chi^{-1}\int d\Omega\sqrt{-g}\Big[\frac{1}{2}fg^{ab}\delta g_{ab} - f_X(R^{ab}\delta g_{ab} - g^{ab}\delta R_{ab}) \\ &\qquad\qquad - 2f_Y(R^{c(a}R^{b)}{}_c\delta g_{ab} - R^{ab}\delta R_{ab}) \\ &\qquad\qquad - 2f_Z(R_{cde}{}^{(b}R^{a)edc}\delta g_{ab} - R_a{}^{bcd}\delta R^a{}_{bcd})\Big]\end{aligned} \tag{2.1.11}$$

where use has again been made of (2.1.4). Using the relations (2.1.5) and

$$\delta R^a{}_{bcd} = \frac{1}{2}g^{ae}(\delta g_{ed;bc} + \delta g_{eb;dc} - \delta g_{db;ec} - \delta g_{ec;bd} - \delta g_{eb;cd} + \delta g_{cb;ed}).$$

We can then write

$$\begin{aligned} f_X g^{ab}\delta R_{ab} &\simeq -f_{X;cd}(g^{ab}g^{cd} - g^{ac}g^{bd})\delta g_{ab} \\ 2f_Y R^{ab}\delta R_{ab} &\simeq -\Big[\Box(f_Y R^{ab}) + (f_Y R^{cd})_{;cd}g^{ab} - 2(f_Y R^{c(a})_{;}{}^{b)}{}_c\Big]\delta g_{ab} \\ 2f_Z R_a{}^{bcd}\delta R^a{}_{bcd} &\simeq 4(f_Z R^{c(ab)d})_{;cd}\delta g_{ab}. \end{aligned}$$

[1] As pointed out by De Witt [79] there is a fourth possibility, namely $\epsilon^{abcd}R_{efab}R^{ef}{}_{cd}$. However, this contraction is of no physical interest due to parity considerations.

Substituting these expressions back into (2.1.11) then gives

$$\delta I = -\chi^{-1} \int d\Omega \sqrt{-g} P^{ab} \delta g_{ab}$$

where

$$P^{ab} \equiv -\frac{1}{2} f g^{ab} + f_X R^{ab} + 2 f_Y R^{c(a} R^{b)}{}_c + 2 f_Z R^{edc(a} R^{b)}{}_{cde} + f_{X;cd}(g^{ab} g^{cd} - g^{ac} g^{bd}) + \Box(f_Y R^{ab}) + g^{ab}(f_Y R^{cd})_{;cd} - 2(f_Y R^{c(a})^{\ b)}_{;\ c} - 4(f_Z R^{d(ab)c})_{;cd}. \quad (2.1.12)$$

The notation f_N denotes partial differentiation of f with respect to N. Looking for a stationary point of the action by setting the first variation to zero gives the field equations

$$P_{ab} = \frac{\chi}{2} T_{ab} - g_{ab} \Lambda \quad (2.1.13)$$

when matter fields and a cosmological constant are included. Here, Λ is the cosmological constant (defined independent of $f(X, Y, Z)$) and T^{ab} is the energy-momentum tensor of the matter. These field equations are generally of fourth-order, with the exception of the cases in which the function f is linear in the second derivatives of the metric [79].

We will often be considering gravitational theories derived from the choice

$$f = f(R) = R^{1+\delta} \quad (2.1.14)$$

where $\delta \neq 0$ is a real number. The limit $\delta \to 0$ gives us the familiar Einstein–Hilbert Lagrangian of GR. We take the quantity R^δ to be the positive real root of R throughout this work. This choice of f gives

$$P_{ab} = \delta(1-\delta^2) R^\delta \frac{R_{,a} R_{,b}}{R^2} - \delta(1+\delta) R^\delta \frac{R_{;ab}}{R} + (1+\delta) R^\delta R_{ab} - \frac{1}{2} g_{ab} R R^\delta - g_{ab} \delta(1-\delta^2) R^\delta \frac{R_{,c} R_{,}{}^c}{R^2} + \delta(1+\delta) g_{ab} R^\delta \frac{\Box R}{R}. \quad (2.1.15)$$

These equations have the useful property that in vacuum they are conformally equivalent to Einstein's equations with a scalar field in an exponential potential, as shown below.

The Newtonian Limit

By comparing the geodesic equation to Newton's gravitational force law it can be seen that, as usual,

$$\Gamma^{\mu}_{00} = \Phi_{,\mu} \tag{2.1.16}$$

where Φ is the Newtonian gravitational potential. All the other Christoffel symbols have $\Gamma^{a}_{\ bc} = 0$, to the required order of accuracy.

We now seek an approximation to the field equations (2.1.15) that is of the form of Poisson's equation; this will allow us to fix the constant χ. Constructing the components of the Riemann tensor from (2.1.16) we obtain the standard results

$$R^{\mu}_{\ 0\nu 0} = \frac{\partial^2 \Phi}{\partial x^{\mu} \partial x^{\nu}} \qquad \text{and} \qquad R_{00} = \nabla^2 \Phi. \tag{2.1.17}$$

The 00 component of the field equations (2.1.15) can now be written

$$(1+\delta) R_{00} - \frac{1}{2} g_{00} R = \frac{\chi}{2} \frac{T_{00}}{R^{\delta}} \tag{2.1.18}$$

where terms containing derivatives of R have been discarded as they will contain third and fourth derivatives of Φ, which will have no counterparts in Poisson's equation. Subtracting the trace of equation (2.1.18) gives

$$(1+\delta) R_{00} = \frac{\chi}{2R^{\delta}} \left(T_{00} - \frac{1}{2(1-\delta)} g_{00} T \right) \tag{2.1.19}$$

where T is the trace of the stress–energy tensor. Assuming a perfect–fluid form for T we should have, to first–order,

$$T_{00} \simeq \rho \qquad \text{and} \qquad T \simeq 3p - \rho \simeq -\rho. \tag{2.1.20}$$

Substituting (2.1.20) and (2.1.17) into (2.1.19) gives

$$\nabla^2 \Phi \simeq \frac{\chi(1-2\delta)}{4(1-\delta^2)} \frac{\rho}{R^{\delta}}.$$

Comparison of this expression with Poisson's equation allows one to read off

$$\chi = 16\pi G \frac{(1-\delta^2)}{(1-2\delta)} R_0^{\delta} \tag{2.1.21}$$

where R_0 is the value of the Ricci tensor at the time G is measured. It can be seen that the Newtonian limit of the field equations (2.1.15) does not reduce to the usual relation $\nabla^2\Phi \propto \rho$, but instead contains an extra factor of R^{δ}. This can be interpreted as being the space–time dependence of Newton's constant, in this theory. Such a dependence should be expected as the Lagrangian (2.1.14) can be shown to be equivalent to a scalar–tensor theory, after an appropriate Legendre transformation[2] (see e.g, [124]). This type of Newtonian gravity theory admits a range of simple exact solutions in the case where the effective value of G is a power-law in time [20].

2.2 Conformal Transformations

A conformal transformation of the metric g_{ab} into $\bar{g}_{ab}$ can be written

$$g_{ab} = e^{2\Gamma(x)} \bar{g}_{ab} \tag{2.2.1}$$

where $\Gamma(x)$ is an arbitrary function of the coordinates x^a. The line-element is then transformed according to

$$ds^2 = e^{2\Gamma(x)} d\bar{s}^2$$

and the square root of the determinant of the metric as

$$\sqrt{-g} = e^{4\Gamma} \sqrt{-\bar{g}},$$

in four dimensions. Conformal transformations of this kind are local, isotropic transformations of the standard of 'size', as defined by the line-element. These transfor-

[2]This equivalence to scalar-tensor theories should not be taken to imply that bounds on the Brans-Dicke parameter ω are immediately applicable to this theory. It can be shown that a potential for the scalar-field can have a non-trivial effect on the resulting phenomenology of the theory [147]. Furthermore, the form of the perturbation to general relativity that we are considering does not allow an expansion of the corresponding scalar field of the form $\phi_0+\phi_1$ where ϕ_0 is constant and $|\phi_1| << |\phi_0|$, so that any constraints obtained in a weak-field expansion of this sort cannot be applied to this situation.

mations are known as conformal as they leave the angle between any two vectors in the space-time unaltered.

After performing such a transformation we use the term 'conformal frame' to distinguish the new, rescaled metric from the original. Among the infinite possible conformal frames there are two which are most commonly used and have specific interpretations: the Jordan frame and the Einstein frame. The Jordan frame is the one in which the energy-momentum tensor is covariantly conserved and in which test-particles follow geodesics of the space-time metric. The Brans-Dicke theory [52], for instance, is most usually formulated in the Jordan frame. The Einstein frame is the conformal frame in which the field equations of the theory take the form of the Einstein equations (unlike the Jordan frame, the Einstein frame can only be defined for some theories). In the Einstein frame the field equations are second order but the energy-momentum tensor of the matter fields is not always covariantly conserved and test-particles do not necessarily follow geodesics of the space-time metric. The Einstein frame, therefore, is particularly useful for finding vacuum solutions, but less useful for finding solutions with matter fields present.

Under the transformation (2.2.1) it can be shown that the Ricci tensor and scalar transform as (see e.g. [193])

$$R_{ab} = \bar{R}_{ab} - 2\Gamma_{;\bar{a}\bar{b}} + 2\Gamma_{,a}\Gamma_{,b} - 2\bar{g}_{ab}\bar{g}^{cd}\Gamma_{,c}\Gamma_{,d} - \bar{g}_{ab}\bar{\Box}\Gamma \tag{2.2.2}$$

$$e^{2\Gamma}R = \bar{R} - 6\bar{g}^{ab}\Gamma_{,a}\Gamma_{,b} - 6\bar{\Box}\Gamma \tag{2.2.3}$$

and the d'Alembertian transforms as

$$e^{2\Gamma}\Box\phi = \bar{\Box}\phi + 2\bar{g}^{ab}\Gamma_{,a}\phi_{,b} \tag{2.2.4}$$

where overbars over operators or indices denote that they are defined using the metric $\bar{g}_{ab}$. We will now use these transformations to show how the scalar-tensor and some fourth-order theories can be transformed from the Jordan frames to the Einstein frame.

2.2.1 Scalar-Tensor Theories

All of the scalar-tensor theories defined by the Lagrangian (2.1.2), in the Jordan frame, can be transformed to an equivalent in the Einstein frame. To see this we will consider the various terms in the generating Lagrangian (2.1.2) seperately. Firstly, we consider the term containing the Ricci scalar

$$\mathcal{L}_1 = \frac{1}{16\pi}\sqrt{-g}\phi R$$

which under the conformal transformation (2.2.1) becomes

$$\mathcal{L}_1 = \frac{1}{16\pi}\sqrt{-\bar{g}}\phi e^{2\Gamma}(\bar{R} - 6\bar{g}^{ab}\Gamma_{,a}\Gamma_{,b} - 6\bar{\Box}\Gamma). \tag{2.2.5}$$

The non-minimal coupling to the Ricci scalar can now be removed by making the choice of conformal factor

$$e^{2\Gamma} = \phi^{-1} \qquad \text{such that} \qquad g_{ab} = \frac{\bar{g}_{ab}}{\phi}. \tag{2.2.6}$$

This choice of Γ defines the conformal transformation between the Jordan and Einstein frames in the scalar-tensor theories. Making this choice of Γ it can be seen that the last term on the right-hand side of (2.2.5) is a total divergence, which can be transformed to an integral over a surface at infinity and therefore ignored.

Considering now the second term in (2.1.2) we get

$$\mathcal{L}_2 = -\frac{1}{16\pi}\sqrt{-g}\frac{\omega}{\phi}g^{ab}\phi_{,a}\phi_{,b} = -\frac{1}{4\pi}\sqrt{-\bar{g}}\omega\bar{g}^{ab}\Gamma_{,a}\Gamma, b$$

under the transformation (2.2.1) and using the definition of Γ above. The third term then gives

$$\mathcal{L}_3 = -\frac{1}{8\pi}\sqrt{-g}\Lambda = -\frac{1}{8\pi}\sqrt{-\bar{g}}e^{4\Gamma}\Lambda$$

so that the whole Lagrangian can be written

$$\mathcal{L} = \frac{1}{16\pi}\sqrt{-\bar{g}}\left(\bar{R} - 2(3+2\omega)\bar{g}^{ab}\Gamma_{,a}\Gamma_{,b} - 2e^{4\Gamma}\Lambda\right) + \mathcal{L}_m(\Psi, e^{2\Gamma}\bar{g}_{ab}). \tag{2.2.7}$$

Now, by making the definitions

$$\sqrt{\frac{4\pi}{(3+2\omega)}} = \frac{\partial\Gamma}{\partial\psi} \qquad \text{and} \qquad 8\pi V(\psi) = e^{4\Gamma}\Lambda \tag{2.2.8}$$

for the scalar ψ and the function $V(\psi)$, we can write the transformed Lagrangian (2.2.7) as

$$\mathcal{L} = \frac{1}{16\pi}\sqrt{-\bar{g}}\bar{R} + \sqrt{-\bar{g}}\left(-\frac{1}{2}\bar{g}^{ab}\psi_{,a}\psi_{,b} - V(\psi)\right) + \mathcal{L}_m(\Psi, e^{2\Gamma}\bar{g}_{ab}). \tag{2.2.9}$$

In the absense of any matter fields the scalar-tensor theories can now clearly be seen to be conformally related to Einstein's theory in the presence of a scalar field in a potential (that potential disappearing in the absense of Λ).

In the Brans-Dicke theory [52] the coupling constant ω is a constant quantity and the scalar fields ϕ and ψ are related by

$$\ln\phi = \sqrt{\frac{16\pi}{(3+2\omega)}}\psi.$$

For more general theories with $\omega = \omega(\phi)$ the definition of ψ, (2.2.8), must be integrated to obtain a relation between ϕ and ψ.

By extremising the action (2.2.9) with respect to $\bar{g}_{ab}$ we get the Einstein frame field equations

$$\bar{R}_{ab} = 8\pi(\bar{T}_{ab} - \frac{1}{2}\bar{g}_{ab}\bar{T} + \psi_{,a}\psi_{,b})$$

and by extremizing with respect to ψ we get the Einstein frame propagation equation

$$\bar{\Box}\psi = -\sqrt{4\pi}\alpha\bar{T},$$

where $\alpha^{-2} \equiv 3 + 2\omega$ and we have defined the energy-momentum tensor $\bar{T}_{ab}$ with respect to $\bar{g}_{ab}$ so that $\bar{T}^{ab} = e^{6\Gamma}T^{ab}$. Correspondingly, whilst the Jordan frame energy-momentum tensor is always covariantly conserved, $T^{ab}{}_{;b} = 0$, its counterpart in the Einstein frame is not, $\bar{T}^{ab}_{;b} = \sqrt{4\pi}\alpha\bar{T}\psi_{,}{}^{a}$. The interaction between the scalar field ψ and the matter fields described by $\bar{T}_{ab}$ can now be seen explicitly.

2.2.2 Fourth-Order Theories

We will now show the conformal transformation between the Jordan frame and the Einstein frame for theories derivable from an abritrary function of the Ricci scalar [25, 122]. Extremising the action

$$S = \int d\Omega \sqrt{-g} f(R) \tag{2.2.10}$$

with respect to the metric g_{ab} gives the field equations, according to (2.1.12),

$$f' R_{ab} - \frac{1}{2} f g_{ab} - f'_{;ab} + g_{ab} \Box f' = \frac{\chi}{2} T_{ab} - g_{ab} \Lambda \tag{2.2.11}$$

where primes denote differentiation with respect to R. Under the conformal transformation

$$\bar{g}_{ab} = f' g_{ab},$$

and making the definition

$$\phi \equiv \sqrt{\frac{3}{\chi}} \ln f',$$

the field equations (2.2.11) then become

$$\bar{R}_{ab} - \frac{1}{2} \bar{g}_{ab} \bar{R} = \frac{\chi}{2} \left(\phi_{,a} \phi_{,b} - \frac{1}{2} \bar{g}_{ab} \bar{g}^{cd} \phi_{,c} \phi_{,d} - \bar{g}_{ab} V \right) + \frac{\chi}{2} \frac{T_{ab}}{f'} \tag{2.2.12}$$

where

$$V = \frac{(Rf' - f)}{2f'^2} + \frac{2\Lambda}{\chi f'}.$$

It can now be seen that, in the absense of any matter fields, theories derived from an action of the form (2.2.10) are conformally equivalent to GR in the presence of a scalar field in a potential.

We will now consider the more specific case of theories derived from the Lagrangian (2.1.14). In this case the relevant conformal transformation can be written as $\bar{g}_{ab} = \Omega_0 R^\delta g_{ab}$, where Ω_0 is a constant. The scalar field can then be defined as

$$\phi \equiv \sqrt{\frac{3}{16\pi G}} \ln R^\delta,$$

and the field equations, in the absense of matter fields and any cosmological constant,

can be rewritten as

$$\bar{G}_{ab} = 8\pi G \left(\phi_{,a}\phi_{,b} - \frac{1}{2}\bar{g}_{ab}(\bar{g}^{cd}\phi_{,c}\phi_{,d} + 2V(\phi)) \right) \tag{2.2.13}$$

and

$$\bar{\Box}\phi = \frac{dV}{d\phi},$$

where $V(\phi)$ is given by

$$V(\phi) = \frac{\delta \ \mathrm{sign}(R)}{16\pi G(1+\delta)\Omega_0} \exp\left\{ \sqrt{\frac{16\pi G}{3}} \frac{(1-\delta)}{\delta}\phi \right\}. \tag{2.2.14}$$

The magnitude of the quantity Ω_0 is not physically important and simply corresponds to the rescaling of the metric by a constant quantity, which can be absorbed by an appropriate rescaling of units. It is, however, important to ensure that $\Omega_0 > 0$ in order to maintain the +2 signature of the metric.

CHAPTER 3

Homogeneous and Isotropic Scalar-Tensor Cosmologies

We will consider in this section the homogeneous and isotropic cosmological solutions to the scalar-tensor fields equations (2.1.8) and (2.1.9). These are space-times with a six-dimensional group of motions, G_6, acting transitively on a three-dimensional space-like subspace.

3.1 Friedmann-Robertson-Walker Cosmologies

Spatially homogeneous and isotropic space-times are described by the Friedmann-Robertson-Walker (FRW) line-element

$$ds^2 = -dt^2 + a^2(t)\left(\frac{dr^2}{1-kr^2} + r^2(d\theta^2 + \sin^2\theta d\phi^2)\right),$$

where $a(t)$ is the scale factor and k is the spatial curvature. Using the FRW metric in the scalar-tensor field equations (2.1.8) and (2.1.9), and setting $\Lambda = 0$, gives

$$2\dot{H} + 3H^2 + \frac{\omega}{2}\frac{\dot{\phi}^2}{\phi^2} + 2H\frac{\dot{\phi}}{\phi} + \frac{\ddot{\phi}}{\phi} = -\frac{8\pi}{\phi}p - \frac{k}{a^2}, \tag{3.1.1}$$

$$\frac{\ddot{\phi}}{\phi} = \frac{8\pi}{\phi}\frac{(\rho - 3p)}{(2\omega + 3)} - 3H\frac{\dot{\phi}}{\phi} - \frac{\dot{\omega}}{(2\omega + 3)}\frac{\dot{\phi}}{\phi}, \tag{3.1.2}$$

and

$$\frac{8\pi}{3\phi}\rho = H^2 + H\frac{\dot{\phi}}{\phi} - \frac{\omega}{6}\frac{\dot{\phi}^2}{\phi^2} + \frac{k}{a^2}, \tag{3.1.3}$$

where $H \equiv \dot{a}/a$ is the Hubble rate, an overdot denotes differentiation with respect to comoving proper time, t, ρ is the matter density, and p is the pressure. Each non-interacting fluid source $p(\rho)$ separately satisfies a conservation equation:

$$\dot{\rho} + 3H(\rho + p) = 0. \tag{3.1.4}$$

Substituting equations (3.1.2) and (3.1.3) into equation (3.1.1) gives

$$\dot{H} + H^2 - H\frac{\dot{\phi}}{\phi} + \frac{\omega}{3}\frac{\dot{\phi}^2}{\phi^2} = -\frac{8\pi}{3\phi}\frac{(3p\omega + 3\rho + \rho\omega)}{(2\omega + 3)} + \frac{1}{2}\frac{\dot{\omega}}{(2\omega + 3)}\frac{\dot{\phi}}{\phi}. \tag{3.1.5}$$

It is the solutions of these equations that concern us in this chapter.

3.2 Brans-Dicke Theory

For the Brans-Dicke theory (ω =constant) there are a variety of known exact homogeneous and isotropic solutions (see e.g. [19, 97, 135, 144]). We will present the solutions here that are of particular significance, and that will be of use later on.

In these theories $\omega(\phi) \equiv \omega$ is a constant. The three essential field equations for the evolution of the scalar field $\phi(t)$ and the expansion scale factor $a(t)$ in a Brans-Dicke universe are (3.1.2), (3.1.3), and (3.1.4). Now ω is a constant parameter and the theory reduces to GR in the limit $\omega \to \infty$ where $\phi = G^{-1} \to$ constant. The general solutions to the FRW Brans-Dicke theory field equations are fully understood. The vacuum solutions are the $t \to 0$ attractors for the perfect-fluid solutions and the general solutions with equation of state

$$p = (\gamma - 1)\rho \tag{3.2.1}$$

and $k = 0$ can all be found. At early times they approach the vacuum solutions but

at late time they approach particular power-law exact solutions [135]:

$$a(t) = t^{[2+2\omega(2-\gamma)]/[4+3\omega\gamma(2-\gamma)]} \tag{3.2.2}$$

$$\phi(t) = \phi_0 t^{[2(4-3\gamma)/[4+3\omega\gamma(2-\gamma)]} \tag{3.2.3}$$

These particular exact power-law solutions for $a(t)$ and $\phi(t)$ are 'Machian' in the sense that the cosmological evolution is driven by the matter content rather than by the kinetic energy of the free ϕ field.

The power-law solutions (3.2.2) and (3.2.3) are valid for any fluid with equation of state (3.2.1). We will now consider seperately the solutions for universes dominated by radiation, matter and vacuum energy. The general solutions for $k = 0$ are known for any fluid that satisfies (3.2.1) [97]. Here we will only present the general solution for a radiation-dominated universe as the late-time power-law attractors for matter and vacuum dominated eras are expected to be sufficient for any realistic universe (see below).

3.2.1 Radiation Domination

We consider first the case of a flat radiation–dominated universe. Assuming the equation of state $p = \frac{1}{3}\rho$ and defining the conformal time variable, η, by $ad\eta \equiv dt$, the equations (3.1.1), (3.1.2) and (3.1.3) integrate to give [97]

$$\frac{a'(\eta)}{a(\eta)} = \frac{\eta + \eta_2}{\eta^2 + (2\eta_2 + 3\eta_1)\eta + \eta_2^2 + 3\eta_1\eta_2 - \frac{3}{2}\omega\eta_1^2} \tag{3.2.4}$$

$$\frac{\phi'(\eta)}{\phi(\eta)} = \frac{3\eta_1}{\eta^2 + (2\eta_2 + 3\eta_1)\eta + \eta_2^2 + 3\eta_1\eta_2 - \frac{3}{2}\omega\eta_1^2} \tag{3.2.5}$$

where η_1 and η_2 are integration constants.

For $\omega > -3/2$ the solutions to these equations are

$$a(\eta) = a_1(\eta + \eta_+)^{\frac{1}{2}+\frac{1}{2\sqrt{1+\frac{2}{3}\omega}}}(\eta + \eta_-)^{\frac{1}{2}-\frac{1}{2\sqrt{1+\frac{2}{3}\omega}}} \tag{3.2.6}$$

$$\phi(\eta) = \phi_1(\eta + \eta_+)^{-\frac{1}{2\sqrt{1+\frac{2}{3}\omega}}}(\eta + \eta_-)^{+\frac{1}{2\sqrt{1+\frac{2}{3}\omega}}} \tag{3.2.7}$$

where $\eta_\pm = \eta_2 + \frac{3}{2}\eta_1 \pm \frac{3}{2}\eta_1\sqrt{1+\frac{2}{3}\omega}$, a_1 and ϕ_1 are integration constants, and $8\pi\rho_{r0}/3\phi_1 a_1^2 = 1$ (subscript 0 indicates a quantity measured at the present day and we rescale so that $a_0 = 1$, throughout).

For $\omega < -3/2$ we find

$$a(\eta) = a_1\sqrt{(\eta+\eta_-)^2+\eta_+^2}\,\exp\left(\frac{-1}{\sqrt{\frac{2}{3}|\omega|-1}}\tan^{-1}\frac{\eta+\eta_-}{\eta_+}\right), \tag{3.2.8}$$

$$\phi(\eta) = \phi_1\left(\frac{2}{\sqrt{\frac{2}{3}|\omega|-1}}\tan^{-1}\frac{\eta+\eta_-}{\eta_+}\right), \tag{3.2.9}$$

where $\eta_+ = \frac{3}{2}\eta_1\sqrt{\frac{2}{3}|\omega|-1}$, $\eta_- = \eta_2 + \frac{3}{2}\eta_1$, $8\pi\rho_{r0}/3\phi_1 a_1^2 = 1$ and constants have been absorbed into a_1 and ϕ_1.

In these solutions η_1 determines the evolution of the scalar field during radiation domination, and is a physically interesting quantity; η_2 sets the origin of the conformal time coordinate. The evolution of a and ϕ, for $\omega > -3/2$ and $\omega < -3/2$, is shown in figures 3.1 and 3.2, respectively. A value of $\omega = 40000$ is chosen, in agreement with recent solar system observations [47].

For $\omega > -3/2$ ($\omega < -3/2$) we see that the scale factor here undergoes an initial period of rapid (slow) expansion and at late times is attracted towards the solution $a(\eta) \propto \eta$, or $a(t) \propto t^{\frac{1}{2}}$. Similarly, ϕ can be seen to be changing rapidly at early times and slowly at late times. We attribute these two different behaviours, at early and late times, to periods of free scalar–field domination and radiation domination, respectively. In fact, setting $\eta_1 = 0$ in (3.2.4) and (3.2.5), we remove the scalar–dominated period and gain the power–law exact solutions $a(\eta) \propto \eta$ and $\phi =$ constant. These are the "Machian" solutions usually considered in the literature. Allowing η_1 to be nonzero we will have a nonconstant ϕ, and hence G, during radiation domination. If $\rho_{r0} = 0$ is chosen then these solutions become vacuum ones that are driven by the ϕ field. For $k = 0$ these solutions do not have GR counterparts.

We see from (3.2.9), and figure 3.2, that for $\omega < -3/2$ the initial singularity is avoided; for a more detailed discussion of this effect, see [31].

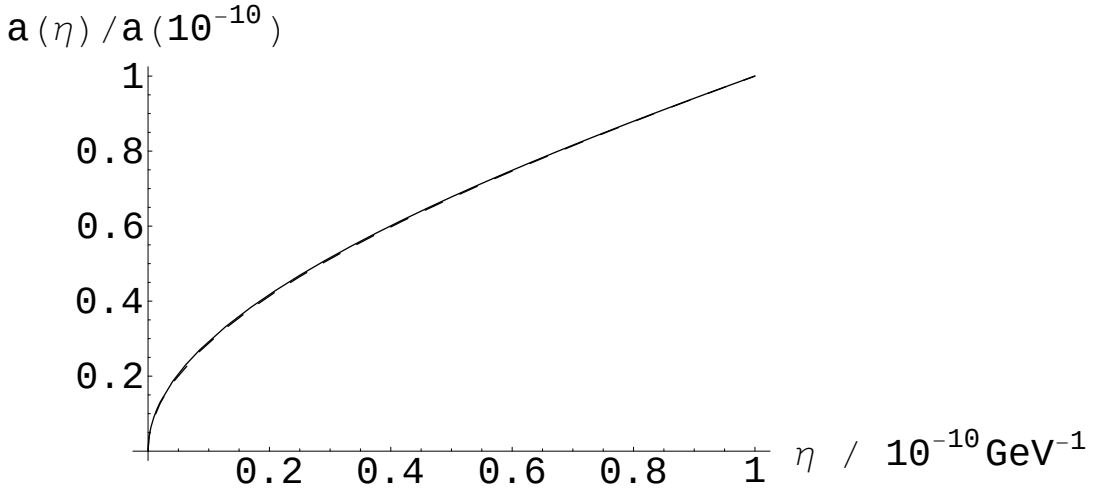

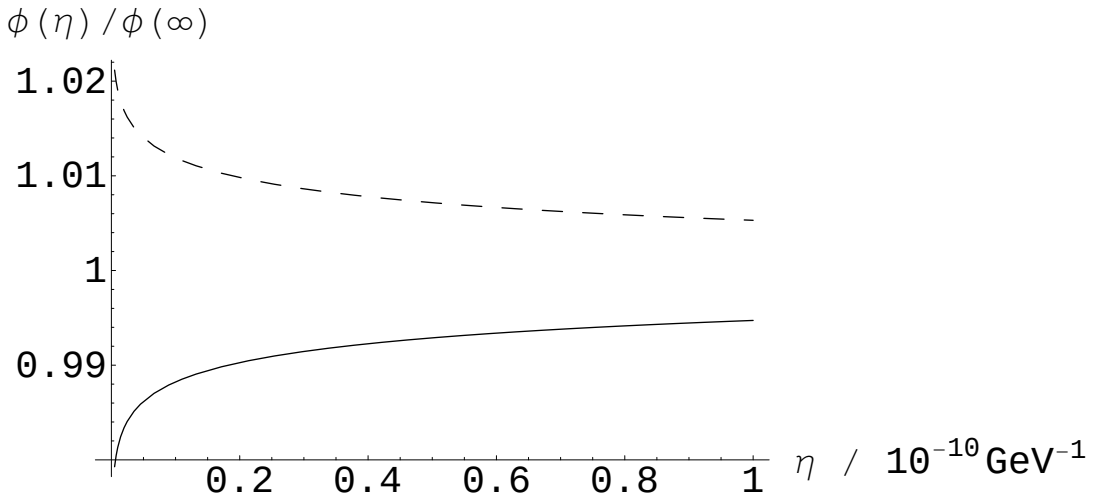

Figure 3.1: *The evolution of a and ϕ as functions of η for $\omega > -\frac{3}{2}$ with $|\eta_1| = 10^{-12} GeV^{-1}$, $\omega = 40000$, and η_2 set so that $a(0) = 0$. The solid line corresponds to $\eta_1 > 0$ and the dashed line to $\eta_1 < 0$.*

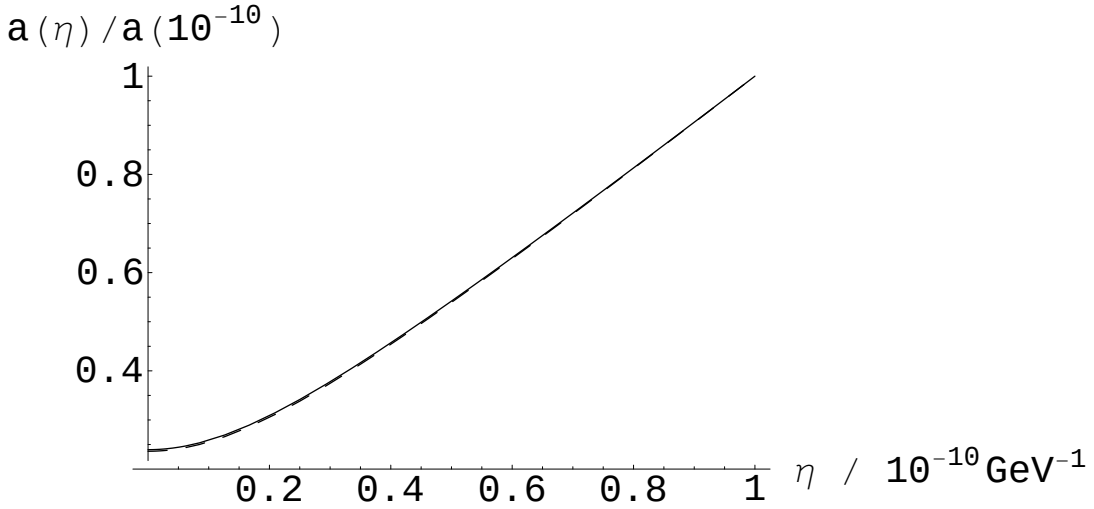

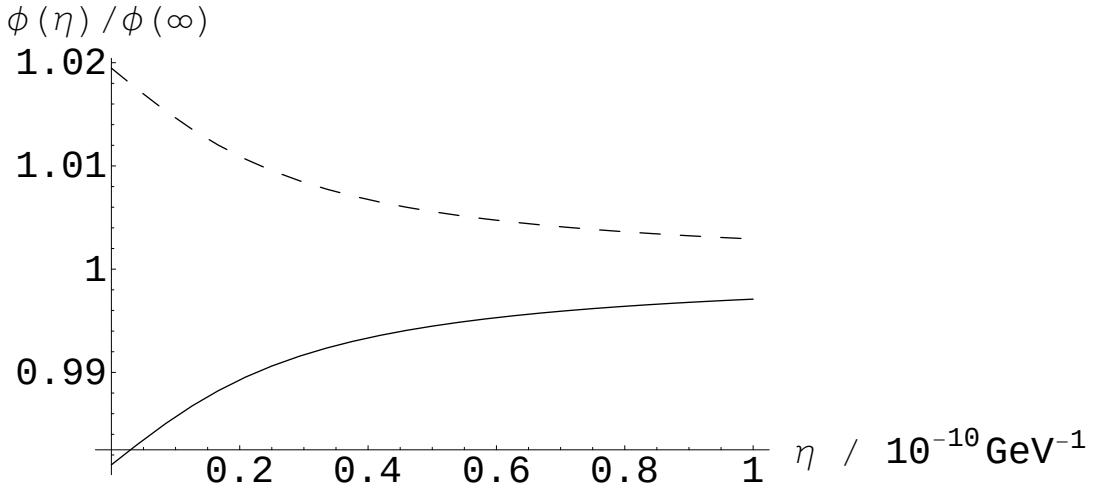

Figure 3.2: *The evolution of a and ϕ as functions of η for $\omega < -\frac{3}{2}$ with $|\eta_1| = 10^{-13} GeV^{-1}$, $\omega = 40000$, and η_2 set so that $a'(0) = 0$. The solid line corresponds to $\eta_1 > 0$ and the dashed line to $\eta_1 < 0$.*

3.2.2 Matter Domination

When considering a matter–dominated universe we could proceed as above and determine a set of general solutions to (3.1.1), (3.1.2) and (3.1.3) that at early times are described by free scalar–field domination and at late times by matter domination (see [97]), but for our purposes this is unnecessary. For a realistic universe we require a period of radiation domination during which primordial nucleosynthesis can occur. If the scalar–field–dominated period of the Universe's history were to impinge upon the usual matter–dominated period then we would effectively lose the radiation–dominated era. For this reason it is sufficient to ignore the free scalar component of the general solution and consider only the Machian component. This is equivalent to imposing the condition $\dot{\phi}a^3 \to 0$ as $a \to 0$. With this additional constraint the solutions to (3.1.1), (3.1.2) and (3.1.3), for $k = 0$ and $p = 0$, are given by [135]

$$a(t) = a_* t^{\frac{2+2\omega}{4+3\omega}} \quad \text{and} \quad \phi(t) = \phi_* t^{\frac{2}{4+3\omega}} \tag{3.2.10}$$

where

$$\frac{8\pi}{3\phi_*}\frac{\rho_{m0}}{a_*^3} = \frac{2(3+2\omega)}{3(4+3\omega)}$$

and a_* and ϕ_* are constants. These solutions can be seen to approach their GR counterparts as $\omega \to \infty$.

3.2.3 Vacuum Energy Domination

Similarly, for a vacuum ($p = -\rho$) dominated period of expansion we can impose the condition $\dot{\phi}a^3 \to 0$ as $a \to 0$ to get the power law exact solutions [135]

$$a(t) = a_\dagger t^{\frac{1}{2}+\omega} \quad \text{and} \quad \phi(t) = \phi_\dagger t^2 \tag{3.2.11}$$

where

$$\frac{8\pi}{3\phi_\dagger}\rho_{\Lambda 0} = \frac{1}{12}(3+2\omega)(5+6\omega)$$

and $a_\dagger$ and $\phi_\dagger$ are constants. Note that this vacuum stress does not produce a de Sitter metric, as in GR.

3.2.4 Vacuum Solutions

In the Brans-Dicke theory it is possible to have spatially flat and positively curved exact vacuum solutions, unlike in the general relativistic cosmologies.

Spatially flat solution

Assuming solutions of the form $\phi \propto t^x$ and $a \propto t^y$ and setting $a(0) = 0$ gives on substitution into (3.1.1), (3.1.2) and (3.1.3) the $k = 0$ Brans-Dicke vacuum solutions [144]

$$a(t) = t^{\frac{1}{3}(1+2(1-\sqrt{3(3+2\omega)})^{-1})} \qquad \text{and} \qquad \phi(t) = \phi_{b0}\left(\frac{t}{t_0}\right)^{-2(1-\sqrt{3(3+2\omega)})^{-1}}. \quad (3.2.12)$$

Closed solution

For the closed region we now follow the method given in [19] to find expressions for $a(\tau)$ and $\phi(\tau)$. We start by introducing conformal time, η, defined by $ad\eta = d\tau$; then equation (3.1.2) becomes

$$\phi_{,\eta\eta} + \frac{2}{a}a_{,\eta}\,\phi_{,\eta} = 0.$$

This integrates directly to yield

$$\phi_{,\eta}\,a^2 = \sqrt{3}A(2\omega+3)^{-1/2} \quad (3.2.13)$$

where A is a constant. We now introduce the variable $y = \phi_p a^2$ to write (3.1.3) as

$$y_{,\eta}^2 = -4ky^2 + \frac{1}{3}\phi_{,\eta}^2\,a^4(2\omega+3). \quad (3.2.14)$$

Equations (3.2.13) and (3.2.14) then give

$$\frac{\phi_{,\eta}}{\phi} = \sqrt{3}Ay^{-1}(2\omega+3)^{-1/2} \qquad \text{and} \qquad y_{,\eta}^2 = -4ky^2 + A^2. \quad (3.2.15)$$

The solutions of equations (3.2.15), when $k > 0$, are given by

$$y(\eta) = \frac{A}{2\sqrt{k}}\sin(2\sqrt{k}(\eta+B)), \quad (3.2.16)$$

and

$$\phi(\eta) = C\tan^{\sqrt{\frac{3}{(2\omega+3)}}}(\sqrt{k}(\eta+B)) \tag{3.2.17}$$

where B and C are arbitrary constants. We now fix the conformal time origin by setting $B = 0$, so that $y = \phi_p a^2$ gives

$$a(\eta) \propto \frac{\sin^{1/2}(2\sqrt{k}\eta)}{\tan^{\sqrt{\frac{3}{4(2\omega+3)}}}(\sqrt{k}\eta)}. \tag{3.2.18}$$

3.3 More General Theories

In order to evaluate more general scalar-tensor theories it is convenient to work in the Einstein frame. In this frame, substituting the FRW line-element into the field equations gives

$$\left(\frac{\dot{\bar{a}}}{\bar{a}}\right)^2 = \frac{8\pi}{3}(\bar{\rho} + \frac{1}{2}\dot{\psi}^2) - \frac{k}{\bar{a}^2}, \tag{3.3.1}$$

$$\frac{\ddot{\bar{a}}}{\bar{a}} = -\frac{4\pi}{3}(\bar{\rho} + 3\bar{p} + 2\dot{\psi}^2) \tag{3.3.2}$$

and

$$\ddot{\psi} + 3\frac{\dot{\bar{a}}}{\bar{a}}\dot{\psi} = -\sqrt{4\pi}\alpha(\bar{\rho} - 3\bar{p}) \tag{3.3.3}$$

where over–dots here denote differentiation with respect to $\bar{t}$ and $\bar{a}(\bar{t}) = e^{-\Gamma}a(t)$ is the scale–factor in the Einstein frame. Defining $N = \ln(\bar{a}/\bar{a}_0)$, Damour and Nordtvedt [76] write (3.3.1), (3.3.2) and (3.3.3) as

$$\frac{2(1-\epsilon)}{(3-4\pi\psi'^2)}\psi'' + (2 - \gamma - \frac{4}{3}\epsilon)\psi' = -(4-3\gamma)\frac{\alpha}{\sqrt{4\pi}}, \tag{3.3.4}$$

where $\epsilon = 3k/8\pi\bar{\rho}\bar{a}^2$, $\bar{p} = (\gamma - 1)\bar{\rho}$ and $'$ denotes differentiation with respect to N.

Now we consider a coupling parameter of the form

$$\Gamma(\psi) = \Gamma(\psi_\infty) + \alpha_0(\psi(\bar{t}) - \psi_\infty) + \frac{1}{2}\beta(\psi(\bar{t}) - \psi_\infty)^2$$

so that

$$\alpha(\bar{t}) = \frac{\alpha_0}{\sqrt{4\pi}} + \frac{\beta}{\sqrt{4\pi}}(\psi(\bar{t}) - \psi_\infty). \tag{3.3.5}$$

This is of the same form as chosen by Santiago, Kalligas and Wagoner [167] and Damour and Pichon [77]. Santiago, Kalligas and Wagoner arrive at this form of α by assuming the evolution of the Universe has been close to the GR solutions throughout the period from primordial nucleosynthesis to the present. They therefore consider themselves justified in performing a Taylor expansion about the asymptotic value of ψ and discarding terms of second order or higher. Damour and Pichon consider Γ to be a potential down which ψ runs. They assume that a particle near a minimum of a potential experiences a generically parabolic form for that potential. This leads them to consider a quadratic form for Γ which gives, on differentiation, α as above. These two lines of reasoning are, of course, equivalent as the parabolic form of a particle near its minimum of potential can be found using a Taylor series. Theories with this form of α belong to the attractor class which approach GR at late times, if we impose the additional condition $\alpha_0 = 0$.

3.3.1 Radiation Domination

For the case of a radiation–dominated flat universe, the general solutions of (3.3.1), (3.3.2) and (3.3.3) with the choice (3.3.5), are, for $\omega > -3/2$:

$$\bar{a}^2(\eta) = \frac{8\pi\bar{\rho}_{r0}}{3}(\eta - \eta_2)(\eta - \eta_2 + |\eta_1|)$$
$$\psi - \psi_1 = \sqrt{\frac{3}{16\pi}}\frac{\eta_1}{|\eta_1|}\ln\left(\frac{\eta - \eta_2}{\eta - \eta_2 + |\eta_1|}\right),$$

and, for $\omega < -3/2$,

$$\bar{a}^2(\eta) = \frac{2\pi\bar{\rho}_{r0}}{3}|\eta_1|^2 + \frac{8\pi\bar{\rho}_{r0}}{3}(\eta - \eta_2)^2$$
$$\psi - \psi_1 = -\sqrt{\frac{3\pi}{16}}\frac{\eta_1}{|\eta_1|} + \sqrt{\frac{3}{4\pi}}\frac{\eta_1}{|\eta_1|}\tan^{-1}\left(\frac{2(\eta - \eta_2)}{|\eta_1|}\right).$$

Here, η_1 determines the evolution of the scalar field, ψ_1 is the value it approaches asymptotically and η_2 sets the origin of the conformal time coordinate defined by $\bar{a}(\eta)d\eta = d\bar{t}$. For $\omega > -3/2$, $\eta_1 \in \mathcal{R}$ such that $\psi \in \mathcal{R}$ whilst for $\omega < -3/2$, $\eta_1 \in \mathcal{I}$ such that $\psi \in \mathcal{I}$ and $\omega \in \mathcal{R}$.

The corresponding solutions in the Jordan frame are

$$\phi(\eta) = \exp\left(-\beta(\psi(\eta) - \psi_\infty)^2\right) \tag{3.3.6}$$

and

$$a^2(\eta) = \frac{\bar{a}^2(\eta)}{\phi}. \tag{3.3.7}$$

They exhibit the same features as their Brans-Dicke counterparts: at early times there is a period of free–scalar–field domination, and at late times they approach $a \propto t^{\frac{1}{2}}$ and ϕ =constant.

3.3.2 Matter Domination

Solutions during the matter–dominated era are difficult to find because the energy–momentum tensor for the matter field is not conserved. However, it is possible to obtain an evolution equation for ψ. Using (3.3.4), we get

$$\frac{2(1-\epsilon)}{(3-4\pi\psi'^2)}\psi'' + (1 - \frac{4}{3}\epsilon)\psi' = -\frac{\beta}{4\pi}(\psi - \psi_\infty). \tag{3.3.8}$$

For a flat universe $\epsilon = 0$ and we can solve (3.3.8) by making the simplifying assumption $4\pi\psi'^2 \ll 3$. This gives the solution

$$\psi(N) - \psi_\infty = Ae^{-\frac{3}{4}(1+\sqrt{1-\frac{2\beta}{3\pi}})N} + Be^{-\frac{3}{4}(1-\sqrt{1-\frac{2\beta}{3\pi}})N} \tag{3.3.9}$$

where A and B are constants of integration.

3.3.3 Vacuum Domination

Similarly, for the case of a vacuum–dominated universe the evolution of ψ can be approximated using (3.3.4) to obtain

$$\psi(N) - \psi_\infty = Ce^{-\frac{3}{2}(1+\sqrt{1-\frac{2\beta}{3\pi}})N} + De^{-\frac{3}{2}(1-\sqrt{1-\frac{2\beta}{3\pi}})N} \tag{3.3.10}$$

where C and D are constants of integration.

CHAPTER 4

Homogeneous and Isotropic Fourth-Order Cosmologies

This chapter is based on the the work of Clifton and Barrow [70].

4.1 Freidmann-Robertson-Walker Cosmologies

In this chapter we will again be concerned with the idealised homogeneous and isotropic space-times described by the FRW metric:

$$ds^2 = -dt^2 + a^2(t)\left(\frac{dr^2}{(1-kr^2)} + r^2 d\theta^2 + r^2 \sin^2\theta d\phi^2\right). \tag{4.1.1}$$

Substituting this metric ansatz into the $\mathcal{L} = R^{1+\delta}$ field equations (2.1.15), and assuming the Universe to be filled with a perfect fluid of pressure p and density ρ, gives the generalised version of the Friedmann equations

$$(1-\delta)R^{1+\delta} + 3\delta(1+\delta)R^{\delta}\left(\frac{\ddot{R}}{R} + 3\frac{\dot{a}}{a}\frac{\dot{R}}{R}\right) - 3\delta(1-\delta^2)R^{\delta}\frac{\dot{R}^2}{R^2} = \frac{\chi}{2}(\rho - 3p) \tag{4.1.2}$$

$$-3\frac{\ddot{a}}{a}(1+\delta)R^{\delta} + \frac{R^{1+\delta}}{2} + 3\delta(1+\delta)\frac{\dot{a}}{a}\frac{\dot{R}}{R}R^{\delta} = \frac{\chi}{2}\rho \tag{4.1.3}$$

where, as usual,

$$R = 6\frac{\ddot{a}}{a} + 6\frac{\dot{a}^2}{a^2} + 6\frac{k}{a^2}. \tag{4.1.4}$$

It can be seen that in the limit $\delta \to 0$ these equations reduce to the standard Friedmann equations of GR. A study of the vacuum solutions to these equations for all k has been made by Schmidt (see the review [171]) and a qualitative study of the perfect-fluid evolution for all k has been made by Carloni et al [58]. Various conclusions are also immediate from the general analysis of $f(R)$ Lagrangians made in reference [36] by specialising them to the case $f = R^{1+\delta}$. In what follows we shall be interested in extracting the physically relevant aspects of the general evolution so that observational bounds can be placed on the allowed values of δ.

Assuming a perfect-fluid equation of state of the form $p = (\gamma - 1)\rho$ gives the usual conservation equation $\rho \propto a^{-3\gamma}$. Substituting this into equations (4.1.2) and (4.1.3), with $k = 0$, gives the power-law exact Friedmann solution for $\gamma \neq 0$

$$a(t) = t^{\frac{2(1+\delta)}{3\gamma}} \tag{4.1.5}$$

where

$$(1 - 2\delta)(2 - 3\delta\gamma - 2\delta^2(1 + 3\gamma)) = 12\pi G(1 - \delta)\gamma^2\rho_c \tag{4.1.6}$$

and ρ_c is the critical density of the universe.

Alternatively, if $\gamma = 0$, there exists the de Sitter solution

$$a(t) = e^{nt}$$

where

$$3(1 - 2\delta)n^2 = 8\pi G(1 - \delta)\rho_c.$$

The critical density (4.1.6) is shown graphically, in figure 4.1, in terms of the density parameter $\Omega_0 = \frac{8\pi G\rho_c}{3H_0^2}$ as a function of δ for pressureless dust ($\gamma = 1$) and black-body radiation ($\gamma = 4/3$). It can be seen from the graph that the density of matter required for a flat universe is dramatically reduced for positive δ, or large negative δ. In order for the critical density to correspond to a positive matter density

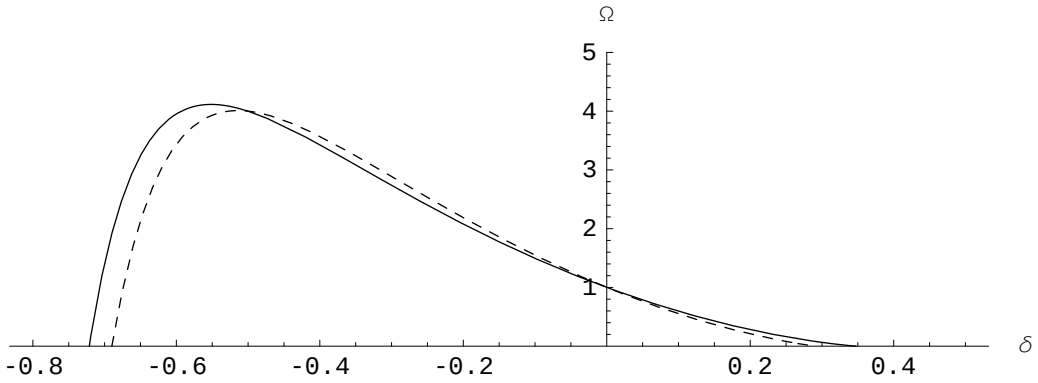

Figure 4.1: *The density parameter, Ω_0, as a function of δ. Solid line corresponds to pressureless dust and dashed line to black-body radiation.*

we require δ to lie in the range

$$-\frac{\sqrt{73+66\omega+9\omega^2}+3\gamma}{4(1+3\gamma)} < \delta < \frac{\sqrt{73+66\omega+9\omega^2}-3\gamma}{4(1+3\gamma)}. \tag{4.1.7}$$

4.2 The Dynamical Systems Approach

The system of field equations (4.1.2) and (4.1.3) have been studied previously using a dynamical systems approach by Carloni, Dunsby, Capozziello and Troisi for general k [58]. We elaborate on their work by studying in detail the spatially flat, $k = 0$, subspace of solutions. This allows us to draw conclusions about the asymptotic solutions of (4.1.2) and (4.1.3) when $k = 0$ and so investigate the stability of the power–law exact solution (4.1.5) and the extent to which it can be considered an attractor solution. By restricting to $k = 0$ we avoid 'instabilities' associated with the curvature which are already present in general relativistic cosmologies.

In performing this analysis we choose to work in the conformal time coordinate

$$d\tau \equiv \sqrt{\frac{8\pi\rho}{3R^\delta}}dt. \tag{4.2.1}$$

Making the definitions

$$x \equiv \frac{R'}{R} \qquad \text{and} \qquad y \equiv \frac{a'}{a},$$

where a prime indicates differentiation with respect to τ, the field equations (4.1.2) and (4.1.3) can be written as the autonomous set of first order equations

$$x' = \frac{2-\delta(3\gamma-2)}{\delta^2(1+\delta)} - \frac{\delta x^2}{2} - \frac{(4-\delta(3\gamma-2))xy}{2\delta} - \frac{2(1-\delta)y^2}{\delta^2} \tag{4.2.2}$$

$$y' = -\frac{1}{\delta} + \frac{1}{2}(2+3\delta)xy + \frac{(2+\delta(3\gamma-2))y^2}{2\delta}. \tag{4.2.3}$$

These coordinate definitions are closely related to those chosen by Holden and Wands [104] for their phase-plane analysis of Brans-Dicke cosmologies and allow us to proceed in a similar fashion.

4.2.1 Locating the Critical Points

The critical points at finite distances in the system of equations (4.2.2) and (4.2.3) are located at

$$x_{1,2} = \pm\frac{4-3\gamma}{\delta\sqrt{(1+\delta)(5-3\gamma)}} \qquad \text{and} \qquad y_{1,2} = \pm\frac{1}{\sqrt{(1+\delta)(5-3\gamma)}} \tag{4.2.4}$$

and at

$$x_{3,4} = \mp\frac{3\sqrt{2\gamma}}{\sqrt{(1+\delta)(2-3\delta\gamma-\delta^2(2+6\gamma))}} \tag{4.2.5}$$

and

$$y_{3,4} = \pm\frac{\sqrt{2(1+\delta)}}{\sqrt{2-3\delta\gamma-\delta^2(2+6\gamma)}}. \tag{4.2.6}$$

The critical points (x_1, y_1) and (x_2, y_2) do not exist for $\gamma = 5/3$.

The exact form of $a(t)$ at these critical points, and the stability of these solutions, can be easily deduced. At the critical point (x_i, y_i) the forms of $a(\tau)$ and $R(\tau)$ are given by

$$a(\tau) = a_0 e^{y_i\tau} \qquad \text{and} \qquad R(\tau) = R_0 e^{x_i\tau}, \tag{4.2.7}$$

where a_0 and R_0 are constants of integration. In terms of τ the perfect-fluid conser-

vation equation can be integrated to give

$$\rho = \rho_0 e^{-3\gamma y_i \tau},$$

where ρ_0 is another positive constant. Substituting into the definition of τ now gives

$$d\tau \propto e^{-\frac{3}{2}\gamma y_i \tau - \frac{\delta}{2} x_i \tau} dt$$

or, integrating,

$$t - t_0 \propto \frac{1}{\frac{3}{2}\gamma y_i + \frac{\delta}{2} x_i} e^{\frac{3}{2}\gamma y_i \tau + \frac{\delta}{2} x_i \tau}. \tag{4.2.8}$$

It can now be seen that if $3\gamma y_i + \delta x_i > 0$ then $t \to \infty$ as $\tau \to \infty$ and $t \to t_0$ as $\tau \to -\infty$. Conversely, if $3\gamma y_i + \delta x_i < 0$ then $t \to t_0$ as $\tau \to \infty$ and $t \to -\infty$ as $\tau \to -\infty$.

In terms of t time the solutions corresponding to the critical points at finite distances can now be written as

$$a(t) \propto (t - t_0)^{\frac{2y_i}{3\gamma y_i + \delta x_i}} \qquad \text{and} \qquad R(t) \propto (t - t_0)^{\frac{2x_i}{3\gamma y_i + \delta x_i}}.$$

The critical points 1 and 2 can now been seen to correspond to $a \propto t^{\frac{1}{2}}$ and the points 3 and 4 correspond to (4.1.5).

In order to analyse the behaviour of the solutions as they approach infinity it is convenient to transform to the polar coordinates

$$x = \bar{r} \cos \phi$$
$$y = \bar{r} \sin \phi.$$

The infinite phase plane can then be compacted into a finite size by introducing the coordinate

$$r = \frac{\bar{r}}{1 + \bar{r}}.$$

The equations (4.2.2) and (4.2.3) then become

$$r' = \frac{-1}{4\delta^2(1+\delta)}\Bigg(4(1-2r)(\delta(1+\delta)\sin\phi - (2-\delta(3\gamma-2))\cos\phi) \\ - r^2((6+8\delta+3\delta^2+\delta^3-12\delta\gamma)\cos\phi + (1+\delta)(2-2\delta-\delta^2-2\delta^3)\cos 3\phi \\ - 2\delta(3-\delta(3\gamma-2)+3\cos 2\phi)\sin\phi)\Bigg) \quad (4.2.9)$$

and

$$\phi' = \frac{-1}{2\delta^2(1+\delta)(1-r)r}\Bigg((2\delta(1+\delta)\cos\phi + 2(2-\delta(3\gamma-2))\sin\phi)(1-2r) \\ - \Big(\delta(1+\delta)\cos\phi(1-3\cos 2\phi) - 4\sin\phi + 4(1-\delta)^2\sin^3\phi \\ + 2\delta(3\gamma-2+\delta(1+\delta)(1+2\delta)\cos^2\phi)\sin\phi\Big)r^2\Bigg). \quad (4.2.10)$$

In the limit $r \to 1$ ($\bar{r} \to \infty$) it can be seen that critical points at infinity satisfy

$$\sin\phi_i(\delta\cos\phi_i + \sin\phi_i)(\delta(1+2\delta)\cos\phi_i + 2(1-\delta)\sin\phi_i) = 0$$

and so are located at

$$\phi_{5,(6)} = 0 \qquad (+\pi) \quad (4.2.11)$$

$$\phi_{7,(8)} = \tan^{-1}(-\delta) \qquad (+\pi) \quad (4.2.12)$$

$$\phi_{9,(10)} = \tan^{-1}\left(-\frac{\delta(1+2\delta)}{2(1-\delta)}\right) \qquad (+\pi). \quad (4.2.13)$$

The form of $a(t)$ can now be calculated for each of these critical points by proceeding

as Holden and Wands [104]. Firstly, as $r \to 1$ equation (4.2.9) approaches

$$\begin{aligned} r' \to \frac{1}{4\delta^2}\Bigg(& \delta(1+2\delta(3\gamma-2))\sin\phi_i - 3\delta\sin 3\phi_i \\ & - (2-\delta(2+\delta))\cos\phi_i + (2-\delta(2+\delta+2\delta^2))\cos 3\phi_i \Bigg) \\ \equiv f(\phi_i) & \end{aligned}$$

which allows the integral

$$r - 1 = f(\phi_i)(\tau - \tau_0)$$

where the constant of integration, τ_0, has been set so that $r \to 1$ as $\tau \to \tau_0$. Now the definition of x allows us to write

$$\frac{R'}{R} = \frac{r}{(1-r)}\cos\phi_i = -\frac{f(\phi_i)(\tau-\tau_0)+1}{f(\phi_i)(\tau-\tau_0)}\cos\phi_i \to -\frac{\cos\phi_i}{f(\phi_i)(\tau-\tau_0)}$$

as $\tau \to \tau_0$. Integrating this it can be seen that

$$R \propto |\tau - \tau_0|^{-\frac{\cos\phi_i}{f(\phi_i)}} \qquad \text{as} \qquad r \to 1.$$

Similarly,

$$a \propto |\tau - \tau_0|^{-\frac{\sin\phi_i}{f(\phi_i)}} \qquad \text{as} \qquad r \to 1.$$

The definition of τ (4.2.1) now gives

$$d\tau \propto |\tau - \tau_0|^{\frac{3\gamma}{2}\frac{\sin\phi_i}{f(\phi_i)} + \frac{\delta}{2}\frac{\cos\phi_i}{f(\phi_i)}} dt$$

which integrates to

$$t - t_0 \propto -\frac{f(\phi_1)}{F(\phi_i)}|\tau - \tau_0|^{-\frac{F(\phi_i)}{f(\phi_i)}} \tag{4.2.14}$$

where

$$F(\phi_i) = \frac{3\gamma\sin\phi_i + \delta\cos\phi_i - 2f(\phi_i)}{2}.$$

The location of critical points at infinity can now be written in terms of t as the power–law solutions

$$R(t) \propto (t-t_0)^{\frac{\cos\phi_i}{F(\phi_i)}} \qquad \text{and} \qquad a(t) \propto (t-t_0)^{\frac{\sin\phi_i}{F(\phi_i)}}. \tag{4.2.15}$$

Direct substitution of the critical points (4.2.11), (4.2.12) and (4.2.13) into (4.2.15) gives

$$a_{5,6}(t) \to \text{constant}$$
$$a_{7,8}(t) \to \sqrt{t - t_0}$$
$$a_{9,10}(t) \to (t - t_0)^{\frac{\delta(1+2\delta)}{(1-\delta)}}$$

as $r \to 1$. Moreover, it can be seen from (4.2.14) that as $r \to 1$ and $\tau \to \tau_0$ so $t \to t_0$ as long as $F(\phi_i)/f(\phi_i) < 0$, as is the case for the stationary points considered here (as long as the value of δ lies within the range given by (4.1.7)).

The exact forms of $a(t)$ at all the critical points are summarised in the table 4.1.

Critical point	**a(t)**
1, 2, 7 and 8	$t^{\frac{1}{2}}$
3 and 4	$t^{\frac{2(1+\delta)}{3\gamma}}$
5 and 6	constant
9 and 10	$t^{\frac{\delta(1+2\delta)}{(1-\delta)}}$

Table 4.1: The form of $a(t)$ at critical points of the phase plane.

4.2.2 Stability of the Critical Points

The stability of the critical points at finite distances can be established by perturbing x and y as

$$x(r) = x_i + u(r) \qquad \text{and} \qquad y(r) = y_i + v(r) \tag{4.2.16}$$

and checking the sign of the eigenvalues, λ_i, of the linearised equations

$$u' = \lambda_i u \qquad \text{and} \qquad v' = \lambda_i v.$$

Substituting (4.2.16) into equations (4.2.2) and (4.2.3) and linearising in u and

v gives

$$u' = -\left(\delta x_i + \frac{(4-\delta(3\gamma-2))}{2\delta}y_i\right)u - \left(\frac{(4-\delta(3\gamma-2))}{2\delta}x_i + 4\frac{(1+\delta)}{\delta^2}y_i\right)v$$
$$v' = \frac{(2+3\delta)}{2}y_0 u + \left(\frac{(2+3\delta)}{2}x_i + \frac{(2+\delta(3\gamma-2))}{\delta}y_0\right)v.$$

The eigenvalues λ_i are therefore the roots of the quadratic equation

$$\lambda_i^2 + B\lambda_i + C = 0$$

where

$$B = -\frac{1}{2}(2+\delta)x_i - \frac{3}{2}(3\gamma-2)y_i$$
$$C = -\frac{\delta}{2}(2+3\delta)x_i^2 - (2+\delta(1+3\delta))x_i y_i + \frac{1}{2\delta}(8-8\delta-6\gamma(1+3\delta)+9\delta\gamma^2)y_i^2.$$

If $B > 0$ and $C > 0$ then both values of λ_i are negative, and we have a stable critical point. If $B < 0$ and $C > 0$ both values of λ_i are positive, and the critical point is unstable to perturbations. $C < 0$ gives a saddle-point.

For points 1 (upper branch) and 2 (lower branch) this gives

$$B = \mp\frac{(4+\delta(3\gamma-1)-3\gamma)}{\delta\sqrt{(1+\delta)(5-3\gamma)}} \qquad \text{and} \qquad C = -\frac{(4+4\delta-3\gamma)}{\delta(1+\delta)}$$

and for points 3 (upper branch) and 4 (lower branch)

$$B = \pm\frac{3(2+2\delta-\gamma(1+2\delta))}{\sqrt{2(1+\delta)(2-3\delta\gamma-2\delta^2(1+3\gamma))}} \qquad \text{and} \qquad C = \frac{(4+4\delta-3\gamma)}{\delta(1+\delta)}.$$

The stability of the critical points at finite distances for a universe filled with pressureless dust, for various different values of δ, are given in table 4.2, and for black-body radiation are given in table 4.3.

Values of $\delta < -\frac{\sqrt{18+38\gamma+9\gamma^2}+3\gamma}{4(1+3\gamma)}$ and $\delta > \frac{\sqrt{18+38\gamma+9\gamma^2}-3\gamma}{4(1+3\gamma)}$ have not been considered here as they lead to negative values of ρ_0 for the solution (4.1.5). (The reader may note the difference here between the range of δ for which point 3 is a stable attractor compared with the analysis of Carloni et. al.).

Critical point	**B**	**C**	$-\frac{\sqrt{73}+3}{16} < \delta < -\frac{1}{4}$	$-\frac{1}{4} < \delta < 0$	$0 < \delta < \frac{\sqrt{73}-3}{16}$
1	$-\frac{(1+2\delta)}{\delta\sqrt{2(1+\delta)}}$	$-\frac{(1+4\delta)}{\delta(1+\delta)}$	Saddle	Stable	Saddle
2	$\frac{(1+2\delta)}{\delta\sqrt{2(1+\delta)}}$	$-\frac{(1+4\delta)}{\delta(1+\delta)}$	Saddle	Unstable	Saddle
3	$\frac{3}{\sqrt{2(1+\delta)(2-3\delta-8\delta^2)}}$	$\frac{(1+4\delta)}{\delta(1+\delta)}$	Stable	Saddle	Stable
4	$-\frac{3}{\sqrt{2(1+\delta)(2-3\delta-8\delta^2)}}$	$\frac{(1+4\delta)}{\delta(1+\delta)}$	Unstable	Saddle	Unstable

Table 4.2: The stability of critical points at finite distances for a universe filled with pressureless dust.

Critical point	**B**	**C**	$-\frac{\sqrt{6}+1}{5} < \delta < \frac{\sqrt{6}-1}{5}$
1	$-\frac{3}{\sqrt{1+\delta}}$	$-\frac{4}{(1+\delta)}$	Saddle
2	$\frac{3}{\sqrt{1+\delta}}$	$-\frac{4}{(1+\delta)}$	Saddle
3	$\frac{(1-\delta)}{\sqrt{(1+\delta)(1-2\delta-5\delta^2)}}$	$\frac{4}{(1+\delta)}$	Stable
4	$-\frac{(1-\delta)}{\sqrt{(1+\delta)(1-2\delta-5\delta^2)}}$	$\frac{4}{(1+\delta)}$	Unstable

Table 4.3: The stability of critical points at finite distances for a universe filled with black-body radiation

Point 3 lies in the $y > 0$ region and so corresponds to the expanding power–law solution (4.1.5). It can be seen from the table above that this solution is stable for certain ranges of δ and a saddle-point for others. In contrast, point 4, the contracting power–law solution (4.1.5), is unstable or a saddle-point. The nature of the stability of these points and the trajectories which are attracted towards them will be explained further in the next subsection.

A similar analysis can be performed for the critical points at infinity. This time only the variable ϕ will be perturbed as

$$\phi(t) = \phi_i + q(t). \tag{4.2.17}$$

The conditions for stability of the critical points are now that $r' > 0$ and the

eigenvalue μ of the linearised equation $q' = \mu q$ satisfies $\mu < 0$ in the limit $r \to 1$. If both of these conditions are satisfied then the point is a stable attractor; if only one is satisfied the point is a saddle; and if neither are satisfied then the point is repulsive.

Substituting (4.2.17) into (4.2.10) and linearising in $q(t)$ gives, in the limit $r \to 1$,

$$q' = \frac{1}{4\delta^2(1-r)}\Big((6(1-\delta)+\delta^2(1+2\delta))\cos\phi_i - 3(2(1-\delta)-\delta^2(1+2\delta))\cos 3\phi_i - 3\delta\sin\phi_i + 9\delta\sin 3\phi\Big)q \equiv \mu q.$$

The sign of r' in the limit $r \to 1$ can be read off from (4.2.9). The stability properties of each of the stationary points at infinity can now be summarised in the table 4.4, where $N_1 = \frac{\sqrt{18+38\gamma+9\gamma^2}+3\gamma}{4(1+3\gamma)}$ and $N_2 = \frac{\sqrt{18+38\gamma+9\gamma^2}-3\gamma}{4(1+3\gamma)}$.

Critical point	$-N_1 < \delta < -\frac{1}{2}$	$-\frac{1}{2} < \delta < 0$	$0 < \delta < \frac{1}{4}$	$\frac{1}{4} < \delta < N_2$
5	Stable	Saddle	Unstable	Unstable
6	Unstable	Saddle	Stable	Stable
7	Unstable	Unstable	Saddle	Stable
8	Stable	Stable	Saddle	Unstable
9	Saddle	Stable	Stable	Saddle
10	Saddle	Unstable	Unstable	Saddle

Table 4.4: The stability of critical points at infinity.

4.2.3 Illustration of the Phase Plane

Some representative illustrations of the phase plane are now presented. Firstly, the compactified phase plane for a universe filled with pressureless dust, $\gamma = 1$, and a value of $\delta = 0.1$ is shown in figure 4.2.

Figure 4.2 is seen to be split into three separate regions labelled I, II and III. The boundaries between these regions are the sub-manifolds $R = 0$. As pointed out by Carloni et. al. the plane $R = 0$ is an invariant sub-manifold of the phase space through which trajectories cannot pass.

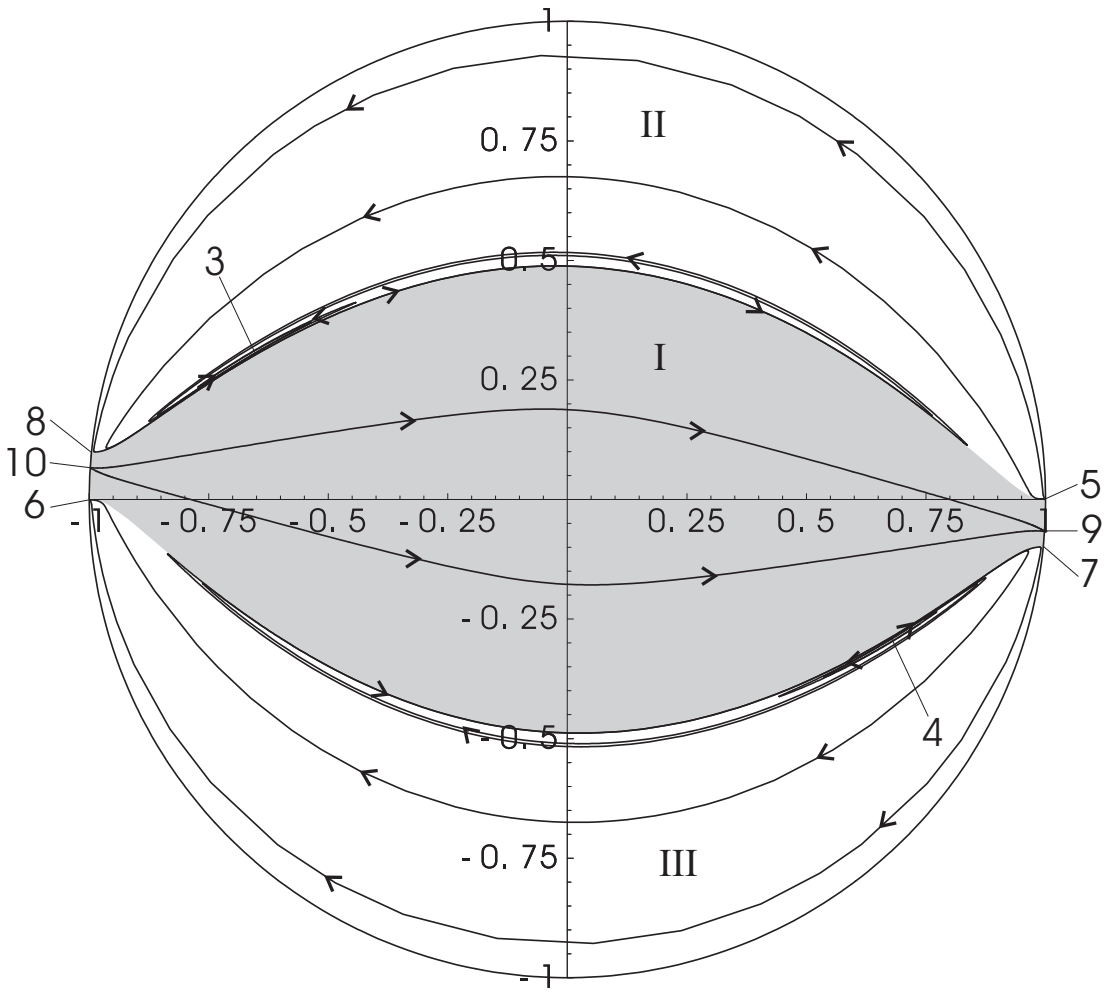

Figure 4.2: *Phase plane of cosmological solutions for* $\gamma = 1$ *and* $\delta = 0.1$. r *is used as the radial coordinate and* ϕ *is measured anti-clockwise from* $y = 0$, $x > 0$.

The equation for R in a FRW universe, (4.1.4), can now be rewritten as

$$R = \frac{16\pi\rho}{\delta R^{\delta}}((1+\delta)y^2 + \delta(1+\delta)xy - 1). \tag{4.2.18}$$

This shows that the boundary $R = 0$ is given in terms of x and y by $(1+\delta)y^2 + \delta(1+\delta)xy - 1 = 0$ and that in region I the sign of R must be opposite to the sign of δ in order to have a positive ρ. Similarly, in regions II and III, R must have the same sign as δ in order to ensure a positive ρ.

It can be seen that regions II and III are symmetric under a rotation of π and a reversal of the direction of the trajectories. As region II is exclusively in the semi–circle $y \geqslant 0$ all trajectories confined to this region correspond to eternally expanding (or expanding and asymptotically static) universes. Similarly, region III is confined to the semi–circle $y \leqslant 0$ and so all trajectories confined to this region correspond to eternally contracting (or contracting and asymptotically static) universes. Region I, however, spans the $y = 0$ plane and so can have trajectories which correspond to universes with both expanding and contracting phases. In fact, it can be seen from figure 4.2 that, for $\delta = 0.1$ all trajectories in region I are initially expanding and eventually contracting.

It can be seen from figure 4.2 that in region I the only stable attractors are, at early times, the expanding point 10 and at late times the contracting point 9. (By 'attractors at early times' we mean the critical points which are approached if the trajectories are followed backwards in time). Both of these points correspond to the solution

$$a \propto t^{\delta\frac{(1+2\delta)}{(1-\delta)}}$$

which describes a slow evolution independent of the matter content of the universe. Notably, region I only has stable attractor points, at both early and late times, which are reached in a finite time as $t \rightarrow$constant. In region II the only stable attractors can be seen to be the static point 5 at some early finite time, t_0, and the expanding matter-driven expansion described by point 3 as $t \rightarrow \infty$. Conversely, in region III the only stable attractors are the contracting point 4 for $t \rightarrow -\infty$ and the static point 6 for $t \rightarrow t_0$.

Figure 4.3 shows the compactified phase plane for a universe containing pres-

sureless dust and having $\delta = -0.1$. Figure 4.3 is split into three separate regions in a similar way to figure 4.2, with the boundary between the regions again corresponding to $R = 0$ and is given in terms of x and y by (4.2.18). Regions II and III again correspond to expanding and contacting solutions, respectively. Region I, still has point 10 as the early-time attractor and point 9 as the late-time attractor, but now has all trajectories initially contracting and eventually expanding. Stable attractors in Region I are still reached in a finite time. Region II now has point 7 as an early-time stable attractor solution and point 1 as a late-time stable attractor solution, corresponding to $a \to t^{\frac{1}{2}}$ as $t \to \infty$. Point 3, which was the stable attractor at late times when $\delta = 0.1$, is now no longer located in Region II and can instead be located in region I where it is now a saddle-point in the phase plane. Interestingly, the value of δ for which point 3 ceases to behave as a stable attractor ($\delta = 0$) is exactly the same value of δ at which the point moves from region II into region I; so as long as point 3 can be located in region I, it is the late-time stable attractor solution and as soon as it moves into region I it becomes a saddle-point. At this same value of δ, point 1 ceases to be a saddle-point and becomes the late-time stable attractor for region II, so that region II always has a stable late-time attractor as $t \to \infty$. Region III behaves in a similar way to the description given for region II above, under a rotation of π and with the directions of the trajectories reversed.

Phase planes diagrams for $\gamma = 1$ with values of δ other than 0.1 and -0.1, but still within the range

$$-\frac{\sqrt{18 + 38\gamma + 9\gamma^2} + 3\gamma}{4(1 + 3\gamma)} < \delta < \frac{\sqrt{18 + 38\gamma + 9\gamma^2} - 3\gamma}{4(1 + 3\gamma)},$$

look qualitatively similar to those above with some of the attractor properties of the critical points being exchanged as they pass each other. In particular, for $\delta < -\frac{1}{4}$ point 3 returns to region II and once again becomes the stable late-time attractor for trajectories in that region. The points that are the stable attractors for any particular value of δ can be read off from the tables in the previous section.

Universes filled with perfect fluid black-body radiation also retain qualitatively similar phase-plane diagrams to the ones above; with the notable difference that the point 3 is always located in region II and is always the late-time stable attractor of that region. This can be seen directly from the Ricci scalar for the solution (4.1.5)

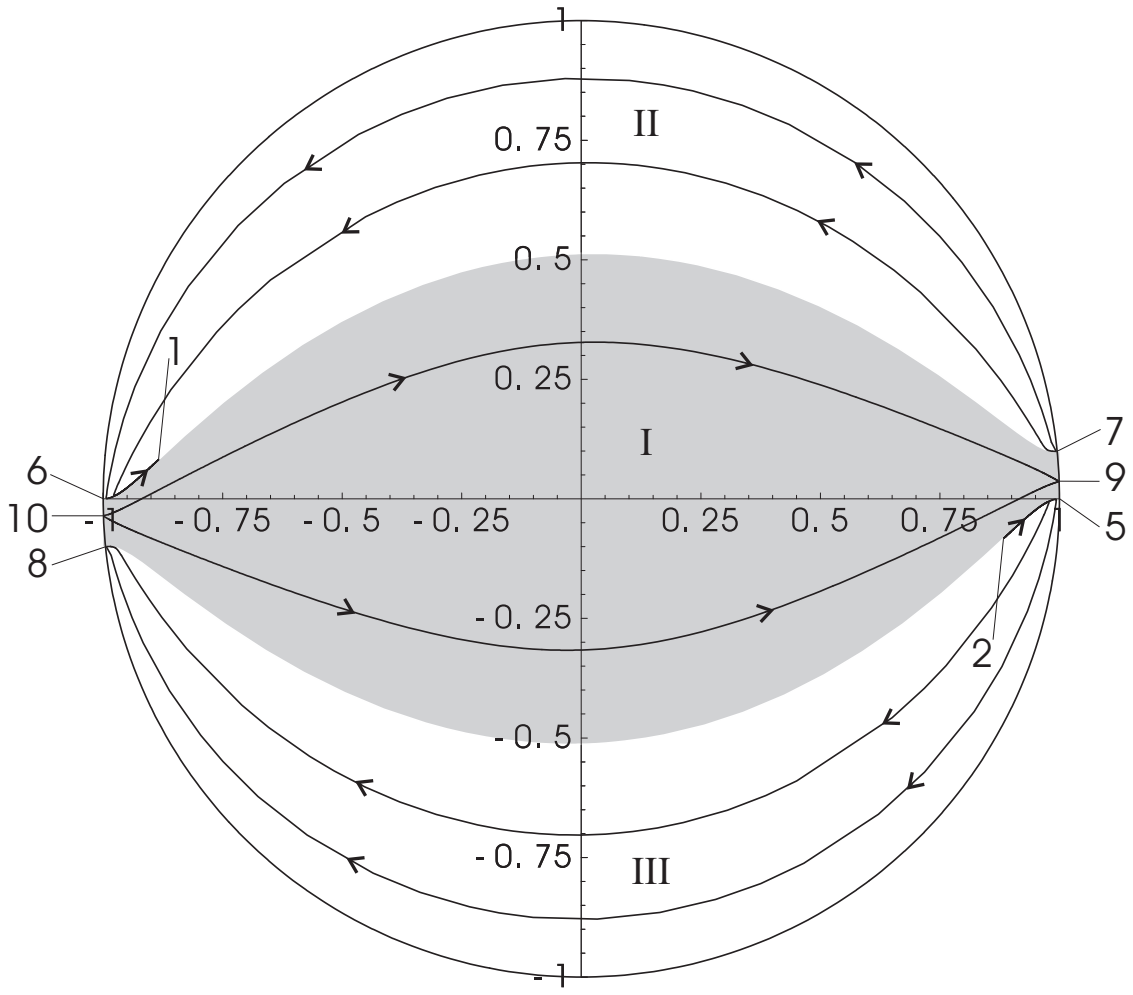

Figure 4.3: *Phase plane of cosmological solutions for* $\gamma = 1$ *and* $\delta = -0.1$. r *is used as the radial coordinate and* ϕ *is measured anti-clockwise from* $y = 0$, $x > 0$.

which is given by

$$R = \frac{3\delta(1+\delta)}{t^2}$$

and can be seen to have the same sign as δ, for $\delta > -1$, and so is always found in region II.

For a spatially-flat, expanding FRW universe containing black-body radiation we therefore have that (4.1.5) is the generic attractor as $t \to \infty$. Similarly, for a spatially-flat, expanding, matter-dominated FRW universe (4.1.5) is the attractor solution as $t \to \infty$; except when $-\frac{1}{4} < \delta < 0$, in which case it is point 1 ($a \propto t^{\frac{1}{2}}$).

If we require a stable period of matter domination, during which $a(t) \sim t^{\frac{2}{3}}$, we therefore have the theoretical constraint $\delta > 0$ (or $\delta < -\frac{1}{4}$). Such a period is necessary for structure to form through gravitational collapse in the post-recombination era of the Universe's expansion.

The effect of a non–zero curvature, $k \neq 0$, on the cosmological dynamics is similar to the general relativistic case. The role of negative curvature ($k = -1$) can be deduced by noting that its effect is similar to that of a fluid with $\gamma = 2/3$. The solution (4.1.5) is unstable to any perturbation away from flatness and will diverge away from $k = 0$ as $t \to \infty$. This is usually referred to as the 'flatness problem' and can be seen to exist in this theory from the analysis of Carloni et. al. [58].

CHAPTER 5

Other Homogeneous Fourth-Order Cosmologies

We will consider in this chapter the conditions required for gravity theories that are derived from Lagrangians that are functions of the scalar curvature and Ricci and Riemann curvature invariants to possess solutions which are homogeneous space-times other than the standard FRW solutions. We will firstly consider space-times of the Gödel [92, 148, 41], Einstein static [27], and de Sitter [102] types. The Gödel solution admits a G_5 group of motions, the Einstein static solution has a G_7 and the de Sitter solution has the maximal G_{10}. In the Gödel case we determine the conditions for the existence or non-existence of closed time-like curves. These three space times share the common property that the three curvature invariants $X = R$, $Y = R^{ab}R_{ab}$ and $Z = R^{abcd}R_{abcd}$ are constant for each of them. This gives the fourth-order field equations a more simple form, allowing solutions to be found more readily.

We will also consider the vacuum Kasner solutions [111] and their fluid-filled counterparts that form type I of the Bianchi classification of three-dimensional homogeneous spaces. These universes have a G_3 group of motions acting transitively on a three dimensional subspace and are geometrically special. In vacuum (or perfect-fluid) cases they are defined by just one (or two) free constant(s) compared to the four (eight) that specify the most general spatially homogeneous vacuum (or per-

fect fluid) solutions. However, they have proved to provide an excellent dynamical description of the evolution of the most general models over finite time intervals. In GR the chaotic vacuum Mixmaster universe of Bianchi Type IX undergoes a infinite sequence of chaotic space-time oscillations on approach to its initial or final singularities which is well approximated by a sequence of different Kasner epochs which form a Poincaré return mapping for the chaotic dynamical system [43, 126, 8, 9, 67, 159].

This chapter is based on the work of Clifton and Barrow [71], [72] and Barrow and Clifton [23].

5.1 Gödel, Einstein and de-Sitter Universes

These three homogeneous space-times, and the investigations of their stability, have played a central role in our understanding of the dynamics of GR and in the possible astrophysical consequences of general relativistic cosmologies. Higher-order modifications of GR are of importance in assessing the corrections that might be introduced in high-curvature environments and can also be of use in explaining the late-time acceleration of the Universe. Furthermore, investigations of these theories allows for an evaluation of the special nature of GR itself. Here we study the conditions under which the Gödel, Einstein static, and de Sitter universes exist in a wide class of non-linear gravity theories.

Considerable simplification of the fourth-order field equations (2.1.12) occurs if the three curvature scalars X, Y and Z are constant. In this case the fourth-order field equations, (2.1.12), reduce to

$$P^{ab} = -\frac{1}{2}fg^{ab}+R^{ab}(f_X-2Rf_Z)-2R^{acdb}R_{cd}(f_Y+4f_Z)+\frac{1}{2}g^{ab}(X^2-4Y+Z)f_Z \quad (5.1.1)$$

where use has been made of the identities [79]

$$\begin{aligned} R^{abcd}{}_{;bc} &= -\Box R^{ad} + R^{ac}{}_{;}{}^{d}{}_{c} \\ R^{ac}{}_{;}{}^{d}{}_{c} &= \frac{1}{2}R_{;}{}^{ad} + R^{abed}R_{be} + R^{a}{}_{c}R^{dc} \\ R^{ab}{}_{;ab} &= \frac{1}{2}\Box R \end{aligned}$$

and

$$2R^a{}_{cde}R^{bcde} + 2g^{ab}Y + 2RR^{ab} = \frac{1}{2}g^{ab}Z - 4R^{acdb}R_{cd} + 4R^a{}_cR^{bc} + \frac{1}{2}g^{ab}R^2.$$

Equation (5.1.1) is only of second order and is therefore a significant simplification of the original system of equations. We will investigate the Gödel, Einstein static and de Sitter universes solutions of these field equations.

5.1.1 Gödel Universes

The Gödel universe [92, 148, 41] is a rotating homogeneous space-time given by the line-element

$$\begin{aligned} ds^2 &= -(dt + C(r)d\psi)^2 + D^2(r)d\psi^2 + dr^2 + dz^2 \\ &= -dt^2 - 2C(r)dtd\psi + G(r)d\psi^2 + dr^2 + dz^2 \end{aligned} \tag{5.1.2}$$

where

$$\begin{aligned} C(r) &= \frac{4\Omega}{m^2}\sinh^2\left(\frac{mr}{2}\right) \\ D(r) &= \frac{1}{m}\sinh(mr) \\ G(r) &= D^2(r) - C^2(r) \\ &= \frac{4}{m^2}\sinh^2\left(\frac{mr}{2}\right)\left[1 + \left(1 - \frac{4\Omega^2}{m^2}\right)\sinh^2\left(\frac{mr}{2}\right)\right] \end{aligned}$$

and m and Ω are constants, and Ω controls the rate of rotation. The existence of Gödel universes in one particular $f(X, Y)$ theory has been previously studied by Accioly [1] where a solution was found in vacuum. We extend this analysis to the more general class of theories above and to universes filled with matter fields.

The Gödel universe is of particular theoretical interest as it allows the possibility of closed time-like curves, and hence time-travel [41, 42]. The condition required to avoid the existence of closed time-like curves is [158, 26]

$$G(r) > 0 \qquad \text{for} \qquad r > 0$$

or

$$m^2 \geqslant 4\Omega^2. \tag{5.1.3}$$

By investigating the existence of Gödel universes in this general class of gravity theories we will also be able to determine those theories in which the condition (5.1.3) is satisfied. Consequently, we will be able to determine those theories in which time travel is a theoretical possibility.

It is convenient to work in the non-holonomic basis defined by

$$\begin{aligned} e^{(0)}{}_0 &= e^{(2)}{}_2 = e^{(3)}{}_3 = 1 \\ e^{(1)}{}_1 &= D(r) \\ e^{(0)}{}_1 &= C(r). \end{aligned}$$

The Gödel line-element (5.1.2) then becomes

$$ds^2 = -(\theta^{(0)})^2 + (\theta^{(1)})^2 + (\theta^{(2)})^2 + (\theta^{(3)})^2$$

where the one-forms $\theta^{(A)}$ are given by $\theta^{(A)} = e^{(A)}{}_a dx^a$ (capital Latin letters denote tetrad indices and lower case Latin letters denote space-time indices). The inverses of $e^{(A)}{}_a$ can be calculated from the relations $e^{(A)}{}_a e^a_{(B)} = \delta^{(A)}{}_{(B)}$ and the non-zero elements of the Riemann tensor in this basis are then given by

$$\begin{aligned} R_{(0)(1)(0)(1)} &= R_{(0)(2)(0)(2)} = \Omega^2 \\ R_{(1)(2)(1)(2)} &= 3\Omega^2 - m^2. \end{aligned}$$

The perfect-fluid energy-momentum tensor is defined in the usual way with respect to the comoving 4-velocity $U^a = (-1, 0, 0, 0)$ and its covariant counterpart $U_a = (1, 0, C(r), 0)$ such that its non-zero components in the non-holonomic basis are given by

$$T_{(0)(0)} = \rho \qquad \text{and} \qquad T_{(1)(1)} = T_{(2)(2)} = T_{(3)(3)} = p.$$

The field equations, (2.1.13), for this space-time can then be manipulated into

the form

$$\Lambda - \frac{\chi}{2}p = \frac{1}{2}f \tag{5.1.4}$$

$$0 = (2\Omega^2 - m^2)(f_X - 4[\Omega^2 - m^2]f_Z) + 2(f_Y + 4f_Z)(8\Omega^4 - 5\Omega^2 m^2 + m^4) \tag{5.1.5}$$

$$\frac{\chi}{2}(\rho + p) = 2\Omega^2(f_X - 4[\Omega^2 - m^2]f_Z) + 4(f_Y + 4f_Z)\Omega^2(2\Omega^2 - m^2). \tag{5.1.6}$$

Solving the field equations has now been reduced to solving these three algebraic relations for some specified $f(X, Y, Z)$.

1 $\boldsymbol{f = f(X)}$

For $\rho + p \neq 0$ we see from (5.1.6) that $f_X \neq 0$. From equation (5.1.5) it can then be seen that $m^2 = 2\Omega^2$, as in general relativity. Therefore for any theory of the type $f = f(X)$ the inequality (5.1.3) is not satisfied and closed time-like curves exist, when $\rho + p \neq 0$.

It now remains to investigate the case $\rho + p = 0$. It can immediately be seen from (5.1.6) that we must have $f_X = 0$ in order for a solution to exist. This sets the relation between m and Ω and automatically satisfies equation (5.1.5). The required value of Λ can then be read off from equation (5.1.4). The condition $f_X = 0$ will now be investigated for a variety of specific theories.

1a $\boldsymbol{f = f(X) = X + \alpha X^2}$

Theories of this kind have been much studied [36, 113] as they have a number of interesting properties, not least of which is that they display divergences which are normalisable at the one loop level [181].

In these theories, the condition $f_X = 0$ is equivalent to

$$m^2 = \Omega^2 + \frac{1}{4\alpha}.$$

The condition under which this theory then satisfies the inequality (5.1.3), and hence does not admit closed time-like curves, is $\Omega^2 \leqslant (12\alpha)^{-1}$. Therefore, for any given theory of this kind, defined only by a choice of the constant α, there is a range of values of Ω for which closed time-like curves do not exist, when $\alpha > 0$ and $\rho + p = 0$.

However, when $\alpha < 0$ this condition is never satisfied and closed time-like curves exist for all values of Ω.

1b $f = f(X) = X + \frac{\alpha^2}{X}$

Theories of this type have generated considerable interest as they introduce cosmological effects at late times, when R is small, which may be able to mimic the effects of dark energy on the Hubble flow [59, 140, 139]. The square in the factor α^2 is introduced here as these theories require a positive value for this coefficient in order for the field equations to have a solution.

When $f_X = 0$ we have the two possible relations

$$m^2 = \Omega^2 \pm \frac{\alpha}{2}$$

where α is the positive real root of α^2. The upper branch of this solution then allows the condition (5.1.3) to be satisfied if $6\Omega^2 \leqslant \alpha$; or, for the lower branch, if $6\Omega^2 \leqslant -\alpha$. For any particular value of $\alpha > 0$, the upper branch always admits a range of Ω for which closed time-like curves do not exist. For the lower branch, however, the inequality (5.1.3) is never satisfied and closed time-like curves are permitted for any value of Ω.

1c $f = f(X) = |X|^{1+\delta}$

This scale-invariant class of theories is of interest as its particularly simple form allows a number of physically relevant exact solutions to be found [75, 23, 50, 58]. In order for solutions of the Gödel type to exist in these theories we must impose upon δ the constraint $\delta \geqslant 0$.

The condition $f_X = 0$ now gives

$$m^2 = \Omega^2.$$

Evidently, the condition (5.1.3) is never satisfied in this case: Gödel solutions always exist and closed time-like curves are permitted for any value of Ω.

2 $f = f(X, Y, Z)$

In this general case, equations (5.1.5) and (5.1.6) can be manipulated into the form

$$f_X - 4(\Omega^2 - m^2)f_Z = \frac{(8\Omega^4 - 5\Omega^2 m^2 + m^4)}{4\Omega^2(4\Omega^2 - m^2)}\chi(\rho + p) \tag{5.1.7}$$

$$f_Y + 4f_Z = -\frac{(2\Omega^2 - m^2)}{8\Omega^2(4\Omega^2 - m^2)}\chi(\rho + p) \tag{5.1.8}$$

when $m^2 \neq 4\Omega^2$. The special case $m^2 = 4\Omega^2$ gives

$$\rho + p = 0 \tag{5.1.9}$$

$$f_X = 4\Omega^2(f_Y + f_Z). \tag{5.1.10}$$

First we consider $\rho + p > 0$. It is clear that $m^2 = 4\Omega^2$ is not a solution in this case. Equations (5.1.7) and (5.1.8) show that in order to satisfy the inequality (5.1.3), and avoid the existence of closed time-like curves, the following two conditions must be satisfied simultaneously

$$f_X + 4(m^2 - \Omega^2)f_Z < 0 \tag{5.1.11}$$

$$f_Y + 4f_Z < 0. \tag{5.1.12}$$

For $\rho + p < 0$ the inequalities must be reversed in these two equations. It is now clear that if it is possible to construct a theory which has a solution of the Gödel type without closed time-like curves for a non-zero $\rho + p$ of a given sign, then this theory cannot ensure the non-existence of closed time-like curves for the opposite sign of $\rho + p$.

It remains to investigate the case $\rho + p = 0$. In order to have a solution in this case we require that the two equations

$$f_X - 4(\Omega^2 - m^2)f_Z = 0 \tag{5.1.13}$$

$$f_Y + 4f_Z = 0 \tag{5.1.14}$$

are simultaneously satisfied, for $m^2 \neq 4\Omega^2$, or

$$f_X = 4\Omega^2(f_Y + f_Z) \tag{5.1.15}$$

for $m^2 = 4\Omega^2$. Any theory which satisfies (5.1.15), therefore, does not allow the existence of closed time-like curves when $\rho + p = 0$.

We now illustrate these considerations by example.

2a $\quad f = X + \alpha X^2 + \beta Y + \gamma Z$

Using the identity [79]

$$\frac{\delta}{\delta g_{ab}}\left(\sqrt{g}(X^2 - 4Y + Z)\right) = \text{pure divergence}$$

it is possible to rewrite f as $f = X + \hat{\alpha}X^2 + \hat{\beta}Y$ where $\hat{\alpha} = \alpha - \gamma$ and $\hat{\beta} = \beta + 4\gamma$. This is the theory considered by Accioly [1].

For the case $\rho + p > 0$, the inequalities (5.1.11) and (5.1.12) then become

$$\hat{\beta} < 0 \qquad \text{and} \qquad \hat{\alpha} > \frac{1}{2|R|}. \tag{5.1.16}$$

The first of these inequalities can be satisfied trivially. The second can be only be satisfied for all Ω if $|R|$ has some non-zero minimum value. From the field equations (5.1.5) and (5.1.6) we can obtain

$$(2\Omega^2 - m^2)(1 + 4\hat{\alpha}[\Omega^2 - m^2]) = -2\hat{\beta}(8\Omega^4 - 5\Omega^2 m^2 + m^4)$$

which gives two solutions for m as a function of Ω, $\hat{\alpha}$ and $\hat{\beta}$. Substituting either of these values of m into $R = 2(\Omega^2 - m^2)$ then gives that $R \to 0$ as $\Omega^2 \to \frac{1}{8|\hat{\beta}|}$. It can now be seen that the second equality in (5.1.16) cannot be satisfied for all Ω if $\hat{\alpha}$ is finite. It is, therefore, not possible to construct a theory of this type which excludes the possibility of closed time-like curves for all Ω, when $\rho + p \neq 0$.

For $\rho + p < 0$ the inequalities in (5.1.16) must be reversed. In this case $\hat{\beta} > 0$ and $\hat{\alpha} > 0$ allows a range of Ω in which closed time-like curves are not permitted and $\hat{\beta} > 0$ and $\hat{\alpha} < 0$ does not allow closed time-like curves for any values of Ω.

The case $\rho + p = 0$ was studied by Accioly [1], who found that equation (5.1.15) is satisfied if

$$4\Omega^2 = m^2 = \frac{1}{(3\hat{\alpha} + \hat{\beta})}.$$

Hence closed time-like curves do not exist in Gödel universes for these theories, when

$\rho + p = 0$.

2b $f = \alpha X + \beta Y$

This class of theories is introduced as an example which excludes the possibility of closed time-like curves for $\rho + p > 0$. The inequalities (5.1.11) and (5.1.12) in this case are

$$\alpha < 0 \qquad \text{and} \qquad \beta < 0,$$

which can be trivially satisfied. For $\rho + p = 0$ the only non-trivial solution is given by $m^2 = 4\Omega^2$, the value of Ω then being given in terms of α and β by (5.1.15).

This example shows explicitly that it is possible to construct a theory in which closed time-like curves do not occur in Gödel universes when $\rho + p \geqslant 0$ (though we do not consider it as physically viable as α is required to have the 'wrong' sign [36, 165]).

Table 5.1 summarises the results found in this section.

5.1.2 Einstein Static Universes

The Einstein static universe is a homogeneous and isotropic space-time with line-element

$$ds^2 = -dt^2 + \frac{dr^2}{(1 - kr^2)} + r^2(d\theta^2 + \sin^2\theta d\phi^2).$$

Here, k parametrizes the curvature of the space-like slices orthogonal to t and the scale-factor has been rescaled to 1. For a universe containing pressureless dust the field equations (2.1.13) can now be written as

$$\chi\rho = 4kf_X + 16k^2(f_Y + f_Z) \tag{5.1.17}$$

$$\Lambda = \frac{1}{2}f - 2kf_X - 8k^2(f_Y + f_Z). \tag{5.1.18}$$

It can now be seen immediately that solutions exist for an Einstein static universe for any $f(X, Y, Z)$ that is differentiable in all its arguments. The corresponding values of ρ and Λ are simply read off from equations (5.1.17) and (5.1.18). It remains to be studied under what circumstances these solutions are stable. The investigation by Barrow, Ellis, Maartens, and Tsagas [27] shows that this is an issue that depends

$f(X,Y,Z)$	Additional conditions	Closed time-like curves exist when		
		$\rho+p>0$	$\rho+p<0$	$\rho+p=0$
$X+\alpha X^2$	$\alpha>0$	✓	✓	✓/×
	$\alpha<0$	✓	✓	✓
$X+\frac{\alpha^2}{X}$	+ve branch	✓	✓	✓/×
	−ve branch	✓	✓	✓
$\lvert X\rvert^{1+\delta}$	$\delta>0$	✓	✓	✓
$X+\alpha X^2+\beta Y+\gamma Z$	$\alpha-\gamma>0,\ \beta+4\gamma<0$	✓/×	✓	×
	$\alpha-\gamma<0,\ \beta+4\gamma<0$	✓	✓	×
	$\alpha-\gamma>0,\ \beta+4\gamma>0$	✓	✓/×	×
	$\alpha-\gamma<0,\ \beta+4\gamma>0$	✓	×	×
$\alpha X+\beta Y$	$\alpha>0,\ \beta<0$	✓	✓	×
	$\alpha>0,\ \beta>0$	✓	×	×
	$\alpha<0,\ \beta<0$	×	✓	×
	$\alpha<0,\ \beta>0$	✓	✓	×

Table 5.1: A summary of the conditions under which closed time-like curves can exist in Gödel universes, for various different gravitational theories, defined by $f(X,Y,Z)$: ✓ denotes their existence for all values of Ω and × denotes that they are not allowed for any value of Ω. The symbol ✓/× means that closed time-like curves are allowed to exist for some restricted range of Ω only; the ranges are given in the main text.

upon the material content and the equation of state of matter in a delicate fashion. In GR, there is first-order stability against density perturbations when the sound speed exceeds a critical value ($1/\sqrt{5}$ of the speed of light) because the Jeans length exceeds the size of the universe [91, 27]. However, there is instability against homogeneous gravitational-wave modes of Bianchi IX type [27]. In general, we expect a universe with compact space sections and Killing vectors to display linearisation instability [40].

5.1.3 de Sitter Universes

The line element for the maximally symmetric de Sitter vacuum universe can be written as

$$ds^2 = -dt^2 + e^{2\sqrt{\frac{\Lambda}{3}}t}(dr^2 + r^2(d\theta^2 + \sin^2\theta d\phi^2))$$

where Λ is the cosmological constant in GR. For de Sitter space-time all components of the Riemann and Ricci tensors can be written in terms of the Ricci scalar using the equations

$$R_{abcd} = -\frac{1}{12}R(g_{ad}g_{bc} - g_{ac}g_{bd})$$
$$R_{ab} = \frac{1}{4}Rg_{ab}$$

where the Ricci scalar is $R = 4\Lambda$. The field equations (2.1.13) can now be reduced to the single equation

$$\frac{1}{2}f - \Lambda = \Lambda f_X + 2\Lambda^2 f_Y + \frac{4}{3}\Lambda^2 f_Z. \tag{5.1.19}$$

This equation must be satisfied by f if the de Sitter universe is to be a solution in any particular gravitational theory. This problem reduces to that studied by Barrow and Ottewill [36] in the case $f = f(X)$. This result establishes the situations where inflation of de Sitter sort can arise from higher-order corrections to the gravitational Lagrangian. In the case where $f = f(X)$ alone it is appreciated that the resulting theory is conformally equivalent to general relativity plus a scalar field [25, 122] with an asymmetric exponential potential and so either de Sitter or power-law inflation is possible. Our results establish when de Sitter inflation is possible in situations where the other invariants, Y and Z contribute to the Lagrangian, and the conformal equivalence with GR is broken. The stability of the de Sitter solutions in these theories will be studied elsewhere.

5.2 Anisotropic Cosmologies

The way in which the Kasner metric has played a central role in the elucidation of the existence and structure of anisotropic cosmological models and their singularities

in GR makes it the obvious starting point for an extension of that understanding to cosmological solutions of higher-order gravity theories. We will determine the conditions for the existence of Kasner-like solutions and find their exact forms. In some cases these solutions are required to be isotropic and correspond to exact FRW vacuum solutions with zero spatial curvature. By studying gravity theories whose Lagrangians are derived from arbitrary powers of the curvature invariants we are able to find simple exact solutions. Past studies have usually focussed on the addition of higher-order curvature terms to the Einstein-Hilbert Lagrangian. This results in enormous algebraic complexity and exact solutions cannot be found. The results presented here provide a tractable route into understanding the behaviours of anisotropic cosmological models in situations where the higher-order curvature corrections are expected to dominate. The solutions we present are vacuum solutions but we provide a simple analysis which determines when the introduction of perfect fluids with non-comoving velocities has a negligible effect on the cosmological evolution at early times.

5.2.1 Field Equations

We will be looking for spatially homogeneous, vacuum solutions of Bianchi type I, described by the line–element

$$ds^2 = -dt^2 + \sum_{i=1}^{3} t^{2p_i} dx_i^2 \tag{5.2.1}$$

where p_1, p_2 and p_3 are constants to be determined. For the special case $p_1 = p_2 = p_3$ these solutions correspond to spatially flat FRW metrics, which will be found to exist for various higher-order theories both in vacuum (where none exist in GR) and in the presence of a perfect fluid.

We can determine the number of independently arbitrary functions of three space variables that will characterise the *general* vacuum solution of the field equations on a Cauchy surface of constant time in these higher-order theories. The field equations are in general fourth order in time; so if we choose a synchronous reference system then we need 6 functions each for the symmetric 3×3 tensors $g_{\alpha\beta}$, $\dot{g}_{\alpha\beta}$, $\dddot{g}_{\alpha\beta}$ and $\ddddot{g}_{\alpha\beta}$. This gives 24 functions, but they may be reduced to 20 by using the 4 constraint

equations, and finally again to 16 by using the 4 coordinate covariances. If a perfect fluid were included as a matter source the final number would rise to 20 due to the inclusion of the density and 3 non-comoving velocity components in the initial data count. We note that in GR the general vacuum solution is prescribed by 3 arbitrary functions of 3 space variables, and that in GR the Kasner vacuum solution is prescribed by one free constant, as the three p_i satisfy two algebraic constraints.

5.2.2 Exact Solutions

For a realistic theory we should expect the dominant term of the analytic function $f(X, Y, Z)$ to be of the Einstein-Hilbert form in the Newtonian limit. However, there is no reason to expect such a term to dominate in the high curvature limit. In fact, this is the limit in which quantum corrections should become dominant. We therefore allow the dominant term in a power series expansion of $f(X, Y, Z)$ to be of the form R^n, $(R_{ab}R^{ab})^n$ or $(R_{abcd}R^{abcd})^n$ on approach to the singularity, where n is a constant. These three different cases will be investigated separately below.

$f = R^n$

Substituting $f = f(X) = R^n$ into the fourth-order field equations (2.1.12) together with the line-element (5.2.1) gives the two independent algebraic constraints,

$$(2n^2 - 4n + 3)P + (n - 2)Q - 3(n - 1)(2n - 1) = 0$$

and

$$2(n^2 - 1)P + (n - 2)(P^2 - Q) - 3(n - 1)^2(2n - 1) = 0,$$

where we have defined

$$P \equiv \sum_i p_i \qquad \text{and} \qquad Q \equiv \sum_i p_i^2. \tag{5.2.2}$$

The constraint equations have two classes of solution. The first is given by

$$P = \frac{3(n - 1)(2n - 1)}{(2 - n)}$$
$$Q = \frac{P^2}{3}$$

which is only solved by the isotropic solution $p_1 = p_2 = p_3 = P/3$. This is the zero-curvature isotropic vacuum universe found by Bleyer and Schmidt [171, 50]. It can be seen that these isotropic cosmologies are valid for all $n \neq 2$ and correspond to expanding universes for $n < 1/2$ or $1 < n < 2$ and to collapsing universes for $1/2 < n < 1$ or $2 < n$.

The second class of solutions to (5.2.2) is given by

$$\begin{aligned} P &= 2n - 1 \\ Q &= (2n-3)(1-2n). \end{aligned} \tag{5.2.3}$$

This class represents a generalisation of the Kasner metric of GR. It can be shown that it only exists for n in the range $1/2 \leqslant n \leqslant 5/4$ and that the values of the constants p_i must then lie within the ranges

$$\begin{aligned} 2n-1-2\sqrt{(2n-1)(5-4n)} &\leqslant 3p_1 \leqslant 2n-1-\sqrt{(2n-1)(5-4n)}, \\ 2n-1-\sqrt{(2n-1)(5-4n)} &\leqslant 3p_2 \leqslant 2n-1+\sqrt{(2n-1)(5-4n)}, \\ 2n-1+\sqrt{(2n-1)(5-4n)} &\leqslant 3p_3 \leqslant 2n-1+2\sqrt{(2n-1)(5-4n)}, \end{aligned}$$

where it has been assumed without loss of generality that $p_1 \leqslant p_2 \leqslant p_3$. These ranges are shown on figure 5.1 and can be read off by drawing a horizontal line of constant n on the plot. The four points at which the horizontal line crosses the two closed curves gives the four boundary values for the allowed ranges of the constants p_i. It can be seen that the points at which the curves cross the abscissa, which corresponds to $n = 1$, give the boundary values $-1/3 \leqslant p_1 \leqslant 0 \leqslant p_2 \leqslant 2/3 \leqslant p_3 \leqslant 1$, in agreement with the Kasner solution of GR. For $n > 1/2$ these solutions correspond to expanding universes with a curvature singularity at $t = 0$. For $n = 1/2$ the only solution is Minkowski space.

For a universe filled with a perfect fluid having an equation of state $p = (\gamma - 1)\rho$, γ constant, relating the fluid pressure p to its density ρ, the field equations (2.1.12) have the isotropic solution

$$p_1 = p_2 = p_3 = \frac{2n}{3\gamma}, \tag{5.2.4}$$

for $\gamma \neq 0$. This reduces to the spatially-flat FRW solution of GR in the limit $n \to 1$. For $n > 0$, these isotropic cosmologies are expanding, and for $n < 0$ they are con-

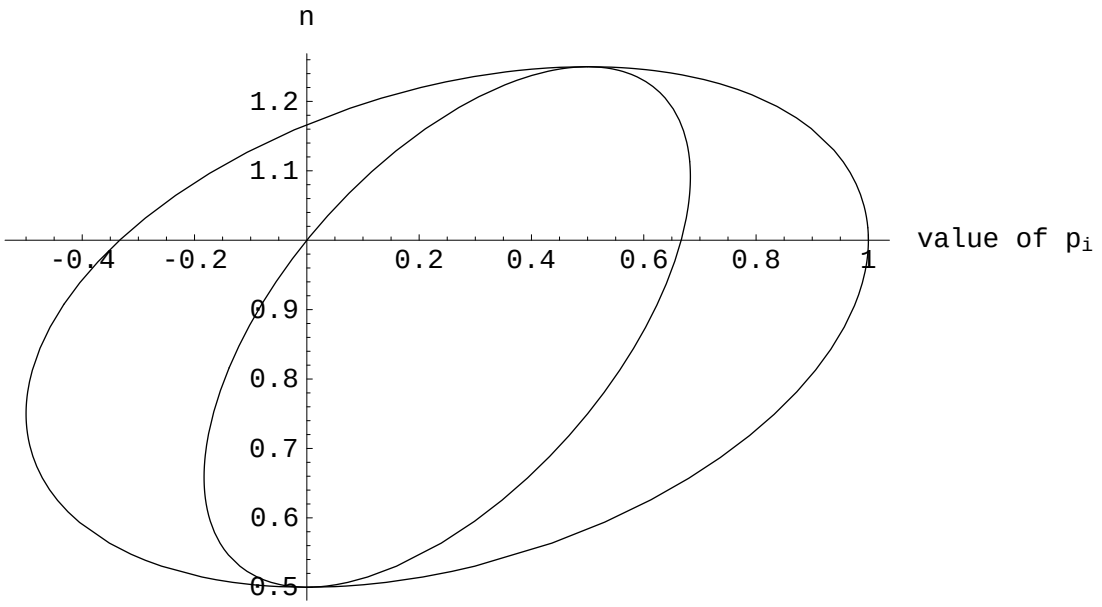

Figure 5.1: *For the solution (5.2.3), the intervals in which the Kasner indices p_i are allowed to lie can be read off from this graph. For any value of n in the range $\frac{1}{2} \leqslant n \leqslant \frac{5}{4}$ a horizontal line is drawn; the boundaries of the intervals in which the p_i lie are then given by the four points at which the horizontal line crosses the two closed curves. For $n = 1$ these boundaries can be seen to be $-\frac{1}{3}$, 0, $\frac{2}{3}$ and 1, as expected for the Kasner solution of general relativity.*

tracting, with $n = 0$ giving Minkowski space. The stability and observational consequences of cosmologies of this type were investigated in [75, 58], where primordial nucleosynthesis and the microwave background were used to impose observational constraints on the admissible values of n.

$f = (R_{ab}R^{ab})^n$

Substituting $f = f(Y) = (R_{ab}R^{ab})^n$ into the fourth-order field equations (2.1.12) along with the metric ansatz (5.2.1) gives the two independent equations,

$$Y^{n-1}\Big((P^2 + Q - 4PQ + P^2Q + Q^2) - 2(3P^2 + P^3 + 3Q - 9PQ + 2Q^2)n + 2(4P^2 + 4Q - 8PQ)\Big) = 0 \quad (5.2.5)$$

and

$$Y^{n-1}\Big((24P - 2P^2 - 2P^3 - 30Q + 10PQ)n + (8P^2 - 32P + 24Q)n^2 + (P^2 - 4P + 2P^3 + 9Q - 10PQ - P^2Q + 3Q^2)\Big) = 0, \quad (5.2.6)$$

where P and Q are defined as before. Equations (5.2.5) and (5.2.6) have five classes of solutions.

The first of these classes is given by

$$P = Q = 0.$$

This is only satisfied for $p_1 = p_2 = p_3 = 0$, which is Minkowski space. It can be seen from (5.2.5) and (5.2.6) that as this solution corresponds to $Y = 0$ it only exists for $n \geqslant 0$ (for $n < 0$ the premultiplicative factor in (5.2.5) and (5.2.6) causes the left-hand side of those equations to diverge).

The second class of solutions is given by

$$P = Q = 1.$$

This is just the Kasner solution of GR, for which the values of the constants p_i are constrained to lie within the ranges $-1/3 \leqslant p_1 \leqslant 0 \leqslant p_2 \leqslant 2/3 \leqslant p_3 \leqslant 1$. Again, this solution corresponds to $Y = 0$ and so is only valid for $n \geqslant 0$.

The third class of solutions is given by

$$P = \frac{3(1-3n+4n^2) \pm \sqrt{3(-1+10n-5n^2-40n^3+48n^4)}}{2(1-n)}$$
$$Q = \frac{P^2}{3}.$$

The only solution belonging to this class corresponds to an isotropic and spatially flat vacuum FRW cosmology. The values of the constants p_i are all equal to $P/3$ in this case and the solution is valid for all $n \neq 1$.

The fourth class of solutions is given by

$$P = (1-2n)^2 \tag{5.2.7}$$
$$Q = 1 - 8n + 16n^2 - 8n^3.$$

The solutions belonging to this class are anisotropic cosmologies which reduce to the standard Kasner form, $P = Q = 1$, in the limit $n \to 1$. For this class of solutions, the values of the constants p_i are in general constrained to lie within the ranges

$$\begin{aligned}(1-2n)^2 - 2A &\leqslant 3p_1 \leqslant (1-2n)^2 - A \\ (1-2n)^2 - A &\leqslant 3p_2 \leqslant (1-2n)^2 + A \\ (1-2n)^2 + A &\leqslant 3p_3 \leqslant (1-2n)^2 + 2A\end{aligned}$$

where $A = \sqrt{(1-2n)(1-6n+4n^3)}$ and the p_i have again been ordered so that $p_1 \leqslant p_2 \leqslant p_3$. These boundaries are shown in figure 5.2 which can be read in the same way as figure 5.1, by taking a horizontal line of constant n and noting the four points at which that line intersects the curves. These intercepts determine the allowed intervals for the values of the p_i.

For real-valued p_i, the value of n must lie either in the range $n_1 \leqslant n \leqslant n_2$ or in the range $1/2 \leqslant n \leqslant n_3$, where n_1, n_2 and n_3 are the roots of the cubic polynomial $1 - 6n + 4n^3 = 0$ and are chosen such that $n_1 < n_2 < n_3$. These generalisations of the Kasner metric always correspond to expanding cosmologies, independent of the value of n.

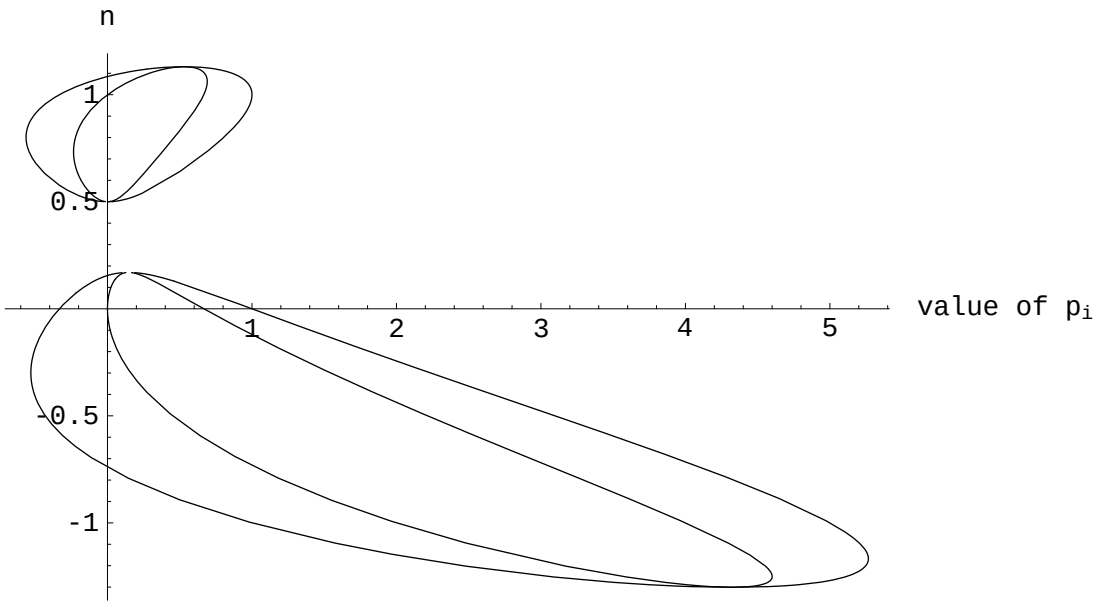

Figure 5.2: *For the solution (5.2.7) the intervals in which the Kasner indices p_i are constrained to lie can be read off this graph, as with figure 5.1. A horizontal line of constant n is drawn; the boundaries of the intervals in which the p_i lie are then given by the four points at which the horizontal line crosses the curves. For $n = 1$ these boundaries can be seen to be $-\frac{1}{3}$, 0, $\frac{2}{3}$ and 1, as expected for the Kasner solution of general relativity.*

The fifth class of solutions to (5.2.5) and (5.2.6) is given by

$$P = 4n - 1$$
$$Q = -3 + 12n - 8n^2 \pm 2(1-2n)\sqrt{2(1-4n+2n^2)}.$$

This class describes complex-valued p_i for all values of n (except for $n = 1/4$, for which this class of solutions reduces to the first class) and is therefore of limited interest.

The isotropic solution for a universe filled with a fluid with equation of state

$p = (\gamma - 1)\rho$ is given by the choice

$$p_1 = p_2 = p_3 = \frac{4n}{3\gamma}.$$

This solution reduces to the spatially-flat FRW cosmology of GR in the limit $n \to 1/2$ and corresponds to an expanding universe for $n > 0$ and to a contracting universe for $n < 0$.

$\boldsymbol{f = (R_{abcd}R^{abcd})^n}$

Substituting $f = f(Z) = (R_{abcd}R^{abcd})^n$ and (5.2.1) into the field equations (2.1.12) gives the two independent equations

$$Z^{n-1}\Bigg(\Big(\frac{P^2Q}{2} - \frac{P^4}{12} - Q - \frac{3Q^2}{4} + 2S - \frac{2PS}{3}\Big) + 8(S-Q)n^2 + \Big(\frac{P^4}{3} + 6Q + 2PQ - 2P^2Q + 3Q^2 - 10S + \frac{2PS}{3}\Big)n\Bigg) = 0 \quad (5.2.8)$$

and

$$Z^{n-1}\Bigg(\Big(\frac{P^4}{4} - P - \frac{3P^2}{2} - \frac{P^3}{2} + \frac{13Q}{2} + \frac{7PQ}{2} - \frac{3P^2Q}{2} + \frac{9Q^2}{4} - 8S\Big) + (6P + 4P^2 - 16Q - 2PQ + 8S)n + 8(Q-P)n^2\Bigg) = 0 \quad (5.2.9)$$

where P and Q are defined as before and we have also now defined

$$S \equiv \sum_i p_i^3.$$

Equations (5.2.8) and (5.2.9) have four different classes of solution.

The first class of solutions is given by

$$P = Q = S = 0.$$

The only solution that belongs to this class is Minkowski space. As $R_{abcd}R^{abcd} = 0$

for Minkowski space it can only be a solution for $n \geqslant 0$, due to the premultiplier in equations (5.2.8) and (5.2.9).

The second class of solutions is given by

$$P = Q = S = 1.$$

The only solution that belongs to this class corresponds to $p_1 = p_2 = 0$ and $p_3 = 1$. Making the coordinate transformations $\bar{z} = t \sinh z$ and $\bar{t} = t \cosh z$ [117] allows the line-element (5.2.1) to then be written in the form

$$ds^2 = -d\bar{t}^2 + dx^2 + dy^2 + d\bar{z}^2$$

which is clearly Minkowski space again. This is only a solution for $n \geqslant 0$, as with the first class of solutions.

The third class of solutions to (5.2.8) and (5.2.9) is given by

$$\begin{aligned} P &= \frac{3(1 - 2n + 4n^2 \pm \sqrt{-1 + 10n - 16n^2 + 16n^4}}{2(1-n)}, \\ Q &= \frac{P^2}{3}, \\ S &= \frac{P^3}{9}, \end{aligned}$$

which only has the isotropic and spatially flat vacuum FRW cosmology as a solution, where $p_1 = p_2 = p_3 = P/3$. This is a solution for all $n \neq 1$.

The fourth and last class of solutions is given by

$$\begin{aligned} P &= 4n - 1 \\ Q &= \frac{1}{3}\{16n^2 - 8n - 1 \pm 4\sqrt{2[n(1-2n) + S(1-n)]}\}. \end{aligned}$$

This class of solutions corresponds to anisotropic metrics with $Z = 0$ and is unusual in that it cannot be expressed in the form $P =$ constant and $Q =$ constant. This feature means that the standard picture of a plane intersecting an ellipsoid is no longer valid for this class. Solutions in this class do not appear to have any range of n for which the constants p_i take real values, and so are of limited physical interest.

The isotropic solution for a universe filled with a fluid with equation of state

$p = (\gamma - 1)\rho$ is given by

$$p_1 = p_2 = p_3 = \frac{4n}{3\gamma}.$$

As before, this reduces to the spatially flat FRW solution of GR in the limit $n \to 1/2$ and corresponds to an expanding universe for $n > 0$ and to a contracting universe for $n < 0$.

5.2.3 Investigation of the Effects of Matter

We have identified above two generalisations of the Kasner metric of GR which are solutions to the scale-invariant theories of gravity we are investigating. The first of these is a solution to the theory defined by $\mathcal{L} = R^n$; the second is a solution to the theory $\mathcal{L} = (R_{ab}R^{ab})^n$. These are the first exact anisotropic solutions to be found for higher-order gravity theories. In this section we will investigate some of the properties of these cosmologies.

The behaviour of these solutions is of particular interest when considering the Bianchi type VIII or type IX 'mixmaster' cosmologies. The field equations for these cosmologies can be cast into the form of the equations of motion of a particle moving inside an exponentially steep triangular potential well with open channels in the corners [126]. The three steep-sided walls are created by the 3-curvature anisotropies. In the region where the potential is negligible (far from the walls) the behaviour of the solutions approaches that of the Kasner metric. As the exponentially steep potential wall is approached the universe 'particle' is reflected and re-enters a Kasner–like regime with the Kasner indices p_i systematically changed to some new values by the rule of reflection from the potential wall. In general relativistic cosmologies of Bianchi types VIII and IX this process is repeated an infinite number of times as the singularity is approached [43, 126, 8, 9, 67, 159] so long as matter obeys an equation of state with $p < \rho$. After reflection from the potential wall the Kasner index that was previously negative is permuted to a positive value and the lowest-valued positive Kasner index is permuted to a negative value. This is repeated *ad infinitum* in the general relativistic cosmology as one of the Kasner indices must be kept negative while the other two are positive. In the generalisations of the Kasner metric presented above this is no longer the case; for some solutions

it is possible for all of the Kasner indices to be positive. If the Kasner indices are being permuted in a chaotic fashion for long enough then, eventually, they will end up in such a configuration. Once this occurs the oscillations will end, as all spatial dimensions will be contracting, and the singularity will be reached monotonically without further oscillation of the scale factors [44, 11].

From figure 5.1 it can be seen that for solution (5.2.3) all Kasner indices can be made positive for values of $1 < n < 5/4$ in the $\mathcal{L} = R^n$ theories. Similarly, from figure 5.2 it can be seen that for the solution (5.2.7), with $n_1 < n < n_2$ or $1 < n < n_3$, all the Kasner indices can be made positive in the theory $\mathcal{L} = (R_{ab}R^{ab})^n$ (where the n_i are defined as before). For both of these solutions, with these ranges of n, there is therefore no infinite series of chaotic mixmaster oscillations as the singularity is approached. However, the solutions to both of these theories are still expected to exhibit an infinite number of chaotic oscillations if $1/2 < n < 1$, as at least one of the Kasner indices must be kept negative whilst another is kept positive. A separate detailed analysis is require to determine where there are differences between this behaviour and the chaotic oscillations found in GR.

It now remains to show that the vacuum solutions found above are the asymptotic attractor solutions in the presence of non-comoving matter motions as $t \to 0$. This analysis will follow closely that of [23] and [117]. We aim to show that the fluid stresses diverge more slowly than the vacuum terms as $t \to 0$ and so produce negligible metric perturbations to an anisotropic Kasner like universe. If this is the case, then the vacuum solutions above can indeed be considered as the asymptotic attractor solutions even in the presence of matter. Matter will just be carried along by the expansion and behave like a test fluid.

We now consider a perfect fluid with equation of state $p = (\gamma - 1)\rho$ where $1 \leqslant \gamma < 2$ and the non-zero 4-velocity components, U^i, are normalised so that $U^i U_i = -1$. The conservation equations $T^{ab}{}_{;b} = 0$ on the metric background (5.2.1) can then be written in the form [117, 11, 9]

$$\frac{\partial}{\partial x^i}(t^p \rho^{\frac{1}{\gamma}} U^i) = 0$$
$$\gamma\rho U^k (U_{i,k} - \frac{1}{2}U^l g_{kl,i}) = -\frac{1}{3}\rho_{,i} - (\gamma - 1)U_i U^k \rho_{,k}.$$

Neglecting spatial derivatives with respect to time derivatives, these equations integrate to

$$\begin{aligned} t^p U_0 \rho^{\frac{1}{\gamma}} &= \text{constant} \\ U_\alpha \rho^{\frac{(\gamma-1)}{\gamma}} &= \text{constant}. \end{aligned}$$

The neglecting of spatial derivatives means that these equations are valid on scales larger than the particle horizon as in the velocity-dominated approximation (although we have not so far restricted the fluid motions to be non-relativistic) [117, 82, 184].

From the second of the integrals above, it can be seen that all the covariant components of the spatial 3-velocity, U_α, are approximately equal. This is not true of the contravariant components as the Kasner indices, p_i, in the metric elements used to raise indices are not equal in these solutions. The contravariant component that diverges the fastest, and dominates the others in the $t \to 0$ velocity-dominated limit, is therefore $U^3 = U_3 t^{2p_3}$, as p_3 is the largest of the p_i. If the 4-velocity is normalised, so that $U_a U^a = -1$, and the contravariant 3-velocity component U^3 diverges the fastest as $t \to 0$, then we must have $U_0 U^0 \sim U_3 U^3 = (U_3)^2 t^{-2p_3}$ in that limit. The integrated conservation equations above can now be solved approximately in this limit to give

$$\begin{aligned} \rho &\sim t^{-\gamma(p_1+p_2)/(2-\gamma)} \\ U_\alpha &\sim t^{(p_1+p_2)(\gamma-1)/(2-\gamma)} \end{aligned}$$

as $t \to 0$.

It is now possible to calculate the leading-order contributions to the energy-momentum tensor, $T^a{}_b = (\rho + p) U^a U_b + p \delta^a{}_b$:

$$\begin{aligned} T^0_0 &\sim \rho U^0 U_0 \sim t^{-P-p_3} \\ T^1_1 &\sim \rho \sim t^{-\gamma(P-p_3)/(2-\gamma)} \\ T^2_2 &\sim \rho U^2 U_2 \sim t^{-2p_2-P+p_3} \\ T^3_3 &\sim \rho U^3 U_3 \sim t^{-P-p_3} \end{aligned}$$

for $\gamma < 4/3$. The component which diverges the fastest here as $t \to 0$ is $T^3_3 \sim t^{-P-p_3}$,

for general γ. For the case $\gamma = \frac{4}{3}$ where the 4-velocity of the fluid is comoving, $U_i = \delta^0_i$, all the components of T^a_b diverge as $\rho \sim t^{-2P+2p_3}$.

For the generalisation of the Kasner metric in the $\mathcal{L} = R^n$ theory, (5.2.3), the vacuum terms diverge as t^{-2n}. We therefore require that $2n > P + p_3$, or $p_3 < 1$, in order for the vacuum terms to dominate over the matter terms for a non-comoving perfect fluid, with general γ, in the limit $t \to 0$. For the $\gamma = \frac{4}{3}$, comoving perfect fluid ($U_i = \delta^0_i$), the condition for vacuum domination is $2n > 2P - 2p_3$, or $p_3 > n - 1$. Both of these conditions are ensured by the boundary values on p_3 given above. In the velocity-dominated limit, the vacuum solutions given here are therefore the appropriate asymptotic solutions on approach to the singularity.

For the generalised Kasner metric in the $\mathcal{L} = (R_{ab}R^{ab})^n$ theory, (5.2.7), the vacuum terms diverge as t^{-4n}. For vacuum domination as $t \to 0$ in this solution we therefore require $4n > P + p_3$, or $p_3 < -1 + 8n - 4n^2$, for the general non-comoving γ fluid; and $4n > 2P - 2p_3$, or $p_3 > 1 - 6n + 4n^2$, for the $\gamma = 4/3$ comoving fluid. From figure 5.2 it can be seen that solutions of this class can be in one of two regions, $n_1 \leqslant n \leqslant n_2$ or $1/2 \leqslant n \leqslant n_3$. The validity of the vacuum solution as $t \to 0$ is different in these two different regions. For the region $1/2 \leqslant n \leqslant n_3$ the boundary conditions on the index p_3 mean that the conditions above are automatically satisfied. For the region $n_1 \leqslant n \leqslant n_2$ these inequalities are not always satisfied. For general γ, the condition for vacuum domination is only met if n lies in the narrow range $1/6 < n < n_2$; for any other value of n in this region the index p_3 can be such that the fluid diverges faster than the vacuum terms. Similarly, for the $\gamma = 4/3$ comoving fluid the condition for vacuum domination is only satisfied if n lies in the narrow range $n_4 < n < n_2$, where n_4 is the real root of the cubic

$$4n^3 - 12n^2 + 10n - 1 = 0.$$

To understand the evolution of an anisotropic solution of the form (5.2.1) in the theory $\mathcal{L} = (R_{ab}R^{ab})^n$, where $n_1 \leqslant n \leqslant n_2$, it is therefore necessary to take into account the relativistic motions of any fluid that is present (except in the narrow ranges of n identified above). This range of n can, however, be regarded as not belonging to physically interesting theories on other grounds. In order to agree with

weak-field experiments it is necessary for a gravitational theory to contain a term which approximates the Einstein-Hilbert action in the weak-field limit (see ref. [75]). Any theory containing such a limit must therefore have a term in its Lagrangian that diverges as t^{-2}. In considering the behaviour of alternative theories close to the singularity it is necessary for the extra terms in the Lagrangian to diverge faster than this if they are to be influential as $t \to 0$. For the theory $\mathcal{L} = (R_{ab}R^{ab})^n$ this requires $n > 1/2$. For $n < 1/2$ such a term will diverge slower than the Einstein-Hilbert term which will then dominate and display the standard Kasner behaviour of GR. For the anisotropic solution (5.2.7) we are therefore only interested in the region lying in the range $1/2 \leqslant n \leqslant n_3$, which has vacuum terms that dominate the fluid stresses in the velocity-dominated approximation.

It remains to investigate the effects of fluids with equations of state, $\gamma > 4/3$. For sufficiently stiff fluids the velocity-dominated approximation is not valid and $U^\alpha U_\alpha \to 0$ as $t \to 0$ due to the very high inertia of the fluid producing a slow down under contraction [10]. In such a limit $U_0 \to 1$ and the conservation equations can be solved to give

$$\rho \sim t^{-\gamma P}$$
$$U_\alpha \sim t^{(\gamma-1)P}.$$

In this approximation we can write $U_\alpha U^\alpha \sim (U_3)^2 t^{-2p_3} \sim t^{2(\gamma-1)P-2p_3}$. It can now be seen that this behaviour occurs when

$$p_3 \ \leqslant (\gamma - 1)P. \tag{5.2.10}$$

In this limit it is only required that ρ diverges more slowly than the vacuum terms, as $\rho U_\alpha U^\alpha << \rho$ when $t \to 0$.

For the solution (5.2.3) to the theory $\mathcal{L} = R^n$ it can be seen from the condition (5.2.10) that it is necessary for $\gamma \geqslant 4/3$ in order for the velocity-dominated approximation to break down (this is derived using the upper limit on n and the lower limit on p_3). The condition that the fluid stresses diverge more slowly than the vacuum terms is now

$$\gamma < \frac{2n}{(2n-1)} \tag{5.2.11}$$

where it has been assumed $n > 1/2$. A sufficient condition to satisfy this for all allowed values of n is $\gamma < 5/3$. For fluids with a stiffer equation of state, $5/3 \leqslant \gamma < 2$, the vacuum terms dominate over the fluid motions provided that $n < 1$. For $n < 1$, however, the Einstein-Hilbert term will be the leading one in the gravitational action, as discussed above.

Similarly, for the solution (5.2.7) to the theory $\mathcal{L} = (R_{ab}R^{ab})^n$ it can be seen from the condition (5.2.10) that it is again necessary to have $\gamma \geqslant 4/3$ in order for the velocity-dominated approximation to break down. In the region $1/2 \leqslant n \leqslant n_3$ the condition for the vacuum solution to be unperturbed by the stiff fluid is always satisfied for any fluid with equation of state $\gamma < 2$. However, in the region $n_1 < n < n_2$ the condition for the vacuum to diverge faster than the energy density of the stiff fluid is never satisfied for a fluid which satisfies the necessary condition for the velocity-dominated approximation to break down (except in the narrow range $(7-\sqrt{33})/8 < n < n_2$ where there are some values of γ for which the vacuum terms can diverge fastest).

5.2.4 Discussion

We have investigated some anisotropic cosmological solutions to higher-order Lagrangian theories of gravity. Whist the standard general relativistic theory appears to be consistent with all weak-field tests, there is less reason to think that it should be valid in high curvature regimes, such as in the vicinity of a possible initial cosmological curvature singularity. In fact, it is in the high-curvature limit that quantum effects should become important and we should expect to see deviations from the standard theory. Without knowing the exact form of such deviations, we have approached this problem by considering a general class of theories that can be derived from an arbitrary analytic function of the three curvature invariants R, $R_{ab}R^{ab}$ and $R_{abcd}R^{abcd}$. Expanding this function as a power series in these variables we then expect the dominant term in the Lagrangian to be of the form R^n, $(R_{ab}R^{ab})^n$ or $(R_{abcd}R^{abcd})^n$ as the singularity is approached. We have found all of the solutions to these theories that can be expressed in terms of the Bianchi type I line–element (5.2.1) in vacuum. These solutions provide simple testing grounds for the exploration of quantum cosmological effects in higher-order gravity theory. We have also

found the homogeneous, isotropic and spatially flat solutions to these theories in the presence of a perfect fluid.

Exact vacuum anisotropic solutions of the form (5.2.1) were found for the theories $\mathcal{L} = R^n$ and $\mathcal{L} = (R_{ab}R^{ab})^n$, whilst it was shown that no such solutions exist for theories defined by $\mathcal{L} = (R_{abcd}R^{abcd})^n$. The properties of these solutions, with respect to their relation to the more general Bianchi type VIII and IX cosmological behaviour, has been investigated. We have argued that for all of the physically relevant new solutions of these theories, the Universe will not experience an infinite number of mixmaster oscillations as the singularity is approached. The extent to which these vacuum solutions can be considered as realistic in the presence of a perfect fluid has also been investigated. It has been shown in the velocity-dominated approximation that all the anisotropic vacuum solutions found for plausible theories are valid in the limit $t \to 0$. The case of stiff fluids that do not satisfy the velocity-dominated approximation as $t \to 0$ has also been investigated. For the solutions to the theories $\mathcal{L} = R^n$ it was found that for a fluid with equation of state $\gamma < 5/3$ the vacuum solutions are good approximations in the vicinity of the singularity. For the theories $\mathcal{L} = (R_{ab}R^{ab})^n$ it was found that the vacuum solutions are good approximations for all $\gamma < 2$.

CHAPTER 6

Static Solutions

In this chapter the vacuum static and spherically symmetric solutions to the Brans-Dicke and R^n theories will be presented. For these theories there is no equivalent of 'Birkhoff's theorem' (in fact, in the next chapter we will present solutions which explicitly violate Birkhoff's theorem). The condition of being static is therefore added as an extra condition, in contrast to the usual treatment in GR.

This chapter is based on the work of Clifton and Barrow [70].

6.1 Scalar-Tensor Theories

The static and spherically symmetric solutions of the Brans-Dicke theory were found long ago by Brans himself [51]. These solutions have been investigated and rediscovered in many papers since, and so we will only present a very brief summary of the situation here, for completeness of this study. In isotropic coordinates

$$ds^2 = -e^{2\alpha}dt^2 + e^{2\beta}(dr^2 + r^2 d\Omega^2)$$

where $\alpha = \alpha(r)$ and $\beta = \beta(r)$, there are four solutions of the Brans-Dicke field equations (2.1.8) and (2.1.9) which are given by [51]

I

$$e^{\alpha} = e^{\alpha_0}\left[\frac{1-\frac{B}{r}}{1+\frac{B}{r}}\right]^{k}$$

$$e^{\beta} = e^{\beta_0}\left(1-\frac{B}{r}\right)^{2}\left[\frac{1-\frac{B}{r}}{1+\frac{B}{r}}\right]^{\frac{(k-1)(k+2)}{k}}$$

$$\phi = \phi_0\left[\frac{1-\frac{B}{r}}{1+\frac{B}{r}}\right]^{\frac{(1-k^2)}{k}}$$

II

$$\alpha = \alpha_0 + \frac{2}{\Lambda}\tan^{-1}\left(\frac{r}{B}\right)$$

$$\beta = \beta_0 - \frac{2(C+1)}{\Lambda}\tan^{-1}\left(\frac{r}{B}\right) - \ln\left[\frac{r^2}{(r^2+B^2)}\right]$$

$$\phi = \phi_0 e^{\frac{2C}{\Lambda}\tan^{-1}\left(\frac{r}{B}\right)}$$

III

$$\alpha = \alpha_0 - \frac{r}{B}$$

$$\beta = \beta_0 - 2\ln\left(\frac{r}{B}\right) + \frac{(C+1)r}{B}$$

$$\phi = \phi_0 e^{-\frac{Cr}{B}}$$

IV

$$\alpha = \alpha_0 - \frac{1}{Br}$$

$$\beta = \beta_0 + \frac{(C+1)}{Br}$$

$$\phi = \phi_0 e^{-\frac{C}{Br}}$$

where

$$k^2 = \frac{(4+2\omega)}{(3+2\omega)}$$

$$\Lambda^2 = C\left(1-\frac{\omega C}{2}\right) - (C+1)^2 > 0$$

$$C = \frac{-1 \pm \sqrt{-2\omega-3}}{(\omega+2)}$$

and B, α_0, β_0 and ϕ_0 are constants. Whilst solution I is valid for all values of ω, solutions II, III and IV are only valid for $\omega < -3/2$. It is probably for this reason that it is most often solution I that is used in the literature for analyses of the static and spherically symmetric situation. Solution I is conformally related to the minimally coupled massless scalar field solution of Buchdahl [53].

It can be seen that these solutions are not all independent of each other. By a transformation of the form

$$r \to \frac{1}{r},$$

and some redefinition of constants, solution II can be transformed into the $\omega < -3/2$ range of solution I [49] and solution III can be transformed into solution IV [48]. It was further shown in [49] that the independent solutions I and IV are both conformally related to the general solution of the static and spherically symmetric case in the Einstein conformal frame, given by Wyman [192].

6.2 Fourth-Order Theories

In the absence of any matter the $\mathcal{L} = R^{1+\delta}$ field equations (2.1.15) can be written as

$$R_{ab} = \delta \left(\frac{R_{;}{}^{cd}}{R} - (1-\delta)\frac{R_{,}{}^{c}R_{,}{}^{d}}{R^2} \right) \left(g_{ac}g_{bd} + \frac{1}{2}\frac{(1+2\delta)}{(1-\delta)} g_{ab}g_{cd} \right). \tag{6.2.1}$$

We find that an exact static spherically symmetric solution of these field equations is given in Schwarzschild coordinates by the line-element

$$ds^2 = -A(r)dt^2 + \frac{dr^2}{B(r)} + r^2(d\theta^2 + \sin^2\theta d\phi^2) \tag{6.2.2}$$

where

$$A(r) = r^{2\delta\frac{(1+2\delta)}{(1-\delta)}} + \frac{C}{r^{\frac{(1-4\delta)}{(1-\delta)}}}$$

$$B(r) = \frac{(1-\delta)^2}{(1-2\delta+4\delta^2)(1-2\delta(1+\delta))} \left(1 + \frac{C}{r^{\frac{(1-2\delta+4\delta^2)}{(1-\delta)}}} \right)$$

and C = constant. This solution is conformally related to the $Q = 0$ limit of the one found by Chan, Horne and Mann for a static spherically–symmetric space-time containing a scalar-field in a Liouville potential [64]. It reduces to Schwarzschild in the limit of GR: $\delta \to 0$.

In order to evaluate whether or not this solution is physically relevant we will proceed as follows. A dynamical systems approach will be used to establish the asymptotic attractor solutions of the field equations (6.2.1). The field equations will then be perturbed around these asymptotic attractor solutions and solved to first order in the perturbed quantities. This linearised solution will then be treated as the physically relevant static and spherically-symmetric weak-field limit of the field equations (6.2.1) and compared with the exact solution (6.2.2).

6.2.1 Dynamical System

The dynamical systems approach has already been applied to a situation of this kind by Mignemi and Wiltshire [125]. We present a brief summary of the relevant points of their work which is relevent to this study, in the above notation.

Taking the value of sign(R) from (6.2.2) as sign$(-\delta(1+\delta)/(1-2\delta(1+\delta)))$ and making a suitable choice of Ω_0 allows the scalar-field potential (2.2.14) to be written as

$$V(\phi) = -\frac{3\delta^2}{8\pi G(1-2\delta(1+\delta))} \exp\left(\sqrt{\frac{16\pi G}{3}}\frac{(1-\delta)}{\delta}\phi\right). \tag{6.2.3}$$

In four dimensions Mignemi and Wiltshire's choice of line–element corresponds to

$$d\bar{s}^2 = e^{2U(\xi)}\left(-dt^2 + \bar{r}^4(\xi)d\xi^2\right) + \bar{r}^2(\xi)(d\theta^2 + \sin^2\theta d\phi^2) \tag{6.2.4}$$

which, after some manipulation, gives the $\mathcal{L} = R^{1+\delta}$ Einstein frame field equations (2.2.13) as

$$\zeta'' = -\frac{2c_1^2(1-\delta)^2 + 6\delta^2\eta'^2 - 24\delta^2\eta'\zeta' - 2(1-2\delta-8\delta^2)\zeta'^2}{1-2\delta+4\delta^2} - e^{2\zeta} \tag{6.2.5}$$

$$\eta'' = \frac{(1-2\delta-8\delta^2)(c_1^2(1-\delta)^2 + 3\delta^2\eta'^2 - 12\delta^2\eta'\zeta' - (1-2\delta-8\delta^2)\zeta'^2)}{3\delta^2(1-2\delta+4\delta^2)} + \frac{(1-2\delta(1+\delta))}{3\delta^2}e^{2\zeta} \tag{6.2.6}$$

and

$$e^{2\eta} = -\frac{(1-2\delta(1+\delta))}{3\delta^2(1-2\delta+4\delta^2)}\left(c_1^2(1-\delta)^2 + 3\delta^2\eta'^2 - 12\delta^2\eta'\zeta'\right.$$
$$\left. -(1-2\delta-8\delta^2)\zeta'^2 + (1-2\delta+4\delta^2)e^{2\zeta}\right) \quad (6.2.7)$$

where

$$\zeta(\xi) = U(\xi) + \log\bar{r}(\xi)$$
$$\eta(\xi) = -\frac{(1-2\delta(1+\delta))}{3\delta^2}U(\xi) + 2\log\bar{r}(\xi) - \frac{(1-\delta)^2}{3\delta^2}c_1\xi + \text{constant}.$$

Primes denote differentiation with respect to ξ and c_1 is a constant of integration.

The variables X, Y and Z are here defined to be

$$X = \zeta' \qquad Y = \eta' \qquad Z = e^{\zeta}$$

(not to be confused with the definitions of the scalar curvature invariants used in other chapters). The field equations (6.2.5) and (6.2.6) can then be written in terms of these new variables as the following set of first-order autonomous differential equations

$$X' = -\frac{2c_1^2(1-\delta)^2 + 6\delta^2Y^2 - 24\delta^2XY - 2(1-2\delta-8\delta^2)X^2}{1-2\delta+4\delta^2} - Z^2 \quad (6.2.8)$$

$$Y' = \frac{(1-2\delta-8\delta^2)(c_1^2(1-\delta)^2 + 3\delta^2Y^2 - 12\delta^2XY - (1-2\delta-8\delta^2)X^2)}{3\delta^2(1-2\delta+4\delta^2)}$$
$$+ \frac{(1-2\delta(1+\delta))}{3\delta^2}Z^2 \quad (6.2.9)$$

$$Z' = XZ. \quad (6.2.10)$$

(The reader should note the different definition of Z here to that of Mignemi and Wiltshire). As identified by Mignemi and Wiltshire, the only critical points at finite values of X, Y and Z are in the plane $Z = 0$ along the curve defined by

$$c_1^2(1-\delta)^2 + 3\delta^2Y^2 - 12\delta^2XY - (1-2\delta-8\delta^2)X^2 = 0.$$

These curves are shown as bold lines in figure 6.1, together with some sample tra-

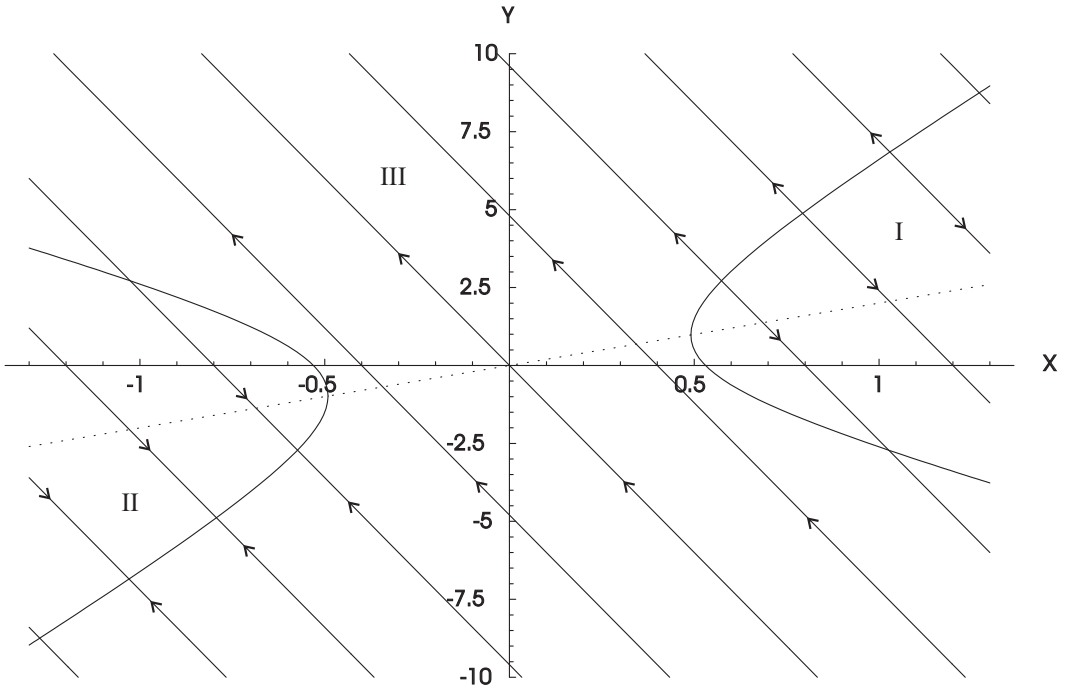

Figure 6.1: *The $Z = 0$ plane of the phase space defined by X,Y and Z for $\delta = 0.1$ and $c_1 = 0.5$. The bold lines show the critical points in this plane and the diagonal lines show the unphysical trajectories confined to this plane. The dotted line is $Y = 2X$ and separates the critical points where $\xi \to \infty$ from the points where $\xi \to -\infty$*

jectories from equations (6.2.8) and (6.2.9). From the definition above we see that the condition $Z = 0$ is equivalent to $\bar{r}e^U = 0$. Whilst we do not consider trajectories confined to this plane to be physically relevant, we do consider the plot to be instructive as it gives a picture of the behaviour of trajectories close to this surface and displays the attractive or repulsive behaviour of the critical points, which can be the end points for trajectories which could be considered as physically meaningful. The dotted line in figure 6.1 corresponds to the line $Y = 2X$ and separates two different types of critical points. The critical points with $Y > 2X$ can be seen to be repulsive to the trajectories in the $Z = 0$ plane and correspond to the limit $\xi \to -\infty$. Conversely, the points with $Y < 2X$ are attractive and correspond to the limit $\xi \to \infty$. As $Z = \bar{r}e^U$, all critical points of this type in the $Z = 0$ plane correspond either to naked singularities, $\bar{r} \to 0$, or regular horizons, $\bar{r} \to$constant.

The two bold lines in figure 6.1 are the points at which the surface defined by

$$c_1^2(1-\delta)^2 + 3\delta^2 Y^2 - 12\delta^2 XY - (1-2\delta-8\delta^2)X^2 + (1-2\delta+4\delta^2)Z^2 = 0$$

crosses the $Z = 0$ plane. This surface splits the phase space into three separate regions between which trajectories cannot move. These regions are labelled I, II and III in figure 6.1. It can be seen from (6.2.7) that trajectories are confined to either regions I or II for the potential defined by (6.2.3). If we had chosen the opposite value of sign(R) in (2.2.14) then trajectories would be confined to region III. We will show, however, that region III does not contain solutions with asymptotic regions in which $\bar{r} \to \infty$ and so is of limited interest for our purposes.

In order to find the remaining critical points it is necessary to analyse the sphere at infinity. This can be done by making the transformation

$$X = \rho \sin\theta \cos\phi \qquad Y = \rho \sin\theta \sin\phi \qquad Z = \rho \cos\theta$$

and taking the limit $\rho \to \infty$. The set of equations (6.2.8), (6.2.9) and (6.2.10) then give

$$\begin{aligned}\frac{d\theta}{d\tau} \to -\frac{\cos\theta}{24\delta^2(1-2\delta+4\delta)}&(6\delta^2\cos\phi(3-3\delta(2-9\delta)+(1-\delta(2+11\delta))\cos 2\theta)\\ &-(3-3\delta(4-\delta(15-22\delta-32\delta^2))\\ &+(5-\delta(20-\delta(3+34\delta+32\delta^2)))\cos 2\theta)\sin\phi\\ &-2(18\delta^2(1-\delta(2+7\delta))\cos 3\phi\\ &-(1-\delta(4+\delta(9-26\delta+32\delta^2)))\sin 3\phi)\sin^2\theta)\end{aligned}$$

and

$$\begin{aligned}\frac{d\phi}{d\tau} \to -\frac{1}{24\delta^2(1-2\delta+4\delta^2)}&(6\delta^2(1-\delta(2+41\delta)-5(1-\delta(2+5\delta))\cos 2\theta)\mathrm{cosec}\theta\sin\phi\\ &+2((1-\delta(4+\delta(9-26\delta+32\delta^2)))\cos 3\phi\\ &+18\delta^2(1-\delta(2+7\delta))\sin 3\phi)\sin\theta\\ &-2\cos\phi(4(1-2\delta(2-\delta(3-2\delta-4\delta^2)))\mathrm{cosec}\theta\\ &-(7-\delta(28+\delta(15-2\delta(43+128\delta))))\sin\theta))\end{aligned}$$

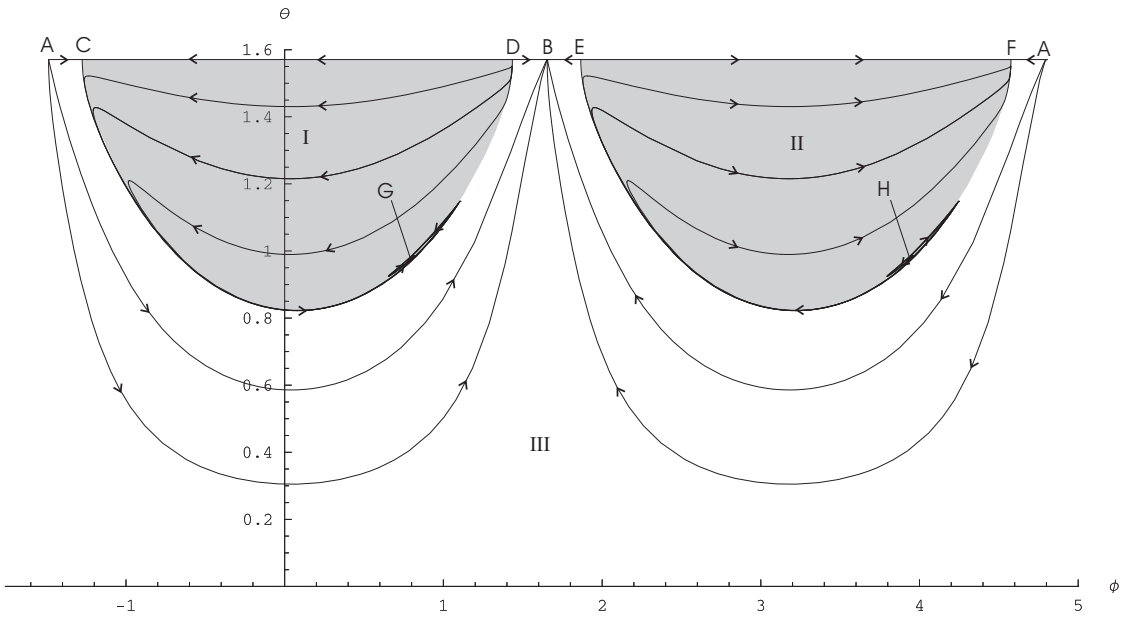

Figure 6.2: *The surface at infinity of the phase space defined by X,Y and Z for $\delta = 0.1$. The shaded areas show where regions I and II. Region III is unshaded.*

where $d\tau = \rho d\xi$. These equations can be used to plot the positions of critical points and trajectories on the sphere at infinity. The result of this is shown in figure 6.2. Once again, these trajectories do not correspond to physical solutions in the phase space but are illustrative of trajectories at large distances and help to show the attractive or repulsive nature of the critical points. The surface at infinity has eight critical points, labelled A-H in figure 6.2. Points A and B are the end-points of the trajectory that goes through the origin in figure 6.1 and are located at

$$\theta = \frac{\pi}{2}, \qquad \text{and} \qquad \phi_{1,(2)} = \cos^{-1}\left(\frac{-6\delta^2}{\sqrt{1-4\delta-12\delta^2+32\delta^3+100\delta^4}}\right)(+\pi)$$

or, in terms of the original functions in the metric (6.2.4),

$$\bar{r} \to (\xi - \xi_1)^{\frac{3\delta^2}{(1-2\delta-8\delta^2)}} \qquad \text{and} \qquad e^U \to (\xi - \xi_1)^{\frac{3\delta^2}{(1-2\delta-8\delta^2)}},$$

where ξ_1 is a constant of integration. The points A and B therefore both correspond to $\xi \to \xi_1$ and hence to $\bar{r} \to 0$.

Points C, D, E and F are the four end points of the two curves in figure 6.1 and

therefore correspond to $\xi \to \infty$ or $-\infty$ and $\bar{r} \to 0$ or constant.

The remaining points, G and H, are located at

$$\phi_{1,(2)} = \frac{\pi}{4}(+\pi) \qquad \text{and} \qquad \theta = \frac{1}{2}\cos^{-1}\left(-\frac{1-2\delta+10\delta^2}{3-6\delta+6\delta^2}\right)$$

or

$$\bar{r}^{\frac{(1-2\delta+4\delta^2)}{(1-\delta)^2}} \to \pm\sqrt{\frac{(1-2\delta-2\delta^2)}{(1-2\delta+4\delta^2)}}\frac{1}{(\xi-\xi_2)}$$

and

$$e^{\frac{(1-2\delta+4\delta^2)U}{3\delta^2}} \to \pm\sqrt{\frac{(1-2\delta-2\delta^2)}{(1-2\delta+4\delta^2)}}\frac{1}{(\xi-\xi_2)}, \tag{6.2.11}$$

where ξ_2 is another integration constant. The positive branch corresponds to point H and the negative branch to point G. These points are, therefore, the asymptotic limit of the exact solution (6.2.2) and correspond to $\xi \to \xi_2$ and hence $\bar{r} \to \infty$.

Whilst it may initially appear that trajectories are repelled from the point H, this is only the case in terms of the coordinate ξ. In terms of the more physically relevant quantity $\bar{r}$, the point H is an attractor. This can be seen from the first equation in (6.2.11). Taking the positive branch here it can be seen that $\bar{r}$ increases as ξ decreases. So, in terms of $\bar{r}$ the points G and H are both attractors, as $\bar{r} \to \infty$.

We can now see that in region I all trajectories appear to start at critical points corresponding to either $\bar{r} \to 0$ or constant and end at point G where $\bar{r} \to \infty$. Region II appears to share the same features as region I with all trajectories starting at either $\bar{r} \to 0$ or constant and ending at H where $\bar{r} \to \infty$. Region III has no critical points corresponding to $\bar{r} \to \infty$ and so all trajectories both begin and end on points corresponding to $\bar{r} \to 0$ or constant.

Therefore solutions with an asymptotic region in which $\bar{r} \to \infty$ only exist in regions I and II where the potential can be described by equation (6.2.3). Furthermore, all trajectories in regions I and II are attracted to the solution

$$ds^2 = -\bar{r}^{\frac{6\delta^2}{(1-\delta)^2}}dt^2 + \frac{(1-2\delta+4\delta^2)(1-2\delta-2\delta^2)}{(1-\delta)^4}d\bar{r}^2 + \bar{r}^2(d\theta^2+\sin^2\theta d\phi^2), \tag{6.2.12}$$

which is the asymptotic behaviour of the solution found by Chan, Horne and Mann [64]. We therefore conclude that all solutions with an asymptotic region in which

$\bar{r} \to \infty$ are attracted towards the solution (6.2.12) as $\bar{r} \to \infty$.

Rescaling the metric back to the original conformal frame, we therefore conclude that the generic asymptotic attractor solution to the field equations, (6.2.1), is

$$ds^2 = -r^{2\delta\frac{(1+2\delta)}{(1-\delta)}}dt^2 + \frac{(1-2\delta+4\delta^2)(1-2\delta-2\delta^2)}{(1-\delta)^2}dr^2 + r^2(d\theta^2 + \sin^2\theta d\phi^2) \quad (6.2.13)$$

as $r \to \infty$, which reduces to Minkowski space in the $\delta \to 0$ limit of GR.

6.2.2 Linearised Solution

We now proceed to find the general solution, to first order in perturbations, around the background described by (6.2.13). Writing the perturbed line-element as

$$\begin{aligned} ds^2 = &-r^{2\delta\frac{(1+2\delta)}{(1-\delta)}}(1+V(r))dt^2 \\ &+ \frac{(1-2\delta+4\delta^2)(1-2\delta-2\delta^2)}{(1-\delta)^2}(1+W(r))dr^2 + r^2(d\theta^2+\sin^2\theta d\phi^2) \end{aligned} \quad (6.2.14)$$

and making no assumptions about the order of R, the field equations (6.2.1) become, up to first order in V and W,

$$\begin{aligned} &\frac{\delta(1+2\delta)(1+2\delta^2)}{(1-\delta)^2r^2} + \frac{(1+2\delta^2)}{(1-\delta)}\frac{V'}{r} - \frac{\delta(1-2\delta)}{2(1-\delta)}\frac{W'}{r} + \frac{V''}{2} \\ &\qquad = \frac{\delta(1+2\delta)}{2}\frac{R'^2}{R^2} - \frac{\delta(1+2\delta)}{2(1-\delta)}\frac{R''}{R} - \frac{3\delta}{4(1-\delta)}\frac{R'}{R}V' \\ &\qquad\qquad - \frac{\delta(1+2\delta)(2+\delta)}{2(1-\delta)^2r}\frac{R'}{R} + \frac{\delta(1+2\delta)}{4(1-\delta)}\frac{R'}{R}W', \end{aligned} \quad (6.2.15)$$

$$\begin{aligned} &\frac{\delta(1+2\delta)(1-2\delta-2\delta^2)}{(1-\delta)^2r^2} - \frac{\delta(1+2\delta)}{(1-\delta)}\frac{V'}{r} + \frac{(2-\delta+2\delta^2)}{2(1-\delta)}\frac{W'}{r} - \frac{V''}{2} \\ &\qquad = -\frac{3\delta}{2}\frac{R'^2}{R^2} + \frac{3\delta}{2(1-\delta)}\frac{R''}{R} + \frac{\delta(1+2\delta)(2-\delta+2\delta^2)}{2(1-\delta)^2r}\frac{R'}{R} \\ &\qquad\qquad + \frac{\delta(1+2\delta)}{4(1-\delta)}\frac{R'}{R}V' - \frac{3\delta}{4(1-\delta)}\frac{R'}{R}W' \end{aligned} \quad (6.2.16)$$

and

$$-\frac{2\delta(3-4\delta+2\delta^2+8\delta^3)}{(1-\delta)^2r^2}+\frac{2(1-2\delta+4\delta^2)(1-2\delta-2\delta^2)}{(1-\delta)^2r^2}W-\frac{V'}{r}+\frac{W'}{r}$$
$$=-\delta(1+2\delta)\frac{R'^2}{R^2}+\frac{\delta(1+2\delta)}{(1-\delta)}\frac{R''}{R}+\frac{\delta(4-\delta+2\delta^2+4\delta^3)}{(1-\delta)^2r}\frac{R'}{R}$$
$$+\frac{\delta(1+2\delta)}{2(1-\delta)}\frac{R'}{R}V'-\frac{\delta(1+2\delta)}{2(1-\delta)}\frac{R'}{R}W'. \quad (6.2.17)$$

Expanding R to first order in V and W gives

$$R=-\frac{6\delta(1+\delta)}{(1-2\delta-2\delta^2)}\frac{1}{r^2}+R_1 \quad (6.2.18)$$

where

$$R_1=\frac{2(1+\delta+\delta^2)}{(1-2\delta-2\delta^2)}\frac{W}{r^2}-\frac{2(1-\delta)(1+2\delta^2)}{(1-2\delta-2\delta^2)(1-2\delta+4\delta^2)}\frac{V'}{r}$$
$$+\frac{(1-\delta)(2-\delta+2\delta^2)}{(1-2\delta-2\delta^2)(1-2\delta+4\delta^2)}\frac{W'}{r}$$
$$-\frac{(1-\delta)^2}{(1-2\delta-2\delta^2)(1-2\delta+4\delta^2)}V''. \quad (6.2.19)$$

Substituting (6.2.18) into the field equations (6.2.15), (6.2.16) and (6.2.17) and eliminating R_1 using (6.2.19) leaves

$$\frac{(1+\delta+\delta^2)(5-12\delta+12\delta^2+4\delta^3)}{3(1-\delta)^2(1+\delta)}\frac{W}{r}+\frac{(16-47\delta+76\delta^2-34\delta^3-16\delta^4+32\delta^5)}{6(1-\delta^2)(1-2\delta+4\delta^2)}W'$$
$$-\frac{(1+\delta+7\delta^2-19\delta^3+44\delta^4+20\delta^5)}{3(1-\delta^2)(1-2\delta+4\delta^2)}\frac{Y}{r}-\frac{(8-15\delta+18\delta^2+16\delta^3)}{6(1+\delta)(1-2\delta+4\delta^2)}Y'$$
$$=-\frac{(1-2\delta-2\delta^2)(5-12\delta+12\delta^2+4\delta^3)}{12(1-\delta^2)(1+\delta)}\frac{\psi}{r}-\frac{(1-2\delta-2\delta^2)}{4(1-\delta^2)}\psi',$$

$$-\frac{(1+2\delta)(1+\delta+\delta^2)(3-4\delta+4\delta^2)}{3(1-\delta)^2(1+\delta)}\frac{W}{r}-\frac{(1+2\delta)(2-\delta+2\delta^2)(3-4\delta+4\delta^2)}{6(1-\delta^2)(1-2\delta+4\delta^2)}W'$$
$$+\frac{(3-2\delta+17\delta^2-4\delta^3+40\delta^2)}{3(1-\delta^2)(1-2\delta+4\delta^2)}\frac{Y}{r}+\frac{(6-\delta+2\delta^2+20\delta^3)}{6(1+\delta)(1-2\delta+4\delta^2)}Y'$$
$$=\frac{(1+2\delta)(1-2\delta-2\delta^2)(3-4\delta+4\delta^2)}{12(1-\delta)^2(1+\delta)}\frac{\psi}{r}+\frac{(1+2\delta)(1-2\delta-2\delta^2)}{12(1-\delta^2)}\psi'.$$

and

$$-\frac{2(8-8\delta+3\delta^2+10\delta^3-28\delta^4-12\delta^5)}{3(1-\delta^2)(1+\delta)(1-2\delta-2\delta^2)}\frac{W}{r}-\frac{(13-22\delta+12\delta^2+26\delta^3-56\delta^4)}{3(1-\delta^2)(1-2\delta-2\delta^2)(1-2\delta+4\delta^2)}W'$$
$$+\frac{2(4+9\delta^2+8\delta^3-12\delta^4)}{3(1+\delta)(1-2\delta-2\delta^2)(1-2\delta+4\delta^2)}\frac{Y}{r}+\frac{(5-4\delta-4\delta^2+12\delta^3)}{3(1+\delta)(1-2\delta-2\delta^2)(1-2\delta+4\delta^2)}Y'$$
$$=\frac{(5-4\delta-4\delta^2+12\delta^3)}{6(1-\delta)^2(1+\delta)}\frac{\psi}{r}+\frac{(1+2\delta)}{6(1-\delta^2)}\psi'$$

where $Y = rV'$ and $\psi = r^3R_1'$, subject to the constraint (6.2.19).

For $-\frac{(7+3\sqrt{21})}{20} < \delta < -\frac{(7-3\sqrt{21})}{20}$ the general solution to this first order set of coupled equations is given, in terms of V and W, by

$$V(r) = c_1V_1(r) + c_2V_2(r) + c_3V_3(r) + \text{constant} \tag{6.2.20}$$
$$W(r) = -c_1V_1(r) + c_2W_2(r) + c_3W_3(r) \tag{6.2.21}$$

where

$$V_1 = -r^{-\frac{(1-2\delta+4\delta^2)}{(1-\delta)}}$$
$$V_2 = \frac{(1+2\delta)r^{-\frac{(1-2\delta+4\delta^2)}{2(1-\delta)}}}{2(2-3\delta+12\delta^2+16\delta^3)}\left((1+2\delta)^2\sin(A\log r)+2A(1-\delta)\cos(A\log r)\right)$$
$$W_2 = r^{-\frac{(1-2\delta+4\delta^2)}{2(1-\delta)}}\sin(A\log r)$$
$$V_3 = \frac{(1+2\delta)r^{-\frac{(1-2\delta+4\delta^2)}{2(1-\delta)}}}{2(2-3\delta+12\delta^2+16\delta^3)}\left((1+2\delta)^2\cos(A\log r)-2A(1-\delta)\sin(A\log r)\right)$$
$$W_3 = r^{-\frac{(1-2\delta+4\delta^2)}{2(1-\delta)}}\cos(A\log r)$$

and

$$A = -\frac{\sqrt{7 - 28\delta + 36\delta^2 - 16\delta^3 - 80\delta^4}}{2(1-\delta)}$$

which is a real number for the any δ in the range specified above. The extra constant in (6.2.20) is from the integration of Y and can be trivially absorbed into the definition of the time coordinate. The above solution satisfies the constraint (6.2.19) without imposing any conditions upon the arbitrary constants c_1, c_2 and c_3.

It can be seen by direct comparison that the constant c_1 is linearly related to the constant C in (6.2.2) by a factor that is a function of δ only. The constants c_2 and c_3 correspond to two new oscillating modes.

CHAPTER 7

Inhomogeneous Cosmological Solutions

We will present in this chapter inhomogeneous cosmological solutions to the scalar-tensor and fourth-order field equations. Considerations will be limited to space-times admitting spherically symmetric three dimensional space-like hypersurfaces. The existence of vacuum solutions with this symmetry shows explicitly that Birkhoff's theorem cannot be formulated in these theories.

In the scalar-tensor case we will also present a study of how the spherical collapse model works in these theories. Closed universes are matched to flat universes at a boundary and allowed to evolve seperately. Following the evolution of the scalar field in each region then allows for consideration of how spatial inhomogeneity in Newton's gravitational constant G can arise in a realistic universe.

This chapter is based on the work by Clifton, Mota and Barrow [75] and Clifton [69].

7.1 Scalar-Tensor Theories

Extensive studies have been made of cosmological solutions of scalar-tensor gravity theories [88], although they are limited in two respects. First, they usually focus on the simplest case of isotropic expansion with zero spatial curvature, where simple

exact solutions exist. Second, they are almost exclusively concerned with spatially homogeneous cosmologies. The latter restriction means that the value of G and its rate of change in time, $\dot{G}$, are required to be the same everywhere in the universe. We want to understand how G and $\dot{G}$ are expected to vary in space in a realistic inhomogeneous universe. Since, even on the scale of a typical galaxy, the amplitude of visible density inhomogeneities are of order 10^6, we need to go beyond linear perturbation theory for such an analysis.

Previous studies on inhomogenieties in physical constants have focussed on the formation of black holes (gravitational memory) and perturbative expansions (see [18, 22, 98, 99, 175, 176, 177]). In this work we confront this problem by tracing the evolution of G, first in exact inhomogeneous solutions and then in a simple, but not unrealistic, inhomogeneous universe in which a zero-curvature Brans-Dicke FRW background universe is populated by spherical overdensities which are modelled by positive curvature Brans-Dicke FRW universes in the dust-dominated era of the Universe's history. This will enable us to track the different evolution followed by $G(t)$ in the background universe and in the overdense regions, which eventually separate off from the background universe and start to contract to high-density separate closed universes. This process can produce significant differences between G and $\dot{G}$ in the background and in the overdensities. Eventually, the collapse of the spherical overdensities will be stopped by pressure and a complicated sequence of dissipative and relaxation processes will lead to virialisation. This state will provide the gravitational environment out of which which stars and planetary systems like our own will form, directly reflecting the local value of $G(t)$ inherited from their virialised protogalaxy or its parent protocluster. The simple model we use for inhomogeneities in density and in G has many obvious limitations, notably in its neglect of pressure, deviations from spherical symmetry, accretion, and interactions between inhomogeneities. Nonetheless, we expect that it will be indicative of the importance of taking spatial inhomogeneity into account. It provides the first step in a clear path towards improved realism in the modelling of inhomogeneities that mirrors the route followed in standard cosmological studies of galaxy formation with constant G.

7.1.1 Exact Solutions

Starting with a solution of Einstein's field equations with a scalar field we can apply a conformal transformation to arrive at a solution of the Brans-Dicke field equations in a vacuum. A spherically symmetric exact solution for the collapse of a minimally-coupled scalar field, ψ, in GR is known and is given by [105]

$$ds^2 = -(qt+b)(f^2(r)dt^2 - f^{-2}(r)dr^2) + R^2(r,t)(d\theta^2 + \sin^2\theta d\phi^2), \tag{7.1.1}$$

where

$$\begin{aligned} f^2(r) &= (1-\frac{2c}{r})^{\alpha}, \\ R^2(r,t) &= (qt+b)r^2(1-\frac{2c}{r})^{1-\alpha}, \\ \alpha &= \pm\frac{\sqrt{3}}{2}. \end{aligned}$$

The evolution of the minimally coupled scalar field, ψ, in the Einstein frame, is given by

$$\psi(r,t) = \pm\frac{1}{4\sqrt{\pi}} ln\left[d\left(1-\frac{2c}{r}\right)^{\frac{\alpha}{\sqrt{3}}}(qt+b)^{\sqrt{3}}\right]. \tag{7.1.2}$$

Here, q, b, c and d are constants. Now under the transformation to the Jordan frame, (2.2.6), where $\phi = \exp\left[\psi\sqrt{\frac{8\pi}{\omega+\frac{3}{2}}}\right]$, we obtain

$$\begin{aligned} d\bar{s}^2 = -\frac{B(t)^{1-\sqrt{3}/\beta}}{d^{1/\beta}A(r)^{\alpha/\sqrt{3}\beta}}\left[A(r)^{\alpha}dt^2 - A(r)^{-\alpha}dr^2\right] \\ + \frac{A(r)^{1-\alpha\frac{1+\sqrt{3}\beta}{\sqrt{3}\beta}}B(t)^{1-\sqrt{3}/\beta}r^2}{d^{1/\beta}}(d\theta^2 + sin^2\theta d\phi^2) \end{aligned} \tag{7.1.3}$$

and

$$\phi(r,t) = \left[dA(r)^{\alpha/\sqrt{3}}B(t)^{\sqrt{3}}\right]^{1/\beta} \tag{7.1.4}$$

where $A(r) = 1-\frac{2c}{r}$, $B(t) = qt+b$ and $\beta = \pm\sqrt{2\omega+3}$. We now assume that $q \neq 0$ (i.e. the metric is not static) and define the new time coordinate $\bar{t} = (qt+b)^{\frac{3}{2}-\frac{\sqrt{3}}{2\beta}}$.

In the limit that $c \to 0$ the r-dependence of the metric is removed and the space

becomes homogeneous. In this case we expect (7.1.3) to reduce to the FRW Brans-Dicke metric given in the last section. We see from the form of (7.1.3) that the metric should reduce to that of a flat FRW Brans-Dicke universe. Insisting on this limit requires us to set $\beta = \sqrt{2\omega+3}$, $q = \frac{2\beta}{3\beta-\sqrt{3}}$ and $d = 1$. This leaves the metric:

$$d\bar{s}^2 = -A(r)^{\alpha(1-\frac{1}{\sqrt{3}\beta})}d\bar{t}^2 + A(r)^{-\alpha(1+\frac{1}{\sqrt{3}\beta})}\bar{t}^{\frac{2(\beta-\sqrt{3})}{3\beta-\sqrt{3}}}\left[dr^2 + A(r)r^2(d\theta^2+\sin^2\theta d\phi^2)\right]. \quad (7.1.5)$$

Rewriting (7.1.4) with these coordinates and constants gives

$$\phi(r,t) = \left(1-\frac{2c}{r}\right)^{\pm\frac{1}{2\beta}}\bar{t}^{2/(\sqrt{3}\beta-1)}. \quad (7.1.6)$$

A comparison of (7.1.5) with the FRW solution (3.2.12) shows that (7.1.5) does indeed reduce to a flat vacuum FRW metric in the limit $c \to 0$ (an inhomogeneous universe requires $c \neq 0$). The metric (7.1.5) is asymptotically flat and has singularities at $\bar{t} = 0$ and $r = 2c$; the coordinates r and $\bar{t}$ therefore cover the ranges $0 \leq \bar{t} < \infty$ and $2 \leq \frac{r}{c} < \infty$.

The equations (7.1.39) and (7.1.6) can now be used to construct a plot of $G(r,t)$; this is done in figure 7.1 which was constructed by choosing the minus sign in (7.1.6). From the form of $G(r,t)$ we see that this choice corresponds to an overdensity in the mass distribution (identified by comparison with the inhomogeneous Brans-Dicke solution with matter, found below). In this figure ω was set equal to 100 and c to 1. This plot shows how G can vary in space and time in an inhomogeneous universe which consists of a static Schwarzschild-like mass sitting at $r = 0$ in an expanding universe. As $r \to \infty$ it can be seen that this solution approaches the behaviour of a Brans-Dicke FRW universe.

An Inhomogeneous Brans-Dicke Solution With Matter

We now seek a solution of the Brans-Dicke field equations (2.1.8) with the form

$$ds^2 = -e^{\nu}dt^2 + e^{\mu}a^2(dr^2 + r^2d\theta^2 + r^2\sin^2\theta d\phi^2) \quad (7.1.7)$$

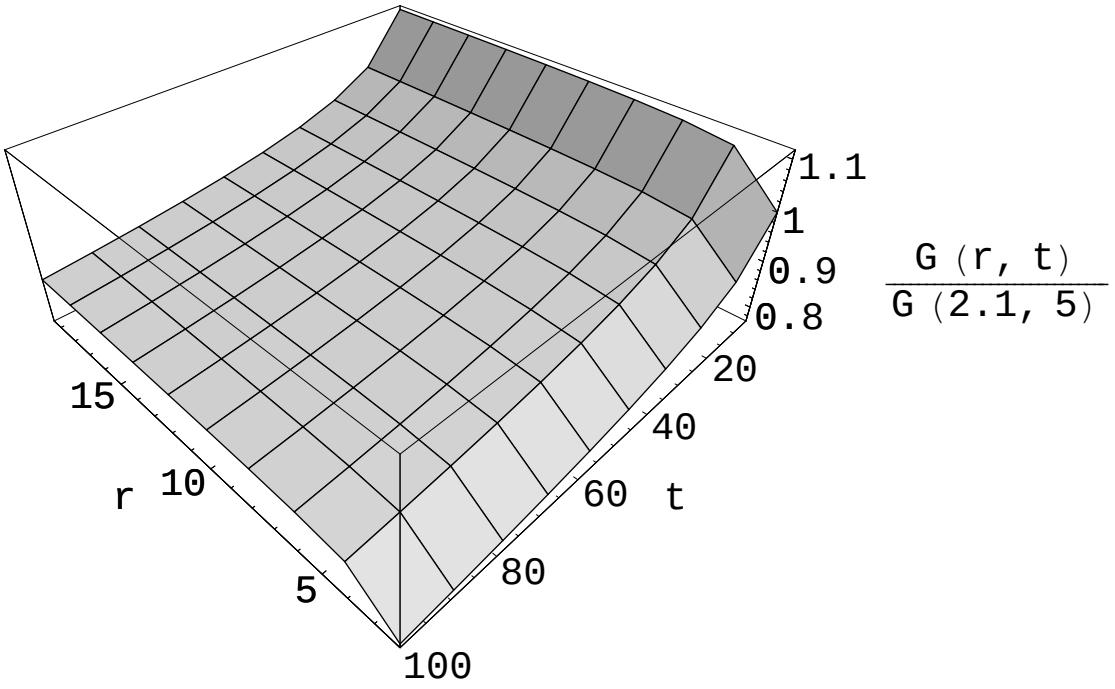

Figure 7.1: *This graph illustrates the possible space and time variations that can arise in G in inhomogeneous solutions to the Brans-Dicke field equations with $\omega = 100$, normalised at $r = 2.1$ and $t = 5$.*

where $e^{\nu} = e^{\nu(r)}$, $e^{\mu} = e^{\mu(r)}$ and $a = a(t)$. Substituting (7.1.7) into (2.1.8) gives, for a perfect fluid

$$\frac{8\pi}{\phi}p = -\left[2\frac{\ddot{a}}{a} + \left(\frac{\dot{a}}{a}\right)^2 + \frac{\omega}{2}\left(\frac{\dot{\phi}}{\phi}\right)^2 + 2\frac{\dot{a}}{a}\frac{\dot{\phi}}{\phi} + \frac{\ddot{\phi}}{\phi}\right]e^{-\nu} + \left[\frac{\mu'^2}{4} + \frac{\mu'\nu'}{r} + \frac{\mu'\nu'}{2} - \frac{\omega}{2}\left(\frac{\phi'}{\phi}\right)^2 + \frac{\phi'}{\phi}\left(\mu' + \frac{\nu'}{2} + \frac{2}{r}\right)\right]e^{-\mu}a^{-2}, \quad (7.1.8)$$

$$\frac{8\pi}{\phi}p = -\left[2\frac{\ddot{a}}{a} + \left(\frac{\dot{a}}{a}\right)^2 + \frac{\omega}{2}\left(\frac{\dot{\phi}}{\phi}\right)^2 + 2\frac{\dot{a}}{a}\frac{\dot{\phi}}{\phi} + \frac{\ddot{\phi}}{\phi}\right]e^{-\nu}$$
$$+\left[\frac{\mu''\nu''}{2} + \frac{\nu'^2}{4} + \frac{\mu'+\nu'}{2r} + \frac{\omega}{2}\left(\frac{\phi'}{\phi}\right)^2 + \frac{\phi''}{\phi} + \left(\frac{\nu'}{2}+\frac{1}{r}\right)\frac{\phi'}{\phi}\right]e^{-\mu}a^{-2}, \quad (7.1.9)$$

and

$$-\frac{8\pi}{\phi}\rho = -\left[3\left(\frac{\dot{a}}{a}\right)^2 - \frac{\omega}{2}\left(\frac{\dot{\phi}}{\phi}\right)^2 + 3\frac{\dot{a}}{a}\frac{\dot{\phi}}{\phi}\right]e^{-\nu}$$
$$+\left[\mu'' + \frac{\mu'^2}{4} + \frac{2\mu'}{r} + \frac{\omega}{2}\left(\frac{\phi'}{\phi}\right)^2 + \frac{\phi''}{\phi} + \left(\frac{\nu'}{2}+\frac{1}{r}\right)\frac{\phi'}{\phi}\right]e^{-\mu}a^{-2} \quad (7.1.10)$$

as the T^{11}, T^{22} and T^{00} equations, respectively. The propagation equation (2.1.9) now becomes

$$\frac{8\pi(\rho-3p)}{(2\omega+3)\phi} = \left[\frac{\ddot{\phi}}{\phi} + 3\frac{\dot{a}}{a}\frac{\dot{\phi}}{\phi}\right]e^{-\nu} - \left[\frac{\phi''}{\phi} + \frac{(\mu'+\nu')}{2}\frac{\phi'}{\phi} + \frac{2}{r}\frac{\phi'}{\phi}\right]e^{-\mu}a^{-2} \quad (7.1.11)$$

and the only other non-trivial field equation is that for T^{10}:

$$\nu'\frac{\dot{a}}{a} - \omega\frac{\dot{\phi}}{\phi}\frac{\phi'}{\phi} - \frac{\dot{\phi}'}{\phi} + \frac{\dot{a}}{a}\frac{\phi'}{\phi} + \frac{\nu'}{2}\frac{\dot{\phi}}{\phi} = \frac{8\pi}{\phi}(\rho+p)ve^{\frac{\nu}{2}} \quad (7.1.12)$$

where v is the three velocity of the perfect fluid. We now assume ϕ is of the form $\phi(r,t) = \phi(r)\phi(t)$ and look for solutions to the set of equations

$$\frac{\mu'^2}{4} + \frac{\mu'\nu'}{r} + \frac{\mu'\nu'}{2} = \frac{\omega(r)}{2}\left(\frac{\phi'(r)}{\phi(r)}\right)^2 - \frac{\phi'(r)}{\phi(r)}\left(\mu' + \frac{\nu'}{2} + \frac{2}{r}\right), \quad (7.1.13)$$

$$\frac{\mu''\nu''}{2} + \frac{\nu'^2}{4} + \frac{\mu'+\nu'}{2r} = -\frac{\omega}{2}\left(\frac{\phi'(r)}{\phi(r)}\right)^2 - \frac{\phi''(r)}{\phi(r)} - \left(\frac{\nu'}{2}+\frac{1}{r}\right)\frac{\phi'(r)}{\phi(r)}, \quad (7.1.14)$$

$$\mu'' + \frac{\mu'^2}{4} + \frac{2\mu'}{r} = -\frac{\omega}{2}\left(\frac{\phi'(r)}{\phi(r)}\right)^2 - \frac{\phi''(r)}{\phi(r)} - \left(\frac{\nu'}{2}+\frac{1}{r}\right)\frac{\phi'(r)}{\phi(r)}, \quad (7.1.15)$$

and

$$\frac{\phi''(r)}{\phi(r)} + \frac{(\mu' + \nu')}{2}\frac{\phi'(r)}{\phi(r)} + \frac{2}{r}\frac{\phi'(r)}{\phi(r)} = 0. \tag{7.1.16}$$

Such solutions are given by [136] as

$$e^{\nu} = \left(\frac{1 - \frac{c}{2kr}}{1 + \frac{c}{2kr}}\right)^{2k}, \tag{7.1.17}$$

$$e^{\mu} = \left(1 + \frac{c}{2kr}\right)^{4}\left(\frac{1 - \frac{c}{2kr}}{1 + \frac{c}{2kr}}\right)^{2(k-1)(k+2)/k}, \tag{7.1.18}$$

and

$$\phi(r) = \phi_0\left(\frac{1 - \frac{c}{2kr}}{1 + \frac{c}{2kr}}\right)^{-2(k^2-1)/k} \tag{7.1.19}$$

where $k = \sqrt{\frac{4+2\omega}{3+2\omega}}$. For e^{ν} and e^{μ} of this form, equations (7.1.8), (7.1.10) and (7.1.11) become

$$\frac{8\pi(\rho e^{\nu} - 3pe^{\nu})}{(2\omega + 3)\phi(t)} = \frac{\ddot{\phi}(t)}{\phi(t)} + 3\frac{\dot{a}}{a}\frac{\dot{\phi}(t)}{\phi(t)}, \tag{7.1.20}$$

$$\frac{8\pi}{\phi(t)}\rho e^{\nu} = 3\left(\frac{\dot{a}}{a}\right)^2 - \frac{\omega}{2}\left(\frac{\dot{\phi}(t)}{\phi(t)}\right)^2 + 3\frac{\dot{a}}{a}\frac{\dot{\phi}(t)}{\phi(t)}, \tag{7.1.21}$$

and

$$-\frac{8\pi}{3\phi(t)}\frac{(3\omega p e^{\nu} + 3\rho e^{\nu} + \omega\rho e^{\nu})}{(2\omega + 3)} = \frac{\ddot{a}}{a} - \frac{\dot{a}}{a}\frac{\dot{\phi}(t)}{\phi(t)} + \frac{\omega}{3}\left(\frac{\dot{\phi}(t)}{\phi(t)}\right)^2. \tag{7.1.22}$$

Here (7.1.22) was obtained by substituting (7.1.8) and (7.1.10) into (7.1.11) and discarding the terms involving r derivatives, as these now sum to zero. We see that (7.1.20), (7.1.21) and (7.1.22) are simply (3.1.1), (3.1.2) and (3.1.3) with $k = 0$, $p_{FRW} = pe^{\nu}$ and $\rho_{FRW} = \rho e^{\nu}$, where subscript FRW denotes a quantity derived from the field equations using the FRW metric. We also have, from $T^{ab}{}_{;b} = 0$, that

$$\frac{d}{dt}(\rho e^{\nu}) + 3H(\rho e^{\nu} + pe^{\nu}) = 0. \tag{7.1.23}$$

Looking for solutions of the form $a \propto t^x$ and $\phi(t) \propto t^y$ gives, on substitution into (7.1.20), the relation $y = 2 - 3x\gamma$ (assuming an equation of state for the Universe

of the form $p = (\gamma - 1)\rho$). Using (7.1.20), (7.1.21), and this relation then gives the solutions

$$a(t) = a_0 \left(\frac{t}{t_0}\right)^{\frac{2\omega(2-\gamma)+2}{3\omega\gamma(2-\gamma)+4}} \tag{7.1.24}$$

and

$$\phi(t) = \phi_0 \left(\frac{t}{t_0}\right)^{\frac{2(4-3\gamma)}{3\omega\gamma(2-\gamma)+4}}. \tag{7.1.25}$$

These are exactly the same as would be expected for the scale factor and the Brans-Dicke field in a flat FRW universe [135]. The form of ρ is then given by (7.1.23) and (7.1.17) as

$$\rho(r,t) = \rho_0 \left(\frac{a_0}{a(t)}\right)^{3\gamma} \left(\frac{1-\frac{c}{2kr}}{1+\frac{c}{2kr}}\right)^{-2k}, \tag{7.1.26}$$

and $\phi(r,t)$ is given as

$$\phi(r,t) = \phi_0 \left(\frac{t}{t_0}\right)^{\frac{2(4-3\gamma)}{3\omega\gamma(2-\gamma)+4}} \left(\frac{1-\frac{c}{2kr}}{1+\frac{c}{2kr}}\right)^{-2(k^2-1)/k}. \tag{7.1.27}$$

This separable solution displays the same time dependence as the power-law FRW Brans-Dicke universes, (3.2.2)-(3.2.3), but with an additional inhomogeneous r-dependence created by the matter source at $r = 0$. Such a distribution of matter in space is illustrated by figure 7.2. Here we have chosen, for illustrative purposes, $\gamma = 1$, $\omega = 100$ and a background value set by the choice $\rho = \rho_{FRW}$ (ρ_{FRW} being the matter density that would be expected in the corresponding homogeneous universe). The temporal evolution of ρ is the same as the FRW case.

We see from figure 7.2 that the matter density is isotropic and asymptotically constant as $r \to \infty$ with a sharp power-law peak near the origin. Now (7.1.27) gives us

$$G(r,t) = G_0 \left(\frac{1-\frac{c}{2kr}}{1+\frac{c}{2kr}}\right)^{2(k^2-1)/k} t^{-\frac{2(4-3\gamma)}{3\omega\gamma(2-\gamma)+4}}. \tag{7.1.28}$$

Equation (7.1.28) is used, with the values $\omega = 100$, $\gamma = 1$ and $c = 0.5$ to create figure 7.3, which shows the space-time evolution of $G(r,t)$.

These results show how $G(r,t)$ can vary in space and time in an asymptotically-flat universe with a peak of matter at the origin. Observers located near the mass concentration will determine different values of G locally, although they will find

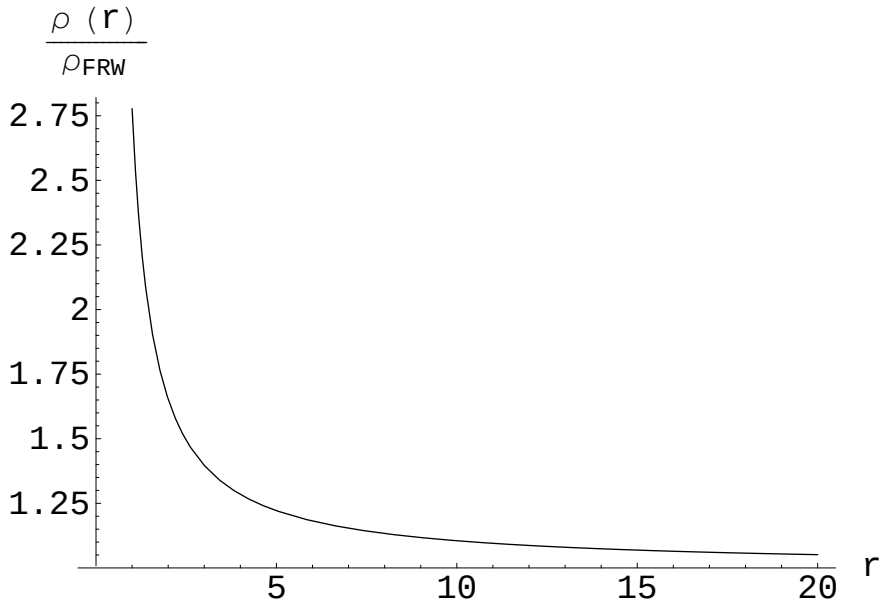

Figure 7.2: *Distribution of ρ as a function of r, with $\omega = 100$, from equation (7.1.26) and $c = 0.5$.*

the same values of $\dot{G}/G$ everywhere because of the separable nature of the $G(r,t)$ evolution in equation (7.1.26). This was also the case for solution (7.1.6) given in subsection 7.1.1. In the next section we shall consider a more realistic model in which both G and $\dot{G}/G$ are different from place to place. Plots like figure 7.3 can be generated for universes dominated by other types of cosmological fluid and with different rates of density fall off with r.

7.1.2 Spherical Collapse Model

Matching Two Vacuum FRW Brans-Dicke Universes

We will now consider a simple model of a spherically symmetric cosmological inhomogeneity produced by matching together flat and positively curved vacuum FRW Brans-Dicke universes. This is a well studied technique, first introduced by Lemaître, for studying the non-linear evolution of overdensities in general relativistic FRW universes. The overdense region is modelled as a closed universe that at first expands more slowly than the background, before reaching an expansion maximum and col-

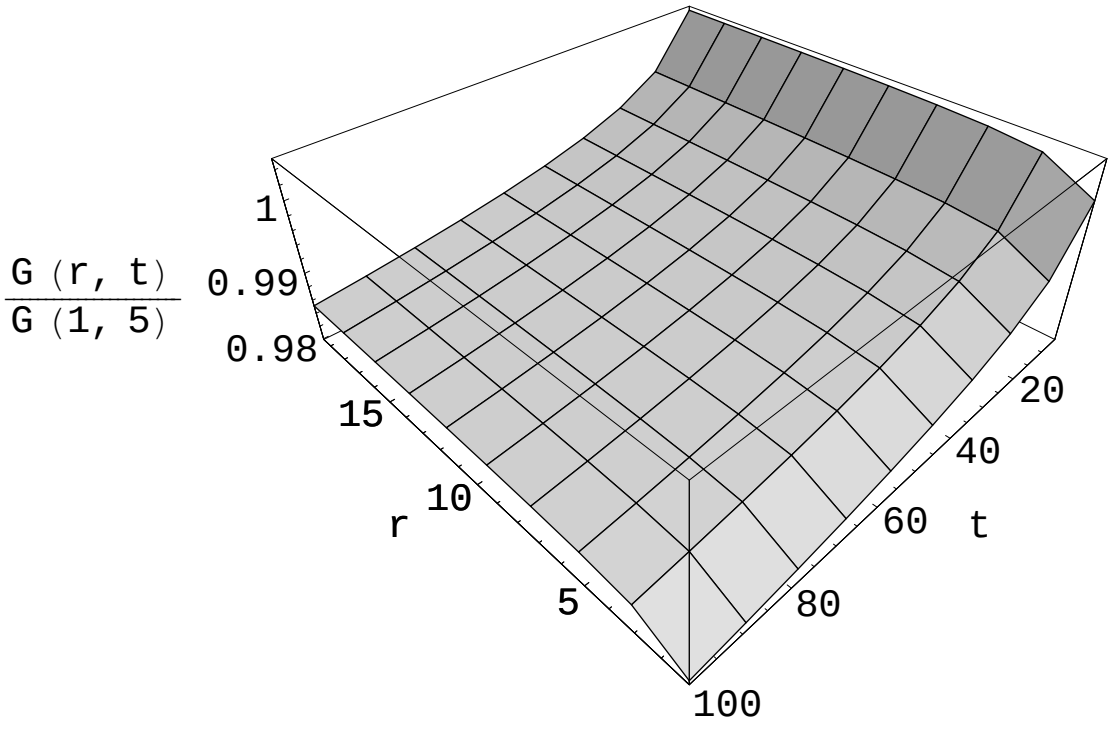

Figure 7.3: *Evolution of $G(r,t)$ in space and time in an inhomogeneous matter dominated Universe, with $\omega = 100$, from equation (7.1.28) and $c = 0.5$.*

lapsing back to high density, whilst the background continues to expand. In this section we consider vacuum universes only, with $\rho = p = 0$.

For flat vacuum FRW universes the Friedmann equation (3.1.3) gives

$$\left(\frac{\dot{a}}{a}\right)^2 + \frac{\dot{a}}{a}\frac{\dot{\phi}_b}{\phi_b} = \frac{\omega}{6}\left(\frac{\dot{\phi}_b}{\phi_b}\right)^2 \tag{7.1.29}$$

where $\dot{} = \frac{d}{dt}$, $\phi_b = \phi_b(t)$ is the Brans-Dicke scalar field and a is the scale factor in the flat background. For a positively curved ($k = +1$) region the scale factor is taken to be $S(\tau)$, which satisfies the Friedmann equation for the closed vacuum Brans-Dicke

universe:

$$\left(\frac{S'}{S}\right)^2 + \frac{S'}{S}\frac{\phi_p'}{\phi_p} = \frac{\omega}{6}\left(\frac{\phi_p'}{\phi_p}\right)^2 - \frac{k}{S^2}, \tag{7.1.30}$$

where $' = \frac{d}{d\tau}$, $\phi_p = \phi_p(\tau)$ and τ and k are the proper time and curvature of this perturbed region.

In matching these two regions at $t = t_0 = \tau_0$ we must satisfy the boundary conditions

$$S(\tau_0) = a(t_0), \qquad \phi_p(\tau_0) = \phi_b(t_0)$$

and

$$\left(\frac{dS}{d\tau}\right)_0 = \left(\frac{da}{dt}\right)_0, \qquad \left(\frac{d\phi_p}{d\tau}\right)_0 = \left(\frac{d\phi_b}{dt}\right)_0.$$

From η to t

The function $\tau(\eta)$ is now obtained by integrating $Sd\eta = d\tau$ and $\tau(\eta)$ can then be used to obtain $S(\tau)$. We now require a relation between t and τ. For this we proceed as in reference [32] and use the equation of relativistic hydrostatic equilibrium [100, 101, 117]

$$\frac{\partial\Phi}{\partial r} = -\frac{\partial p/\partial r}{p+\rho} \tag{7.1.31}$$

where Φ is the Newtonian gravitational potential and r is radial distance. Equation (7.1.31) is derived under the assumptions that the configuration is static and the gravitational field is weak, so Φ completely determines the metric; then (7.1.31) is given by the conservation of energy-momentum for a perfect fluid. We now use $d\tau = e^{\Phi}dt$, and for a scalar field we have an effective equation of state with $p = \rho$ and $\rho = \frac{\omega}{\phi}\dot{\phi}^2$. Combining these results gives

$$\frac{d\tau}{dt} = \frac{\dot{\phi}_b}{\phi_p'}\frac{\phi_p^{1/2}}{\phi_b^{1/2}}. \tag{7.1.32}$$

Now $\dot{\phi}_b \propto a^{-3}$ and $\phi_p' \propto S^{-3}$, and so with the solutions (3.2.17) and (3.2.12) this gives

$$\frac{d\tau}{dt} = \frac{\sin^{1/2}(2\sqrt{k}\eta)}{\sin^{1/2}(2\sqrt{k}\eta_0)} \frac{S^2}{S_0^2} \frac{a^{\sqrt{1+\frac{2}{3}\omega}-4}}{a_0^{\sqrt{1+\frac{2}{3}\omega}-4}} \tag{7.1.33}$$

Equation (7.1.33) and the relation $Sd\eta = d\tau$ allow us to obtain $S(t)$ from (3.2.18). This is done numerically. Now fixing the constants of proportionality together with k in equations (3.2.18), (3.2.17) and (3.2.12), in order to satisfy the boundary conditions, we find equations for the evolution of the scale factors and scalar fields in the flat background and perturbed region. These are matched at a boundary, at time $t_0 = \tau_0 = \eta_0$.

Results

Figure 7.4 shows the evolution of $a(t)$ and $S(t)$ when the region described by $S(t)$ becomes positively curved at initial time $t_0 = 1$. In figure 7.4 we choose $\omega = 100$, for illustrative purposes, and $a_0 = S_0 = 1$ so that the boundary condition for the matching of the first derivatives of the scale factors is given by $\left(\frac{dS}{d\tau}\right)_0 = \left(\frac{dS}{d\eta}\right)_0 = \left(\frac{da}{dt}\right)_0$.

We can now express $G = G(t)$ in the regions of different curvature using equation (7.1.39) and the flat and closed FRW solutions (3.2.17) and (3.2.12), along with the appropriate coordinate transformations. This gives figure 7.5. It is clearly seen that the evolution of $G(t)$ is quite different in the two regions, as expected. The collapsing overdensity evolves faster than the background and possesses a smaller value of G but a larger value of $|\dot{G}/G|$ at all times after the matching.

7.1.3 A More Refined Spherical Collapse Model

We now generalise the spherical collapse model described in the last section to the more realistic case of a flat universe containing matter and a cosmological constant (see. e.g. refs. [149], [150] or [116]). As before, we match a flat Brans-Dicke FRW background to a spherically symmetric overdensity at an appropriate boundary and allow the two regions to evolve separately.

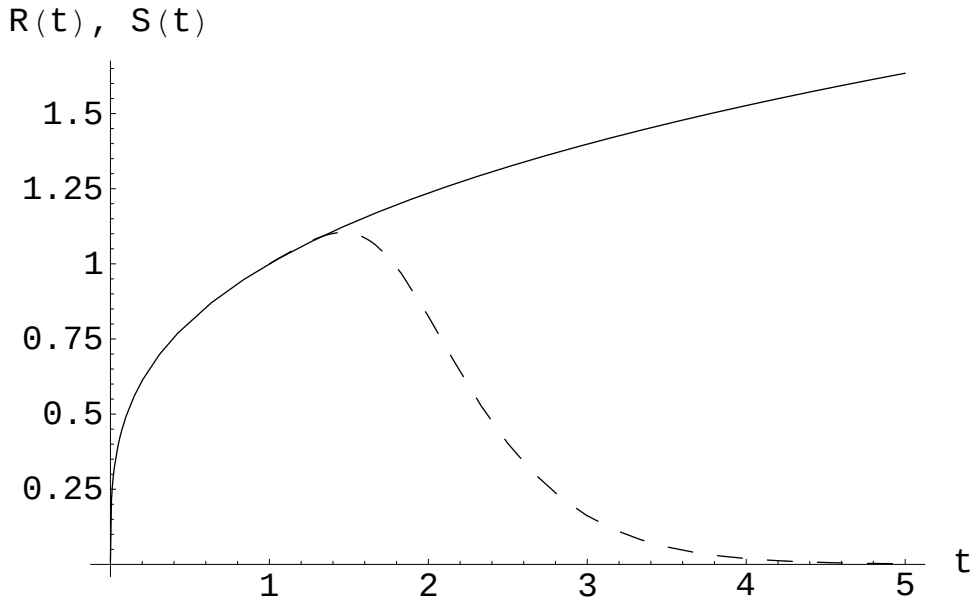

Figure 7.4: *Evolution of the scale factor S in the perturbed overdense region (dashed line) and in the background a(solid line) with respect to the comoving proper time in the flat background.*

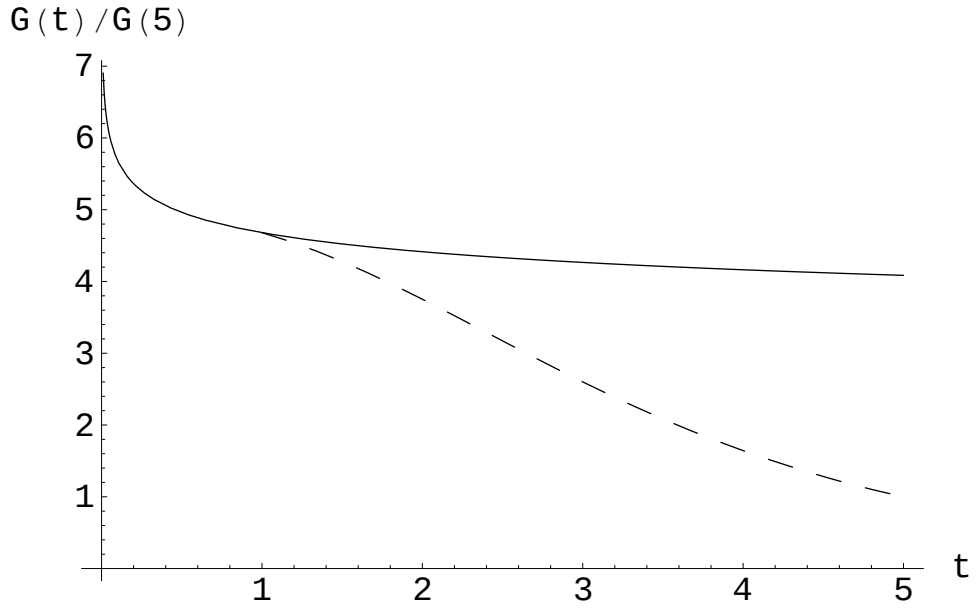

Figure 7.5: *Evolution of $G(t)$ in the overdense perturbed overdense region of positive curvature (dashed line) and in the spatially flat background universe (solid line).*

The background universe

Again, we consider a flat ($k = 0$), homogeneous and isotropic background universe. Since we are interested in the matter-dominated epoch, when structure formation starts, we can assume that our universe contains only matter and a vacuum energy contribution so that $\rho = \rho_m + \rho_\Lambda$ and $p = p_\Lambda = -\rho_\Lambda$ give the total density and pressure, respectively. So, for the flat background, the Friedmann equation (3.1.3) gives for a general $\omega(\phi)$ theory,

$$\left(\frac{\dot{a}}{a}\right)^2 + \frac{\dot{a}}{a}\frac{\dot{\phi}}{\phi} = \frac{\omega}{6}\frac{\dot{\phi}^2}{\phi^2} + \frac{8\pi}{3\phi}(\rho_m + \rho_\Lambda) \tag{7.1.34}$$

and the scalar field equation (3.1.2) gives

$$\ddot{\phi} + 3\frac{\dot{a}}{a}\dot{\phi} = \frac{8\pi}{(2\omega+3)}(\rho_m + 4\rho_\Lambda) - \frac{\dot{\omega}\dot{\phi}}{(2\omega+3)}. \tag{7.1.35}$$

Here, $\rho_m \propto a(t)^{-3}$ and $\rho_\Lambda =$ constant. These equations govern the evolution of $\phi(t)$ and $a(t)$ in the flat expanding cosmological background. The contribution of the vacuum energy stress ($p = -\rho$) to the Friedmann equation (7.1.34) in Brans-Dicke cosmology differs from that in GR because of the presence of the variable ϕ field: it is not the same as the addition of a cosmological constant term to the right-hand side of (7.1.34). However, with this proviso, we shall continue to refer to ΛCDM models in Brans-Dicke theories in the following sections.

The overdensity

Again, we consider a spherical overdense region of radius S and model the interior space-time as a closed FRW Brans-Dicke universe, ignoring any anisotropic effects of gravitational instability or collapse. As usual, we assume there is no shell-crossing; this implies mass conservation inside the overdensity [149]. The evolution equations can now be written in a form that ignores the spatial dependence of the fields. Now $\rho = \rho_{CDM} + \rho_\Lambda$ and $p = p_\Lambda = -\rho_\Lambda$, where 'CDM' corresponds to cold dark matter,

so that the acceleration equation (3.1.5) gives

$$\ddot{S} - \dot{S}\frac{\dot{\phi_c}}{\phi_c} = -S\left(\frac{\omega_c}{3}\frac{\dot{\phi_c}^2}{\phi_c^2} - \frac{1}{2}\frac{\dot{\omega}_c}{(2\omega_c+3)}\frac{\dot{\phi_c}}{\phi_c} + \frac{8\pi}{3\phi_c}\frac{(\rho_{CDM}(3+\omega_c)+\rho_\Lambda(3-2\omega_c))}{(2\omega_c+3)}\right), \quad (7.1.36)$$

while the scalar field equation (3.1.2) reduces to

$$\ddot{\phi_c} + 3\frac{\dot{S}}{S}\dot{\phi_c} = \frac{8\pi}{(2\omega_c+3)}(\rho_{CDM}+4\rho_\Lambda) - \frac{\dot{\omega}_c\dot{\phi_c}}{(2\omega_c+3)} \quad (7.1.37)$$

where $S = S(t)$ is the scale factor and $\phi_c = \phi_c(t)$ is the Brans-Dicke scalar field in the collapsing region of positive curvature where $\rho_{CDM} \propto S(t)^{-3}$ and $\rho_\Lambda =$ constant. These equations give the evolution of $\phi_c(t)$ and $S(t)$.

We have assumed that the equation of motion of the field inside the cluster overdensity is described by the local space-time geometry. This means that the field follows the dark-matter collapse from the beginning of the cluster's formation. We do not consider this to be fully realistic since there is expected to be an outflow of energy associated with ϕ from the overdensity to the background universe, as first noticed by Mota and van de Bruck ([130]). The details of this outflow of energy and its effect on the collapse can only be determined by a fully relativistic hydrodynamical calculation, which is beyond the scope of this study. Nevertheless, at late times during the collapse of the dark matter (and especially when the density contrast in the dark matter is very large) the field should no longer feel the effects of the expanding background and will decouple from it. We are also neglecting the effects of deviations from spherical symmetry, which grow during the collapse in the absence of pressure, along with rotation, gravitational tidal interactions between different overdensities, and all forms of non-linear hydrodynamical complexity.

Evolution of the overdensity

Consider a spherical perturbation in the dark matter fluid with a spatially constant internal density. Initially, this perturbation is assumed to have a density amplitude $\delta_i > 0$ where $|\delta_i| \ll 1$. The initial density of dark matter inside the overdensity is

therefore $\rho_{CDM} = \rho_m(1 + \delta_i)$.

Four characteristic phases of the overdensity's evolution can be identified:

- *Expansion*: we employ the initial boundary condition $\phi_c = \phi$ and assume that at early times the overdensity expands along with the background.
- *Turnaround*: for a sufficiently large δ_i, gravity prevents the overdensity from expanding forever; the spherical overdensity breaks away from the general expansion and reaches a maximum radius. Turnaround is defined as the time when $S = S_{max}$, $\dot{S} = 0$ and $\ddot{S} < 0$.
- *Collapse*: the overdensity subsequently collapses ($\dot{S} < 0$). If pressure and dissipative physics are ignored the overdensity would collapse to a singularity where the density of matter would tend to infinity. In reality this singularity does not occur; instead, the kinetic energy of collapse is transformed into random motions.
- *Virialisation*: dynamical equilibrium is reached and the system becomes stationary with a fixed radius and constant energy density.

We require our spherical overdensity to evolve from the linear perturbation regime at high redshift until it becomes non-linear, collapses, and virialises.

Virialisation

In scalar-tensor theories we expect that the gravitational potential will not be of the standard local r^{-1} form. This requires reconsideration of the virial condition. According to the virial theorem, equilibrium will be reached when [93]

$$T = \frac{1}{2} S \frac{\partial U}{\partial S} \tag{7.1.38}$$

where T is the average total kinetic energy, U is the average total potential energy and S here denotes the radius of the spherical overdensity.

The potential energy for a given component x can be calculated from its general form in a spherical region [117]

$$U_x = 2\pi \int_0^S \rho_{tot} \Phi_x r^2 dr,$$

where ρ_{tot} is the total energy density and Φ_x is the gravitational potential due to the density component ρ_x.

The gravitational potential Φ_x can be obtained from the weak-field limit of the field equations (2.1.8). This results in a Poisson equation where the terms associated to the scalar field can be absorbed into the definition of the Newtonian constant as [191]

$$G_c = \frac{4 + 2\omega_c(\phi_c)}{3 + 2\omega_c(\phi_c)} \frac{1}{\phi_c}. \tag{7.1.39}$$

This results in the usual form for the Newtonian potential

$$\Phi_x(s) = -2\pi G_c \rho_x (3\gamma_x - 2) \left(S^2 - \frac{r^2}{3} \right)$$

where G_c is given by equation (7.1.39) and $\gamma_x - 1$ is p_x/ρ_x for the fluid component with density ρ_x and pressure p_x (appearing due to the relativistic correction to Poisson's equation: $\Delta\Phi = 4\pi G(\rho + 3p)$).

In ΛCDM models of structure formation it is entirely plausible to set $\gamma_x = 1$ as the energy density of the cosmological constant is negligible on the virialised scales we are considering [188, 130]. The potential energy associated with a given component x inside the overdensity is now given by

$$U_x = -\frac{16\pi^2}{15} G_c \rho_{tot} \rho_x S^5. \tag{7.1.40}$$

Therefore, the virial theorem will be satisfied when

$$T_{vir} = \frac{1}{2} S_{vir} \left(\frac{\partial U}{\partial S} \right)_{vir},$$

where

$$\frac{\partial U}{\partial S} = -\frac{16\pi^2}{15} \left[\frac{\partial G_c}{\partial S} \rho_{tot} \rho_x S^5 + G_c \frac{\partial \rho_{tot}}{\partial S} \rho_x S^5 + G_c \rho_{tot} \frac{\partial \rho_x}{\partial S} S^5 + G_c \rho_{tot} \rho_x 5 S^4 \right] \tag{7.1.41}$$

and we have used $U_{tot} = U_{CDM} + U_\Lambda + U_{\phi_c}$, $\rho_{tot} = \rho_{CDM} + \rho_\Lambda + \rho_{\phi_c}$, $\rho_{\phi_c} = \omega_c \dot{\phi}^2/\phi$ and

$$\frac{\partial G_c}{\partial S} = \frac{\dot{G}_c}{\dot{S}} = -G_c \, \dot{\phi}_c \frac{3 + 2\omega_c}{4 + 2\omega_c} \left(G_c + \frac{2\omega_c'(\phi_c)}{(3 + 2\omega_c)^2} \right).$$

The other components of equation (7.1.41) are obtained from equations (7.1.36) and (7.1.37).

Using equation (7.1.38), together with energy conservation at turnaround and virialisation, we obtain an equilibrium condition in terms of potential energies only

$$\frac{1}{2}S_{vir}\left(\frac{\partial U}{\partial S}\right)_{z_v} + U_{tot}(z_v) = U_{tot}(z_{ta}), \tag{7.1.42}$$

where z_v is the redshift at virialisation and z_{ta} is the redshift of the over-density at its turnaround radius. The behaviour of G during the evolution of an overdensity can now be obtained by numerically evolving the background equations (7.1.34) and (7.1.35) and the overdensity equations (7.1.36) and (7.1.37) until the virial condition (7.1.42) holds.

We point out here an inconsistency when one makes use of equation (7.1.42) together with the assumption that energy is conserved. This inconsistency is removed by assuming a negligible outflow of ϕ from the overdensity, in which case we regain energy conservation within the system and so retain self-consistency.

Overdensities vs Background

Brans-Dicke theory

The Brans-Dicke coupling parameter ω is constant and constrained by a variety of local gravitational tests (see [186] for a review). The strongest constraint to date is derived from observations of the Shapiro time delay of signals from the Cassini space craft as it passes behind the Sun. These considerations led Bertotti, Iess and Tortora [47], after a complicated data analysis process, to claim that ω must have a value greater than 40000, to 2σ. This limit on ω must be satisfied at all times in all parts of the universe, and leads to the conclusion that Brans-Dicke theory must be phenomenologically very similar to GR throughout most of the history of the universe. However, we do still expect a cosmological evolution of the Brans-Dicke field ϕ which determines the value of Newton's G; and we expect this evolution to be different in regions that collapse to form the structure probed by Cassini compared to that in the idealised expanding cosmological background, as described above. Hence we expect the measurable value of G to be different in these two distinct

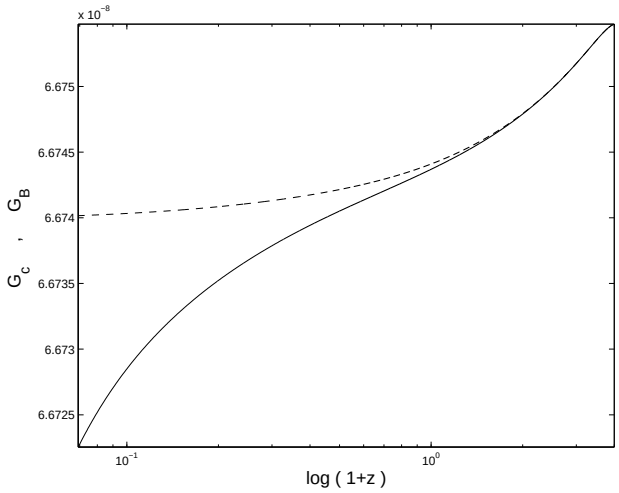

(a) $\omega = 40000$

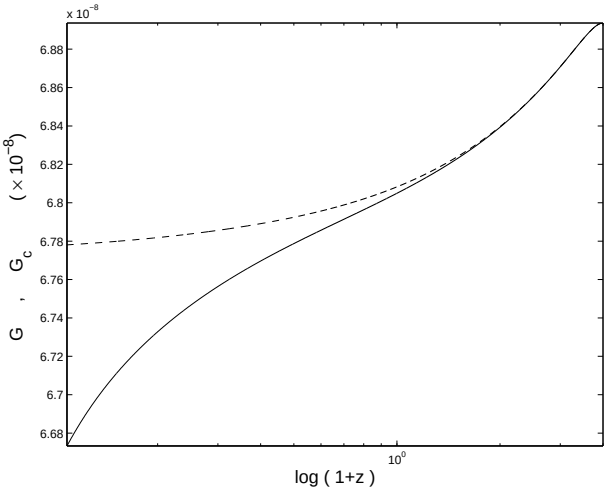

(b) $\omega = 500$

Figure 7.6: *Plots of G against $\ln(1+z)$ in the background (dashed-line) and in an overdensity (solid-line), for different values of ω. Initial conditions are chosen in both cases so as to give $G = G_0$, the present value of the Newton constant, at virialisation. We note that increasing ω decreases the difference in G between the overdensity and the background.*

regions with different histories.

The plots in figure 7.6 were constructed using the representative values $\omega = 40000$ and $\omega = 500$ and the boundary condition $\phi_{c0} \simeq G_0^{-1}$, so that the value of G measured inside the overdensity at present is equal to the value of Newton's G, as measured locally. The evolution of the background was determined by matching ϕ_c to ϕ at the time when the overdensity decouples from the background, t_i. We see a clear difference in the evolution of G in the two regions, as expected. This example shows that we expect different values of G and $\dot{G}/G$ inside and outside virialised overdensities. The present value of G and $\dot{G}/G$ depends on the history of the region where it was sampled, as well as on the Brans-Dicke coupling parameter, ω.

It can be seen from the plots in figure 7.6 that increasing ω has the effect of decreasing the difference in G between the background universe and the overdensity. The size of this inhomogeneity is found to be of order $1/\omega$ and, correspondingly, reduces to zero as $\omega \to \infty$. This is an important consistency check for the methods used as we expect Brans-Dicke theory to reduce to GR, with a constant G, in this limit.

Scalar-tensor theory with $2\omega + 3 = 2A\left|1 - \frac{\phi}{\phi_\infty}\right|^{-p}$

Next, we consider a scalar-tensor theory with a variable $\omega(\phi)$. We investigate the class of theories defined by the choice of coupling function

$$2\omega(\phi) + 3 = 2A\left|1 - \frac{\phi}{\phi_\infty}\right|^{-p},$$

where A, ϕ_∞, and p are positive definite constants. We refer to this as Theory 1. Such a choice of coupling was considered by Barrow and Parsons and was solved exactly for the case of a flat FRW universe containing a perfect fluid [37].

Setting the constants as $2A = (\phi_\infty/\beta)^2$ and $p = 2$ gives us the scalar-tensor theory considered by Damour and Pichon [77] and by Santiago, Kalligas and Wagoner [167]. This choice of $\omega(\phi)$ corresponds to setting $\ln A(\phi) = \ln A(\phi_0) + \frac{1}{2}\beta(\phi_\infty - \phi)^2$, where $A^2(\phi)$ is the conformal factor $1/\phi$ from equation (2.2.6). Damour and Nordvedt [76] consider this function as a potential and therefore justify its choice in relation to the generic parabolic form near a potential minimum. Expecting the

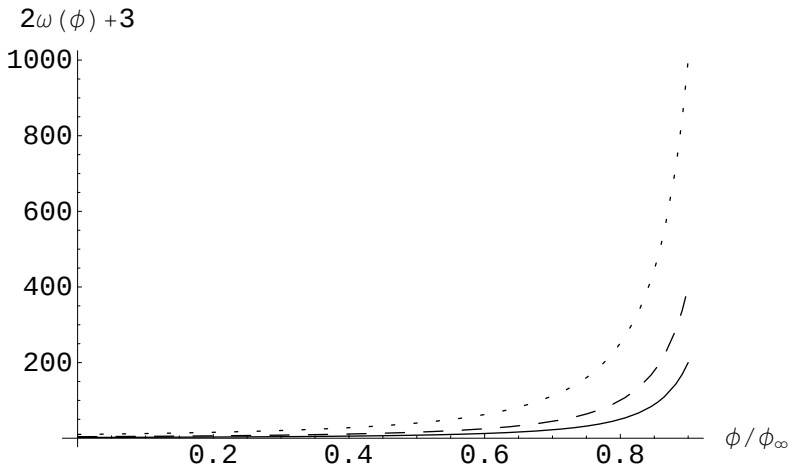

(a) $2\omega(\phi)+3$ for p=2 and A=1, 2 and 5 (solid, dashed and dotted lines, respectively).

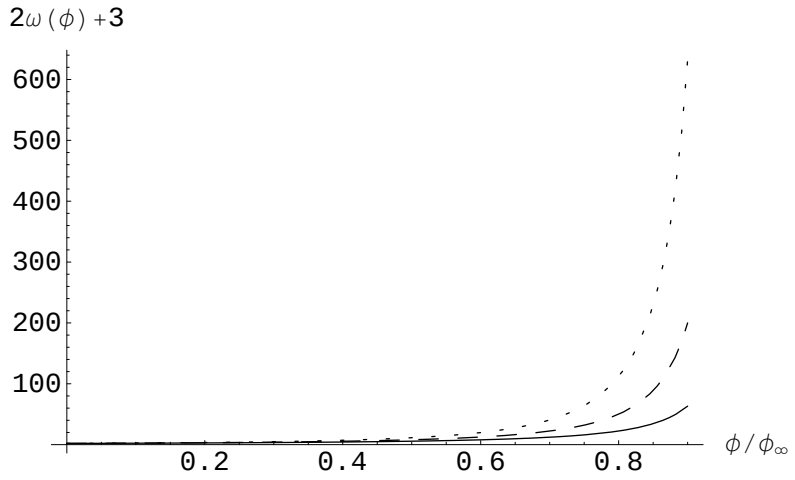

(b) $2\omega(\phi)+3$ for A=1 and p=1.5, 2 and 2.5 (solid, dashed and dotted lines, respectively).

Figure 7.7: In these gravity theories there is fast approach to general relativity at late times when $\phi \to \phi_\infty$, but significantly different behaviour at early times.

function to be close to zero (i.e. GR), Santiago, Kalligas and Wagoner justify its expression as a perturbative expansion. This choice of $\omega(\phi)$ with $p > 1/2$ corresponds to a general two-parameter class of scalar-tensor theories that are close to GR and will be drawn ever closer to it with $\omega \to \infty$ and $\omega'/\omega^3 \to 0$ as the universe expands and $\phi \to \phi_\infty$. We therefore consider it as a representative example of a wide family of plausible varying-G theories that generalise Brans-Dicke theory.

The evolution of this form of $\omega(\phi)$ is shown graphically in figure 7.7 for different values of A and p. Clearly the evolution of $\omega(\phi)$ is sensitive to both A and p and so the choice of these parameters is important for the form of the underlying theory. For illustrative purposes we choose here the values $p = 1.5, 2$ and 5 and $A = 1, 2$ and 5.

In a similar way to the Brans-Dicke case we now create an evolution of ϕ_c that virialises at $z = 0$ to give the value $G_{c0} = 6.673 \times 10^{-11}$, as observed experimentally. The corresponding evolution for ϕ_b is calculated as before by matching it to the value of ϕ_c at the time the overdensity decouples from the background and begins to collapse. In creating these plots we have used the conservative parameter values $p = 2$, $\omega_{c0} = 1.2 \times 10^5$ and $A = 6 \times 10^{-7}$ which are consistent with observation and allow structure formation to occur in a similar way to GR. The results of this are plotted in figure 7.8.

Again, we note the different evolution of $G(t)$ in the two regions, and the difference in the asymptotic values of G. We note that experimental measurements of G on Earth have a significant uncertainty with the 1998 CODATA value carrying an uncertainty 12 times *greater* than the standard value adopted in 1987. The 1998 value is given as [127, 169]

$$G_{1998} = 6.673 \pm 0.010 \times 10^{-8} cm^3 gm^{-1} s^{-2},$$

while the 2002 CODATA pre-publication announcement reverts to the earlier higher accuracy consensus with [138]

$$G_{2002} = 6.6742 \pm 0.0010 \times 10^{-8} cm^3 gm^{-1} s^{-2}$$

We could re-run the above analysis with different values of A and p, but expect that the results would look qualitatively similar. From figure 7.7 we see that in-

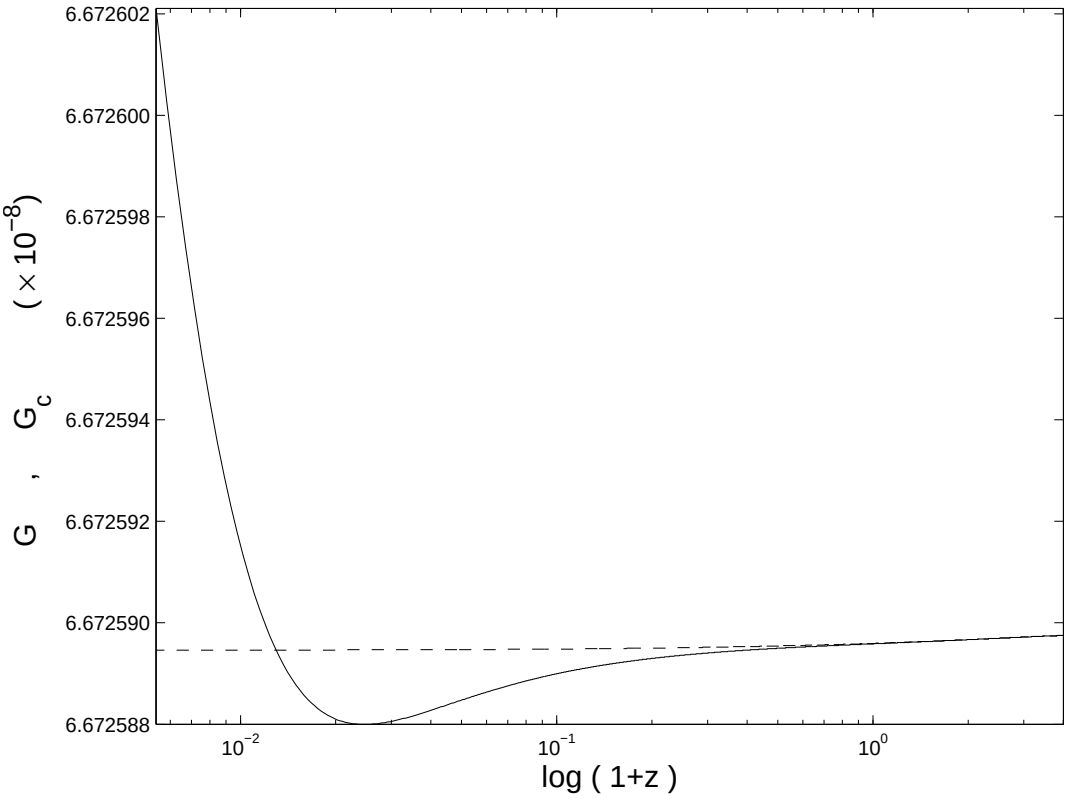

Figure 7.8: $2\omega+3 = 2A\left|1-\frac{\phi}{\phi_\infty}\right|^{-2}$ *A graph of the variation* G *against* $\ln(1+z)$ *for the background universe (dashed-line) and inside an overdensity (solid-line) which give* $G = G_0$*,the presently observed terrestrial value, at virialisation.*

creasing (decreasing) the values of A and p will increase (decrease) the value of $\omega(\phi)$ for a given ϕ, thereby making the theory more (less) like GR. We therefore expect an analysis with a higher (lower) value of A and/or p to look very similar to the analysis presented above with a less (more) rapid evolution of $G(t)$. For the sake of brevity we omit such an analysis here.

Space and Time variations of G

We now calculate how time and space variations of G evolve with redshift and depend on the dark matter density contrast, Δ_c. In order to do this, we make the definitions

$$\frac{\Delta G}{G}(t) \equiv \frac{G(t) - G_0}{G_0}, \qquad \frac{\delta G}{G}(t) \equiv \frac{G_c(t) - G_b(t)}{G_b(t)}$$

and

$$\Delta_c \equiv \frac{\rho_{CDM}(z_v)}{\rho_m(z_v)},$$

where G_c and G_b correspond to G as measured in the overdensity and in the background universe, respectively.

The results of our numerical calculations, for a cluster which virialises at $z_v = 0$, are presented in figures 7.9, 7.10 and 7.11, respectively. These plots display the evolution of $\dot{G}/G$, $\Delta G/G$, and $\delta G/G$ with redshift for Brans-Dicke theory, the theory of subsection 7.1.3, and some other choices of $\omega(\phi)$ that are specified in the captions. The parameters used in generating these plots are $B = 0.4$, $C = 10^{-16}$, $D = 80$, $A = 6 \times 10^{-7}$, $p = 2$ and $\omega = 4 \times 10^6$. These values were chosen so as to agree with observation and so that structure formation is not significantly different from that which occurs in GR.

It is clear from the plots that different scalar-tensor theories lead to different variations of G. The predictions of these models can be quite diverse. While some models produce higher values of G inside the overdensity, others produce a lower one. A feature common to all models is that the value of G and $\dot{G}/G$ inside an overdensity is different from G and $\dot{G}/G$ in the background universe. The reason for these differences is that in the non-linear regime, when the overdensity decouples from the background expansion at turnaround, the field ϕ that drives variations in the Newtonian gravitational 'constant' stops feeling the background expansion.

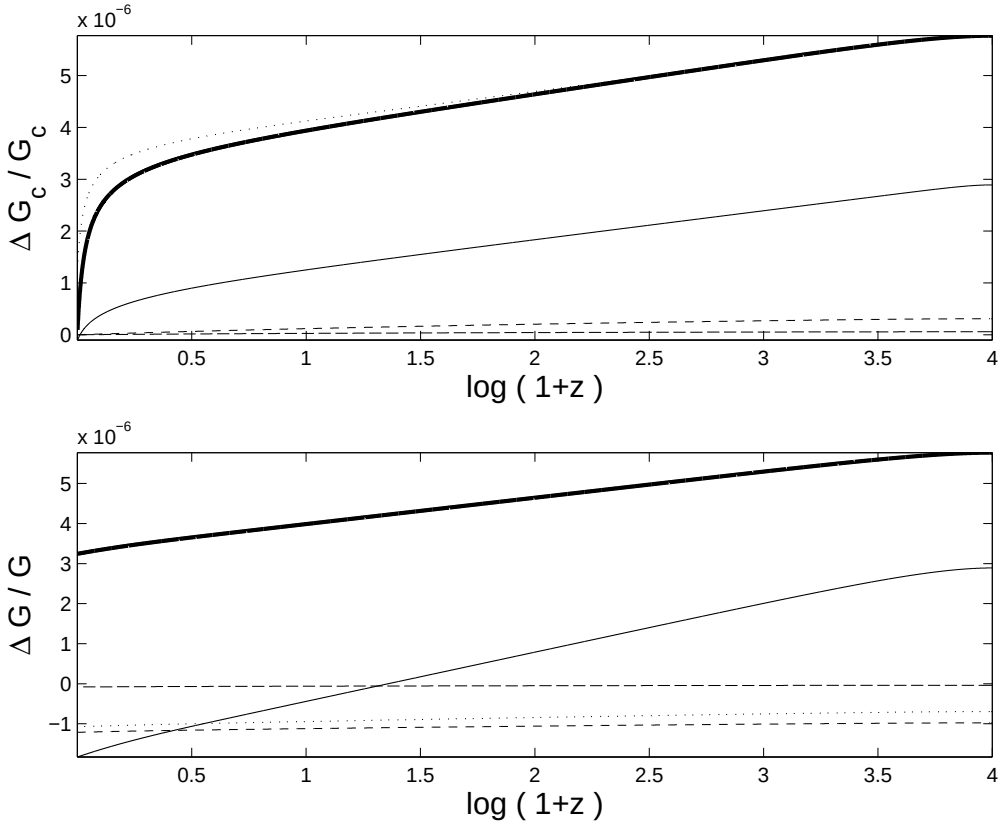

Figure 7.9: *Evolution of $\Delta G/G$ as a function of $log(1+z)$ for overdensities which virialise at $z=0$ in a ΛCDM model. Upper plot: evolution inside the overdensity. Lower plot: evolution in the background universe. Thick solid line $2\omega+3=4\times10^6$, thin solid line $2\omega+3=B^2\phi$, dashed-line $2\omega+3=2A|1-\frac{\phi}{\phi_0}|^{-2}$, dash-dotted line $2\omega+3=C|\ln(\frac{\phi}{\phi_0})|^{-4}$, dotted line $2\omega+3=D|1-(\frac{\phi}{\phi_0})^2|^{-1}$. Each model is normalised in order to have $G_0=G_c(z=0)$ inside the overdensities.*

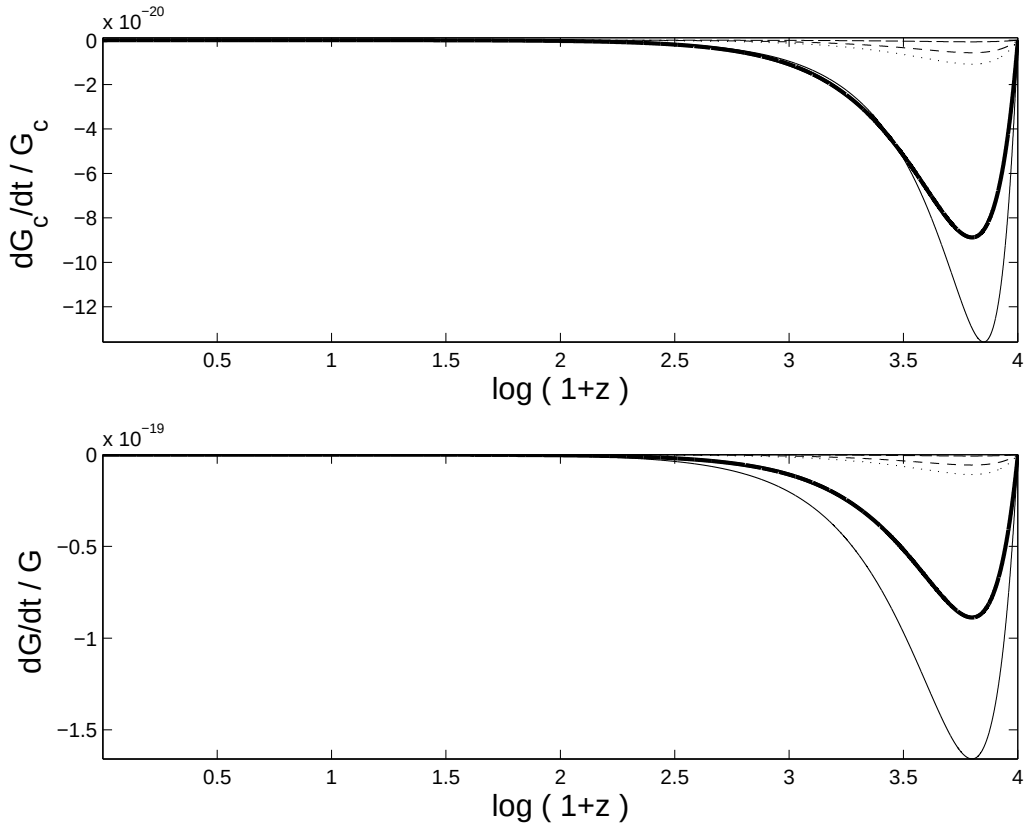

Figure 7.10: *Evolution of $\dot{G}/G$ as a function of $log(1+z)$ for overdensities which virialise at $z=0$ in a ΛCDM model. Upper plot: evolution inside the overdensity. Lower plot: evolution in the background universe. Thick solid line $2\omega+3 = 4\times10^6$, thin solid line $2\omega+3 = B^2\phi$, dashed-line $2\omega+3 = 2A|1-\frac{\phi}{\phi_0}|^{-2}$, dash-dotted line $2\omega+3 = C|\ln(\frac{\phi}{\phi_0})|^{-4}$, dotted line $2\omega+3 = D|1-(\frac{\phi}{\phi_0})^2|^{-1}$. Each model is normalised in order to have $G_0 = G_c(z=0)$ inside the overdensities.*

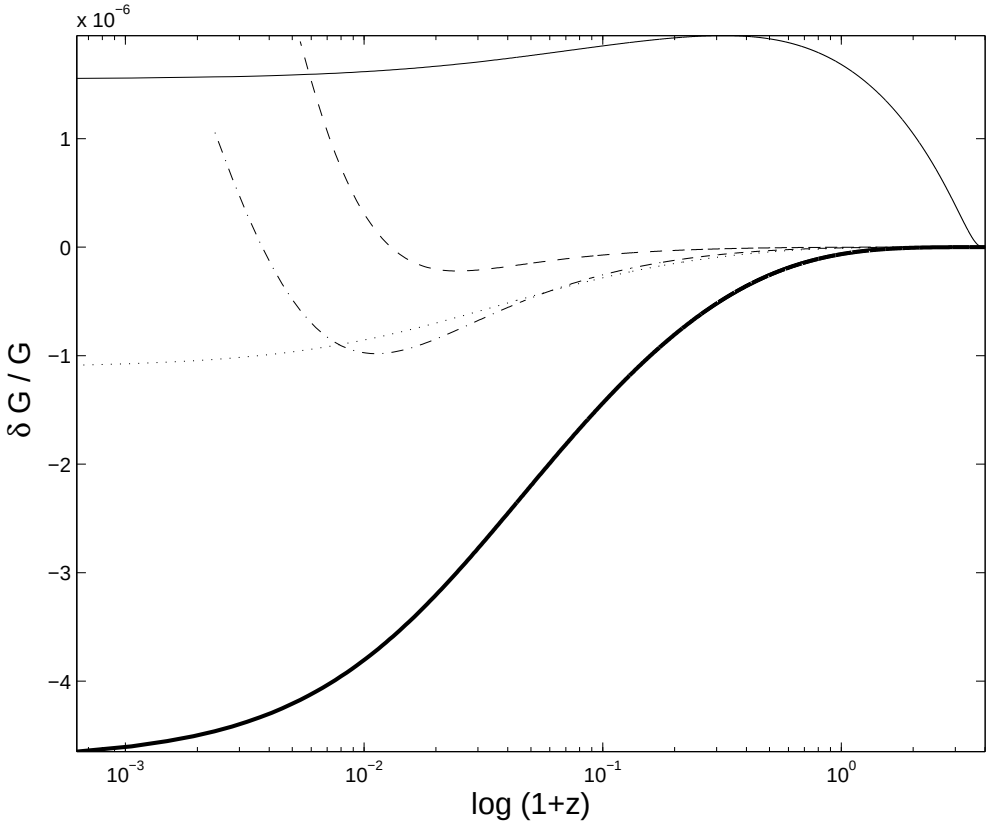

Figure 7.11: *Evolution of $\delta G/G$ as a function of $log(1+z)$ for overdensities which virialise at $z = 0$ in a ΛCDM model. Thick solid line $2\omega + 3 = 4 \times 10^6$, thin solid line $2\omega + 3 = B^2\phi^{2(p+1)}$, dashed-line $2\omega + 3 = 2A|1 - \frac{\phi}{\phi_0}|^{-2}$, dash-dotted line $2\omega+3 = C|\ln(\frac{\phi}{\phi_0})|^{-4}$, dotted line $2\omega+3 = D|1-(\frac{\phi}{\phi_0})^2|^{-1}$. Each model is normalised in order to have $G_0 = G_c(z = 0)$ inside the overdensities.*

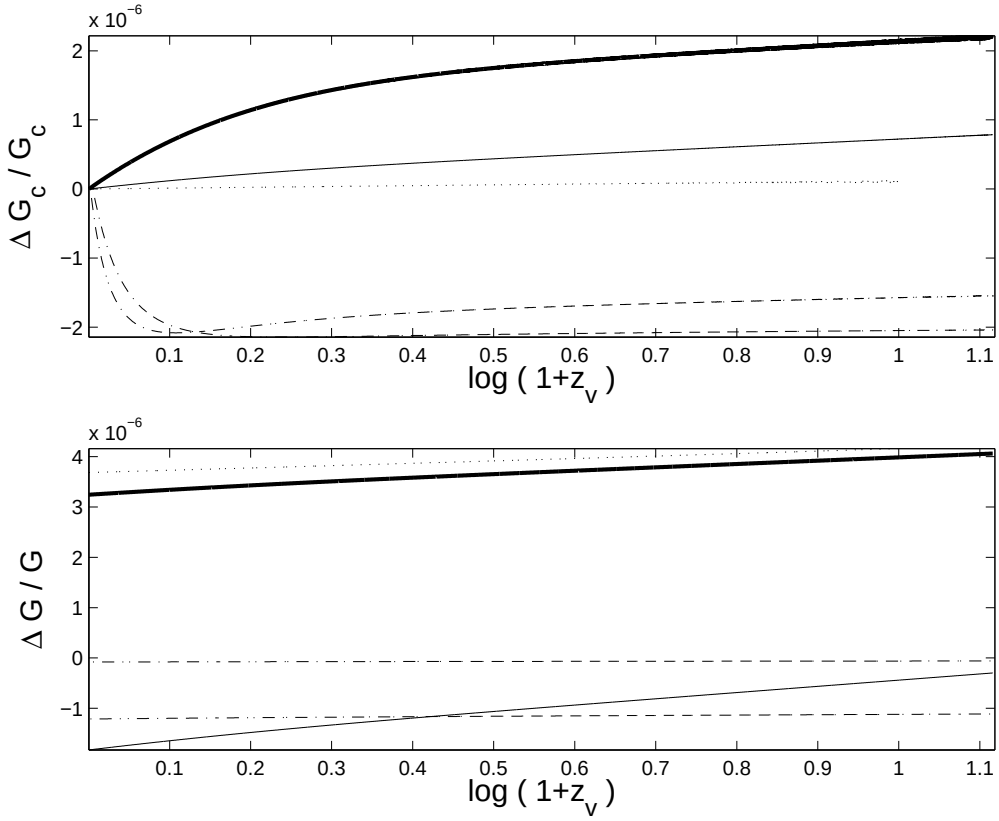

Figure 7.12: *Values of $\Delta G/G$ as a function of $log(1+z_v)$ at virialisation. Upper plot: evolution inside the overdensity. Lower plot: evolution in the background universe. Thick solid line $2\omega+3 = 4\times10^6$; thin solid line $2\omega+3 = B^2\phi$; dashed-line $2\omega+3 = 2A|1-\frac{\phi}{\phi_0}|^{-2}$; dash-dotted line $2\omega+3 = C|\ln(\frac{\phi}{\phi_0})|^{-4}$; dotted line $2\omega+3 = D|1-(\frac{\phi}{\phi_0})^2|^{-1}$. Each model is normalised to have $G_0 = G_c(z=0)$ inside the overdensities.*

After turnaround, the field inside the overdensity, ϕ_c, deviates from the field, ϕ, in the background universe, leading to spatial variations in G. In reality, such spatial inhomogeneities in the value of G are small: $\delta G/G \approx 10^{-6}$, figure 7.11. The time variations of G are even smaller than the spatial inhomogeneities but with a marked difference between the inside and outside rates of change. We find $\dot{G}_c/G_c \leq 10^{-20} s^{-1}$ inside the clusters and $\dot{G}/G \leq 10^{-19} s^{-1}$ in the background, figure 7.10.

Figures 7.12, 7.13 and 7.14 represent the values of $\Delta G/G$, $\delta G/G$ and $\dot{G}/G$ at the redshift of virialisation (z_v). Once again the differences between the different scalar-tensor theories and between $G_c(z_v)$ and $G(z_v)$ are evident.

Figure 7.15 shows how the dark matter contrast, $\Delta_c \equiv \rho_{CDM}(z_v)/\rho_m(z_v)$, affects the difference between the value of G inside an overdensity and in the cosmological background. (Recall that, in the Einstein-de Sitter model $\Delta_c \equiv \rho_{CDM}(z_v)/\rho_m(z_v) \approx 147$ at virialisation, and $\Delta_c \equiv \rho_{CDM}(z_v)/\rho_m(z_c) \approx 187$ at collapse). It is interesting to see that different scalar-tensor theories produce a different dependence.

From the numerical simulations, we see that a variation of the Newtonian gravitational constant, *of the order presented here*, does not affect the predictions of the structure formation models. For instance, the virialisation radius and the density contrast Δ_c of the virialised clusters are very similar to the ΛCDM and standard CDM models with constant G . Nevertheless, one should point out that different scalar-tensor theories lead to slightly different results. Besides that, there is also a dependence on the initial conditions, as with many other cosmological scalar fields (see e.g. [130, 128, 129]). Different initial conditions will lead to slightly different allowed values of ω and to different cosmological behaviours of G and G_c.

7.1.4 Discussion

We have studied the inhomogeneous cosmological evolution of the Newtonian gravitational 'constant' G within the framework of relativistic scalar-tensor theories of gravity, of which Brans-Dicke theory is the simplest and best known case. We began by first exploiting the conformal equivalence between these theories and GR to transform an existing solution of Einstein's field equations to a new exact spherically symmetric inhomogeneous vacuum cosmological solution of the Brans-Dicke field equations. We then present a second spherically symmetric perfect-fluid solution to

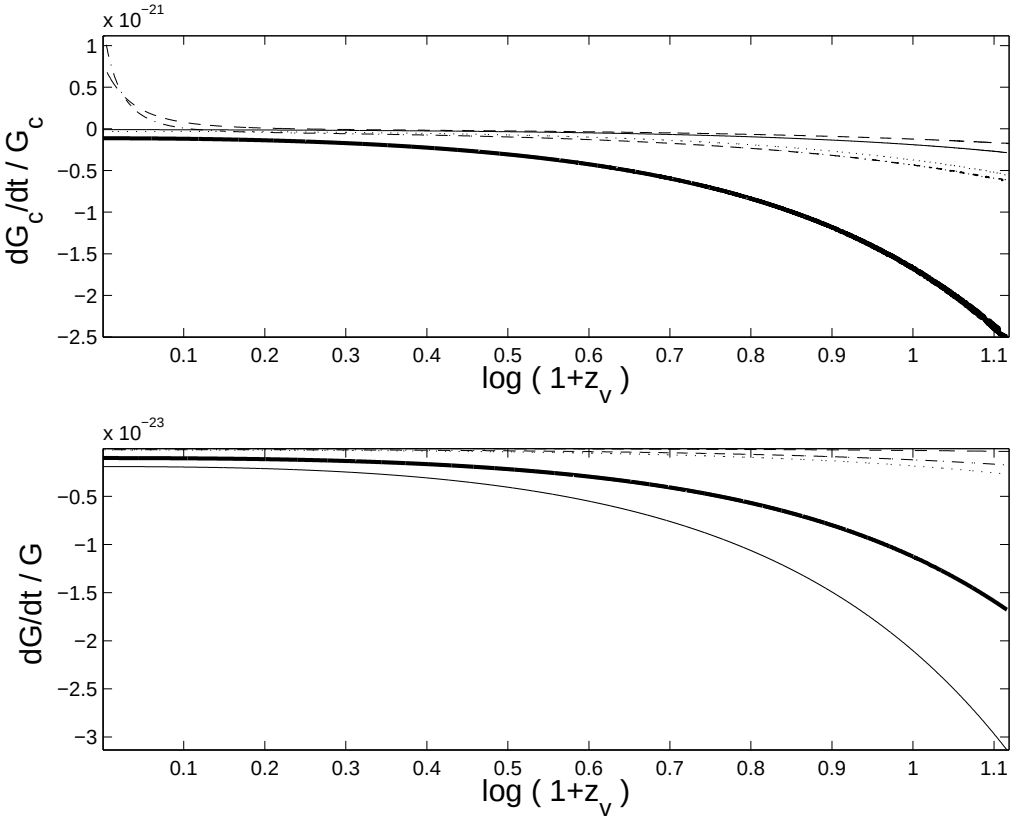

Figure 7.13: *Values of $\dot{G}/G$ as a function of $log(1+z_v)$ at virialisation. Upper plot: evolution inside the overdensity. Lower plot: evolution in the background universe. Thick solid line $2\omega+3 = 4\times10^6$; thin solid line $2\omega+3 = B^2\phi$; dashed-line $2\omega+3 = 2A|1-\frac{\phi}{\phi_0}|^{-2}$; dash-dotted line $2\omega+3 = C|\ln(\frac{\phi}{\phi_0})|^{-4}$; dotted line $2\omega+3 = D|1-(\frac{\phi}{\phi_0})^2|^{-1}$. Each model is normalised to have $G_0 = G_c(z=0)$ inside the overdensities.*

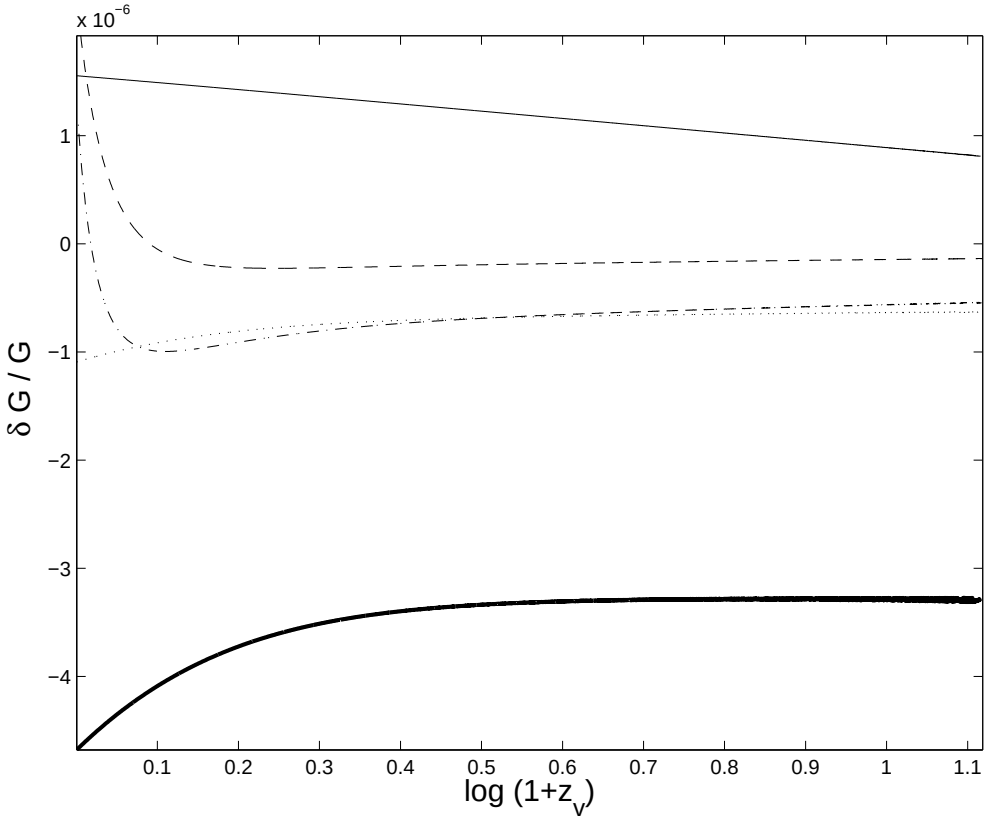

Figure 7.14: *Values of $\delta G/G$ as a function of $log(1+z_v)$ at virialisation. Thick solid line $2\omega+3 = 4\times10^6$; thin solid line $2\omega+3 = B^2\phi$; dashed-line $2\omega+3 = 2A|1-\frac{\phi}{\phi_0}|^{-2}$; dash-dotted line $2\omega+3 = C|\ln(\frac{\phi}{\phi_0})|^{-4}$; dotted line $2\omega+3 = D|1-(\frac{\phi}{\phi_0})^2|^{-1}$. Each model is normalised to have $G_0 = G_c(z=0)$ inside the overdensities.*

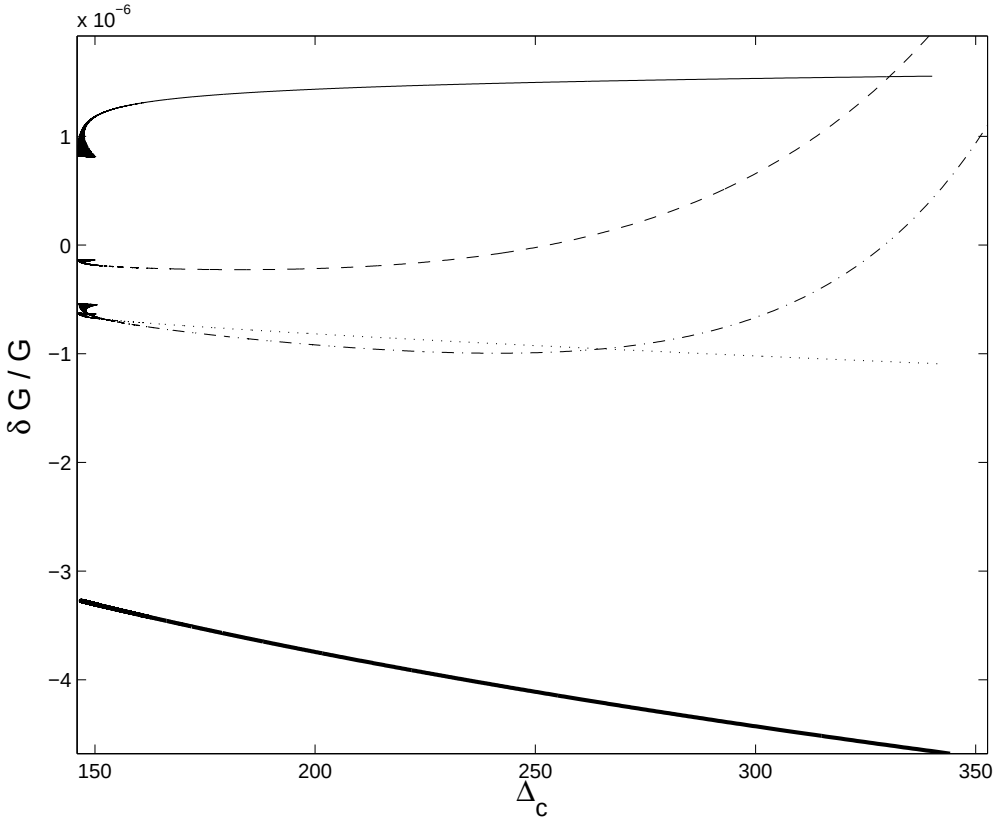

Figure 7.15: *Values of $\delta G/G$ as a function of Δ_c for a ΛCDM model. Thick-solid line $2\omega + 3 = 4 \times 10^6$; solid line $2\omega + 3 = B^2\phi$; dashed-line $2\omega + 3 = 2A|1 - \frac{\phi}{\phi_0}|^{-2}$; dash-dotted line $2\omega + 3 = C|\ln(\frac{\phi}{\phi_0})|^{-4}$; dotted line $2\omega + 3 = D|1 - (\frac{\phi}{\phi_0})^2|^{-1}$. Each model is normalised to have $G_0 = G_c(z = 0)$ inside the overdensities.*

the Brans-Dicke field equations which corresponds to an overdense inhomogeneity in an asymptotically homogenous and isotropic expanding cosmological background. These exact solutions have simple enough form to allow the $G(r,t)$ evolution to be investigated directly and can be used to model the presence of a Schwarzschild-like mass in an expanding Brans-Dicke universe that approaches an idealised FRW universe asymptotically as $r \to \infty$. It is noted that far from the mass G varies very slowly with r and that as $r \to \infty$ the variation of G with r is removed altogether and only the cosmological evolution of G with time is relevant. Close to the mass, the r variation of G becomes more significant and we see that $G \to 0$ at small r. We also note that in the limit $\omega \to \infty$ all space and time variation in G is removed from these solutions and GR is recovered.

Next, we increased the complexity of the model by matching together two vacuum FRW Brans-Dicke universes of zero and positive curvature on a spacelike time slice. This results in a simple model for a spherically symmetric perturbation in the density and curvature that is followed into the non-linear regime. The different evolutions of G in the two regions were determined and a comparison was made of the different evolutions of G on spacelike slices of differing time. We see from this toy model that the value of G does indeed have a different value in regions that have decoupled from the expanding cosmological background and collapsed, compared to its value in the background itself. We were then able to repeat this construction for a more realistic matching of two FRW ΛCDM universes of different curvature in an arbitrary scalar-tensor gravity theory. We followed the development of spherical overdensities through their expansion, separation from the background, turnaround, and subsequent collapse. Applying a simple approximation to virialise the collapsing overdensities, we were then able to study the differences in $G(x^\mu, t)$ between the non-expanding overdensity and the expanding background universe. We highlighted as a special case the simple Brans-Dicke theory but also presented results for other scalar-tensor gravity theories, specified by their defining coupling function $\omega(\phi)$. Although each theory predicts a different detailed cosmological evolution of G, a feature common to all of them is the difference between the value and time evolution of G inside bound overdensities and in the background universe. These differences will produce spatial inhomogeneities in G with a value which depends on the scalar-tensor theory used. While some models produce higher values of G

inside the overdensity, others produce lower ones. In spite of these differences, such spatial inhomogeneities are small: $\delta G/G \approx 10^{-6}$. The differences in the time variations of G were found, with typically $\dot{G}_c/G_c \leq 10^{-20}s^{-1}$ inside the clusters and $\dot{G}/G \leq 10^{-19}s^{-1}$ in the background universe in the range of theories studied. Such variations in G do not significantly alter the virialisation radius and the density contrast Δ_c of the virialised clusters from those in standard ΛCDM and CDM models with constant G. Nevertheless, different scalar-tensor theories lead to slightly different results. There is also a dependence on the initial conditions. Different initial conditions will lead to a different value of ω and to different cosmological behaviours of G and G_c. Taken as a whole, these analyses show that local observational limits on varying G made within our solar system or Galaxy must be used with caution when placing constraints upon the allowed cosmological variation of G on extragalactic scales or in the early universe. The universe is not spatially homogeneous and, in cosmological models where it can vary, nor is G.

7.2 Fourth-Order Theories

It has been known for some time that Birkhoff's theorem is not ensured in the vacuum solutions of generalised fourth-order theories of gravity, as they are in GR (see e.g. [151, 181]). We will now present an exact solution that shows this behaviour explicitly; a non-static, vacuum solution admitting spherically symmetric three-dimensional space-like hypersurfaces. A perturbation expansion will be performed about the background ($r \to \infty$ limit) of the exact solution.

7.2.1 Exact Solution

A solution to the spherically symmetric vacuum field equations of R^n theory (6.2.1) is given by

$$ds^2 = -A_2(r)dt^2 + a^2(t)B_2(r)(dr^2 + r^2 d\Omega^2) \tag{7.2.1}$$

where

$$A_2(r) = \left(\frac{1-\frac{C_2}{r}}{1+\frac{C_2}{r}}\right)^{\frac{2}{q}} \qquad a(t) = t^{\delta\frac{(1+2\delta)}{(1-\delta)}}$$

$$B_2(r) = \left(1+\frac{C_2}{r}\right)^4 A(r)^{q+2\delta-1} \qquad q^2 = 1-2\delta+4\delta^2$$

and C_2 is a constant. This solution is conformally related to one found by Fonarev [86] and reduces to the Schwarzschild solution in the limit $\delta \to 0$. It shows explicitly the lack of validity of Birkhoff's theorem in these theories. It becomes r-independent in the limit $r \to \infty$, but still displays strong curvature in this limit as the metric reduces to the spatially flat vacuum FRW cosmology found in [70].

We will now continue to find the general form of spherically symmetric perturbations to the background of the above solution. It will be seen that there exist extra modes which are not excited in the exact solutions, but that the modes corresponding to the linearised exact solutions above are the ones most interesting for performing gravitational experiments in this space-time.

7.2.2 Linear perturbation analysis

Perturbative analyses in the literature are often performed about Minkowski space or de Sitter space. This is perfectly acceptable practise in GR and fourth-order theories in which an Einstein-Hilbert term dominates in the low curvature regime. In other fourth-order theories, of the type considered here, in which the Einstein-Hilbert term does not dominate the low curvature regime then there is good reason to consider perturbing about other backgrounds. We have shown explicitly, with exact solutions, the existence of other spherically symmetric space-times. We will now proceed to perform a linear perturbation analysis about the background of solution (7.2.1). The general solution to first order in perturbations will be found.

Writing the perturbed line-element as

$$ds^2 = -(1+P(r))dt^2 + b^2(t)(1+Q(r))(dr^2+r^2d\Omega^2) \tag{7.2.2}$$

allows the vacuum field equations to be linearised in P and Q. These linearised field

equations are

$$6\delta(1-2\delta-2\delta^2)(5-14\delta-12\delta^2)\nabla P - 12(1-2\delta-2\delta^2)(1-6\delta+4\delta^2+4\delta^3)\nabla Q + (1+2\delta)(1-\delta)^2 t^{\frac{2(1-2\delta-2\delta^2)}{(1-\delta)}}\nabla\psi = 0$$

$$(2-17\delta+18\delta^2+52\delta^3+8\delta^4)P'' - 2(1-\delta+3\delta^2-34\delta^3-32\delta^4)\frac{P'}{r} + 2(2-8\delta-9\delta^2+16\delta^3+8\delta^4)Q'' + 2(1-4\delta-15\delta^2+20\delta^3+16\delta^4)\frac{Q'}{r} + 3(1-\delta)^2 t^{\frac{2(1-2\delta-2\delta^2)}{(1-\delta)}}\left(\frac{\psi''}{2(1+2\delta)}+\frac{\psi'}{3r}\right) = 0$$

and

$$\psi' = 0$$

where

$$\psi = \nabla P + 2\nabla Q.$$

Primes here denote differentiation with respect to r and ∇ is the Laplacian on the three-dimensional subspace. These equations have the general solution

$$P = -\frac{c_4}{r} + \frac{2c_5(1-6\delta+4\delta^2+4\delta^3)}{(5-14\delta-12\delta^2)}r^2 + \text{constant}$$
$$Q = \frac{(1-2\delta)c_4}{r} + \delta c_5 r^2 + \text{constant}$$

where c_4 and c_5 are constants and the two other constant terms in P and Q are independent of each other and can be absorbed into t and s by redefinitions. It can be seen that one of the modes, c_4, corresponds to the linearised version of the exact solution (7.2.1).

We immediately see that the form of these linearised solutions are quite different to those obtained by expanding around the background of the static spherically symmetric solution (6.2.2). Whist the expansion about (6.2.2) produces damped oscillatory modes, as well as the mode corresponding to the linearised exact solution, the expansion about (7.2.1) produces more familiar looking terms proportional to

r^2. Aside from the different form of these extra modes, there is also a noticeable difference in the terms corresponding to the linearised exact solutions, which both go as r^{-1} in the limit $\delta \to 0$, but behave differently from each other when $\delta \neq 0$. This shows explicitly the differences that can arise when linearising about different backgrounds. Not only are there extra modes which can take different functional forms, but even the modes which reduce to the Schwarzschild limit as $\delta \to 0$ are different, depending on the background that has been chosen.

CHAPTER 8

Scalar-Tensor Cosmologies with Energy Exchange

Non-minimally coupled scalar fields arise in a variety of different theories, including Kaluza-Klein theory [109, 110], string theories [94] and brane-worlds [156, 157]. The same mechanism that creates a scalar field non-minimally coupled to the curvature in these theories can also lead to a coupling between the scalar and matter fields. This coupling manifests itself through the matter Lagrangian becoming a function of ϕ. The possibility of such a coupling is usually neglected in the literature, where the matter Lagrangian is *a priori* assumed to be independent of ϕ. It is the possibility of a coupling between the scalar and matter fields in scalar-tensor theories that will be the subject of this chapter.

The introduction of a coupling between ϕ and matter greatly enlarges the phenomenology of the theory. Potentially, this allows greater variability of G in the early universe whilst still satisfying the solar system bounds on varying G [47]. We will investigate the extent to which G can vary when energy is exchanged between the ϕ field and ordinary matter. As well as giving a window into the four-dimensional cosmologies associated with higher-dimensional theories, we hope that this direction of study might be useful in understanding why the present value of G is so small compared to the proton mass scale ($Gm_{pr}^2 \sim 10^{-39}$). The direct exchange of energy between ϕ and the matter fields offers a non-adiabatic mechanism for G to 'decay'

towards its present value from a potentially different initial value. There have been a variety of studies which investigate the drain of energy from ordered motion by entropy generation, due to bulk viscosity [15, 17, 68] or direct decay [38, 87] or energy exchange [183], but few studies of the drain of energy by non-adiabatic processes from a scalar field that defines the strength of gravity [90, 78, 95]. This creates a range of new behaviours in scalar-tensor cosmologies.

In considering a coupling between ϕ and matter we are forced to reconsider the equivalence principle. The energy-momentum tensor of perfect-fluid matter fields will no longer be covariantly conserved and the trajectories of test-particles will no longer follow exact geodesics of the metric. These violations of the experimentally well verified weak equivalence principle exclude most possible couplings between ϕ and matter [191]. Such violations are not necessarily fatal though. We show that whilst energy-momentum is not separately conserved by the matter fields there is still an exact concept of energy-momentum conservation when the energy density of the scalar field is included. Furthermore, the non-geodesic motion of test particles is only problematic if the coupling increases above experimentally acceptable levels as the Universe ages. The theory we consider is still a geometric one and it remains true that at any point on the space-time manifold it is possible to choose normal coordinates so that it looks locally flat.

This chapter is based on the work of Clifton and Barrow [73].

8.1 Field Equations

The conservation of T^{ab}, whilst appealing, is not absolutely necessary in deriving a theory in which G can vary. There are numerous examples where one might expect ${T^{ab}}_{;b} \neq 0$. For example, when considering two fluids the energy-momentum tensor of each fluid is not separately conserved unless the fluids are completely non-interacting [24]. It is only required that the energy-momentum being lost by one of the fluids is equal to the energy-momentum being gained by the other.

In what follows we will consider the scalar and matter fields as two fluids (or more than two fluids if there is more than one matter fluid present) and introduce a transfer of energy and momentum between them. Such an interaction can be introduced by allowing $\mathcal{L}_m$ to be a function of ϕ and will change the nature of the

resulting FRW cosmologies.

The field equations take their usual form in the Brans-Dicke theory (2.1.8) and the scalar-field propagation equation and matter energy-momentum conservation equations are now

$$\Box\phi = \frac{8\pi T}{(2\omega+3)} - \frac{16\pi\phi}{(2\omega+3)}\frac{\sigma^a}{\phi_{;}{}^a} \tag{8.1.1}$$

$$T^{ab}{}_{;b} = \sigma^a \tag{8.1.2}$$

where T is the trace of the energy-momentum tensor and σ^a is an arbitrary vector function of the space-time coordinates x^b that determines the rate of transfer of energy and momentum between the scalar field ϕ and the ordinary matter fields. The precise form of σ^a depends on the detailed form of the interaction between the scalar and matter fields in $\mathcal{L}_m$. For example, a conformal transformation of the form $g_{ab} \to A^2(\phi)g_{ab}$ from a frame in which $T^{ab}{}_{;b} = 0$ gives

$$\sigma^a = \frac{T}{A}\frac{dA}{d\phi}\phi_{;}{}^a.$$

This particular choice of energy transfer can be interpreted as a space-time variation of the rest masses of matter described by $\mathcal{L}_m$. For the moment, we consider the case of more general interactions by leaving σ^a as an arbitrary function. Later, we will consider specific forms of σ^a that allow direct integration of the field equations.

Substituting the spatially flat FRW metric into the field equations (2.1.8), (8.1.1) and (8.1.2) gives the generalised Friedmann equations:

$$\left(\frac{\dot{V}}{V}\right)^2 = -3\frac{\dot{V}}{V}\frac{\dot{\phi}}{\phi} + \frac{3\omega}{2}\left(\frac{\dot{\phi}}{\phi}\right)^2 + 3(3+2\omega)\alpha\frac{\rho}{\phi} \tag{8.1.3}$$

$$\frac{(\dot{V}\phi)^{\cdot}}{\rho V} = 3\alpha((2-\gamma)\omega+1) + 3\frac{\alpha}{\rho}\frac{\phi}{\dot{\phi}}\sigma^0 \tag{8.1.4}$$

$$\frac{(V\dot{\phi})^{\cdot}}{\rho V} = \alpha(4-3\gamma) - 2\frac{\alpha}{\rho}\frac{\phi}{\dot{\phi}}\sigma^0 \tag{8.1.5}$$

$$\dot{\rho} + \gamma\frac{\dot{V}}{V}\rho = \sigma^0 \tag{8.1.6}$$

where we have defined a comoving volume $V = a^3$ and a constant $\alpha = \frac{8\pi}{(3+2\omega)}$; the energy-momentum tensor is assumed to be a perfect barotropic fluid with density ρ and pressure p which are linked by a linear equation of state $p = (\gamma - 1)\rho$, and over-dots denote differentiation with respect to the comoving proper time, t. It is this set of differential equations that we need to solve in order to determine the evolution of $a(t)$ and $G \propto \phi(t)^{-1}$ in cosmological models of this type.

8.2 Transfer of Energy and Entropy

The conservation of energy and momentum, as well as the second law of thermodynamics, are of basic importance to physics. In considering an interaction between a gravitational scalar field ϕ and the matter fields Ψ, it is therefore necessary to investigate the extent to which we can consider energy and momentum to be conserved and the second law to be obeyed.

When we consider the thermodynamics of an exchange of energy between the scalar field and matter it is useful to define an effective energy density, ρ_ϕ, for the scalar field ϕ. Defining

$$\rho_\phi \equiv \frac{\dot{\phi}^2}{16\pi\omega\phi}, \tag{8.2.1}$$

the scalar-field propagation equation (8.1.4) can then be rewritten as

$$\dot{\rho}_\phi + 2\frac{\dot{V}}{V}\rho_\phi = -\frac{R}{16\pi}\dot{\phi} - \sigma^0. \tag{8.2.2}$$

Comparison of this equation with (8.1.6) shows that ϕ acts as a fluid with equation of state $\gamma = 2$ ($p_\phi = \rho_\phi$). The two terms on the right hand side of this equation act as sources for the energy density ρ_ϕ. The first is the standard Brans-Dicke source term for the scalar field and the second, $\sigma^0(t)$, is new and describes the energy exchange between ϕ and the matter fields. It can be seen that the second term is exactly the opposite of the source term in equation (8.1.3), and it is in this sense that the total energy is conserved in this theory.

It is also useful to consider the entropy. Contracting the divergence of the energy-

momentum tensor with the comoving four-velocity U^a we obtain

$$\begin{aligned} U^a\sigma_a &= U^a T_a{}^b{}_{;b} \\ &= U^a p_{;a} + U^a((\rho+p)U_a U^b)_{;b} \\ &= U^a p_{;a} - ((\rho+p)U^b)_{;b}, \end{aligned}$$

where, in the last line, we have used the normalisation $U^a U_a = -1$ and $(U^a U_a)_{;b} = U^a{}_{;b}U_a + U^a U_{a;b} = 0$. Defining the particle current by $N^a \equiv nU^a$, where n is the number density in a comoving Lorentz frame, this expression can be rewritten as

$$\begin{aligned} U^a\sigma_a &= U^a\left[p_{;a} - n\left(\frac{(\rho+p)}{n}\right)_{;a}\right] - \frac{(\rho+p)}{n}N^a{}_{;a} \\ &= -nU^a\left[p\left(\frac{1}{n}\right)_{;a} + \left(\frac{\rho}{n}\right)_{;a}\right], \end{aligned}$$

where we have used the conservation of particle number, $N^a{}_{;a} = 0$. Recalling the first law of thermodynamics,

$$\Theta dS = pdV + dE = pd\left(\frac{1}{n}\right) + d\left(\frac{\rho}{n}\right),$$

where Θ is the temperature and S is the entropy, we now get

$$U^a\sigma_a = -n\Theta U^a S_{;a}$$

or, making use of our assumption of spatial homogeneity,

$$\dot{S} = \frac{\sigma^0}{n\Theta}.$$

This tells us that, as energy is transferred from ϕ to the matter fields, the entropy of the matter fields increases, as expected. Conversely, the matter fields can decrease their entropy by transferring energy into ϕ.

Unfortunately, there is currently no known way of defining the entropy of a non-static gravitational field so it is not possible to perform an explicit calculation of the entropy changes in ϕ and g_{ab}. We can only assume that if the Universe can be treated as a closed system, and the exchange of energy is an equilibrium process,

then the entropy that is lost or gained by the matter through this exchange will be gained or lost by the gravitational fields. This direct interaction of the matter with ϕ then allows an additional mechanism for increasing or decreasing the entropy of the matter content of the Universe.

8.3 General Solutions

It is convenient to define a new time coordinate τ by

$$d\tau \equiv \rho V dt \tag{8.3.1}$$

and to re-parametrise the arbitrary function σ^0 by

$$\sigma^0 = \rho^2 V \frac{\phi'}{\phi} \lambda' \tag{8.3.2}$$

where a prime denotes differentiation with respect to τ and $\lambda(\tau)$ is a new arbitrary function. This re-parameterisation of the interaction is chosen to enable a direct integration of the field equations and does not imply any loss of generality, as λ is an arbitrary function. The field equations (8.1.4) and (8.1.5) can now be integrated to

$$\rho\phi V V' = 3\alpha((2-\gamma)\omega + 1)(\tau - \tau_1) + 3\alpha\lambda \tag{8.3.3}$$

$$\rho V^2 \phi' = \alpha(4 - 3\gamma)\tau + \alpha\tau_2 - 2\alpha\lambda \tag{8.3.4}$$

where τ_1 and τ_2 are constants of integration. We have a freedom in where we define the origin of τ and can, therefore, absorb the constant τ_1 into τ and the definition of τ_2 by the transformations $\tau \to \tau + \tau_1$ and $\tau_2 \to \tau_2 - (4 - 3\gamma)\tau_1$. It can now be seen from (8.3.4) that ϕ' is sourced by three terms. The first corresponds to the source term in (8.1.2) and can be seen to disappear for $\gamma = 4/3$, as expected for black-body radiation. The second term is constant and is the contribution of the free scalar to the evolution of ϕ; it is this term which distinguishes the general spatially-flat Brans-Dicke FRW solutions [97] from the power-law late-time attractor solutions [137]. The third term is new and gives the effect of the energy transfer on the evolution of ϕ. This term is dependent on the arbitrary function λ, which

specifies the interaction between ϕ and the matter fields.

The problem is now reduced to solving the coupled set of first-order ordinary differential equations (8.3.3) and (8.3.4) with the constraint equation (8.1.6). The remaining equation (8.1.3) is rewritten in terms of τ and λ as

$$\frac{\rho'}{\rho} + \gamma \frac{V'}{V} = \lambda' \frac{\phi'}{\phi}, \tag{8.3.5}$$

and can be solved for ρ once V and ϕ have been found for some λ.

We can decouple the set of equations (8.3.3) and (8.3.4) by differentiating (8.3.4) and substituting for (8.3.3) to get the second-order ordinary differential equation

$$\begin{aligned} &((4-3\gamma)\tau + \tau_2 - 2\lambda)\,\frac{\phi''}{\phi} - ((4-3\gamma) - 2\lambda')\,\frac{\phi'}{\phi} \\ &= -\left[((4-3\gamma)\tau + \tau_2 - 2\lambda)\lambda' + 3(2-\gamma)(((2-\gamma)\omega + 1)\tau + \lambda)\right]\left(\frac{\phi'}{\phi}\right)^2 \end{aligned}$$

which can be integrated to

$$\frac{\phi'}{\phi} = \frac{(4-3\gamma)\tau + \tau_2 - 2\lambda}{(A\tau^2 + B\tau + C)}, \tag{8.3.6}$$

where

$$\begin{aligned} A &= 3\gamma^2\omega/2 - 3\gamma(1+2\omega) + (5+6\omega) \\ B &= \tau_2 + (4-3\gamma)\lambda \\ C &= -\lambda^2 + \lambda\tau_2 + D \end{aligned}$$

and D is a constant of integration. The three source terms for ϕ' appear in the numerator on the right-hand side of equation (8.3.6). The equations (8.3.3) and (8.3.4) can now be combined to give a'/a in terms of ϕ'/ϕ as

$$\frac{a'}{a} = \frac{((2-\gamma)\omega + 1)\tau + \lambda}{(A\tau^2 + B\tau + C)} \tag{8.3.7}$$

where A, B, C and D are defined as before. The constant D can be set using the

constraint equation (8.1.6). Using (8.3.3) and (8.3.7) we obtain the expression

$$\rho V^2 \phi = \alpha(A\tau^2 + B\tau + C).$$

This can then be substituted into (8.1.6) which, in terms of τ and a, gives the generalised Friedmann equation:

$$3\left(\frac{a'}{a}\right)^2 + 3\frac{a'}{a}\frac{\phi'}{\phi} - \frac{\omega}{2}\left(\frac{\phi'}{\phi}\right)^2 = \frac{(3+2\omega)}{(A\tau^2 + B\tau + C)}.$$

Substituting (8.3.6) and (8.3.7) into this, we find that

$$D = -\frac{\tau_2^2 \omega}{2(3+2\omega)}.$$

8.4 Particular Solutions

If λ is specified in terms of τ, we now have a set of two decoupled first-order ordinary differential equations for the two variables a and ϕ. It is the solution of these equations, for specific choices of $\lambda(\tau)$, that we give in this section.

$\boldsymbol{\lambda(\tau) = c_1 + c_2\tau}$

A simple form for λ that allows direct integration of equations (8.3.6) and (8.3.7) is the linear function $\lambda = c_1 + c_2\tau$. From equations (8.3.3) and (8.3.4) it can be seen that the constant c_1 can be absorbed into τ_1 and τ_2 by simple redefinitions. The equations (8.3.6) and (8.3.7) then become

$$\frac{\phi'}{\phi} = \frac{(4 - 3\gamma - 2c_2)\tau + \tau_2}{(\hat{A}\tau^2 + \hat{B}\tau + \hat{C})}$$
$$\frac{a'}{a} = \frac{((2-\gamma)\omega + 1 + c_2)\tau}{(\hat{A}\tau^2 + \hat{B}\tau + \hat{C})}$$

where $\hat{A} = A - c_2^2$, $\hat{B} = B + c_2\tau_2$ and $\hat{C} = D$. The solutions of these equations depend upon the sign of the discriminant

$$\Delta = \hat{B}^2 - 4\hat{A}\hat{C}. \tag{8.4.1}$$

For the case $\Delta = 0$, there exist simple exact power-law solutions

$$a(\tau) \propto \tau^{\frac{2(2-\gamma)\omega+2+2c_2}{3\gamma^2\omega-6\gamma(1+2\omega)+2(5+6\omega)-2c_2^2}} \tag{8.4.2}$$

$$\phi(\tau) \propto \tau^{\frac{2(4-3\gamma)-4c_2}{3\gamma^2\omega-6\gamma(1+2\omega)+2(5+6\omega)-2c_2^2}}. \tag{8.4.3}$$

Substituting these power-law solutions into (8.3.5), we can obtain the corresponding power-law form

$$\rho \sim \tau^{\frac{4c_2(2-3\gamma-c_2)-6\gamma(1+(2-\gamma)\omega)}{3\gamma^2\omega-6\gamma(1+2\omega)+2(5+6\omega)-2c_2^2}}.$$

The relationship between τ and the cosmological time t can now be obtained by integrating the definition $d\tau = \rho a^3 dt$ given in eq. (8.3.1). This gives (8.4.2) and (8.4.3) in terms of t time as

$$a(t) \sim t^{\frac{2+2(2-\gamma)\omega+2c_2}{4+3\gamma\omega(2-\gamma)-2c_2(7-6\gamma-c_2)}} \tag{8.4.4}$$

$$\phi(t) \sim t^{\frac{2(4-3\gamma)-4c_2}{4+3\gamma\omega(2-\gamma)-2c_2(7-6\gamma-c_2)}}. \tag{8.4.5}$$

The condition required for the occurrence of power-law inflation is obtained by requiring the power of time in equation (8.4.5) to exceed unity (for the case with out energy transfer see refs. [122, 115]). For $\omega > -3/2$ we always have $\Delta \geqslant 0$, and the case $\Delta > 0$ possesses the exact solutions

$$a(\tau) = a_0(\hat{A}\tau^2 + \hat{B}\tau + \hat{C})^{\frac{(2-\gamma)\omega+1+c_2}{2\hat{A}}} \left(\frac{2\hat{A}\tau + \hat{B} + \sqrt{\Delta}}{2\hat{A}\tau + \hat{B} - \sqrt{\Delta}}\right)^{\frac{\hat{B}((2-\gamma)\omega+1+c_2)}{2\hat{A}\sqrt{\Delta}}} \tag{8.4.6}$$

$$\phi(\tau) = \phi_0(\hat{A}\tau^2 + \hat{B}\tau + \hat{C})^{\frac{4-3\gamma-2c_2}{2\hat{A}}} \left(\frac{2\hat{A}\tau + \hat{B} + \sqrt{\Delta}}{2\hat{A}\tau + \hat{B} - \sqrt{\Delta}}\right)^{\frac{(4-3\gamma-2c_2)\hat{B}-\tau_2\hat{A}}{2\hat{A}\sqrt{\Delta}}}. \tag{8.4.7}$$

where a_0 and ϕ_0 are constants of integration. For $\omega < -3/2$ we have $\Delta \leqslant 0$, and the case $\Delta < 0$ has the exact solutions

$$a(\tau) = a_0(\hat{A}\tau^2 + \hat{B}\tau + \hat{C})^{\frac{(2-\gamma)\omega+1+c_2}{2\hat{A}}} \times \exp\left[-\frac{((2-\gamma)\omega+1+c_2)\hat{B}}{\hat{A}\sqrt{-\Delta}} \tan^{-1}\left(\frac{\hat{B}+2\hat{A}\tau}{\sqrt{-\Delta}}\right)\right] \tag{8.4.8}$$

$$\phi(\tau) = \phi_0(\hat{A}\tau^2 + \hat{B}\tau + \hat{C})^{\frac{4-3\gamma-2c_2}{2\hat{A}}} \times \exp\left[\frac{2\tau_2\hat{A} - 2(4-3\gamma-2c_2)\hat{B}}{\hat{A}\sqrt{-\Delta}}\tan^{-1}\left(\frac{\hat{B}+2\hat{A}\tau}{\sqrt{-\Delta}}\right)\right]. \quad (8.4.9)$$

These solutions have the same functional form as those found by Gurevich, Finkelstein and Ruban [97] for Brans-Dicke theory, in the absence of energy exchange ($\lambda =$ constant), and reduce to them in the limit $c_2 \to 0$. The behaviour of these solutions at early and late times will be discussed in the next section.

$\boldsymbol{\lambda(\tau) = c_3\tau^n,\ n \neq 1}$

We now consider forms of $\lambda(\tau)$ that are more general than a simple linear function of τ. Making the choice $\lambda = c_3\tau^n$, where $n \neq 1$ and c_3 is constant, and setting the free scalar component to zero ($\tau_2 = 0$), we find that (8.3.6) and (8.3.7) can be integrated exactly. The form of the solutions again depends upon the roots of the denominator. For real roots we require $\omega > -3/2$, for which we find the solutions

$$a(\tau) = a_0\tau^{\frac{2+2(2-\gamma)\omega}{\kappa}}\left[\pm 2c_3\tau^{n-1} \mp (4-3\gamma) \pm (2-\gamma)\sqrt{3(3+2\omega)}\right]^{-\frac{3+3(2-\gamma)\omega-\sqrt{3(3+2\omega)}}{3\kappa(n-1)}} \times \left[\pm 2c_3\tau^{n-1} \mp (4-3\gamma) \mp (2-\gamma)\sqrt{3(3+2\omega)}\right]^{-\frac{3+3(2-\gamma)\omega+\sqrt{3(3+2\omega)}}{3\kappa(n-1)}} \quad (8.4.10)$$

$$\phi(\tau) = \phi_0\tau^{\frac{2(4-3\gamma)}{\kappa}}\left[\pm 2c_3\tau^{n-1} \mp (4-3\gamma) \pm (2-\gamma)\sqrt{3(3+2\omega)}\right]^{-\frac{(4-3\gamma)+(2-\gamma)\sqrt{3(3+2\omega)}}{\kappa(n-1)}} \times \left[\pm 2c_3\tau^{n-1} \mp (4-3\gamma) \mp (2-\gamma)\sqrt{3(3+2\omega)}\right]^{-\frac{(4-3\gamma)-(2-\gamma)\sqrt{3(3+2\omega)}}{\kappa(n-1)}} \quad (8.4.11)$$

where $\kappa \equiv 2(5-3\gamma) + 3(2-\gamma)^2\omega$. For a denominator with imaginary roots we require $\omega < -3/2$, for which we find

$$a(\tau) = a_0\left[\pm 2(4-3\gamma)c_3\tau^{1-n} \pm \kappa\tau^{2(1-n)} \mp 2c_3^2\right]^{\frac{1+(2-\gamma)\omega}{\kappa(1-n)}} \times \exp\left\{\frac{2\sqrt{-3(3+2\omega)}}{3\kappa(1-n)}\tan^{-1}\left(\frac{(4-3\gamma)-2c_3t^{n-1}}{(2-\gamma)\sqrt{-3(3+2\omega)}}\right)\right\} \quad (8.4.12)$$

$$\phi(\tau) = \phi_0 \left[\pm 2(4-3\gamma)c_3\tau^{1-n} \pm \kappa\tau^{2(1-n)} \mp 2c_3^2\right]^{\frac{(4-3\gamma)}{\kappa(1-n)}} \times \exp\left\{-\frac{2(2-\gamma)\sqrt{-3(3+2\omega)}}{\kappa(1-n)}\tan^{-1}\left(\frac{(4-3\gamma)-2c_3t^{n-1}}{(2-\gamma)\sqrt{-3(3+2\omega)}}\right)\right\} \quad (8.4.13)$$

with κ defined as above. The $\pm$ and $\mp$ signs here indicate that there are multiple solutions that satisfy the field equations. These signs should be chosen consistently within each set of square brackets (solutions (8.4.10) and (8.4.11) can have upper or lower branches chosen independently in each set of square brackets, as long as a consistent branch is taken within each separate set of square brackets). The physical branch should be chosen as the one for which the quantity in brackets remains positive as $\tau \to \infty$, so ensuring the existence of a positive real root in this limit,

These solutions display interesting new behaviours at both early and late times, which will be discussed in the next section.

8.5 Behaviour of Solutions

$\boldsymbol{\lambda(\tau) = c_1 + c_2\tau}$

At late times, as $\tau \to \infty$, the solutions (8.4.6)-(8.4.9) all approach the exact power-law solutions (8.4.2) and (8.4.3). It can be seen that these solutions reduce to the usual spatially flat FRW Brans-Dicke power-law solutions [137] in the limit that the rate of energy transfer goes to zero, $c_2 \to 0$. It can also be seen that these solutions reduce to the spatially-flat FRW general relativistic solutions in the limit $\omega \to \infty$, irrespective of any (finite) amount of energy transfer.

The early-time behaviour of these solutions approaches that of the general Brans-Dicke solutions [97], without energy transfer. Generally, we expect an early period of free-scalar-field domination except in the case $\tau_2 = 0$, in which case the power-law solutions (8.4.2) and (8.4.3) are valid right up to the initial singularity. For $\omega > -3/2$, the scalar-field dominated phase causes an early period of power-law inflation. In this case there is always an initial singularity and the value of the scalar field diverges to infinity or zero as it is approached, depending on the sign of τ_2. For $\omega < -3/2$ there is a 'bounce' and the scale factor has a minimum non-

zero value. In these universes there is a phase of contraction followed by a phase of expansion, with no singularity separating them. Solutions of this type were the focus of [38] where the evolution of ϕ through the bounce was used to model the variation of various physical constants in such situations. The energy exchange term does not play a significant role at early times in these models. The asymptotic solutions as the singularity (or bounce) is approached are the same as if the energy exchange term had been neglected, and are given by [144], up to the absorption of c_1 into τ_2 previously described.

$\boldsymbol{\lambda(\tau) = c_3\tau^n,\ n \neq 1}$

The behaviour of the solutions (8.4.10)-(8.4.13) depends upon the signs of $n-1$ and c_3, as well as on the sign of $\omega + 3/2$. For illustrative purposes we will consider the radiation case $\gamma = 4/3$ which is appropriate for realistic universes dominated by asymptotically-free interactions at early times.

For $n > 1$ it can be seen that the late-time attractors of solutions (8.4.10)-(8.4.13) are $a \to$ constant and $\phi \to$ constant as $\tau \to \infty$, for both $\omega > -3/2$ and $\omega < -3/2$. At late times these universes are asymptotically static; the evolution of the scale-factor ceases as $\tau \to \infty$ and both ϕ and ρ become constant. Further analysis is required to establish whether these static universes are stable or not (we expect them to be stable as no tuning of parameters or initial conditions has been performed to obtain these solutions).

The early-time behaviour of solutions with $n > 1$ depends upon the sign of c_3 as well as whether ω is greater or less than $-3/2$. We will consider first the case of $\omega > -3/2$. For $c_3 > 0$, we see that $a \to \infty$ as $\tau^{n-1} \to \tau_0^+$; for $c_3 < 0$ we see that $a \to \infty$ as $\tau^{n-1} \to \tau_0^-$ (where $\tau_0^+ = ((2-\gamma)\sqrt{3(3+2\omega)} + (4-3\gamma))/2c_3$ and $\tau_0^- = -((2-\gamma)\sqrt{3(3+2\omega)} - (4-3\gamma))/2c_3$). For $n > 1$ and $\omega > -3/2$ we therefore have the generic behaviour that $a \to \infty$ at early times and $a \to$ constant at late times. The behaviour of a at intermediate times varies in form depending on the sign of c_3, as can be seen in figures 8.1 and 8.2. The asymptotic form of ϕ for $n > 1$ and $\omega > -3/2$ depends critically on the sign of c_3. For $c_3 > 0$ it can be seen that $\phi \to 0$ as $\tau^{n-1} \to \tau_0^+$, whereas for $c_3 < 0$ it can be seen that $\phi \to \infty$ as $\tau^{n-1} \to \tau_0^-$. The behaviour of ϕ in these two cases is illustrated in figures 8.1 and 8.2.

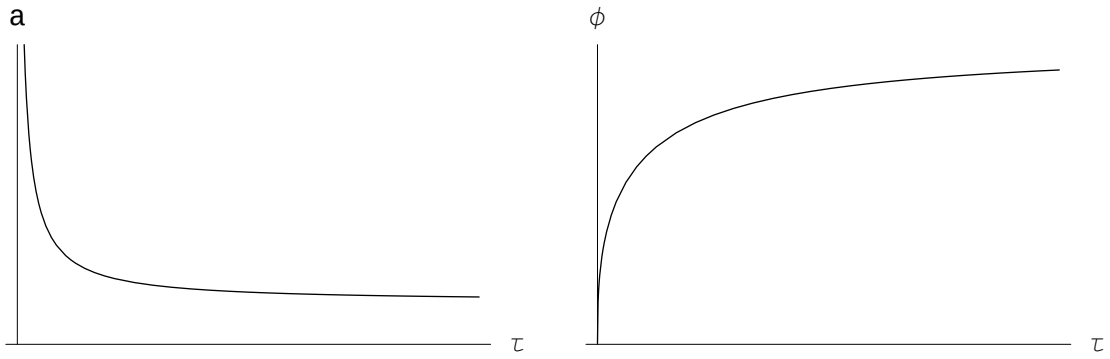

Figure 8.1: *The evolution of a and ϕ for $n = 2$, $\omega = 10$, $c_3 = 10$ and $\gamma = 4/3$.*

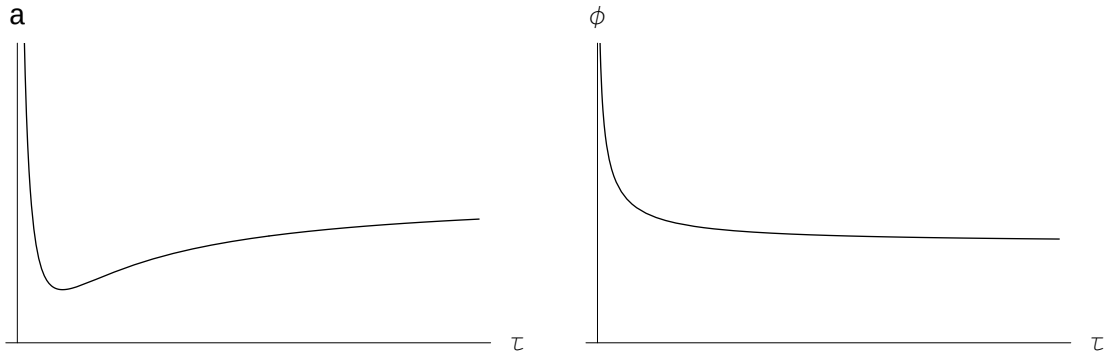

Figure 8.2: *The evolution of a and ϕ for $n = 2$, $\omega = 10$, $c_3 = -10$ and $\gamma = 4/3$.*

We now consider the early-time behaviour of solutions with $n > 1$ and $\omega < -3/2$. It can be seen that $a \to 0$ as $\tau \to 0$ irrespective of the sign of c_3, so that we find the generic behaviour $a \to 0$ at early times and $a \to$ constant at late times (this is in contrast to the standard theory where an initial singularity is avoided when $\omega < -3/2$). Again, the behaviour of a at intermediate times is dependent on the sign of c_3, as can be seen from figures 8.3 and 8.4. As $\tau \to 0$ we see that ϕ has a finite non-zero value and is either increasing or decreasing depending on the sign of c_3. This behaviour is shown in figures 8.3 and 8.4.

It remains to investigate the nature of the solutions with $n < 1$. At late times

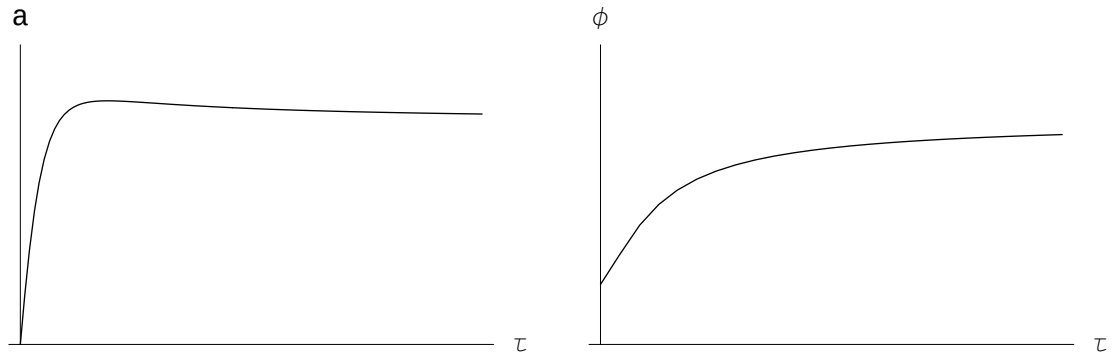

Figure 8.3: *The evolution of a and ϕ for $n = 2$, $\omega = -10$, $c_3 = 10$ and $\gamma = 4/3$.*

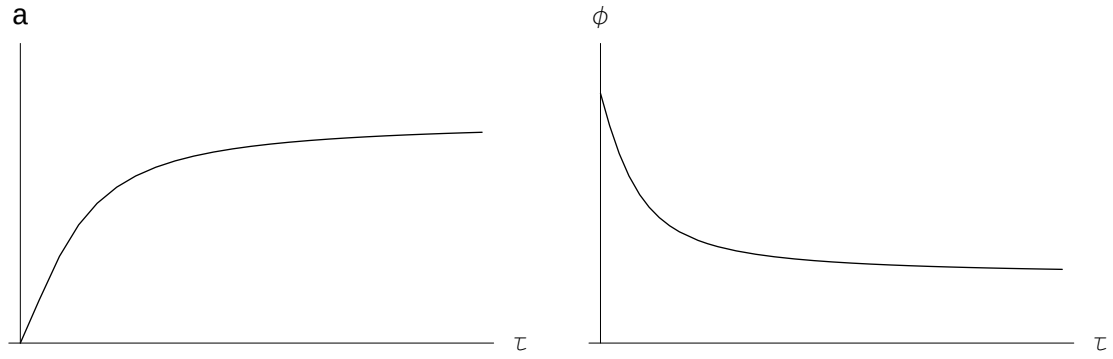

Figure 8.4: *The evolution of a and ϕ for $n = 2$, $\omega = -10$, $c_3 = -10$ and $\gamma = 4/3$.*

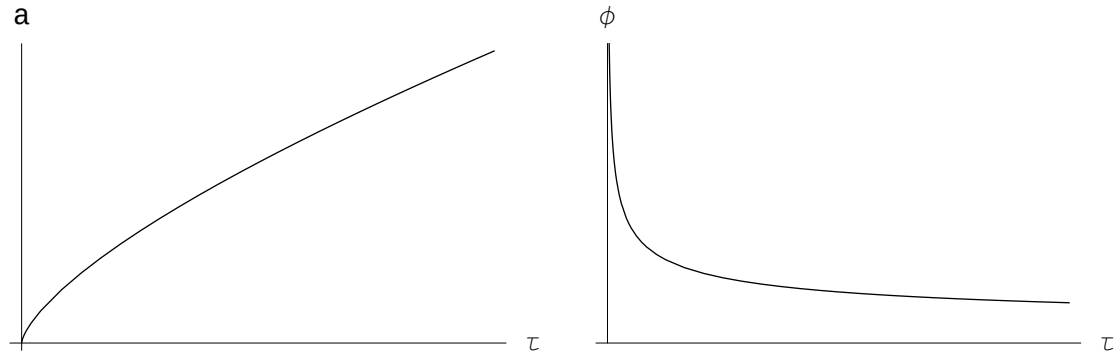

Figure 8.5: *The evolution of a and ϕ for $n = 0$, $\omega = 10$, $c_3 = 10$ and $\gamma = 4/3$.*

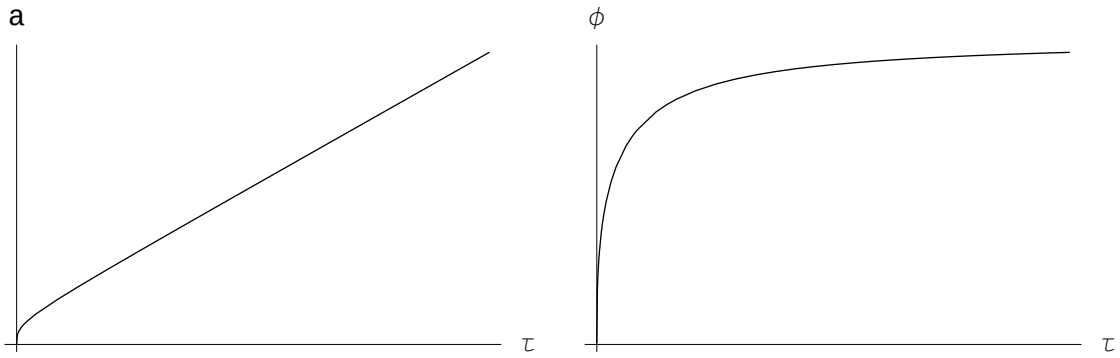

Figure 8.6: *The evolution of a and ϕ for $n = 0$, $\omega = 10$, $c_3 = -10$ and $\gamma = 4/3$.*

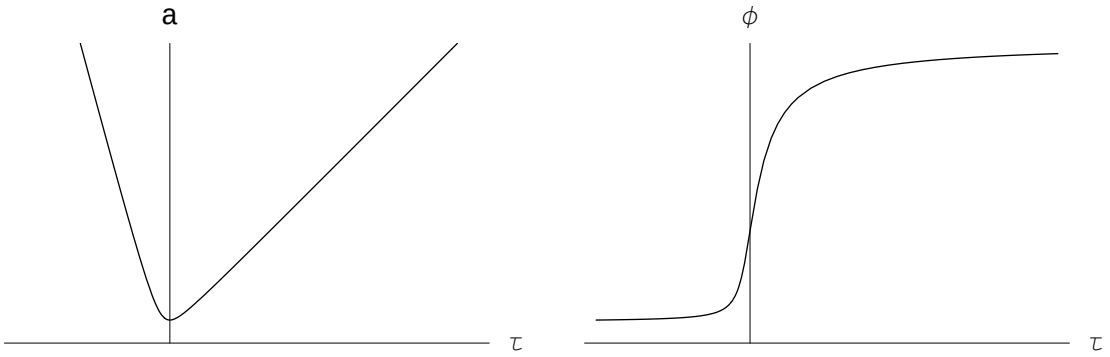

Figure 8.7: *The evolution of a and ϕ for $n = 0$, $\omega = -10$, $c_3 = 10$ and $\gamma = 4/3$.*

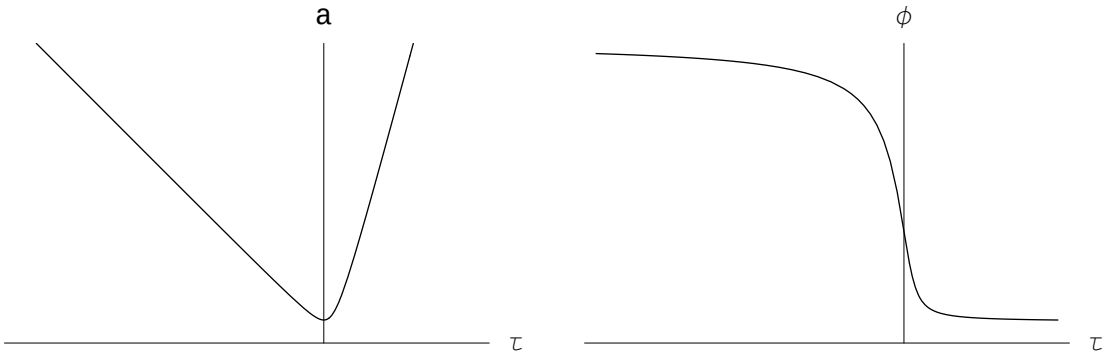

Figure 8.8: *The evolution of a and ϕ for $n = 0$, $\omega = -10$, $c_3 = -10$ and $\gamma = 4/3$.*

we see that

$$a \longrightarrow \tau^{\frac{2+2(2-\gamma)\omega}{2(5-3\gamma)+3(2-\gamma)^2\omega}},$$
$$\phi \longrightarrow \tau^{\frac{2(4-3\gamma)}{2(5-3\gamma)+3(2-\gamma)^2\omega}},$$

as $\tau \to \infty$, irrespective of the sign of c_3 or the value of ω. These late-time attractors are the flat FRW power-law Brans-Dicke solutions [137] which reduce to the standard general relativistic solutions in the limit $\omega \to \infty$.

The early-time behaviour when $n < 1$ depends on the sign of c_3 and the sign of $\omega + 3/2$. We consider first the case $\omega > -3/2$. In this case it can be seen that $a \to 0$ as $\tau^{n-1} \to \tau_0^+$ or $\tau^{n-1} \to \tau_0^-$, for $c_3 > 0$ or $c_3 < 0$ respectively. The behaviour of a for both $c_3 > 0$ and $c_3 < 0$ is shown in figure 8.5 and 8.6. The behaviour of ϕ at early times depends on the sign of c_3 and goes to ∞ for $c_3 > 0$ or to 0 for $c_3 < 0$. The behaviour of ϕ in these cases is shown in figures 8.5 and 8.6. For $\omega < -3/2$ the scale factor a contracts to a finite, but non-zero, minimum value and then expands. The exact form of the minimum depends on the values of n, ω and c_3, but it is interesting to note that odd values of n produce symmetric bounces and even values of n produce asymmetric bounces, as illustrated in figures 8.7 and 8.8. The evolution of ϕ through these bounces is smooth with a time direction prescribed by the value of c_3, as shown in figures 8.7 and 8.8 (increasing for $c_3 > 0$ and decreasing for $c_3 < 0$). The effect of changing the sign of c_3 is seen to be a mirroring of the evolution of a and ϕ in the $y-$axis.

8.6 Physical Consequences

The solutions found in the previous sections are of physical interest for a number of reasons. The transfer of energy and momentum between a non-minimally coupled scalar field ϕ and matter fields is a prediction of a number of fundamental theories of current interest, including string theories, Kaluza-Klein theories and brane-worlds. The cosmologies produced by such an interaction, therefore, should be of direct interest in the consideration of these theories. Furthermore, the solutions we have found display modified behaviour at both early and late times. The investigation of modified theories of gravity at early times is of particular interest as it is in

the high-energy limit that deviations from general relativity are usually expected. Modified behaviour at late times is also of interest as it is at these times that we can make direct observations which can be used to constrain deviations from the standard general relativistic model. We will now summarise the behaviour of the solutions found in the previous section, highlighting the physically significant results and constraints that can be placed on the theory by observations.

For the case of λ linear in τ it was shown that the late-time attractors of the general solutions are no longer the power-law solutions of the Brans-Dicke theory, but are given by equations (8.4.4) and (8.4.5). These attractors are of special interest as they have a simple power-law form that reduces to the general relativistic result in the limit $\omega \to \infty$ and to the Brans-Dicke result in the limit $c_2 \to 0$. Observations of cosmic microwave background anisotropies and the products of primordial nucleosynthesis will therefore be able to constraint any potential late-time deviations of this kind, and hence the underlying model. The process of primordial nucleosynthesis in scalar-tensor theories has been used by a number of authors to place constraints on the coupling parameter $\omega(\phi)$ [61, 62, 173, 172, 167, 77, 70]. In these studies the different value of G during nucleosynthesis causes the weak interactions to freeze out at a different time and hence the proton to neutron ratio at this time is different to the standard case. This modification causes different abundances of the light elements to be produced, which can be compared with observations to constrain the underlying theory. Studies of this kind usually assume G to be constant during nucleosynthesis, which will not be the case when energy is allowed to be exchanged between ϕ and the matter fields. The effects of a non-constant G were studied in [70]. A similar study would be required to place constraints upon the parameters c_2 and ω in this theory. The cosmic microwave background power spectrum has also often been used to constrain scalar-tensor theories of gravity [118, 65, 133, 194, 134, 2]. In these studies the redshift of matter-radiation equality is different from its usual general relativistic value due to the modified late-time evolution of the Universe. This change in the redshift of equality is imprinted on the spectrum of perturbations as it is only after equality that sub-horizon scale perturbations are allowed to grow. The main effect is seen as a shift in the first peak of the power-spectrum, which can be compared with observations to constrain the theory. Again, the late-time evolution of the Universe is modified from the usual Brans-Dicke case by the energy exchange

that we consider, so that the previous constraints are not directly applicable.

For the case of a non-linear power-law exchange of energy, described by $\lambda \propto \tau^n$, the late-time evolution of a and ϕ can be significantly modified. For $n > 1$, the solutions do not continue to expand eternally, but are attracted towards a static state where the time-evolutions of a, ϕ and ρ cease. For $n < 1$ the generic late-time attractor is the power-law solution of a flat FRW Brans-Dicke universe. It appears that theories of energy exchange with $n > 1$ are ruled out immediately by observations of an expanding universe whilst the case of $n < 1$ is subject to the same late-time constraints as the standard Brans-Dicke theory [61, 62, 173, 172, 167, 77, 70, 118, 65, 133, 194, 134, 2].

It remains to investigate the physical consequences of the early-time behaviour of our solutions. For λ linear in τ these solutions approach those of the standard Brans-Dicke theory as either the initial singularity or the minimum of the bounce are approached, according to the sign of $\omega - 3/2$. The physical significance of this behaviour has been discussed many times before, usually focusing on the avoidance of the initial singularity and the inflation that can result from the presence of the free component of the scalar field.

For $\lambda \propto \tau^n$ the early-time behaviour can be significantly changed from that of the standard theory. For $n > 1$ the scale factor a either approaches infinity or zero, depending on our choice of ω and c_3, as previously described. For the more realistic case of $n < 1$ the evolution of a at early times either undergoes a period of rapid expansion or a non-singular bounce, depending on whether ω is greater or less than $-3/2$. This behaviour is similar to that of the general solutions of the standard theory, but in this case the free scalar-field-dominated epoch has not been invoked and there is more freedom as to the exact form of the evolution. For example, with a suitable choice of parameters it is possible to create a universe that contracts and then is briefly static before 'bouncing' and continuing on to its late-time power-law evolution. This is shown in figure 8.9 for the case $\omega = -10$, $n = -2$ and $c_3 = 10$. (It is interesting to note that Peter and Pinto-Neto remark that a static period followed by a bounce could potentially produce a scale-invariant spectrum of perturbations [152]). For the physically reasonable models with $n \leqslant 1$ the evolution of ϕ, and hence of G, can be significantly altered at early times from what is generally assumed to be the case in scalar-tensor theories of gravity. For the case $\omega > -3/2$, the value of G

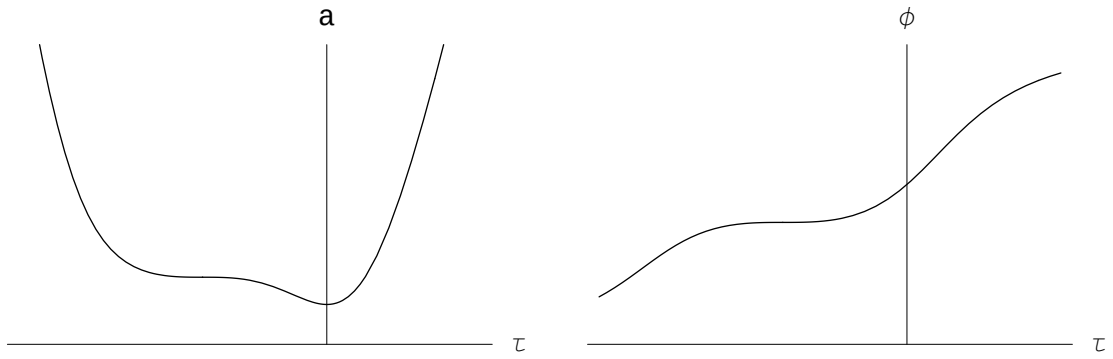

Figure 8.9: *The evolution of a and ϕ for $n = -2$, $\omega = -10$, $c_3 = 10$ and $\gamma = 4/3$.*

can be made to diverge to infinity or to zero as the initial singularity is approached, independent of whether or not there was an early scalar-dominated phase to the universe's history. For the case $\omega < -3/2$, the value of G evolves smoothly through the bounce in the scale-factor, and is again independent of whether or not there was a scalar-dominated phase. More complicated evolutions of ϕ can also be constructed, as can be seen in figure 8.9.

In performing this analysis we have allowed the coupling constant ω to lie in the ranges $\omega > -3/2$ and $\omega < -3/2$. It should be noted that when $\omega < -3/2$ the scalar field ϕ should be considered as having negative energy. Allowing an interaction with matter fields may then be considered as problematic as energy could potentially be transferred from the scalar field to the matter fields without bound, allowing runaway solutions.

8.7 Discussion

We have considered spatially flat FRW universes in scalar-tensor theories of gravity where energy is allowed to be exchanged between the Brans-Dicke scalar field that determines the strength of gravity and any perfect fluid matter fields in the space-time. We have presented a prescription for integrating the field equations exactly for some unknown function λ which describes the rate at which energy is exchanged. For the case of λ being a linear function of τ we have found the general solutions to the problem and for the case of λ being a non-linear power law function of τ

we have been able to find a wide class of exact solutions. These solutions display behaviours that can deviate substantially from the corresponding solutions in the standard case, where the exchange of energy is absent. Depending upon the values of the parameters defining the theory and the exchange of energy, deviations in the evolution of a and ϕ can occur at both early and late times, providing a richer phenomenology than is available in the standard theory.

We have found that the parameter n must be bounded by the inequality $n \leqslant 1$ if the Universe is to be expanding at late times. For $n = 1$ we have found late-time power-law attractor solutions which can be used to constrain the parameters c_2 and ω. For $n < 1$ we have seen that the late-time evolution will be the same as in the standard Brans-Dicke case, and so is subject to the same observational constraints as these theories. The parameters c_3 and τ_2 have been shown to be influential only in the vicinity of the initial singularity, or at the minimum of expansion in non-singular solutions. These parameters are therefore less accessible to constraint by late-time observations (see, however, [70] where the influence on primordial nucleosynthesis is used to constrain τ_2). The parameter ω is, as always, subject to the very tight solar system constraint $\omega > 40000$ to 2σ [47].

These results could be of interest in attempting to explain why G is so small in the present day Universe compared to the proton mass scale ($Gm_{pr}^2 \sim 10^{-39}$). In these models the value of G can decay away by a coupling between the scalar field ϕ and the matter fields which allows energy to be transferred. The small value of G is then due to the age of the Universe. It remains to see whether or not the late-time modifications found above are consistent with observations of the primordial abundance of light elements, microwave background formation and other late-time physical processes. These studies should be able to be performed in an analogous way to the ones that already exist for the standard Brans-Dicke theory.

Using the late-time solutions that have been found it is possible to comment on the case of FRW cosmologies with non-zero spatial curvature. At early times it is expected that the effect of any spatial curvature on the evolution of $a(t)$ should be negligible. From the solution (8.4.2) we can see that spatial curvature will dominate the late time evolution if the condition

$$\frac{2 + 2(2-\gamma)\omega + 2c_2}{4 + 3\gamma\omega(2-\gamma) - 2c_2(7 - 6\gamma - c_2)} < 1$$

is satisfied. If this condition is not satisfied, then the power-law solution (8.4.2) will be an attractor as $t \to \infty$ even in the case of non-zero spatial curvature, offering a potential solution to the flatness problem. This behaviour corresponds to power-law inflation and it can be seen that the condition for equation (8.4.2) to dominate over the spatial curvature at late times is, indeed, also the condition that power-law inflation should occur.

In conclusion, we have found that a direct coupling between ϕ and the matter fields in scalar-tensor cosmologies provides a richer frame-work within which one can consider variations of G. We have shown that it is possible to construct models where the late-time violations of the equivalence principle can be made arbitrarily small (for $\lambda \propto \tau$) or are attracted to zero (for $\lambda \propto \tau^n$ where $n < 1$). This enlarged phenomenology is of interest for the consideration of the four-dimensional cosmologies associated with higher-dimensional theories as well as for more general considerations of the variation of G and its late-time value. This study has been limited to scalar-tensor theories with constant coupling parameters, to flat FRW cosmologies, and to special cases of σ^0 that allow direct integration of the field equations. Obvious extensions exist in which these assumptions are partially or completely relaxed.

CHAPTER 9

Cosmological Constraints

Observations of physical processes occuring in an expanding universe can be used to constrain the underlying gravitational theory in a number of ways. These observations can range from galaxy surveys in the nearby Universe to the results of processes occuring in the very early Universe. We will concentrate in this work on the processes of primordial nucleosynthesis and microwave background formation. Both of these processes occur early in the Universe's history and the results of both are well observed by astronomers and astrophysicists.

This chapter is based on the work of Clifton, Barrow and Scherrer [74] and Clifton and Barrow [70].

9.1 Scalar-Tensor Theories and Primordial Nucleosynthesis

Using the scalar-tensor theories we investigate the earliest well understood physical process, primordial nucleosynthesis. Previous studies on this subject have been carried out by a number of authors. In particular, the Brans-Dicke theory has been especially well studied in this context by, for example, Casas, Garcia-Bellido and Quiros [61], [62] and Serna, Dominguez-Tenreiro and Yepes [173]. The more general

class of Scalar-Tensor theories has also been well studied, most notably by Serna and Alimi [172], Santiago, Kalligas and Wagoner [167] and Damour and Pichon [77]. More recently, a number of studies have been performed investigating the effect of a nonminimally coupled quintessence field on primordial nucleosynthesis (see e.g. [66],[153]). Although these studies are very detailed, they all make the simplifying assumption of a constant G during the radiation-dominated phase of the Universe's history (with the exception of [173], who numerically investigate the effect of an early scalar-dominated phase on the Brans-Dicke theory, and [77] who use the idea of a "kick" on the scalar field during electron-positron annihilation). We relax this assumption and investigate the effects of entering the radiation-dominated phase with a non-constant G. The constraints we impose upon the variation of G during primordial nucleosynthesis are then used to constrain the parameters of the theory. In carrying out this study we consider the more general class of scalar-tensor theories, paying particular attention to the Brans-Dicke theory.

9.1.1 Modelling the Form of $G(t)$

If primordial nucleosynthesis were to occur during the scalar-dominated period then the very different expansion rate would have disastrous consequences for the light-element abundances (see e.g. [173]). Therefore we limit our study to times at which the scale factor can be approximated by a form that is close to $a(t) \propto t^{\frac{1}{2}}$, and so primordial nucleosynthesis can safely be described as occurring during radiation domination. Performing a power-series expansion of the FRW Brans-Dicke solutions (3.2.6), (3.2.7), (3.2.8) and (3.2.9) in $\eta_1/(\eta+\eta_2)$ we find

$$a(\eta) = a_1(\eta + \eta_2 + 3\eta_1) + O(\eta_1^2) \tag{9.1.1}$$

$$\phi(\eta) = \phi_1 \left(1 - \frac{3\eta_1}{\eta + \eta_2}\right) + O(\eta_1^2) \tag{9.1.2}$$

for both $\omega > -3/2$ and $\omega < -3/2$. We can then set the origin of the η coordinate such that $a(0) = 0$ with the choice $\eta_2 = -3\eta_1$. The solutions (9.1.1) and (9.1.2)

then become, in terms of the time coordinate t,

$$a(t) = a_1 t^{\frac{1}{2}} + O(\eta_1^2)$$
$$\phi(t) = \phi_1 \left(1 + \frac{a_2}{a(t)}\right) + O(\eta_1^2),$$

where $a_2 = -3\eta_1 a_1$ and the origin of t has been chosen to coincide with the origin of η.

Similarly, expanding the FRW $\omega(\phi)$ solutions (3.3.6) and (3.3.7) in $\eta_1/(\eta + \eta_2)$ we find that, for both $\omega > -3/2$ and $\omega < -3/2$,

$$a(t) = a_1 t^{\frac{1}{2}} + O(\eta_1^2)$$
$$\phi(t) = \phi_1 \left(1 + \frac{a_2}{a(t)}\right) + O(\eta_1^2)$$

where

$$a_1 = \sqrt{8\pi\bar{\rho}_{r0}/3}\exp(\beta(\psi_1 - \psi_\infty)^2/2)$$
$$a_2 = \sqrt{2\bar{\rho}_{r0}}\beta\eta_1(\psi_1 - \psi_\infty)\exp(\beta(\psi_1 - \psi_\infty)^2/2)$$
$$\phi_1 = \exp(-\beta(\psi_1 - \psi_\infty)^2)$$

and η_2 has been set so that $a(0) = 0$.

In the limit $\dot{\phi} \to 0$ we can see from equations (3.1.2), (3.1.3) and (3.1.5) that the standard GR Friedmann equations are recovered, with a different value of Newton's constant given by

$$G(t) = \frac{1}{\phi(t)} = G_1 \frac{a(t)}{a(t) + a_2} \tag{9.1.3}$$

where $G_1 = 1/\phi_1$. We conclude that the solutions found above correspond to a situation that can be described using the GR Friedmann equations with a different, and adiabatically changing, value of G. This is just the situation considered by Bambi, Giannotti and Villante [5], but we now have an explicit form for the evolution of $G(t)$ derived from scalar-tensor gravity theory.

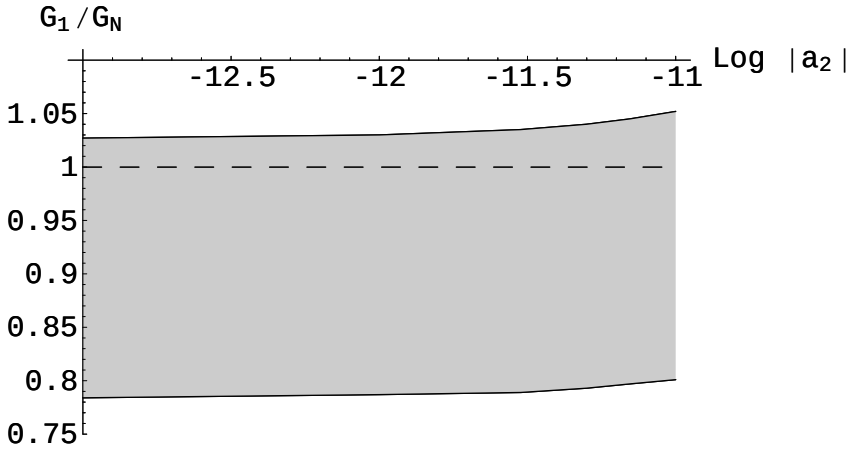

(a) 2σ bounds for $a_2 > 0$

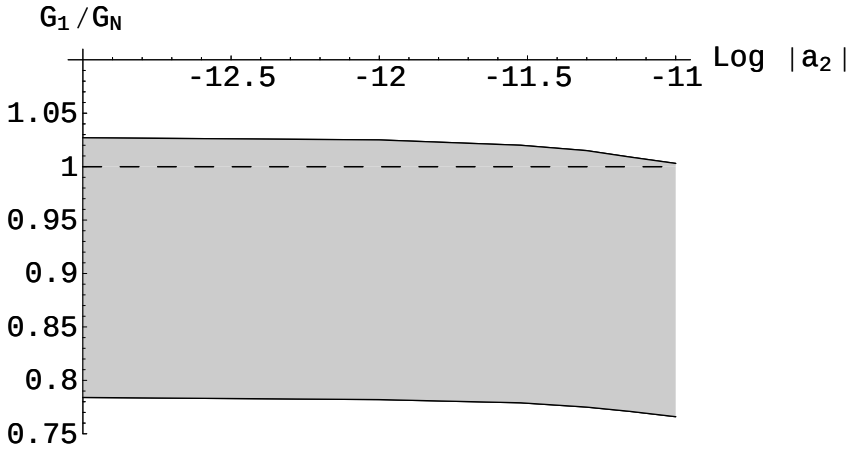

(b) 2σ bounds for $a_2 < 0$

Figure 9.1: *The upper and lower bounds on G_1/G_N as a function of a_2 are shown by the solid lines. The shaded regions correspond to the allowed parameter space and the dashed lines show $G_1 = G_N$.*

9.1.2 The Effect of a Non-Constant G

The time at which weak interactions freeze out in the early Universe is determined by equality between the rate of the relevant weak interactions and the Hubble rate. When the weak interaction rate is the greater then the ratio of neutrons to protons tracks its equilibrium value, $n/p = \exp(-(m_n - m_p)/T)$ where m_n and m_p are the neutron and proton masses. If, however, the Hubble rate is greater than the weak-interaction rate then the ratio of neutrons to protons is effectively 'frozen-in', and β decay is the only weak process that still operates with any efficiency. This will be the case until the onset of deuterium formation, at which time the neutrons become bound and β-decay ceases. The onset of deuterium formation is primarily determined by the photon to baryon ratio, η_γ, which inhibits the formation of deuterium nuclei until the critical temperature for photodissociation is past. As the vast majority of neutrons end up in ^{4}He the primordial abundance of this element is influenced most significantly by the number of neutrons at the onset of deuterium formation, which is most sensitive to the temperature of weak-interaction freeze-out, and hence the Hubble rate, and so G, at this time. Conversely, the primordial abundances of the other light elements are most sensitive to the temperature of deuterium formation, and hence η_γ, when nuclear reactions occur and the light elements form. (See [5] for a more detailed discussion of these points).

Using the simple forms of $a(t)$ and $G(t)$ derived above we use a modified version of the Kawano code [112] to investigate the effect of this variation of G on primordial nucleosynthesis directly. We use the deuterium abundance estimated by Kirkman et al. [114]

$$\log\left(\frac{D}{H}\right) = -4.556 \pm 0.064 \quad \text{to } 1\sigma, \tag{9.1.4}$$

and the ^{4}He abundance estimated by Barger et al. [7]

$$Y_P = 0.238 \pm 0.005 \quad \text{to } 1\sigma, \tag{9.1.5}$$

to create a parameter space in (η_γ, G_1, a_2). The three-dimensional 95% χ^2 confidence region is projected into the G_1, a_2 plane to give figure 9.1, where three species of light neutrinos and a neutron mean lifetime of $\tau = 885.7$ seconds have been assumed.

The apparent disfavoring of the value of G_1 much greater than G_N in figure

9.1 is due to the observational limits we have adopted for Y_P (equation (9.1.5)), which suggest a helium abundance that is already uncomfortably low compared to the theoretical prediction for Y_P derived from the baryon density corresponding to equation (9.1.4). We expect these constraints to be updated by future observations (see e.g. [185]); this will require a corresponding update of any work, such as this, that seeks to use these constraints to impose limits on physical processes occuring during primordial nucleosynthesis.

These limits on the parameters G_1 and a_2 can be used to construct plots showing the explicit evolution of $G(t)$ for various limiting combinations of the two parameters, this is done in figure 9.2. It is interesting to note that in both of these plots the lines corresponding to different values of a_2 all appear to cross at approximately the same point, $\log a \sim -9.4$. This confirms our earlier discussion, and the results of [5], that the ^{4}He abundance is mostly only sensitive to the value of G at the time when the weak interactions freeze out. In reality, this freeze-out happens over a finite time interval, but from figure 9.2 we see that it is a good approximation to consider it happening instantaneously - where the lines cross. To a reasonable accuracy one could then take G throughout primordial nucleosynthesis to be its value during the freeze-out process.

9.1.3 Constraining the Theory

Using the results in the previous section it is possible to constrain the underlying scalar-tensor gravitational theory. This is done separately for the Brans-Dicke theory and for the more general scalar-tensor theories. For each theory we consider the case of a universe containing matter and radiation only and then a universe containing matter, radiation and a non-zero vacuum energy, with equation of state $p = -\rho$.

Brans-Dicke theory

Universe containing matter and radiation

Using the Brans-Dicke matter-dominated FRW solutions (3.2.10) we can write the ratio of G at matter-radiation equality, G_{eq}, to its present-day laboratory value, G_N,

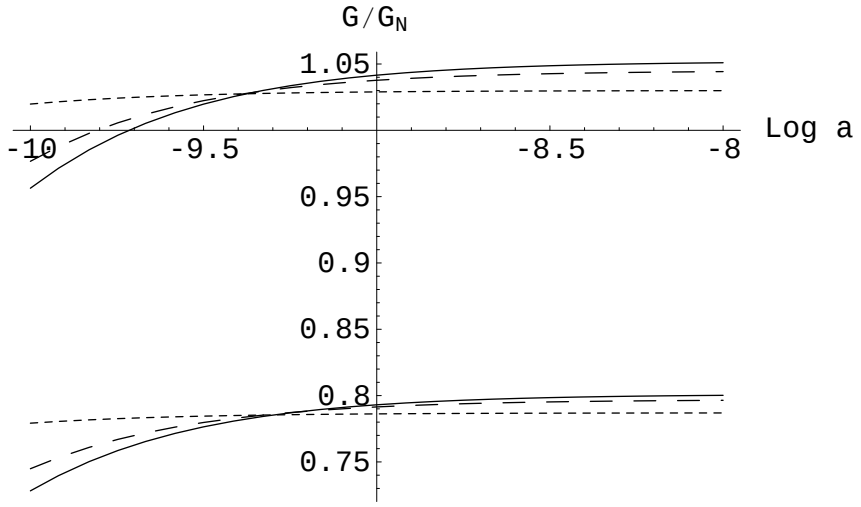

(a) $a_2 > 0$

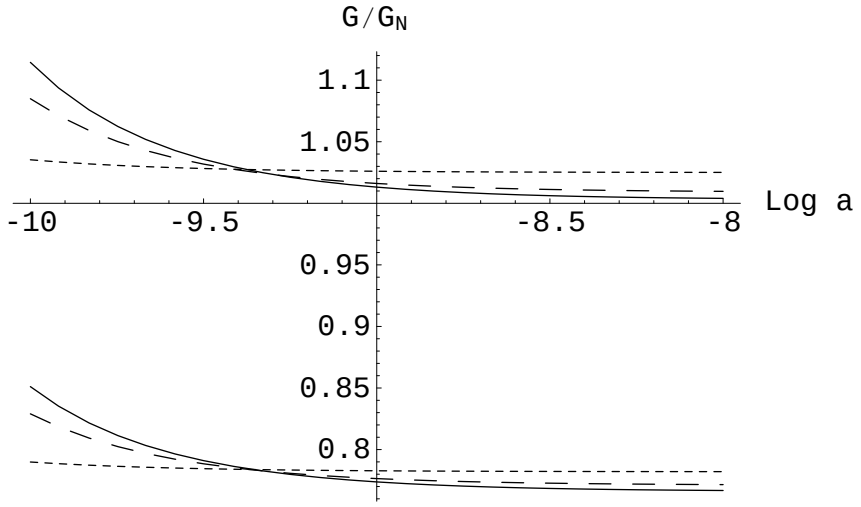

(b) $a_2 < 0$

Figure 9.2: *These plots show the explicit evolution of G for some limiting values of G_1, as taken from figure 9.1, for various values of a_2. Solid lines correspond to $|a_2| = 10^{-11}$, dashed lines correspond to $|a_2| = 10^{-11.155}$ and dotted lines correspond to $|a_2| = 10^{-12}$.*

as

$$\frac{G_{eq}}{G_N} = \frac{(2\omega+3)}{(2\omega+4)}\frac{\phi_N}{\phi_{eq}} = \frac{(2\omega+3)}{(2\omega+4)}\left(\frac{a_0}{a_{eq}}\right)^{1/(\omega+1)} \equiv \frac{(2\omega+3)}{(2\omega+4)}(1+z_{eq})^{1/(\omega+1)} \quad (9.1.6)$$

where we have used the expression for G in the weak-field limit [191]:

$$G(\phi) = \frac{(2\omega+4)}{(2\omega+3)}\frac{1}{\phi}, \quad (9.1.7)$$

for G_N, and $G(\phi) = 1/\phi$ for G_{eq}, as in (9.1.3). In reality, the laboratory value of G today is not equal to that in the background cosmology [75], although we take it to be so here for simplicity as this effect should be small.

We now proceed by calculating $1 + z_{eq}$ in the Brans-Dicke cosmology, following Liddle, Mazumdar and Barrow [118]. As $T^{ab}{}_{;b} = 0$ in the Jordan frame we have that $\rho_r \propto a^{-4}$ and $\rho_m \propto a^{-3}$. For a universe containing matter and radiation only, this gives

$$1 + z_{eq} = \frac{a_0}{a_{eq}} = \frac{\rho_{m0}}{\rho_{r0}}\frac{\rho_{req}}{\rho_{meq}} = \frac{\rho_{m0}}{\rho_{r0}}$$

as well as the usual relation $T \propto a^{-1}$, when entropy increase is neglected.

Photons and neutrinos both contribute to the value of ρ_{r0}, the present-day energy-density of radiation. From $T_{\gamma 0} = 2.728 \pm 0.004K$ [85], we get $\rho_{\gamma 0} = 4.66 \times 10^{-34} g\ cm^{-3}$ and using the well known result $T_{\nu 0} = (4/11)^{1/3} T_{\gamma 0}$, and assuming three families of light neutrinos, we also have $\rho_{\nu 0} = 0.68\rho_{\gamma 0}$. This gives the total present-day radiation density as $\rho_{r0} = 7.84 \times 10^{-34} g\ cm^{-3}$. Now, recalling our assumption of spatial flatness and (3.1.3), we can write

$$\rho_{tot0} = \rho_{m0} + \rho_{r0} = \frac{3H_0^2}{8\pi G_N}\frac{(4+3\omega)(4+2\omega)}{6(1+\omega)^2}.$$

For $G_N = 6.673 \times 10^{-11}\ Nm^2kg^{-2}$, $H_0 = 100h\ kms^{-1}Mpc^{-1}$, and the value of ρ_{r0} above, we have

$$\begin{aligned} 1 + z_{eq} &= 2.39 \times 10^4 h^2 \frac{(4+3\omega)(4+2\omega)}{6(1+\omega)^2} - 1 \\ &= 2.39 \times 10^4 h^2 \left(1 + \frac{4}{3\omega}\right) + O(\omega^{-2}). \end{aligned}$$

This correction to $1 + z_{eq}$ has direct observational consequences in the power spectrum of cosmic microwave background perturbations. After $1 + z_{eq}$ the subhorizon scale perturbations, that were previously effectively frozen, are allowed to grow. Changing the value of $1 + z_{eq}$ therefore causes a shift in the power-spectrum peaks, which is potentially observable (see [118], [65], [133] [194], [134] and [2] for a more detailed discussion of the effect of a varying G on microwave background formation). For our purposes this modified expression for $1 + z_{eq}$ can then be substituted into (9.1.6) to give an equation in terms of ω, G_{eq} and h. Assuming a value of $h = 0.7$ and that $G_{eq} = G_1$, as appears a very good approximation for the models above, we can use our bounds on G_1 in terms of a_2 to create an allowed parameter space in the (ω,a_2) plane. This is shown in figure 9.3.

We remind the reader that a large ω corresponds to a slowly varying Machian component of $\phi(1 + z)$, as can be seen directly from equations (3.2.10), (3.2.11) and the late-time limits of (3.2.6), (3.2.7), (3.2.8) and (3.2.9). The parameter a_2 determines the evolution of the free component of ϕ, as can be seen from the early time limits of (3.2.6), (3.2.7), (3.2.8) and (3.2.9). In the limits $\omega \to \infty$ and $a_2 \to 0$ the Machian and free components of $\phi(1 + z)$ both become constant, respectively, resulting in a constant $G(1 + z)$. The constraints imposed upon ω and a_2 in figure 9.3 therefore correspond to constraints upon the evolution of $G(1+z)$ in this theory, valid both during primordial nucleosynthesis and at other cosmological epochs.

Universe containing matter, radiation and a nonzero vacuum energy

A more realistic constraint would involve taking into account a late-time period of vacuum domination; so as well as $\rho_r \propto a^{-4}$ and $\rho_m \propto a^{-3}$, we now also have $\rho_\Lambda =$ constant. Hence,

$$\begin{aligned}\frac{G_{eq1}}{G_N} &= \frac{(2\omega+3)}{(2\omega+4)}\frac{\phi_0}{\phi_{eq1}} = \frac{(2\omega+3)}{(2\omega+4)}\frac{\phi_{eq2}}{\phi_{eq1}}\frac{\phi_0}{\phi_{eq2}} \\ &= \frac{(2\omega+3)}{(2\omega+4)}\,(1+z_{eq1})^{\frac{1}{(1+\omega)}}\,(1+z_{eq2})^{-\frac{\omega}{(1+\omega)(1+2\omega)}}\end{aligned}$$

where we have defined the redshift of matter-radiation equality, z_{eq1}, and the redshift of matter-vacuum equality, z_{eq2}, as

$$1 + z_{eq1} = \frac{\rho_{m0}}{\rho_{r0}} \quad \text{and} \quad 1 + z_{eq2} = \left(\frac{\rho_{\Lambda 0}}{\rho_{m0}}\right)^{\frac{1}{3}}.$$

As above, we still have $\rho_{r0} = 7.84 \times 10^{-34} g\ cm^{-3}$ but now our assumption of spatial flatness gives

$$\rho_{tot0} = \rho_{\Lambda 0} + \rho_{m0} + \rho_{r0} = \frac{3H_0^2}{8\pi G_N} \frac{(4+3\omega)(4+2\omega)}{6(1+\omega)^2}.$$

or, using $G_N = 6.673 \times 10^{-11}\ Nm^2kg^{-2}$ and $H_0 = 100h\ kms^{-1}Mpc^{-1}$,

$$1 + z_{eq1} = \frac{\left(2.39 \times 10^4 h^2 \frac{(4+3\omega)(4+2\omega)}{6(1+\omega)^2} - 1\right)}{\left(1 + \frac{\rho_{\Lambda 0}}{\rho_{m0}}\right)}.$$

Taking the value $\rho_{\Lambda 0}/\rho_{m0} = 2.7$, consistent with WMAP observations [45], we get the results shown in figure 9.3.

Dynamically-coupled theories

Constraints on $\omega(\phi)$ at matter-radiation equality

Recalling that $e^{2\Gamma} = 1/\phi$ and $\alpha^{-2} = 2\omega + 3$ allows us to re-write (9.1.7) as

$$G = e^{2\Gamma}(1 + \alpha^2),$$

the ratio G_{eq}/G_N can then be expressed in terms of Γ and α as

$$\frac{G_{eq}}{G_N} = \frac{e^{\Gamma_{eq}}}{e^{\Gamma_0}\sqrt{1 + \alpha_0^2}}.$$

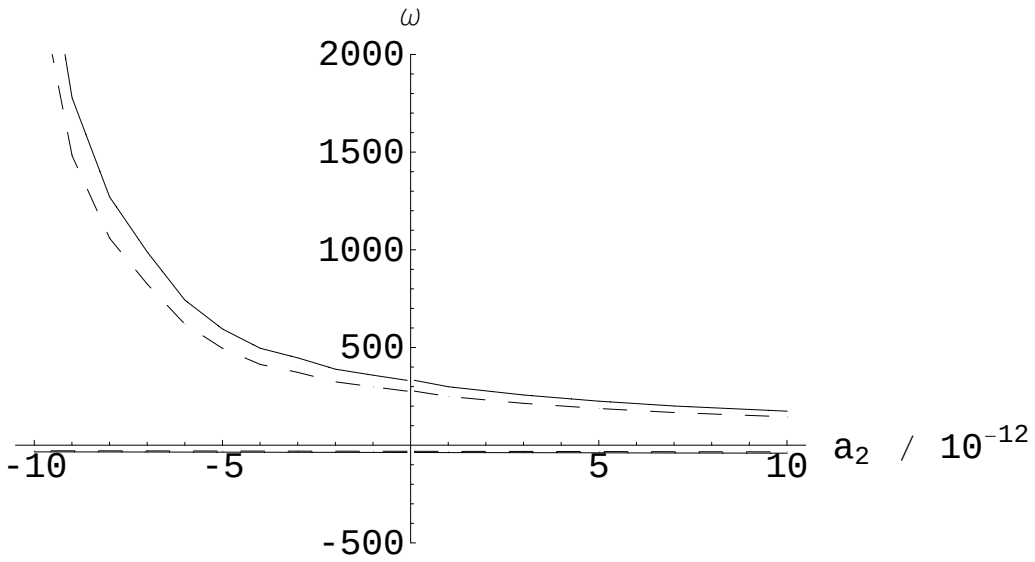

Figure 9.3: *The allowed parameter space in this plot is the region above the higher solid line and below the lower solid line, with $h = 0.7$ to 2σ for a universe containing matter and radiation only. The dashed lines show the corresponding result for a universe with a non-zero vacuum energy.*

Assuming that Γ_0 and $\ln(1+\alpha_0)$ are negligible compared to Γ_{eq} (i.e. the Universe is close to GR today, [47]) we can write

$$\ln\left(\frac{G_{eq}}{G_N}\right) \simeq \Gamma_{eq} = \frac{1}{2}\beta(\psi_{eq}-\psi_\infty)^2 = \frac{2\pi}{(2\omega_{eq}+3)}\frac{1}{\beta}.$$

This allows us to constrain ω_{eq} in terms of β and a_2, as shown in figure 9.4. Constraints imposed upon ω and a_2 have the same consequences for the evolution of G as previously discussed. The parameter β controls the evolution of ω, as can be seen from (3.3.5). In the limit $\beta \to 0$ it can be seen that ω becomes constant and this class of scalar-tensor theories becomes indistinguishable from the Brans-Dicke the-

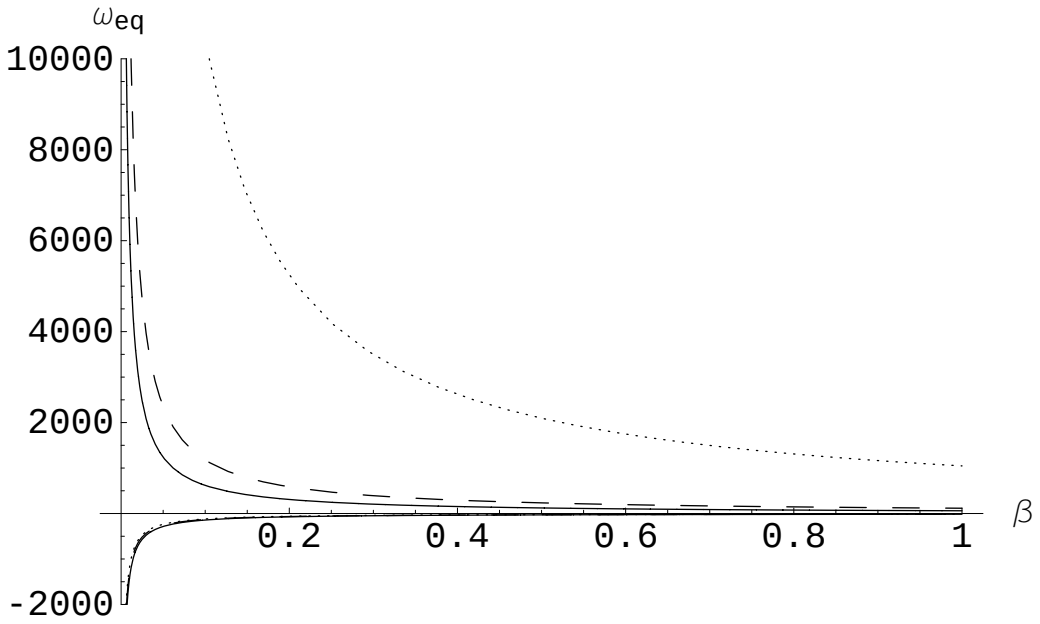

Figure 9.4: *The allowed parameter space in this graph is the region above the line in the region $\omega > 0$ and below the line in the region $\omega < 0$, to 2σ. The solid lines correspond to $a_2 = 10^{-11}$ the dashed lines to $a_2 = 10^{-13}$ and the dotted lines to $a_2 = -10^{-11}$. ω_{eq} is the value of ω at matter-radiation equality and β is a parameter of the theory, defined in (3.3.5).*

ory. Constraints upon β therefore correspond to constraints on the allowed variation of ω and hence G.

The parameter β is taken to be small here so that the "kick" on the scalar field during electron-positron annihilation can be neglected. These effects have been explored by Damour and Pichon in [77], for the case $a_2 = 0$, and are expected to have the same result in this more general scenario; we will not repeat their analysis of this effect here.

Constraints on ω_0 for a universe containing matter and radiation

The scalar field can be evolved forward in time from the time of matter-radiation equality to the present, using the solution (3.3.9). The two arbitrary constants in

this expression can be fixed using our limiting values of G_{eq} derived above and by assuming that the evolution of the scalar field has effectively ceased by this time, i.e. $\psi'_{eq} = 0$, as is the case for the models considered here.

In order to gain a quantitative limit on $\psi_1 - \psi_\infty$, and hence on ω_0, it is necessary to calculate N_{eq}. From the definition of N, we can write

$$\begin{aligned} N_{eq} &= -\ln(1+z_{eq}) - \Gamma_{eq} + \Gamma_0 \\ &\simeq -\ln(1+z_{eq}) - \frac{1}{2}\beta(\psi_{eq} - \psi_\infty)^2 \end{aligned}$$

where z_{eq} is the redshift at t_{eq} and we have assumed, as before, the term $\ln A_0$ to be negligible.

It now remains to determine $1 + z_{eq} = \rho_{m0}/\rho_{r0}$ for the case $\omega = \omega(\phi)$. If we now assume ω_0 to be moderately large, and recall our assumption of spatial flatness, we can write

$$\rho_{tot0} = \rho_{m0} + \rho_{r0} = \frac{3H_0^2}{8\pi G_N}.$$

For $\rho_{r0} = 7.84 \times 10^{-34} g\ cm^{-3}$ this gives $\rho_{m0} \simeq 1.87 \times 10^{-29}\ h^2 g\ cm^{-3}$. We have $1 + z_{eq} \simeq 2.4 \times 10^4\ h^2$ and so finally obtain, for $h = 0.7$,

$$N_{eq} \simeq -9.37 - \frac{1}{2}\beta(\psi_{eq} - \psi_\infty)^2.$$

Evolving $\psi - \psi_\infty$ from N_{eq} to $N_0 = 0$ and using

$$\omega_0 = \frac{2\pi}{\beta^2(\psi_0 - \psi_\infty)^2} - \frac{3}{2} \tag{9.1.8}$$

we obtain the results shown in figure 9.5.

Constraints on ω_0 for a universe containing matter, radiation and nonzero vacuum energy

We can repeat the previous analysis for the more realistic case of a universe with a period of late-time vacuum domination. We now need the time of matter-radiation equality, N_{eq1}, and the time of matter-vacuum equality, N_{eq2}.

Assuming spatial flatness, a large ω_0, $h = 0.7$, $\rho_{\Lambda 0}/\rho_{m0} = 2.7$, and ρ_{r0} as above

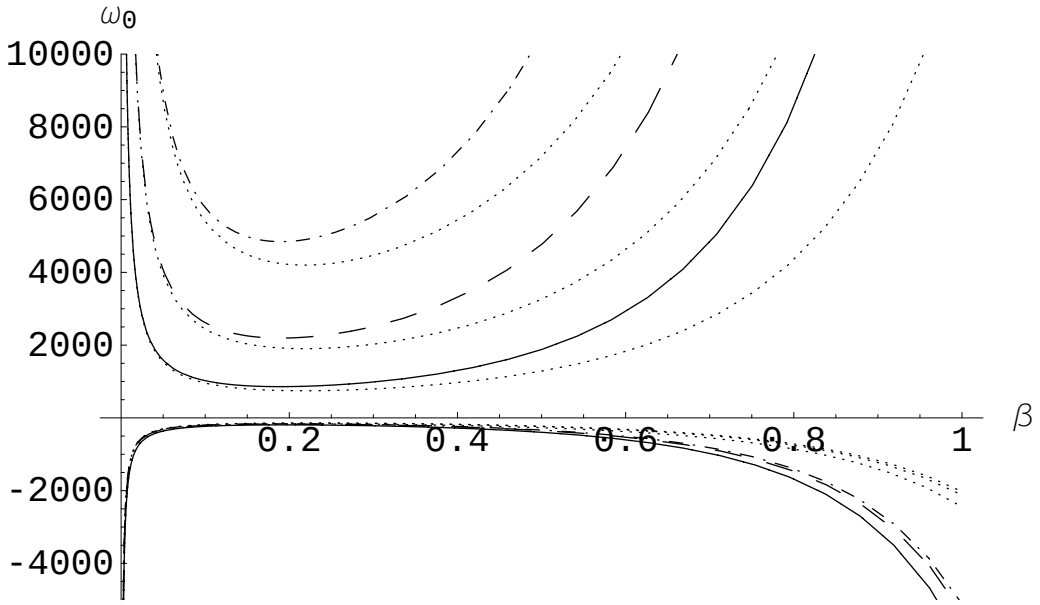

Figure 9.5: *The allowed parameter space in this graph is the region above the line in the region $\omega > 0$ and below the line in the region $\omega < 0$, to 2σ for a universe containing matter and radiation only. The solid lines correspond to $a_2 = 10^{-11}$, the dashed lines to $a_2 = -10^{-11.523}$, and the dot-dashed lines to $a_2 = -10^{-11.155}$. The dotted lines show the corresponding results for a universe with a non-zero vacuum energy.*

gives

$$N_{eq1} \simeq -8.06 - \frac{1}{2}\beta(\psi_{eq1} - \psi_\infty)^2,$$

and

$$N_{eq2} \simeq -0.33 - \frac{1}{2}\beta(\psi_{eq2} - \psi_\infty)^2.$$

We can now evolve $\psi(N) - \psi_\infty$ from N_{eq1} to N_{eq2} using (3.3.9) and the same boundary conditions as before. (In finding N_{eq2} we used an iterative method to evaluate $\psi_{eq2} - \psi_\infty$). We then use the solution (3.3.10) to evolve the field from N_{eq2} to N_0; the constants C and D in (3.3.10) are set by matching $\psi(N) - \psi_\infty$ and its first derivative with the solution (3.3.9) at N_{eq2}. Finally, we can calculate ω_0 using

(9.1.8). The results of this procedure are shown in figure 9.5.

9.1.4 Discussion

Using the framework provided by scalar-tensor theories of gravity we have investigated the effect of a time-varying G during primordial nucleosynthesis. We determined the effect on primordial nucleosynthesis numerically, using a modified version of the Kawano code [112], and constrained the parameters of the underlying theory using these results. Our results are consistent with the interpretation that the abundance of ^{4}He is primarily only sensitive to the value of G at the time when weak interactions freeze out, for the class of scalar-tensor models studied.

Using our numerically determined constraints on the evolution of G, we imposed the 2σ upper and lower bounds shown in figure 9.3 on the Brans-Dicke parameter ω. For a constant G (i.e. $a_2 = 0$) we get the bounds $\omega \gtrsim 332$ or $\omega \lesssim -37$, for a universe containing matter and radiation only, and the bounds $\omega \gtrsim 277$ or $\omega \lesssim -31$, for a universe containing matter, radiation and a nonzero vacuum energy. As the parameter a_2 is increased, the strength of the upper bound decreases whilst that of the lower bound increases; the opposite behaviour occurs as a_2 is decreased. This is because the strength of the bound on ω is essentially due to the allowed value of G at matter-radiation equality. If primordial nucleosynthesis allows this value to be vastly different from G_N then a significant evolution of G during matter domination, and hence a low $|\omega|$, is permitted. A value of G_{eq} close to G_N means that only a very slow variation of G, and hence large $|\omega|$ is permitted. As $a_2 > 0$ corresponds to an increasing G during primordial nucleosynthesis this corresponds to a higher value of G_{eq} and hence a looser upper bound on ω and a tighter lower bound (as G decreases during matter domination for $\omega > -3/2$ and increases for $\omega < -3/2$); $a_2 < 0$ corresponds to G decreasing during radiation domination, and so has the opposite effect.

The more stringent effect of a nonzero value of a_2 on the upper bounds is due to the current observational determinations of the ^{4}He abundance [7] disfavouring $G > G_N$ during primordial nucleosynthesis (see e.g. [38]).

The interpretation of the constraints on the more general ST theories is a little more complicated, due to the increased complexity of the theories. The bounds on

$\omega(\phi)$ at matter-radiation equality, shown in figure 9.4, are seen to be stronger for smaller β and weaker for larger for β (assuming β to be small enough to safely ignore the effect of the e^-e^+ kick analysed by [77]). This should be expected as $\omega \sim \beta^{-2}$ in the models we are studying. We see from the constraints on ω at the present day, shown in figure 9.5, that the bounds on ω become tighter as β gets very small and large, with an apparent minimum in the bound at $\beta \sim 0.2$. The tight bounds for very small β are due to the tight bounds on ω_{eq} for small β. The tight bounds at large β are due to the attraction towards GR at late times that occurs for this class of scalar-tensor theories (see e.g. [76]). This attractor mechanism is more efficient for larger values of β, as can be seen from the solution (3.3.4), and at late times so ω is drawn to a larger value for a larger β.

The effect of including a late-time vacuum-dominated stage of the Universe's evolution is to weaken slightly the bounds that can be placed on ω at the present day, as can be seen from figures 9.3 and 9.5. This weakening of the bounds is due to a shortening of the matter-dominated period of the Universe's history which is essentially the only period, after the effects of the free scalar-dominated phase become negligible, during which G evolves.

We find that the constraints that can be imposed upon the present day value of ω from primordial nucleosynthesis are, for most of the allowed parameter space, considerably weaker than those obtained from observations within the solar system. To date, the tightest constraint upon ω_0 are imposed by Bertotti, Iess and Tortora [47] who find $|\omega_0| \gtrsim 40000$, to 2σ. This constraint is obtained from observations of the Shapiro delay of radio signals from the Cassini spacecraft as it passes behind the Sun. We consider the constraints imposed upon ω here to be complementary to these results as they probe different length and time scales, as well as different epochs of the Universe's history.

9.2 Fourth-Order Theories

The modified cosmological dynamics for fourth-order gravity lead to different predictions for the outcomes of primordial nucleosynthesis and microwave background formation, compared to the standard general relativistic model. The relevant modifications to these physical processes, and the bounds that they can impose upon

the theory, will be discussed in this section. We will use the solutions (4.1.5) as they have been shown to be the generic attractors as $t \to \infty$ (except for the case $-\frac{1}{4} < \delta < 0$ when $\gamma = 1$, which has been excluded as physically unrealistic on the grounds of structure formation).

9.2.1 Primordial Nucleosythesis

We find that the temperature-time adiabat during radiation domination for the solution (4.1.5) is given by the exact relation

$$t^{2(1+\delta)} = \frac{A}{T^4} \tag{9.2.1}$$

where, as usual (with units $\hbar = c = 1 = k_B$),

$$\rho = \frac{g\pi^2}{15} T^4$$

where g is the total number of relativistic spin states at temperature T. The constant A can be determined from the generalised Friedmann equation (4.1.3) and is dependent on the present day value of the Ricci scalar, through equation (2.1.21). (This dependence is analogous to the dependence of scalar-tensor theories on the evolution of the non-minimally coupled scalar, as may be expected from the relationship between these theories [124]). As a first approximation, we assume the universe to have been matter dominated throughout its later history; this allows us to write

$$A = \left(\frac{45(1-2\delta)(1-2\delta-5\delta^2)}{32(1-\delta)g\pi^3 G} \right) \left(\frac{2(1+\delta)}{3H_0} \right)^{2\delta} \tag{9.2.2}$$

where H_0 is the value of Hubble's constant today and we have used the solution (4.1.5) to model the evolution of $a(t)$. Adding a recent period of accelerated expansion will refine the constant A, but in the interests of brevity we exclude this from the current analysis. As usual, the weak-interaction time is given by

$$t_{wk} \propto \frac{1}{T^5}.$$

The freeze-out temperature, T_f, for neutron-proton kinetic equilibrium is then defined by

$$t(T_f) = t_{wk}(T_f).$$

Hence the freeze-out temperature in this theory, with $\delta \neq 0$, is related to that in the general relativistic case with $\delta = 0$, T_f^{GR}:

$$T_f = C(T_f^{GR})^{\frac{3(1+\delta)}{(3+5\delta)}} \tag{9.2.3}$$

where

$$C = \left(\frac{(1-\delta)}{(1-2\delta)(1-2\delta-5\delta^2)}\right)^{\frac{1}{2(2+5\delta)}} \left(\frac{45}{32g\pi^3 G}\right)^{\frac{\delta(1+\delta)}{2(3+5\delta)}} \left(\frac{3H_0}{2(1+\delta)}\right)^{\frac{\delta}{(3+5\delta)}}. \tag{9.2.4}$$

The neutron-proton ratio, n/p, is now determined at temperature T when the equilibrium holds by

$$\frac{n}{p} = \exp\left(-\frac{\Delta m}{T}\right).$$

where Δm is the neutron-proton mass difference. Hence the neutron-proton ratio at freeze-out in the $R^{1+\delta}$ early universe is given by

$$\frac{n}{p} = \exp\left(-\frac{\Delta m}{C(T_f^{GR})^{1-\varepsilon}}\right),$$

where

$$\varepsilon \equiv \frac{2\delta}{3+5\delta}.$$

The frozen-out n/p ratio in the $R^{1+\delta}$ theory is given by a power of its value in the general relativistic case, $\left(\frac{n}{p}\right)_{GR} \approx 1/7$, by

$$\frac{n}{p} = \left(\frac{n}{p}\right)_{GR}^{C(T_f^{GR})^{\varepsilon}}.$$

It is seen that when $C(T_f^{GR})^{\varepsilon} > 1$ ($\delta < 0$) there is a smaller frozen-out neutron-proton ratio that in the general relativistic case and consequently a lower final helium-4 abundance than in the standard general-relativistic early universe containing the same number of relativistic spin states. This happens because the freeze-out

temperature is lower than in GR. The neutrons remain in equilibrium to a lower temperature and their slightly higher mass shifts the number balance more towards the protons the longer they are in equilibrium. Note that a reduction in the helium-4 abundance compared to the standard model of GR is both astrophysically interesting and difficult to achieve (all other variants like extra particle species [178, 180], anisotropies [103, 8, 9, 14], magnetic fields [28, 30], gravitational waves [8, 9, 21], or varying G [33, 20, 74], lead to an *increase* in the expansion rate and in the final helium-4 abundance). Conversely, when $C(T_f^{GR})^{\varepsilon} < 1$ ($\delta > 0$) freeze-out occurs at a higher temperature than in general relativity and a higher final helium-4 abundance fraction results. The final helium-4 mass fraction Y is well approximated by

$$Y = \frac{2n/p}{(1 + n/p)}. \tag{9.2.5}$$

It is now possible to constrain the value of δ using observational abundances of the light elements. In doing this we will use the results of Carroll and Kaplinghat [60] who consider nucleosynthesis with a Hubble constant parametrised by

$$H(T) = \left(\frac{T}{1MeV}\right)^{\alpha} H_1.$$

Our theory can be cast into this form by substituting

$$\alpha = \frac{2}{(1+\delta)}$$

and

$$H_1 = \frac{(1+\delta)}{2} A^{-\frac{1}{2(1+\delta)}} (1MeV)^{\frac{2}{(1+\delta)}},$$

so, taking $g = 43/8$, $G = 6.72 \times 10^{-45} MeV^{-2}$ and $H_0 = 1.51 \times 10^{-39} MeV$ [45], this can be rewritten as

$$H_1 = \frac{(1+\delta)}{2} \left(\frac{7.96 \times 10^{-43}(1-\delta)}{(1-2\delta)(1-2\delta-5\delta^2)}\right)^{\frac{1}{2(1+\delta)}} \left(\frac{2.23 \times 10^{-39}}{(1+\delta)}\right)^{\frac{\delta}{(1+\delta)}} MeV.$$

Carroll and Kaplinghat use the observational abundances inferred by Olive et. al.

[146],

$$0.228 \leqslant Y_P \leqslant 0.248$$
$$2 \leqslant 10^5 \times \frac{D}{H} \leqslant 5$$
$$1 \leqslant 10^{10} \times \frac{^7Li}{H} \leqslant 3,$$

to impose the constraint

$$H_1 = H_c \left(\frac{T_c}{MeV} \right)^{-\alpha}$$

where $H_c = 2.6 \pm 0.9 \times 10^{-23} MeV$ at $T_c = 0.2 MeV$ for $0.5 \leqslant \eta_{10} \leqslant 50$, or $H_c = 2.0 \pm 0.3 \times 10^{-23}$ for $1 \leqslant \eta_{10} \leqslant 10$ and η_{10} is 10^{10} times the baryon to photon ratio.

These results can now be used to impose upon δ the constraints

$$-0.017 \leqslant \delta \leqslant 0.0012,$$

for $0.5 \leqslant \eta_{10} \leqslant 50$, or

$$-0.0064 \leqslant \delta \leqslant 0.0012, \tag{9.2.6}$$

for $1 \leqslant \eta_{10} \leqslant 10$.

9.2.2 Microwave Background Formation

The horizon size at the epoch of matter-radiation equality is of great observational significance. During radiation domination cosmological perturbations on sub-horizon scales are effectively frozen. Once matter domination commences, however, perturbations on all scales are allowed to grow and structure formation begins. The horizon size at matter-radiation equality is therefore frozen into the power spectrum of perturbations and is observable. Calculation of the horizon sizes in this theory proceeds in a similar way to that in Brans-Dicke theory [118].

In making an estimate of the horizon size in $R^{1+\delta}$ theory we will use the generalised Friedmann equation, (4.1.3), in the form

$$H^2 + \delta H \frac{\dot{R}}{R} - \frac{\delta R}{6(1+\delta)} = \frac{8\pi G(1-\delta)}{3(1-2\delta)} \frac{R_0^\delta}{R^\delta} \rho. \tag{9.2.7}$$

Again, we assume the form (4.1.5) to model the evolution of the scale factor during the epoch of matter domination. This gives

$$\begin{aligned} a(t) &= a_0 \left(\frac{t}{t_0}\right)^{\frac{2(1+\delta)}{3}} \\ H_0 &= \frac{2(1+\delta)}{3t_0} \\ \rho_m &= \frac{3H_0^2}{16\pi G}\frac{(1-2\delta)(2-3\delta-8\delta^2)}{(1-\delta)(1+\delta)^2}\frac{a_0^3}{a^3} \\ R(t) &= \frac{4(1+5\delta+4\delta^2)}{3t^2} \end{aligned}$$

during the matter-dominated era. In order to simplify matters, we assume the above solutions to hold exactly from the time of matter-radiation equality up until the present (neglecting the small residual radiation effects and the late time acceleration). Substituting them into (9.2.7), along with $\rho_{eq} = 2\rho_{meq}$ at equality, we can then solve for H_{eq} to first order in δ to find

$$\frac{a_{eq}H_{eq}}{a_0H_0} \simeq \sqrt{2}\sqrt{1+z_{eq}}^{\frac{1-2\delta}{1+\delta}}(1-2.686\delta) + O(\delta^2) \tag{9.2.8}$$

where z_{eq} is the redshift at matter radiation equality and H has been treated as an independent parameter. The value of $1 + z_{eq}$ can now be calculated in this theory as

$$1 + z_{eq} = \frac{\rho_{r0}}{\rho_{m0}}. \tag{9.2.9}$$

Taking the present day temperature of the microwave background as $T = 2.728 \pm 0.004K$ [85] gives

$$\rho_{r0} = 3.37 \times 10^{-39} MeV^4 \tag{9.2.10}$$

where three families of light neutrinos have been assumed at a temperature lower than that of the microwave background by a factor $(4/11)^{\frac{1}{3}}$. Using the same values for G and H_0 as above we than find from the above expression for ρ_m that

$$\rho_{m0} = 2.03 \times 10^{-35}\frac{(1-2\delta)(2-3\delta-8\delta^2)}{(1-\delta)(1+\delta)^2} MeV^4. \tag{9.2.11}$$

Substituting (9.2.10), (9.2.11) and (9.2.9) into (9.2.8) then gives the expression for

the horizon size at equality, to first order in δ, as

$$\frac{a_{eq}H_{eq}}{a_0 H_0} \simeq 155(1 - 19\delta) + O(\delta^2). \tag{9.2.12}$$

This expression shows that the horizon size at matter-radiation equality will be shifted by $\sim 1\%$ for a value of $\delta \sim 0.0005$. This shift in horizon size should be observable in a shift of the peak of the power spectrum of perturbations, compared to its position in the standard general relativistic cosmology. Microwave background observations, therefore, allow a potentially tight bound to be derived on the value of δ. This effect is analogous to the shift of power-spectrum peaks in Brans-Dicke theory (see e.g. [118], [65]).

A full analysis of the spectrum of perturbations in this theory requires a knowledge of the evolution of linearised perturbations as well as a marginalisation over other parameters which can mimic this effect (e.g. baryon density). Such a study is beyond the scope of the present work.

CHAPTER 10

Weak-Field Constraints

It is the weak-field limit of gravity that is most readily accessible to us for experiment and observation. By performing gravitational experiments in the solar system, and comparing the results of these experiments to the predictions from different gravitational theories, it is possible to place constraints on the theory under consideration. To date, it is weak field gravitational experiments that have so far offered the best constraints on the theory (though with astrophysical and cosmological observations becoming ever more accurate there is a possibility of the situation changing in the not too distant future).

The consideration of gravitational experiments in the weak-field, low velocity limit is usually performed within the frame-work of the parameterised post-Newtonian (PPN) formalism. In this chapter we will give a brief explanation of the PPN formalism, and explain how it can be used to constrain scalar-tensor and fourth-order theories of gravity. We will also point out the areas in which this formalism cannot be applied so easily, and provide alternative ways to proceed.

This chapter is based on the work of Clifton and Barrow [70] and Clifton [69].

10.1 Parameterised Post-Newtonian Approach

We will provide in this section a brief explanation of the PPN approach (for a more detailed explanation of this formalism the reader is referred to Will, [191]).

The PPN formalism does not deal with exact solutions, but instead uses perturbative expansions about a Minkowski background. In the weak-field, low velocity limit we need only deal with the lowest orders of the perturbative expansion. Solving the field equations order by order, we can then find approximate solutions which can be compared with observation.

Following Will we define an "order of smallness" such that

$$U \sim v^2 \sim \frac{p}{\rho} \sim \Pi \sim O(2)$$

where U is the Newtonian potential, v is the velocity of a body in the space-time, p is pressure, ρ is energy density and Π is specific energy density (ratio of energy density to rest mass density) and $O(2)$ means second order in "smallness". In the solar system we have that $U \leqslant 10^{-5}$ is a small perturbation to flatness, and all of the other above quantities are less that U and so are also small (see Will [191] for more details). It is also assumed that the time evolution of the solar system is slow

$$\frac{|\partial/\partial t|}{|\partial/\partial x|} \sim O(1).$$

A perturbative expansion about the Minkowski background can now be performed in the order of smallness that has just been defined.

To obtain the Newtonian limit for particles following time-like geodesics we now need to know only the $O(2)$ term in the g_{00} component of the metric. The Newtonian limit of light rays are straight lines, so for null geodesics the Newtonian limit is given simply by the Minkowski background. The post-Newtonian limit is then given by the next non-zero order in the perturbative expansion of the metric components. For time-like particles this is given by g_{00} to $O(4)$, $g_{0\mu}$ to $O(3)$ and $g_{\mu\nu}$ to $O(2)$. For null particles it is given by g_{00} to $O(2)$ and $g_{\mu\nu}$ to $O(2)$.

The usual approach at this point is to construct a metric containing a number of the possible functionals of the matter variables, to the required post-Newtonian order. Giving the different functionals (often referred to as potentials) arbitrary

coefficients it is then possible to construct a generalised metric. The values of the coefficients are then given by solving the field equations of the theory being considered, order by order in perturbation. To restrict the number of potentials in the metric a number of conditions are usually imposed such as asymptotic flatness and simplicity of the functional form. After specifying a particular gauge the generalised metric can then be written down explicitly.

The appeal of this approach is that the generalised metric can be used by experimenters to place constraints on the coefficients of the metric potentials, independent of any further considerations of the specific gravitational theory being tested. For any particular gravitational theory (that fits into this framework) the values of the coefficients can then be expressed in terms of the parameters of the theory. In this way the results of gravitational experiments can be applied to any gravitational theory that fits into the PPN frame-work.

A simplified version of the post-Newtonian metric is given by

$$\begin{aligned} g_{00} &= -1 + 2U - 2\beta U^2 + (2 + 2\gamma + \zeta_1)\Phi_1 \\ &\quad + 2(1 - 2\beta + 3\gamma + \zeta_2)\Phi_2 + 2(1 + \zeta_3)\Phi_3 + 2(3\gamma + 3\zeta_4)\Phi_4 \\ g_{\mu\nu} &= (1 + 2\gamma U)\delta_{\mu\nu} \\ g_{0\mu} &= -\frac{1}{2}(3 + 4\gamma + \zeta_1 + \alpha_1 - \alpha_2)V_\mu - \frac{1}{2}(1 - \zeta_1 + \alpha_2)W_\mu) \end{aligned} \tag{10.1.1}$$

where β, γ, ζ_1, ζ_2, ζ_3, ζ_4, α_1 and α_2 are some of the possible post-Newtonian coefficients and Φ_1, Φ_2, Φ_3, Φ_4, V_μ and W_μ are post-Newtonian potentials. (See [191] for a more comprehensive version of the post-Newtonian metric, and definitions of the above post-Newtonian potentials). For an idealised spherical and non-rotating massive object at the origin, in an otherwise empty space-time, this metric reduces to

$$ds^2 = -\left(1 - \frac{2Gm}{r} + \beta\frac{2G^2m^2}{r^2}\right)dt^2 + \left(1 + \gamma\frac{2Gm}{r}\right)\delta_{\mu\nu}dx^\mu dx^\nu$$

which is exactly the metric considered by Eddington [83], Robertson [161] and Schiff [170].

The PPN approach has been shown to work very well for a number of gravitational theories, but it does have some drawbacks. From the point of view of the present study the principle drawback is the assumption of the Minkowski back-

ground. Whilst the Minkowski background is very well justified in GR, it is less well justified in some alternative theories. This is principally due to the lack of any equivalent to Birkhoff's theorem. In fact, in a previous chapter we have shown explicitly the existence of solutions which are spherically symmetric, non-static vacuum solutions. This breakdown of Birkhoff's theorem can be understood quite simply in terms of the conformal equivalence of these theories in vacuum to GR in the presence of a scalar field. Just as it conceivable that a scalar field in GR could cause a cosmological evolution (even in the absence of any other matter sources), so it is conceivable here that the vacuum solutions of these modified theories could evolve cosmologically.

These problems are especially evident in the R^n theories. In these theories, even in the static case, it has already been shown that at asymptotically large spatial distances the general solution is not attracted towards flatness. This strange asymptotic behaviour means that the theories do not fit straightforwardly into the PPN frame-work. We develop new ways of dealing with this strange behaviour below, and apply the results of gravitational experiments to these theories.

10.2 Scalar-Tensor Theories

The post-Newtonian limit of the scalar-tensor theories of gravity has been well studied numerous times in the past. We present here a brief illustration of how the post-Newtonian coefficients are obtained, and how they can be used to constrain the theory.

In order to fit into the PPN formalism the metric and scalar field must be subjected to a perturbative expansion of the form

$$g_{\mu\nu} = \eta_{\mu\nu} + h_{\mu\nu}$$
$$\phi = \phi_0 + \varphi$$

where

$$\begin{aligned} h_{00} &\sim O(2) + O(4) \\ h_{\mu\nu} &\sim O(3) \\ h_{0\mu} &\sim O(2) \\ \varphi &\sim O(2) + O(4). \end{aligned}$$

These expansions can then be substituted into the scalar-tensor field equations (2.1.8) and (2.1.9), which can be solved order by order in perturbations to obtain (after an appropriate gauge choice) [191]

$$\begin{aligned} g_{00} &= -1 + 2U - 2(1+\Lambda)U^2 + 4\left(\frac{3+2\omega}{4+2\omega}\right)\Phi_1 \\ &\quad + 4\left(\frac{1+2\omega}{4+2\omega} - \Lambda\right)\Phi_2 + 2\Phi_3 + 6\left(\frac{1+\omega}{2+\omega}\right)\Phi_4 \\ g_{\mu\nu} &= \left(1 + 2\left(\frac{1+\omega}{2+\omega}\right)U\right)\delta_{\mu\nu} \\ g_{0\mu} &= -\frac{1}{2}\left(\frac{10+7\omega}{2+\omega}\right)V_\mu - \frac{1}{2}W_\mu \end{aligned} \tag{10.2.1}$$

where

$$\Lambda \equiv \frac{d\omega/d\phi}{(4+2\omega)(3+2\omega)^2}$$

and Newton's constant has been set to

$$G \equiv \left(\frac{4+2\omega}{3+2\omega}\right)\frac{1}{\phi_0}.$$

A direct comparison of (10.1.1) and (10.2.1) allows the PPN coefficients to be read off as

$$\begin{aligned} \gamma &= \frac{1+\omega}{2+\omega} \\ \beta &= 1 + \Lambda \\ \zeta_1 &= \zeta_2 = \zeta_3 = \zeta_4 = \alpha_1 = \alpha_2 = 0. \end{aligned}$$

The Brans-Dicke theory can be particularly well constrained by observations con-

straining the PPN coefficients. For the Brans-Dicke theory ω =constant, so $\Lambda = 0$, and the constraints on the coefficient γ,

$$\gamma = 1 + (2.1 \pm 2.3) \times 10^{-5},$$

from observations of the Shapiro time delay of radio signals from the Cassini space-probe [47], gives the constraint

$$\omega > 40000.$$

This constraint is very limiting indeed for the Brans-Dicke theory, but less so for theories in which ω is allowed to be a function of ϕ. For these theories, whilst the present day value of ω in the solar system is tightly constrained, the value of ω at other points in the Universe's history (particularly in the early Universe) is less restricted. To better constrain these theories we need to obtain limits on the parameter β or, even better, use cosmological constraints from the early Universe, such as those which were discussed in the last chapter.

10.3 Fourth-Order Theories

In order to calculate the classical tests of metric theories of gravity (i.e. bending and time-delay of light rays and the perihelion precession of Mercury) we require a spherically symmetric solution to the $\mathcal{L} = R^{1+\delta}$ field equations (2.1.15). Due to the complicated form of these equations we are unable to find the general solution; instead we propose to use first-order solutions around attractors as $r \to \infty$ or $t \to \infty$. This method should be applicable to gravitational experiments performed in the solar system as the gravitational field in this region can be considered weak and we will be considering experiments performed at large r (in terms of the Schwarzschild radius of the massive objects in the system) and at late times.

10.3.1 Static Space-Time

In this section we will use the static and spherically symmetric solution found previously (6.2.2). We choose to arbitrarily set the oscillatory parts of the solution to zero, and hence ensure that the gravitational force is always attractive. This

considerable simplification of the solution also allows a straightforward calculation of both null and time-like geodesics which can be used to compute the outcomes of the classical tests in this space-time.

Solution in isotropic coordinates

Having removed the oscillatory parts of the solution we are left with the part corresponding to the exact solution (6.2.2). Making the coordinate transformation

$$r^{(1-2\delta+4\delta^2)/(1-d)} = \left(1 - \frac{C}{4\hat{r}\sqrt{\frac{(1-2\delta+4\delta^2)}{(1-2\delta-2\delta^2)}}}\right)^2 \hat{r}^{\sqrt{\frac{(1-2\delta+4\delta^2)}{(1-2\delta-2\delta^2)}}}$$

the solution (6.2.2) can be transformed into the isotropic coordinate system

$$ds^2 = -A(\hat{r})dt^2 + B(\hat{r})(d\hat{r}^2 + \hat{r}^2(d\theta^2 + \sin^2\theta d\phi^2)) \tag{10.3.1}$$

where

$$A(\hat{r}) = \hat{r}^{\frac{2\delta(1+2\delta)}{\sqrt{(1-2\delta-2\delta^2)(1-2\delta+4\delta^2)}}} \left(1 + \frac{C}{4\hat{r}\sqrt{\frac{(1-2\delta+4\delta^2)}{(1-2\delta-2\delta^2)}}}\right)^2 \left(1 - \frac{C}{4\hat{r}\sqrt{\frac{(1-2\delta+4\delta^2)}{(1-2\delta-2\delta^2)}}}\right)^{-\frac{2(1+4\delta)}{(1-2\delta+4\delta^2)}}$$

and

$$B(\hat{r}) = \hat{r}^{-2+2\frac{(1-\delta)}{\sqrt{(1-2\delta-2\delta^2)(1-2\delta+4\delta^2)}}} \left(1 - \frac{C}{4\hat{r}\sqrt{\frac{(1-2\delta+4\delta^2)}{(1-2\delta-2\delta^2)}}}\right)^{\frac{4(1-\delta)}{(1-2\delta+4\delta^2)}}.$$

This is, to linear order in C,

$$A(\hat{r}) = \hat{r}^{\frac{2\delta(1+2\delta)}{\sqrt{(1-2\delta-2\delta^2)(1-2\delta+4\delta^2)}}} \left(1 + \frac{(1-\delta)(1-2\delta)}{(1-2\delta+4\delta^2)} \frac{C}{\hat{r}\sqrt{\frac{(1-2\delta+4\delta^2)}{(1-2\delta-2\delta^2)}}}\right)$$

and

$$B(\hat{r}) = \hat{r}^{-2+2\frac{(1-\delta)}{\sqrt{(1-2\delta-2\delta^2)(1-2\delta+4\delta^2)}}} \left(1 - \frac{(1-\delta)}{(1-2\delta+4\delta^2)} \frac{C}{\hat{r}\sqrt{\frac{(1-2\delta+4\delta^2)}{(1-2\delta-2\delta^2)}}}\right).$$

Newtonian limit

We first investigate the Newtonian limit of the geodesic equation in order to set the constant C in the solution (10.3.1) above. As usual, we have

$$\Phi_{,\mu} = \Gamma^{\mu}_{00}$$

where Φ is the Newtonian gravitational potential. Substituting in the isotropic metric (10.3.1) this gives

$$\begin{aligned}\nabla\Phi &= \frac{\nabla A(\hat{r})}{2B(\hat{r})} \qquad (10.3.2)\\ &= \frac{\delta(1+2\delta)\hat{r}^{1-2\sqrt{\frac{1-2\delta-2\delta^2}{1-2\delta+4\delta^2}}}}{\sqrt{(1-2\delta-2\delta^2)(1-2\delta+4\delta^2)}}\\ &\quad - \frac{(1-\delta)(1-8\delta+4\delta^2)C\hat{r}^{1-\frac{3(1-2\delta)}{\sqrt{(1-2\delta-2\delta^2)(1-2\delta+4\delta^2)}}}}{2\sqrt{(1-2\delta-2\delta^2)(1-2\delta+4\delta^2)^3}} + O(C^2).\end{aligned}$$

The second term in the expression goes as $\sim \hat{r}^{-2+O(\delta^2)}$ and so corresponds to the Newtonian part of the gravitational force. The first term, however, goes as $\sim \hat{r}^{-1+O(\delta^2)}$ and has no Newtonian counterpart. In order for the Newtonian part to dominate over the non-Newtonian part we must impose upon δ the requirement that it is at most

$$\delta \sim O\left(\frac{C}{r}\right).$$

If δ were larger than this then the non-Newtonian part of the potential would dominate over the Newtonian part, which is clearly unacceptable at scales over which the Newtonian potential has been measured and shown to be accurate.

This requirement upon the order of magnitude of δ allows (10.3.2) to be written

$$\nabla\Phi = \frac{\delta}{\hat{r}^{1+O(C^2)}} - \frac{C}{2\hat{r}^{2+O(C^2)}} + O(C^2) \qquad (10.3.3)$$

where expansions in C have been carried out separately in the coefficients and the powers of $\hat{r}$ of the two terms.

Comparison of (10.3.3) with the Newtonian force law

$$\nabla\Phi_N = \frac{Gm}{r^2}$$

allows the value of C to be read off as

$$C = -2Gm + O(\delta).$$

Post-Newtonian limit

We now wish to calculate, to post-Newtonian order, the equations of motion for test particles in the metric (10.3.1). The geodesic equation can be written in its usual form

$$\frac{d^2x^\mu}{d\lambda^2} + \Gamma^\mu_{ij}\frac{dx^i}{d\lambda}\frac{dx^j}{d\lambda} = 0,$$

where λ can be taken as proper time for a time-like geodesic or as an affine parameter for a null geodesic. In terms of coordinate time this can be written

$$\frac{d^2x^\mu}{dt^2} + \left(\Gamma^\mu_{ij} - \Gamma^0_{ij}\frac{dx^\mu}{dt}\right)\frac{dx^i}{dt}\frac{dx^j}{dt} = 0. \tag{10.3.4}$$

We also have the integral

$$g_{ij}\frac{dx^i}{dt}\frac{dx^j}{dt} = S \tag{10.3.5}$$

where $S = -1$ for particles and 0 for photons.

Substituting (10.3.1) into (10.3.4) and (10.3.5) gives, to the relevant order, the equations of motion

$$\begin{aligned}\frac{d^2\mathbf{x}}{dt^2} = &-\frac{Gm}{r^2}\left(1 + \left|\frac{d\mathbf{x}}{dt}\right|^2\right)\mathbf{e_r} + 4\frac{G^2m^2}{r^3}\mathbf{e_r} + 4\frac{Gm}{r^2}\mathbf{e_r}\cdot\frac{d\mathbf{x}}{dt}\frac{d\mathbf{x}}{dt} \\ &- \frac{\delta}{r}\left(1 - \left|\frac{d\mathbf{x}}{dt}\right|^2\right)\mathbf{e_r} - 4\frac{\delta^2}{r}\mathbf{e_r} + \delta\frac{Gm}{r^2}\mathbf{e_r} + O(G^3m^3)\end{aligned} \tag{10.3.6}$$

and

$$\left|\frac{d\mathbf{x}}{dt}\right|^2 = 1 - 4\frac{Gm}{r} + \frac{S}{r^{2\delta}} - 2S\frac{Gm}{r^{1+2\delta}} + O(G^2m^2). \tag{10.3.7}$$

(In the interests of concision we have excluded the $O(\delta^2)$ terms from the powers of

r; the reader should regard them as being there implicitly). The first three terms in equation (10.3.6) are identical to their general relativistic counterparts. The next two terms are completely new and have no counterparts in general relativity. The last term in equation (10.3.6) can be removed by rescaling the mass term by $m \to m(1+\delta)$; this has no effect on the Newtonian limit of the geodesic equation as any term $Gm\delta$ is of post-Newtonian order.

The bending of light and time delay of radio signals

From equation (10.3.7) it can be seen that the solution for null geodesics, to zeroth order, is a straight line that can be parametrised by

$$\mathbf{x} = \mathbf{n}(t - t_0)$$

where $\mathbf{n} \cdot \mathbf{n} = 1$. Considering a small departure from the zeroth order solution we can write

$$\mathbf{x} = \mathbf{n}(t - t_0) + \mathbf{x}_1$$

where $\mathbf{x}_1$ is small. To first order, the equations of motion (10.3.6) and (10.3.7) then become

$$\frac{d^2\mathbf{x}}{dt^2} = -2\frac{Gm}{r^2}\mathbf{e_r} + 4\frac{Gm}{r^2}(\mathbf{n} \cdot \mathbf{e_r})\mathbf{n} \tag{10.3.8}$$

and

$$\mathbf{n} \cdot \frac{d\mathbf{x}}{dt} = -2\frac{Gm}{r}. \tag{10.3.9}$$

Equations (10.3.8) and (10.3.9) can be seen to be identical to the first-order equations of motions for photons in GR. We therefore conclude that any observations involving the motion of photons in a stationary and spherically symmetric weak field situation cannot tell any difference between GR and this $R^{1+\delta}$ theory, to first post-Newtonian order. This includes the classical light bending and time delay tests, which should measure the post-Newtonian parameter γ to be one in this theory, as in GR.

Perihelion precession

In calculating the perihelion precession of a test particle in the geometry (10.3.1) it is convenient to use the standard procedures for computing the perturbations of

orbital elements (see [179] and [162]). In the notation of Robertson and Noonan [162] the measured rate of change of the perihelion in geocentric coordinates is given by

$$\frac{d\tilde{\omega}}{dt} = -\frac{p\mathcal{R}}{he}\cos\phi + \frac{\mathcal{J}(p+r)}{he}\sin\phi \tag{10.3.10}$$

where p is the semi-latus rectum of the orbit, h is the angular-momentum per unit mass, e is the eccentricity and $\mathcal{R}$ and $\mathcal{J}$ are the components of the acceleration in radial and normal to radial directions in the orbital plane, respectively. The radial coordinate, r, is defined by

$$r \equiv \frac{p}{(1+e\cos\phi)} \tag{10.3.11}$$

and ϕ is the angle measured from the perihelion. We have, as usual, the additional relations

$$p = a(1-e^2)$$

and

$$h \equiv \sqrt{Gmp} \equiv r^2\frac{d\phi}{dt}. \tag{10.3.12}$$

From (10.3.6), the components of the acceleration can be read off as

$$\mathcal{R} = -\frac{Gm}{r^2} - \frac{Gm}{r^2}v^2 + 4\frac{Gm}{r^2}v_{\mathcal{R}}^2 + 4\frac{G^2m^2}{r^3} - \frac{\delta}{r} + \frac{\delta}{r}v^2 - 4\frac{\delta^2}{r} \tag{10.3.13}$$

and

$$\mathcal{J} = 4\frac{Gm}{r^2}v_{\mathcal{R}}v_{\mathcal{J}} \tag{10.3.14}$$

where we now have the radial and normal-to-radial components of the velocity as

$$v_{\mathcal{R}} = \frac{eh}{p}\sin\phi$$
$$v_{\mathcal{J}} = \frac{h}{p}(1+e\cos\phi)$$

and $v^2 = v_{\mathcal{R}}^2 + v_{\mathcal{J}}^2$. In writing (10.3.13), the last term of (10.3.6) has been absorbed by a rescaling of m, as mentioned above.

The expressions (10.3.13) and (10.3.14) can now be substituted into (10.3.10) and integrated from $\phi = 0$ to 2π, using (10.3.11) and (10.3.12) to write r and dr in terms of ϕ and $d\phi$. The perihelion precession per orbit is then given, to post-Newtonian

accuracy, by the expression

$$\Delta\tilde{\omega} = \frac{6\pi Gm}{a(1-e^2)} - \frac{2\pi\delta}{e^2}\left(e^2 - 1 - \frac{(1+4\delta)a(1-e^2)}{Gm}\right). \tag{10.3.15}$$

The first term in (10.3.15) is clearly the standard general relativistic expression. The second term is new and contributes to leading order the term

$$\frac{2\pi a}{Gm}\left(\frac{1-e^2}{e^2}\right)\delta.$$

Comparing the prediction (10.3.15) with observation is a non-trivial matter. The above prediction is the highly idealised precession expected for a time-like geodesic in the geometry described by (10.3.1). If we assume that the geometry (10.3.1) is a good approximation to the weak field for a static Schwarzschild-like mass then it is not trivial to assume that the time-like geodesics used to calculate the rate of perihelion precession (10.3.15) are the paths that material objects will follow. Whilst we are assured from the generalised Bianchi identities [124] of the covariant conservation of energy-momentum, $T^{ab}{}_{;b} = 0$, and hence of the geodesic motion of an ideal fluid of pressureless dust, $U^i U^j_{;i} = 0$, this does not ensure the geodesic motion of extended bodies. This deviation from geodesic motion is known as the Nordvedt effect [141] and, whilst being zero for GR, is generally non-zero for extended theories of gravity. From the analysis so far it is also not clear how orbiting matter and other nearby sources (other than the central mass) will contribute to the geometry (10.3.1).

In order to make a prediction for a physical system such as the solar system, and in the interests of brevity, some assumptions must be made. It is firstly assumed that the geometry of space-time in the solar system can be considered, to first approximation, as static and spherically symmetric. It is then assumed that this geometry is determined by the Sun, which can be treated as a point-like Schwarzschild mass at the origin, and is isolated from the effects of matter outside the solar system and from the background cosmology. It is also assumed that the Nordvedt effect is negligible and that extended massive bodies, such as planets, follow the same time-like geodesics of the background geometry as neutral test particles.

In comparing with observation it is useful to recast (10.3.15) in the form

$$\Delta\tilde{\omega} = \frac{6\pi Gm}{a(1-e^2)}\lambda$$

where

$$\lambda = 1 + \frac{a^2(1-e^2)^2}{3G^2m^2e^2}\delta.$$

This allows for easy comparison with results which have been used to constrain the standard post-Newtonian parameters, for which

$$\lambda = \frac{1}{3}(2 + 2\gamma - \beta).$$

The observational determination of the perihelion precession of Mercury is not clear cut and is subject to a number of uncertainties; most notably the quadrupole moment of the Sun (see e.g. [155]). We choose to use the result of Shapiro et. al. [174],

$$\lambda = 1.003 \pm 0.005, \tag{10.3.16}$$

which for standard values of a, e and m [3] gives us the constraint

$$\delta = 2.7 \pm 4.5 \times 10^{-19}. \tag{10.3.17}$$

In deriving (10.3.16) the quadrupole moment of the Sun was assumed to correspond to uniform rotation. For more modern estimates of the anomalous perihelion advance of Mercury see [155].

10.3.2 Non-Static Space-Time

We will now proceed to calculate the equations of motion of particles following geodesics of the space-time (7.2.1), to post-Newtonian order. It will be shown that not only are the terms due to the linear perturbations different to the static case (as should be expected as the perturbations themselves have been shown to be background dependant) but that the background itself contributes an extra term to the post-Newtonian equation of motion.

Equation of motion

We will now proceed to calculate the geodesics of the non-static solution (7.2.2). In doing this we will neglect the contribution of the r^2 mode to (7.2.2) so that we only take into account the modes which go as r^{-1}, in the limit $\delta \to 0$. This is the mode corresponding to the linearisation of the exact solution (7.2.1).

The geodesic equation can be written, as usual, in the form

$$\frac{d^2x^\mu}{d\lambda^2} + \Gamma^\mu_{ij}\frac{dx^i}{d\lambda}\frac{dx^j}{d\lambda} = 0,$$

where λ can be taken as proper time for a time-like geodesic, or as an affine parameter for a null geodesic. In terms of coordinate time this can be re-written as

$$\frac{d^2x^\mu}{dt^2} + \left(\Gamma^\mu_{ij} - \Gamma^0_{ij}\frac{dx^\mu}{dt}\right)\frac{dx^i}{dt}\frac{dx^j}{dt} = 0. \tag{10.3.18}$$

Substituting the linearised solution into this equation will then give the equations of motion for test particles in this space-time.

Substituting (7.2.1) into (10.3.18) gives, to post-Newtonian order, the equation of motion

$$\frac{d^2\mathbf{x}}{d\tau^2} = -\frac{Gm}{r^2}\mathbf{e}_r + 4(1-\delta)\frac{G^2m^2}{r^3}\mathbf{e}_r - (1-2\delta)\frac{Gm}{r^2}\left(\frac{d\mathbf{x}}{d\tau}\right)^2 + 4(1-\delta)\frac{Gm}{r^2}\mathbf{e}_r\cdot\frac{d\mathbf{x}}{d\tau}\frac{d\mathbf{x}}{d\tau} - \mathcal{H}\frac{d\mathbf{x}}{d\tau}\left(1-\left(\frac{d\mathbf{x}}{d\tau}\right)^2\right) \tag{10.3.19}$$

where

$$\mathcal{H} \equiv \frac{1}{a}\frac{da}{d\tau}.$$

The conformal time coordinate τ is defined by $dt \equiv ad\tau$ and c_4 has been set by the appropriate Newtonian limit. The equations of motion for this solution are considerably simpler than those of the static solution (6.2.2), but still differ from those of GR in significant ways. All of the terms except the last in equation (10.3.19) have GR counterparts and the powers of r in these terms are all the same as in the general relativistic case. The premultiplicative factors of these terms are, however, modified and can be described adequately within the frame-work of the PPN approach by

assigning

$$\beta = 1 \qquad \text{and} \qquad \gamma = 1 - 2\delta.$$

By making this identification, the constraints on γ from observations of the Shapiro time delay of radio signals from the Cassini space probe [47] can be used to impose upon δ the constraint

$$\delta = -1.1 \pm 1.2 \times 10^{-5}. \tag{10.3.20}$$

As well as the usual effects associated with $\gamma - 1$ being non-zero there are extra effects in this space-time due to the last term in (10.3.19). This term is proportional to the velocity of the test-particle (when $v << c$) and is zero for photons. For this reason we identify it as a friction term, with the friction coefficient being given by $\mathcal{H}$. This 'friction' is a purely gravitational effect and is not due to any non-gravitational interaction of test particles with any other matter.

It is clear that the constraints which can be imposed on this theory depend crucially on whether or not the space-time of the solar system can be assumed to be static. This is a non-trivial matter, as Birkhoff's theorem is no longer valid. Taking the usual assumption of the geometry of the solar system being static leads us to a solution with a non-trivial asymptotic dependence on r, as $r \to \infty$. These unusual asymptotics can be removed, but this appears to require that the usual assumption of the solar system having a static geometry be abandoned. Further study is required on this subject to determine which of these solutions is the most appropriate for application to the solar system.

CHAPTER 11

Conclusions

The objective of this work has been to develop the framework of alternative theories of gravity, to investigate the solutions to their field equations and to identify the principle ways in which they deviate from GR. This framework has then been used to study the ways in which GR can be considered to be special or unique, to identify new behaviour that was not previously present and to place observational constraints on deviations from the standard theory. In achieving these goals a number of approaches have been used in both cosmological and weak-field environments.

The focus of the analysis of cosmological solutions has been on, but not limited to, studies of FRW universes. These universes are appealing for a number of reasons. As well as having the same symmetries as our own observable Universe (on the largest scales) their high degree of symmetry is particularly useful for finding simple exact solutions to the complicated field equations of the theory. These solutions have been used to model a variety of physical processes such as structure formation, primordial nucleosynthesis and microwave background formation. All of these processes have been seen to behave differently from the corresponding cases in the standard model. In this way we have been able to see explicitly what effect such modifications to GR would have on the evolution of the Universe, as well as on the physical processes occurring within it.

Further to studying FRW universes we have also considered a variety of other cosmological solutions. In particular we have found the conditions for the existence of Gödel, Einstein static and de Sitter universes in a wide variety of theories. For the case of the Gödel universe the existence of closed time-like curves, and hence time travel into the past, has been analysed in detail. Furthermore, anisotropic solutions of Bianchi type I have been found and used to study the approach to anisotropic singularities in this extended framework. Using these solutions it has been found that an infinite sequence of chaotic mixmaster oscillations does not occur in all theories, as it does in GR. As well as studying homogeneous cosmologies, investigation has also been made of the effects of inhomogeneity on cosmological models within this framework. We have used FRW universes to model spherical collapse and have found exact inhomogeneous, spherically symmetric and time-dependent vacuum solutions. The very existence of these solutions is forbidden in GR by Birkhoff's theorem, and so they are of particular interest in looking for new behaviour which is not available in the standard model.

The tightest constraints currently available on gravitational theory are from experiments in the solar system and astrophysical tests in the proximity of (almost) spherical massive bodies. With this in mind the spherically symmetric vacuum solutions to the field equations are of particular interest. We have found exact solutions for this situation, and analysed their behaviour. These solutions have been shown to exhibit entirely new behaviour not previously obtainable in GR, including time dependence and non-asymptotic flatness. The weak field limit of these solutions has been found and the geodesics calculated to Post-Newtonian order. Comparison of these solutions with observational results has allowed tight constraints to be placed on the theory.

In summary, the principle new results in this work are that it has:

- Investigated the spatially flat FRW solutions of theories with Lagrangian density $\mathcal{L} = R^n$.
- Found the conditions for the existence of Gödel, Einstein static and de Sitter universes in a wide class of fourth-order theories.
- Investigated the phenomenon of closed time-like curves in these theories.

- Found exact Bianchi type I anisotropic solutions for a wide class of scale invariant fourth-order gravity theories.
- Investigated the approach to anisotropic singularities in these theories.
- Found exact static and spherically symmetric solutions in vacuum for R^n theories and investigated their stability.
- Found exact inhomogeneous cosmological solutions for scalar-tensor and R^n theories.
- Explicitly shown the lack of validity of Birkhoff's theorem in scalar-tensor and R^n theories.
- Investigated the spherical collapse model in scalar-tensor theories, and the spatial variations in G that can result from it.
- Investigated the possibility of generalising the usual scalar-tensor theories by allowing a transfer of energy between scalar and matter fields.
- Used primordial nucleosynthesis to impose constraints upon scalar-tensor and R^n theories, and their resulting cosmologies.
- Considered microwave background formation in R^n theories.
- Imposed constraints on R^n theories by modelling the solar system as either a static or non-static spherically symmetric vacuum space-time.

This work has confirmed the excellent agreement between GR and gravitational experiment and observation. It has uncovered new effects of modifying the standard theory and it has shown that such modifications are very strongly constrained, particularly in the low curvature regime of the solar system.

There are a variety of directions in which future research on this subject can proceed. Firstly, new effects and behaviours that have been found in this work can be used to model other physical processes. Particular processes of interest may be particle production near anisotropic singularities, modelling of anomalous observations (such as the Pioneer anomaly) or effects on structure formation and

the dynamics of astrophysical bodies. A second avenue of investigation would be to further investigate the effects that can be found to arise in theories of gravity which do not allow Birkhoff's theorem to be formulated. A start has been made on this by identifying exact vacuum solutions in Brans-Dicke and R^n theories which are spherically symmetric and either static or non-static. More work is required to fully understand how these solutions should be interpreted and what their physical effects would be. Other future research may focus on the effects of self-interacting scalar fields in some of the contexts that have been explored here. The gravitational scalars that have been considered in this work have all been massless. Self-interactions are of direct interest for problems such as the late-time acceleration of the Universe as well as early-time behaviour, such as that which occurs during inflation. Understand these theories, and their physical effects, would be of direct interest for considerations of these scenarios.

Bibliography

[1] A. J. Accioly, Nuovo Cimento **100B**, 703 (1987).

[2] V. Acquaviva, C. Baccigalupi, S. M. Leach, A. R. Liddle and F. Perrotta, Phys. Rev. D **71**, 104025 (2005).

[3] C. W. Allen, *Astrophysical quantities*, The Athlone Press, London (1965).

[4] T. Ashenfelter, G. J. Mathews and K. A. Olive, Phys. Rev. Lett. **92**, 41102 (2004).

[5] C. Bambi, M. Giannotti and F. L. Villante, Phys. Rev. D **71**, 123524 (2005).

[6] N. Banerjee and S. Sen, Phys. Rev. D **56**, 1334 (1997).

[7] V. Barger, J. P. Kneller, H. S. Lee, D. Marfatia and G. Steigman, Phys. Lett. B **566**, 8 (2003).

[8] J. D. Barrow, Mon. Not. Roy. astr. Soc., **175**, 359 (1976).

[9] J. D. Barrow, Mon. Not. Roy. astr. Soc., **178**, 625 (1977).

[10] J. D. Barrow, Mon. Not. Roy. Astr. Soc. **179** 47P, (1977).

[11] J. D. Barrow, Nature **272**, 211 (1978).

[12] J. D. Barrow, Phys. Rev. Lett. **46**, 963 (1981).

[13] J. D. Barrow, Physics Reports **85**, 1 (1982).

[14] J. D. Barrow, Mon. Not. Roy. Astr. Soc. **211**, 221 (1984).

[15] J. D. Barrow, Phys. Lett. B **180**, 335 (1986).

[16] J. D. Barrow, Phys. Lett. B **187**, 12 (1987).

[17] J. D. Barrow, Nucl. Phys. B **310**, 743 (1988).

[18] J. D. Barrow, Phys. Rev. D **46**, R3227 (1992).

[19] J. D. Barrow, Phys. Rev. D **47**, 5329 (1992).

[20] J. D. Barrow, Mon. Not. Roy. Astr. Soc. **282**, 1397 (1996).

[21] J. D. Barrow, Phys. Rev. D **55**, 7451 (1997).

[22] J. D. Barrow and B. J. Carr, Phys. Rev. D **54**, 3920 (1996).

[23] J. D. Barrow and T. Clifton, Class. Quant. Grav. **23**, L1 (2006).

[24] J. D. Barrow and T. Clifton, Phys. Rev. D **73**, 103520 (2006).

[25] J. D. Barrow and S. Cotsakis, Phys. Lett. B **214**, 515 (1988).

[26] J. D. Barrow and M. P. Dąbrowski, Phys. Rev. D **58**, 103502 (1998).

[27] J. D. Barrow, G. F. R. Ellis, R. Maartens and C. Tsagas Class. Quant. Grav. **20**, L155 (2003).

[28] J. D. Barrow, P. G. Ferreira, J. Silk, Phys. Rev. Lett. **78**, 3610 (1997).

[29] J. D. Barrow and S. Hervik, Phys. Rev. D **73**, 023007 (2006).

[30] J. D. Barrow, Y. Jin, and K.-I. Maeda, Phys. Rev. D **72**, 103512 (2005).

[31] J. D. Barrow, D. Kimberly and J. Magueijo, Class. Quant. Grav. **21**, 4289 (2004).

[32] J. D. Barrow and C. Kunze, Phys. Rev. D, **57**, 2255 (1997).

[33] J. D. Barrow and K.-I. Maeda, Nucl. Phys. B **341**, 294 (1990).

[34] J. D. Barrow and J. P. Mimoso, Phys. Rev. D **50**, 3746 (1994).

[35] J. D. Barrow and C. O'Toole, Mon. Not. Roy. Astron. Soc. **322**, 585 (2001).

[36] J. D. Barrow and A. C. Ottewill, J. Phys. A **16**, 2757 (1983).

[37] J. D. Barrow and P. Parsons, Phys. Rev. D **55**, 1906 (1997).

[38] J. D. Barrow and R. J. Scherrer, Phys. Rev. D **70**, 103515 (2004).

[39] J. D. Barrow and J. Stein-Schabes, Phys. Rev. D **32**, 1595 (1985).

[40] J. D. Barrow and F. J. Tipler, Phys. Reports **56**, 371 (1979).

[41] J. D. Barrow and C. Tsagas, Class. Quant. Grav. **21**, 1773 (2004).

[42] J. D. Barrow and C. Tsagas, Phys. Rev. D **69** 064007, (2004).

[43] V. A. Belinskii, I. M. Khalatnikov and E. M. Lifshitz, Sov. Phys. Usp. **13**, 745 (1971).

[44] V. A. Belinskii and I. M. Khalatnikov I M, Sov. Phys. JETP **36**, 591 (1973).

[45] C. L. Bennett et. al., Astrophys. J. Suppl. **148**, 1 (2003).

[46] P. G. Bergmann, Int. J. Theo. Phys. **1**, 25 (1968).

[47] B. Bertotti, L. Iess and P. Tortora, Nature **425**, 374 (2003).

[48] A. Bhadra and K. K. Nandi, Mod. Phys. Lett. **16**, 2079 (2001).

[49] A. Bhadra and K. Sarkar, Gen. Rel. Grav. **37**, 2189 (2005).

[50] U. Bleyer and H. J. Schmidt, Int. J. Mod. Phys. A **5**, 4671 (1990).

[51] C. Brans, Phys. Rev. D **125**, 2194 (1962).

[52] C. Brans and R. H. Dicke, Phys. Rev. D **124**, 925 (1961).

[53] H. A. Buchdahl, Phys. Rev. **115**, 1325 (1959).

[54] H. A. Buchdahl, Mon. Not. R. Astron. Soc. **150**, 1 (1970).

[55] H. A. Buchdahl, J. Phys. A **12**, 1229 (1979).

[56] S. Capozziello, R. De Ritis, C. Rubano and P. Scudellaro, Int. J. Mod. Phys. D **5**, 85 (1996).

[57] S. Capozziello, F. Occhionero and L. Amendola, Int. J. Math. Phys. D **1**, 615 (1993).

[58] S. Carloni, P. K. S. Dunsby, S. Capoziello and A. Troisi, Class. Quant. Grav. **22**, 4839 (2005).

[59] S. M. Carroll, A. De Felice, V. Duvvuri, D. A. Easson, M. Trodden and M. S. Turner, Phys. Rev. D **71**, 063513 (2005).

[60] S. M. Carroll and M. Kaplinghat, Phys. Rev. D **65**, 063507 (2002).

[61] J. A. Casas, J. Garcia-Bellido and M. Quiros, Mod. Phys. Lett. A **7**, 447 (1992).

[62] J. A. Casas, J. Garcia-Bellido and M. Quiros, Phys. Lett. B **278**, 94 (1992).

[63] J. L. Cervantes-Cota and M. Nahmad, Gen. Rel. Grav. **33**, 767 (2001).

[64] K. C. K. Chan, J. H. Horne and R. B. Mann, Nucl. Phys. **B447**, 441 (1995).

[65] X. Chen and M. Kamionkowski, Phys. Rev. D **60**, 104036 (1999).

[66] X. Chen, R. J. Scherrer and Gary Steigman, Phys. Rev. D **63**, 123504 (2001).

[67] D. Chernoff and J. D. Barrow, Phys. Rev. Lett. **50**, 134 (1983).

[68] L. P. Chimento, A. S. Jakubi and D. Pavon, Int. J. Mod. Phys. D **9**, 43 (2000).

[69] T. Clifton, *gr-qc/0607096* (2006).

[70] T. Clifton and J. D. Barrow, Phys. Rev. D **72**, 103005 (2005).

[71] T. Clifton and J. D. Barrow, Phys. Rev. D **72**, 123003 (2005).

[72] T. Clifton and J. D. Barrow, Class. Quant. Grav. **23**, 2951 (2006).

[73] T. Clifton and J. D. Barrow, Phys. Rev. D **73**, 104022 (2006).

[74] T. Clifton, J. D. Barrow and R. Scherrer, Phys. Rev. D **71**, 123526 (2005).

[75] T. Clifton, D. F. Mota and J. D. Barrow, Mon. Not. Roy. Ast. Soc. **358**, 601 (2005).

[76] T. Damour and K. Nordtvedt, Phys. Rev. D **48**, 3436 (1993).

[77] T. Damour and B. Pichon, Phys. Rev. D **59**, 123502 (1999).

[78] S. Das and N. Banerjee, Gen. Rel. Grav. **38**, 785 (2006).

[79] B. De Witt, *The Dynamical Theory of Groups and Fields*, Gordon and Breach, New York (1965).

[80] R. H. Dicke, Phys. Rev. **125**, 2163 (1962).

[81] R. H. Dicke, *The Theoretical Significance of Experimental Relativity*, Blackie, London (1964).

[82] D. Eardley, E. Liang and R. Sachs R, J. Math. Phys. **13**, 99 (1972).

[83] A. S. Eddington, *The Mathematical Theory of Relativity, 2nd. edn.*, Cambridge University Press, Cambridge (1924).

[84] Y. Fenner, B. Gibson and M. Murphy, Mon. Not. Roy. Ast. Soc. **358**, 468 (2005).

[85] D. J. Fixsen, E. S. Cheng, J. M. Gales, J. C. Mather, R. A. Shafer and E. L. Wright, Astrophys. J. **473**, 576 (1996).

[86] O. A. Fonarev, Class. Quant. Grav. **12**, 1739 (1995).

[87] K. Freese, F. C. Adams, J. A. Friedman, and E. Mottola, Nucl. Phys. B **287**, 797 (1987).

[88] Y. Fuji and I.-K. Maeda, *The Scalar-Tensor Theory of Gravitation*, Cambridge University Press, Cambridge (2003).

[89] J. Garcia-Bellido, A. Linde, D. Linde, Phys. Rev. D **50**, 730 (1994).

[90] B. Geyer, S. D. Odintsov and S. Zerbini, Phys. Lett. B **460**, 58 (1999).

[91] G. W. Gibbons, Nucl. Phys. B **292**, 784 (1987) and ibid **310**, 636 (1988)

[92] K. Gödel, Rev. Mod. Phys. **21**, 447 (1949).

[93] H. Goldstein, *Classical Mechanics, 2nd edn.* Addison-Wesley, Reading, Mass. (1980).

[94] M. B. Green, J. H. Schwartz and E. Witten, *Superstring Theory*, Cambridge University Press, Cambridge (1987).

[95] B. Guberina, R. Horvat and H. Nikolic, Phys. Lett. B **636**, 80 (2006).

[96] V. T. Gurovich, Sov. Phys. JETP **46**, 193 (1977).

[97] L. E. Gurevich, A. M. Finkelstein and V. A. Ruban, Astrophys. Space Sci. **22**, 231 (1973).

[98] T. Harada, B. J. Carr and C. A. Goymer, *astro-ph/0102058*, contribution to proceedings of JGRG10, Osaka, Japan (2000).

[99] T. Harada, C. A. Goymer and B. J. Carr, Phys. Rev. D **66**, 104023 (2002).

[100] E. R. Harrison, Phys. Rev. D, **1**, 2726 (1970).

[101] E. R. Harrison, in *Cargèse Lectures in Physics*, Vol. 6, ed. E. Schatzmann, Gordon and Breach, NY (1973).

[102] S. W. Hawking and G. F. R. Ellis, *The large scale structure of spacetime*, Cambridge University Press, Cambridge (1973).

[103] S. W. Hawking and R. J. Tayler, Nature **209**, 1278 (1966).

[104] D. J. Holden and D. Wands, Class. Quant. Grav. **15**, 3271 (1998).

[105] V. Husain, E. A. Martinez and D. Nunez, Phys. Rev. D, **50**, 3783 (1994).

[106] P. Jordan, Nature **164**, 637 (1949).

[107] P. Jordan, *Schwerkraft und Weltall*, Vieweg, Baunschweig (1995).

[108] P. Jordan, Z. Phys. **157**, 112 (1959).

[109] T. Kaluza, Sitzungber. Preus. Akad. Wiss. 966 (1920)

[110] O. Klein, Z. Phys. **37**, 895 (1926).

[111] E. Kasner, Trans. Am. Math. Soc. **27**, 101 (1925).

[112] L. Kawano, Fermilab-pub-92/04-A, 1992.

[113] R. Kerner, Gen. Rel. Grav. **14**, 453 (1982).

[114] D. Kirkman, D. Tytler, N. Suzuki, J. M. O'Meara and D. Lubin, Astrophys. J. Suppl. **149**, 1 (2003).

[115] D. La and P.J. Steinhardt, Phys. Rev. Lett. **62**, 376 (1989).

[116] O. Lahav *et al.*, Mon. Not. Roy. Astron. Soc. **251**, 128 (1991).

[117] L. D. Landau and E. M. Lifshitz, *The Classical Theory of Fields* 4th rev. edn. Pergamon, Oxford (1975).

[118] A. R. Liddle, A. Mazumdar and J. D. Barrow, Phys. Rev. D **58**, 027302 (1998).

[119] E. M. Lifshitz and I. M. Khalatnikov, Adv. Phys. **12**, 185 (1963).

[120] B. Losic and W. G Unruh, Phys. Rev. D **71**, 044011 (2005).

[121] M. S. Madsen and J. D. Barrow, Nucl. Phys. B **323**, 242 (1989).

[122] K.-I. Maeda, Phys. Rev. D **39**, 3159 (1989).

[123] G. Magnano, M. Ferraris and M. Francaviglia, Gen. Rel. Grav. **19**, 465 (1987).

[124] G. Magnano and M. Sokolowski, Phys. Rev. D **50**, 5039 (1994).

[125] S. Mignemi and D. L. Wiltshire, Class. Quant. Grav. **6**, 987 (1989).

[126] C. W. Misner, Phys. Rev. Lett. **22**, 1071 (1969).

[127] J. P. Mohr and B. Taylor, Rev. Mod. Phys. **72**, 351 (2000).

[128] D. F. Mota and J. D. Barrow, Mon. Not. Roy. Astron. Soc. **349**, 281 (2004).

[129] D. F. Mota and J. D. Barrow, Phys. Lett. B **581**, 141 (2004).

[130] D. F. Mota and C. van de Bruck, Astron. Astrophys. **421**, 71 (2004).

[131] M. T. Murphy *et al*, Mon. Not. Roy. Aast. Soc. **327**, 1208 (2001)

[132] M. T. Murphy, J. K. Webb and V. V. Flambaum, MNRAS **345**, 609 (2003).

[133] R. Nagata, T. Chiba and N. Sugiyama, Phys. Rev. D **66**, 103510 (2002).

[134] R. Nagata, T. Chiba and N. Sugiyama, Phys. Rev. D **69**, 083512 (2004).

[135] H. Nariai, Prog. Theo. Phys. **40**, 49 (1968).

[136] H. Nariai, Prog. Theo. Phys. **42**, 742 (1969).

[137] H. Nariai, Prog. Theo. Phys. **42**, 544 (1969).

[138] National Institute of Standards and Technology, *www.physics.nist.gov/cuu/Constants* (2002).

[139] I. Navarro and K. van Acoleyen, J. Cosm. Astopart. Phys. **0603**, 008 (2006).

[140] S. Nojiri and S. D. Odintsov, Phys. Rev. D **68**, 123512 (2003).

[141] K. Nordvedt, Phys. Rev. **169**, 1014 (1968)

[142] K. Nordvedt, Phys. Rev. **169**, 1017 (1968).

[143] K. Nordtvedt, Astrophys. J. **161**, 1059 (1970).

[144] J. O'Hanlon and B. Tupper, Nuovo Cimento **137**, 305 (1970).

[145] A. Ohashi, H. Tagoshi and M. Sasaki, Prog. Theo. Phys. **96**, 713 (1996).

[146] K. A. Olive, G. Steigman and T. P. Walker, Physics Reports **333**, 389 (2000).

[147] G. J. Olmo, Phys. Rev. D **72**, 083505 (2005).

[148] I. Ozsváth and E. Schücking, Class. Quant. Grav. **18**, 2243 (2001).

[149] T. Padmanabhan, *Structure formation in the universe*, Cambridge University Press, Cambridge (1995).

[150] J. Peacock, *Cosmological Physics*, Cambridge University Press, Cambridge (1999)

[151] E. Pechlaner and R. Sexl, Comm. Math. Phys. **2**, 165 (1966).

[152] P. Peter and N. Pinto-Neto, Phys. Rev. D **66**, 063509 (2002).

[153] V. Pettorino, C. Baccigalupi and G. Mangano, J. Cosmol. Astropart. Phys. **01**, 014 (2004).

[154] O. L. Pimentel, Mod. Phys. Lett. A **12**, 1865 (1997).

[155] S. Pireaux, J. P. Rozelot and S. Godier, Astrophys. Space Sci. **284**, 1159 (2003).

[156] L. Randall and R. Sundrum, Phys. Rev. Lett. **83**, 3370 (1999).

[157] L. Randall and R. Sundrum, Phys. Rev. Lett. **83**, 4690 (1999).

[158] M. J. Reboucas and J. Tiomno, Phys. Rev. D **28**, 1251 (1983).

[159] A. D. Rendall, Class. Quantum Grav. **14**, 2341 (1997).

[160] N. Riazi, E. Ahmadi-Azar, Astrophys. Sp. Sci. **226**, 1 (1995).

[161] H. P. Robertson, in *Space Age Astronomy*, Academic, New York (1962).

[162] H. P. Robertson and T. W. Noonan, *Relativity and Cosmology*, Saunders, Philadelphia (1968).

[163] C. Romero and A. Barros, Phys. Lett. A **173**, 243 (1993).

[164] I. Roxburgh, Gen. Rel. Grav. **8**, 219 (1977).

[165] T. V. Ruzmaikina and A. A. Ruzmaikin, Sov. Phys. JETP **57**, 680 (1969).

[166] T. V. Ruzmaikina and A. A. Ruzmaikin, Sov. Phys. JETP **30** , 372 (1970).

[167] D. I. Santiago, D. Kalligas and R. V. Wagoner, Phys. Rev. D **56**, 7627 (1997).

[168] M. A. Scheel, S. L. Shapiro and S. A. Teukolsky, Phys. Rev. D **51**, 4208 (1995).

[169] R. J. Scherrer, Phys.Rev. D **69**, 107302 (2004).

[170] L. I. Schiff, in *Relativity Theory and Astrophysics. I. Relativity and Cosmology*, American Mathematical Society, Providence (1967).

[171] H. J. Schmidt, *Lectures on Mathematical Cosmology, gr-qc/0407095* (2004).

[172] A. Serna and J. M. Alimi, Phys. Rev. D. **53**, 3087 (1996).

[173] A. Serna, R. Dominguez-Tenreiro and G. Yepes, Astrophys. J. **391**, 433 (1992).

[174] I. I. Shapiro, C. C. Counselman III and R. W. King, Phys. Rev. Lett. **36**, 555 (1976).

[175] D. J. Shaw and J. D. Barrow, Phys. Rev. D **73**, 123505 (2006).

[176] D. J. Shaw and J. D. Barrow, Phys. Lett. B **639**, 569 (2006).

[177] D. J. Shaw and J. D. Barrow, Phys. Rev. D **73**, 123506 (2006).

[178] V. F. Shvartsman, Sov. Phys. JETP Lett. **9**, 184 (1969).

[179] W. M. Smart, *Celestial Mechanics*, Longman Green, London (1953).

[180] G. Steigman, Phys. Scripta T **121**, 142 (2005).

[181] K. S. Stelle, Phys. Rev. D **16**, 953 (1977).

[182] T. Tamaki, K.-I. Maeda and T. Torii, Phys. Rev. D **60**, 104049 (1999).

[183] R. C. Tolman, *Relativity, Thermodynamics and Cosmology*, Oxford University Press, Oxford, (1934), section 165.

[184] K. Tomita, Prog. Theo. Phys. **54**, 730 (1975).

[185] R. Trotta and S. H. Hansen, Phys. Rev. D **69**, 023509 (2004).

[186] J. P. Uzan, Rev. Mod. Phys. **75**, 403 (2003).

[187] R. V. Wagoner, Phys. Rev. D **1**, 3209 (1970).

[188] L. M. Wang and P. J. Steinhardt, Astrophys. J. **508**, 483 (1998).

[189] J. K. Webb *et al*, Phys. Rev Lett. **82**, 884 (1999)

[190] J. K. Webb *et al*, Phys. Rev. Lett. **87**, 91301 (2001)

[191] C. M. Will, *Theory and Experiment in Gravitational Physics* (rev. edn.), Cambridge University Press, Cambridge (1993).

[192] M. Wyman, Phys. Rev. D **24**, 839 (1981).

[193] K. Yano, *Integral Formulas in Riemannian Geometry* (Pure and Applied Mathematics: A Series of Monographs), Marcel Dekker Inc., New York (1970).

[194] O. Zahn and M. Zaldarriaga, Phys. Rev. D **67**, 063002 (2003).

[195] Y. B. Zeldovich, Sov. Phys. JETP Lett. **12**, 307 (1970).